

**Identification and first characterization of pairing-
dependently transcribed genes in
Schistosoma mansoni males**

Inaugural-Dissertation

zur Erlangung des Doktorgrades der Naturwissenschaften (Dr. rer. nat.)

im Fachbereich Biologie und Chemie der

Justus-Liebig-Universität Gießen

vorgelegt von

Dipl.-Biol. Silke Leutner

aus Gießen

Juni 2013

Die vorliegende Arbeit wurde am Institut für Parasitologie,
des Fachbereiches Veterinärmedizin der Justus-Liebig-Universität,
im Rahmen eines DFG geförderten Projektes und
mit Unterstützung der Studienstiftung des deutschen Volkes, angefertigt.

Dekan des Fachbereiches Biologie und Chemie: Prof. Dr. H. Zorn

1. Gutachter: Prof. Dr. A. Bindereif
Institut für Biochemie, Fachbereich Biologie & Chemie
Justus-Liebig-Universität Gießen

2. Gutachter: Prof. Dr. C.G. Grevelding
Institut für Parasitologie, Fachbereich Veterinärmedizin
Justus-Liebig-Universität Gießen

Eingereicht am: 11.06.2013

Disputation am: 07.10.2013

Eidesstattliche Erklärung

Ich, Silke Leutner geboren am 09.02.1981 in Gießen, erkläre: Ich habe die vorgelegte Dissertation selbständig und ohne unerlaubte fremde Hilfe und nur mit den Hilfen angefertigt, die ich in der Dissertation angegeben habe. Alle Textstellen, die wörtlich oder sinngemäß aus veröffentlichten Schriften entnommen sind, und alle Angaben, die auf mündlichen Auskünften beruhen, sind als solche kenntlich gemacht. Bei den von mir durchgeführten und in der Dissertation erwähnten Untersuchungen habe ich die Grundsätze guter wissenschaftlicher Praxis, wie sie in der „Satzung der Justus-Liebig-Universität Gießen zur Sicherung guter wissenschaftlicher Praxis“ niedergelegt sind, eingehalten.

Gießen, den

Silke Leutner

*I have not failed.
I've just found 10,000 ways that won't work.*

[Thomas A. Edison]

Contents

1. Introduction	1
1.1. <i>Schistosoma mansoni</i>	1
1.2. Schistosome reproduction biology and the hypothesized male stimulus	3
1.3. Parasite development and host-factors	6
1.4. Signal transduction molecules in schistosomes with a focus on males	7
1.4.1. Serine-threonine kinases	8
1.4.2. TGF β -pathway	8
1.5. Transcriptomics in schistosome research	11
1.6. Aims of the study	13
2. Materials and Methods	15
2.1. Materials	15
2.1.1. Buffers and solutions	15
2.1.2. Media and additives	17
2.1.3. Enzymes	19
2.1.4. Molecular weight standards	20
2.1.5. Primers	20
2.1.6. Plasmids	28
2.1.7. Bacteria and yeasts	29
2.1.8. Antibodies	29
2.1.9. Databases and online software-tools	29
2.1.10. Sequencing	30
2.2. Methods	31
2.2.1. <i>Schistosoma mansoni</i> laboratory cycle	31
2.2.1.1. Infection of hamsters	31
2.2.1.2. Hamster perfusion and <i>Schistosoma in vitro</i> culture	31
2.2.1.3. Snails	32
2.2.1.4. Obtaining <i>Schistosoma</i> larval stages	32
2.2.2. Isolation of nucleic acids	33
2.2.2.1. Isolation of RNA from <i>Schistosoma mansoni</i>	33
2.2.2.2. Isolation of DNA from <i>S. mansoni</i>	33

Content

2.2.2.3.	Isolation of plasmid DNA from bacteria	34
2.2.2.4.	Determination of nucleic acid concentration	34
2.2.3.	Gel electrophoresis of nucleic acids	34
2.2.3.1.	DNA	35
2.2.3.2.	RNA	35
2.2.4.2.	Gel-elution	35
2.2.4.	Polymerase chain reactions	36
2.2.4.1.	Standard PCR	36
2.2.4.2.	Colony-PCR	36
2.2.4.3.	Sexing-PCR	37
2.2.4.4.	Reverse transcriptase reactions	37
2.2.4.5.	Real-time PCR	38
2.2.4.6.	Mutagenesis	40
2.2.5.	Cloning of DNA into plasmid vectors	41
2.2.5.1.	Restriction enzyme digestions	41
2.2.5.2.	Ligation	41
2.2.6.	Bacteria	42
2.2.6.1.	Production of heat-shock competent bacteria	42
2.2.6.2.	Transformation of heat-shock competent bacteria	42
2.2.6.3.	Blue-white selection	42
2.2.6.4.	Liquid culture	43
2.2.6.5.	Glycerin-stocks	43
2.2.7.	Yeasts	43
2.2.7.1.	Liquid culture	43
2.2.7.2.	Glycerin-stocks	43
2.2.7.3.	Production of yeast cells competent for transformation	43
2.2.7.4.	Transformation of yeast – lithium acetate method	44
2.2.7.5.	Yeast two-hybrid system	44
2.2.7.6.	Colony lift filter assay	45
2.2.7.7.	β -galactosidase-liquid assay	45
2.2.8.	<i>In situ</i> hybridization	46
2.2.8.1.	Fixation	46

2.2.8.2. Preparation of glass slides	46
2.2.8.3. Tissue sections	46
2.2.8.4. Probe synthesis	47
2.2.8.5. <i>In situ</i> hybridization protocol	48
2.2.9. Determination of mitotic activity	49
2.2.10. Carmine red staining of adult schistosomes	50
2.2.11. Pairing experiments	51
2.2.12. TNF α treatment	51
2.2.13. Inhibitor treatment	51
2.2.14. Transcriptome studies	51
2.2.14.1. Microarrays	52
2.2.14.2. Super-SAGE	55
2.2.14.3. Merging data from microarray and SuperSAGE experiments	55
2.2.14.4. Gene ontology and network analysis	57
2.2.14.5. Comparative analysis to previous studies	58
3. Results	59
3.1. Analyses on mitotic activity in male worms	59
3.1.1. Pairing inconsistently stimulates male mitotic activity	59
3.1.2. TNF α treatment has a dose-dependent effect on male mitotic activity	61
3.2. The cGMP-dependent protein kinase SmcGK1 may have a function in schistosome gonads	62
3.2.1. SmcGK1 sequence identification	63
3.3.2. Other <i>S. mansoni</i> cGKs	63
3.2.3. SmcGK1 action in <i>S. mansoni</i> reproductive organs	64
3.2.4. SmcGK1 anti-sense transcription	66
3.2.5. Differential transcription of SmcGK1 between male stages was not confirmed	67
3.3. Transcriptome analyses comparing EM and UM	68
3.3.1. Microarray analysis detected 1572 significantly regulated transcripts	69
3.3.2. SuperSAGE detected 53 or 815 significantly regulated transcripts depending on the applied statistics	74
3.3.2.1. SuperSAGE – EdgeR statistical analysis of SuperSAGE data	75

Content

3.3.2.2. SuperSAGE – Audic & Claverie statistical analysis of SuperSAGE data	75
3.3.3. Combinatory analysis of microarray and SuperSAGE data	79
3.4. Real-time PCR	87
3.4.1. Establishing real-time PCR	87
3.4.2. Verification of significantly transcribed genes	88
3.5. Data-analyses with refined criteria drastically reduced the number of interesting genes	96
3.6. First characterization studies	103
3.6.1. Follistatin	103
3.6.2. <i>In situ</i> hybridization experiments for SmInAct and SmBMP	106
4. Discussion	109
4.1. Male mitotic activity	109
4.1.1. The effect of pairing on mitotic activity in males	109
4.1.2. The effect of TNF α treatment on schistosome mitotic activity	111
4.2. The role of SmcGKI in schistosomes	113
4.3. Transcriptomic comparison between EM and UM	117
4.3.1. Comparison of microarrays and SuperSAGE revealed methodological and statistical differences	118
4.3.2. Real-time PCR experiments led to a more stringent streamlining of the data	120
4.3.3. Comparisons to previous studies on the differences between EM and UM support data reliability	121
4.3.4. EM and UM differ in metabolic processes	123
4.3.5. Signal transduction processes during UM to EM transition	124
4.3.6. Involvement of neurological processes during pairing	128
4.3.7. Detection of egg shell-related transcripts indicates leaky expression in males	129
4.3.8. Regulatory RNAs may be a future research focus	130
4.3.9. Further aspects of research	131
4.4. The role of SmFst in schistosomes	133
4.5. Conclusion	137
5. Summary	139
Zusammenfassung	140

6. References	143
List of abbreviations	163
List of units	167
List of figures	169
List of tables	171
List of supplementary files	173
Publications and scholarships	175
Acknowledgements	177

Appendix

1. Introduction

1.1. *Schistosoma mansoni*

S. mansoni and other parasitic flatworms of the genus *Schistosoma* cause a tropical disease of world-wide import. Transmission of this chronic disease, schistosomiasis, was reported for 78 countries, with an estimated 90% of infected people living in Africa under poor and sanitarily insufficient conditions (WHO Fact sheet N°115, updated March 2013, <http://www.who.int/mediacentre/factsheets/fs115/en/>). In 2011 at least 243 million people required treatment (WHO Fact sheet N°115, updated March 2013, <http://www.who.int/mediacentre/factsheets/fs115/en/>), while approximately 800 million are at risk (Ross *et al.*, 2012). Besides the resulting and underestimated socio economic importance (King, 2010), schistosomes are also of basic economic relevance as they can infect animals as well (Quack *et al.*, 2006; DeBont & Vercruyse, 1998).

Pathology is not induced by adult worms, but by eggs. One female deposits up to 300 eggs per day into the bloodstream (Moore & Sandground 1956). To continue the life cycle eggs have to pass from the mesenteric veins, where adult worms finally reside, through different tissue layers into the gut lumen, from where they are excreted and reach the environment. This process causes severe damage and chronic inflammation of the according tissues, as eggs secrete lytic enzymes and serologically active proteins (Ashton *et al.*, 2001; Schramm & Haas, 2010). A number of eggs are accidentally transported via the blood stream to inner organs such as the liver and spleen, where they cause additional inflammatory processes, resulting in granuloma formation and finally leading to hepatosplenomegaly and cirrhosis (Ross *et al.*, 2012).

Successful tissue passage of eggs takes approximately ten days, during which the embryo develops into the next larval stage, the miracidium. When the egg reaches the water, the already sexually determined miracidium hatches. Upon contact it penetrates the intermediate host, in case of *S. mansoni* the aquatic snail *Biomphalaria glabrata*. Within the snail asexual reproduction occurs and miracidia develop into mother sporocysts, which generate a large number of daughter sporocysts. These produce another larval stage, the cercariae, which is infective for the final host (Mehlhorn & Piekarski, 2002; Dönges, 1988). Infection of the final host occurs through enzymatically facilitated penetration of the host's skin (Ross *et al.*, 2012). During the skin-passage cercariae develop into schistosomula, which start the migration through the host's blood-stream towards the portal vein system of the liver. During their body passage, schistosomula develop into adult male and female flukes (Ross *et al.*, 2012). The existence of separate sexes is a singular trait

1. Introduction

of the family Schistosomatidae within the class Trematoda (flukes). All other animals within this class are hermaphrodites (Mehlhorn & Piekarski, 2002; Dönges, 1988). Male and female *S. mansoni* pair in the liver and migrate to the mesenteric veins, where they live permanently paired. During pairing the female resides within a ventral groove of the male, the gynaecophoral canal (Ross *et al.*, 2012; Mehlhorn & Piekarski, 2002; Dönges, 1988) (Figure 1.1.).

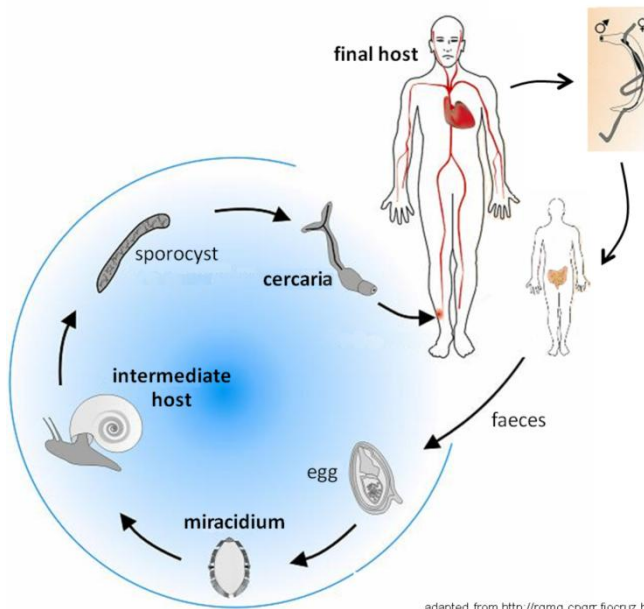


Figure 1.1: *S. mansoni* life cycle.

Adult *S. mansoni* couples live in the blood vessels of the human intestines. Eggs deposited by the female pervade the tissue between blood vessel and intestine and are excreted with the faeces. Miracidia hatch from eggs reaching a water body and penetrate into the snail intermediate host (*Biomphalaria glabrata*). After two sporocyst stages within the snail cercariae are produced. Leaving the intermediate host, cercariae render great damage to the host's tissue. In the water they move with their bifurcate tails and are attracted to the main host by chemotaxis. After penetration of the human skin, the cercariae lose their tails and become schistosomula, which develop into adult flukes while passing the heart and lung. Mating takes place in the liver.

The current drug of choice to treat schistosomiasis is praziquantel (PZQ) (Chitsulo *et al.*, 2004), which acts on adult worms, but not on juvenile stages (reviewed in: Doenhoff *et al.*, 2009; Greenberg & , 2005; Cioli & Pica-Mattoccia, 2003). Also first evidence exists for reduced PZQ effects in patients and from laboratory studies justifying the fear of upcoming resistance against this drug (Doenhoff *et al.*, 2009; Melman *et al.*, 2009; Cioli & Pica-Mattoccia, 2003). The mechanism of action of praziquantel is unknown, though evidence exists that the molecular target of the drug are calcium channels (reviewed in: Doenhoff *et al.*, 2009). In response to praziquantel treatment, schistosomes are paralyzed which is accompanied by an influx of calcium-ions into the worms (reviewed in: Greenberg & , 2005; Cioli & Pica-Mattoccia, 2003). Recently, the involvement of calcium/calmodulin-dependent kinase II (CaMKII) was demonstrated (You *et al.*, 2013). Oxamniquine, another anti-schistosomal drug, is only effective against *S. mansoni*, not against other parasites of the same genus, and therefore not widely used in the field (Pica-Mattoccia *et al.*, 2006; Cioli & Pica-Mattoccia, 2003). Vaccines against cercariae or adults are not available. Therefore, the search for new drugs and drug targets is a major focus of schistosome research. Recent studies have reported the schistosomicidal activity of established anti-cancer drugs such as Imatinib (Beckmann *et al.*, 2012a; Dissous & Grevelding, 2011; Beckmann & Grevelding, 2010) or

plumbagin (Lorsuwannarat *et al.*, 2013). Plant derived agents like the cyclotides kalata B1 and B2 (Malagón *et al.*, 2013), (+)-Limonene Epoxide (deMoraes *et al.*, 2013) or Curcumin (Morais *et al.*, 2013) were also described to negatively affect the worms.

In an attempt to gain new insights into the biology of schistosome parasites, transcriptome and genome projects were performed, leading to a nearly complete coverage of the genomes of the most important schistosome species with respect to human health (Protasio *et al.*, 2012; Young *et al.*, 2012; Berriman *et al.*, 2009; *Schistosoma japonicum* Genome Sequencing and Functional Analysis Consortium *et al.*, 2009; Verjovski-Almeida *et al.*, 2004; Verjovski-Almeida *et al.*, 2003).

1.2. Schistosome reproduction biology and the hypothesized male stimulus

Males play an essential role in the biology of schistosomes infectious to humans. Without a constant pairing-contact to a male, females are not able to reach sexual maturation or, if paired before, lose their maturation status following separation from the male (Kunz, 2001; Grevelding *et al.*, 1997a; Popiel *et al.*, 1984; Clough, 1981; Shaw, 1977; Erasmus, 1973). It has been proposed that this strong dependence has evolutionary roots since schistosomes likely originated from hermaphroditic ancestors (Loker & Brant, 2006; Basch, 1990). Sexual maturation of the female includes the differentiation of the reproductive organs as a prerequisite for egg production. Since the eggs cause pathogenesis, the search for the stimulating male factor(s) has been one research focus for a long time. Closely related to this research subject is the question whether the capacity of the male to stimulate developmental processes in the female is of constitutional nature or has to be induced itself by an initial pairing event.

While morphological differences between pairing-unexperienced females (UF) and pairing-experienced females (EF) are evident, pairing causes no obvious morphological changes in males. UF have no developed vitellarium or ovary, and they are much smaller than EF (Kunz, 2001). Pairing-unexperienced males (UM) and pairing-experienced males (EM) are similar in size, and have both well developed testes. Male sizes differ between schistosome species. While sizes are comparable for EM and UM in *S. mansoni*, *H. americana* and *S. japonicum* UM are much smaller than corresponding EM, also size differences depend additionally on the worm age as observed for *S. japonicum* (Armstrong, 1965; Severinghaus, 1928). This size difference is an indication that males also need a stimulus from the female to complete maturation. Indeed, further supporting evidence was obtained that pairing has an influence on males, too: compared to EM, UM need 24 h longer to induce mitotic activity (MA) in the female (Den Hollander & Erasmus, 1985).

1. Introduction

Furthermore, it has been shown, that females induce lipid accumulation and lipase activity in males (Haseeb *et al.*, 1989). However, research on a factor transferred from the female to the male was neglected as it was assumed to be uncertain and less promising concerning schistosomiasis control compared to the male factor influencing the female.

Since the male exerts a prominent role in pairing, much attention was given to the identification of a male factor. This factor was proposed to be: purely tactile, a glycoprotein, a hormone, sperm or components of the seminal fluid:

Cross-mating between adults of different schistosome species indicated that there are different stimuli for female development and size (Basch & Basch, 1984; Armstrong, 1965). Initial pairing was hypothesized to be a result of random encounters followed by tactile stimulation rather than a hormonal one, because homosexual pairing between males was observed (Armstrong, 1965).

To obtain more evidence on the nature of the stimulus from males to females, Michaels (1969) conducted pairing experiments with transected males and females. Using egg production as an indicator for female stimulation he concluded that the posterior half of a male is more competent in stimulating the female than the anterior one, indicating a local production or concentration of a male factor. Performing similar experiments with transected as well as whole worms *in vivo* and *in vitro*, and using differentiation of the vitellarium as an indicator for female stimulation, Popiel and Basch (1984a) concluded that the stimulus was indeed a local one, not propagated longitudinally in the female. This was taken as supportive evidence for the presence of either a tactile stimulus or a locally concentrated soluble factor.

In 1985 Aronstein and Strand reported the finding of a glycoprotein that was located exclusively to the gynaecophoral canal and therefore named "gynaecophoral canal protein" (GCP). Immunolocalization found GCP to a higher extent in EM compared to UM, the latter, however, was deduced from a non-quantitative method (Aronstein & Strand, 1985). Using the antibody generated by Aronstein and Strand, Gupta and Basch (1987) found that GCP was expressed on the surface of the gynaecophoral canal and within structures interpreted as connections to cytons within the subtegument in EM and UM. The authors concluded that GCP-expression was pairing-dependent as it was not detected in older UM (6 wks) but in EM. In paired females, GCP was detected on the surface only, giving rise to the idea that the glycoprotein may be transferred from the male to the female. However, further evidence indicating GCP as the sought-after male stimulus was not obtained (Gupta & Basch, 1987).

Shaw (1977) proposed that the gynaecophoral canal provides “an essential microenvironment”, serving not only in holding the female but concentrating the male-stimulus to a critical amount to activate processes in the female. In search for a chemical stimulus Basch and Nicolas (1989) paired complete and bisected halves of males to calcium alginate fibers that served as surrogate females. Analyses of the substances bound to these artificial fibers by PAGE revealed two molecules of 40 and 46 kDa that were not present in the controls. However, these molecules were not further analyzed (Basch & Nicolas, 1989).

Atkinson and Atkinson (1980) identified a 66 kDa molecule as a male product that was later detected in females, hypothesizing that it might be the sought-after stimulus transferred to the female. This study was discussed controversially since other groups were not able to detect this molecule in similar experiments (Popiel & Basch, 1984b; Ruppel & Cioli, 1977). On the gels presented in the work of Ruppel and Cioli (1977) a band of this size was found in EF and not in males; also, it represented a very minor band compared to others. Instead, Ruppel and Cioli (1977) found a 29 kDa molecule to be specific for females in comparison to males, schistosomula and cercariae. However, this result could not be reproduced as reported by Popiel and Basch (1984b). Thus definitive candidate molecule(s) for the male stimulus still remain elusive.

Shaw *et al.* (1977) were successful in inducing female development under *in vitro* conditions by applying acetone and ether extracts of male worms. Females from unisexual infections increased in size, and further development of their vitelline cells was observed. These results however, were contradictory discussed since similar experiments failed in other hands (Popiel, 1986). Moore *et al.* (1954) tried to stimulate UF *in vivo* by injecting UF-infected hosts with suspensions from pulverized males or testosterone. While the male suspensions showed no effect, testosterone induced abnormal ovaries in some individuals.

Since schistosomes are not capable of *de novo* synthesis of sterols and fatty acids, they depend on host-molecules that are used for the synthesis of lipids (Meyer *et al.*, 1970). It is known that cholesterol is transferred from males to females (Silveira *et al.*, 1986; Cornford & Fitzpatrick, 1985) and vice versa (Popiel & Basch, 1986; Haseeb *et al.*, 1985). Furthermore, it has been reported that ecdysteroids are synthesized and secreted by adult worms (Nirde *et al.*, 1984; Nirde *et al.*, 1983; Torpier *et al.*, 1982), though their function remains uncertain. Besides the described hormones nuclear receptors have been identified in schistosomes, with a putative role in female processes (Freebern *et al.*, 1999a; Freebern *et al.*, 1999b). Such hormone receptors could be the last link in the signaling chain induced by a male stimulus and leading to female differentiation.

Sperms were also considered as a possible stimulator of female development. In contrast to this hypothesis, females paired to males made anorchid by X-ray or males with non-functional sperm, still sexually matured (Michaels, 1969; Armstrong, 1965). Other studies found that vitelline cell development was independent of the presence of sperm in the oviduct (Shaw, 1977). However, while the first studies provided insufficient evidence on presence of sperm in the female receptaculum seminis, the latter reduced placement of male sperm within the female to the oviduct. Thus, all these studies reasoning that sperm or seminal fluid did not contain a stimulus could not provide conclusive evidence on the relevance of these factors for female maturation.

After more than 50 years of schistosome research and many attempts to identify a male stimulus towards the female, it still remains elusive.

1.3 Parasite development and host-factors

Besides the direct male-female interaction host factors have an influence on schistosome development (Lamb *et al.*, 2010; Salzet *et al.*, 2000). The presence of ecdysteroids was demonstrated in *S. mansoni* (Basch, 1986; Nirde *et al.*, 1984; Nirde *et al.*, 1983; Torpier *et al.*, 1982), but also in the related parasite *Trichobilharzia ocellata*. There it was hypothesized to be derivative from the snail host and/or important in host-parasite interaction (Schallig *et al.*, 1991). The schistosome epidermal growth factor (EGF)-receptor SER (Shoemaker *et al.*, 1992) has been shown *in vitro* to be able to bind human EGF, activate down-stream signaling, and enhance DNA synthesis (Vicogne *et al.*, 2004). It is primarily expressed in muscle cells (Ramachandran *et al.*, 1996), but also in female gonads (Buro *et al.* in preparation). Two insulin-receptors have been identified in *S. japonicum* and *S. mansoni* each, and it could be shown that transcript-levels for many genes are regulated in response to insulin treatment (You *et al.*, 2010; Ahier *et al.*, 2008; Khayath *et al.*, 2007). Thyroxine deficiency of hosts leads to dwarfed worms (Wahab *et al.*, 1971). Parasite development with regard to worm size (Davies *et al.*, 2001) and egg production was reported to be coupled to the presence of DC4⁺ T-cells (Davies *et al.*, 2001; Doenhoff *et al.*, 1978), probably by their modulation of monocyte/macrophage function (Lamb *et al.*, 2010). IL-7 seems to influence the parasite migration and development while also modulating the host immune response (Wolowczuk *et al.*, 1999). A lack of IL-7 reduces worm and egg burden and leads to reduced worm size, while increased IL-7 levels have the opposite effect (Wolowczuk *et al.*, 1999). Another cytokine, tumor necrosis factor α (TNF α), was linked to increased egg production and granuloma formation (Amiri *et al.*, 1992), but also adult schistosome viability (Davies *et al.*, 2004).

Previous, unpublished results from our group additionally indicated a TNF α -induced stimulation of MA in males.

1.4 Signal transduction molecules in schistosomes with a focus on males

Molecular signaling is of great importance for growth, differentiation and metabolic events. Signals are transduced from the cell-membrane to the nucleus or between cells (Lodish *et al.*, 2001), and even between whole organisms as proposed for the male and female schistosomes. Several recent publications (Wilson, 2012; Beckmann *et al.*, 2012a; Andrade *et al.*, 2011; Avelar *et al.*, 2011; Beckmann *et al.*, 2010b; LoVerde *et al.*, 2009; Knobloch *et al.*, 2007; LoVerde *et al.*, 2007; Bahia *et al.*, 2006a) have summarized the different protein kinases (PKs) and signal transduction molecules described in schistosomes and their functional importance. Functional characterizations of signaling molecules were so far mostly associated with female reproduction. Extensive signal transduction models for female oocytes and vitellocytes exist (Beckmann *et al.*, 2010b; Knobloch *et al.*, 2007). However, it has been hypothesized that similar events are important in males, especially concerning spermatogenesis since most of the described molecules have been localized in the testes by *in situ* hybridization (Beckmann *et al.*, 2010b). Three tyrosine kinases (TK), the Src kinase SmTK3 (Kapp *et al.*, 2001), the Syk kinase SmTK4 (Beckmann *et al.*, 2010a; Knobloch *et al.*, 2002b) and the Src/Abl hybrid kinase SmTK6 (Beckmann *et al.*, 2011), were postulated to form a trimeric complex that interacts with receptor tyrosine kinases but also with integrin and mucin receptors in the oocyte (Beckmann *et al.*, 2011). Transcripts for the trimeric kinase complex and two further interaction partners, discs-large homolog (DLG) and mucin were localized in EM testes (Beckmann *et al.*, 2011; Beckmann *et al.*, 2010a; Knobloch *et al.*, 2002b). Treatment of couples with the SmTK4-specific inhibitor Piceatannol as well as RNAi (RNA interference) experiments negatively affected male and female worms, among others spermatogenesis was impaired (Beckmann *et al.*, 2010a). Also, the down-stream target of SmTK3, SmDia, and its interaction partner SmRho were localized within the testicular lobes by *in situ* hybridization experiments (Quack *et al.*, 2009). As up-stream partners of the trimeric TK complex integrins were identified, and also localized in the testes (Beckmann *et al.*, 2012b).

Transcripts for two other TKs were detected in testes as well as female organs, the Fyn-like kinase TK5 (Knobloch *et al.*, 2002b; Kapp *et al.*, 2001) and *S. mansoni* receptor tyrosin kinase 1 (SmRTK1), a venus kinase receptor (VKR) (Gouignard *et al.*, 2012; Beckmann, 2008; Vicogne *et al.*, 2003).

1.4.1. Serine-threonine kinases

Serine threonine kinases are a family of protein kinases involved in multiple biological processes including development, proliferation, cell survival, metabolism, ion channel control and others (Krauss, 2008). A cAMP-dependent protein kinase (PKA) has been identified in schistosomes and was linked to egg production, parasite viability and most recently to neuronal and muscular activity in adult worms (de Saram *et al.*, 2013; Swierczewski & Davies, 2010a; Swierczewski & Davies, 2010b; Swierczewski & Davies, 2009). Similarly the protein kinase C (PKC) was cloned and localized to larval stages but not adult worms; it has a proposed role in the transformation from the miracidium to the mother sporocyst (Ludtmann *et al.*, 2009; Bahia *et al.*, 2006b).

Polo-like kinases (PLK) are regulators of the cell-cycle and more specifically of mitosis. Two PLKs are described in schistosomes, SmPLK1 and SmPLK2 (also SmSAK). Besides its role in oocyte development SmPLK1 is important for male spermatogenesis, inhibition of this kinase induced morphological changes in testes (Dissous *et al.*, 2011; Long *et al.*, 2010). SmPLK2 was weakly detected in the testes showing lower transcript levels in males than in other life cycle stages of the parasite. As RNAi experiments were unsuccessful and a specific inhibitor unavailable, the role of SmPLK2 in males remains unclear (Long *et al.*, 2012). A potential up-stream binding partner of SmPLK1 was SmSLK, a kinase of the Ste20 group shown to be linked to growth, apoptosis and morphogenesis in other systems, was also identified in schistosomes. In males, SmSLK was localized to the tegument and parenchyma of male worms (Yan *et al.*, 2007).

Another PK associated to spermatogenesis, sperm chemotaxis and motility in other organisms is the cGMP-dependent protein kinase (cGK) (Miraglia *et al.*, 2011; Teves *et al.*, 2009; Yuasa *et al.*, 2000). Evidence existed from a previous study on *S. mansoni* males that this kinase is differentially expressed between EM and UM (Schulze, 1997).

1.4.2. TGF β -pathway

For approximately 10 years now it was speculated that the transformin growth factor β (TGF β)-pathway may be important for the differentiation of the female as well as functions in the male (LoVerde *et al.*, 2009; Knobloch *et al.*, 2007; LoVerde *et al.*, 2007). In general, members of the TGF β -family can be categorized into two subclasses: (i) the TGF β /Activin/Nodal- associated class and (ii) the “bone morphogenic protein” (BMP) / “growth and differentiation factor” (GDF) associated class (Massague *et al.*, 2000). The first group acts via the receptor-regulated Smads (R-Smads) Smad2 and Smad3, the second one via the R-Smads Smad1, Smad5, and Smad8. Two types

of TGF β receptors (TGF β R) are distinguished, for each type several receptors are differentiated according to their ligand. The function of type II receptors is the binding to, and activation of type I receptors upon ligand binding. TGF β RI then phosphorylates and activates R-Smads, which form complexes with Co-Smads to translocate to the nucleus. Here, these Smad complexes regulate target gene transcription in conjunction with other transcription regulators (Massague *et al.*, 2000; Massague & Wotton, 2000; Massagué & Chen, 2000; Massagué, 2000).

Several members of the TGF β -pathway have been identified in *Schistosoma mansoni* (reviewed in: LoVerde *et al.*, 2007). The first molecule discovered was *S. mansoni* receptor kinase I (SmRKI) (Davies *et al.*, 1998), later renamed SmTGF β RI. A SmTGF β RII, for which three different transcripts were detected, could also be localized to the tegument and parenchyma cells of both males and females leading to the hypothesis that the SmTGF β Rs are interaction partners (Osman *et al.*, 2006; Forrester *et al.*, 2004). Transcription for both receptors is relatively constant throughout the life cycle. However, transcription of SmTGF β RII was always significantly higher than that of SmTGF β RI. SmFKBP12, an inhibitor of phosphorylation of the EGF-receptor and TGF β RI, was found to be expressed in the tegument (in males mainly in the dorsal area) and parenchyma of both genders as well as the female gonads (Knobloch *et al.*, 2004). By yeast two hybrid (Y2H) studies it was shown that SmFKBP12 interacted with SmTGF β RI, which was also localized to the female gonads (Knobloch *et al.*, 2004). Additionally, a calcineurin A homologous molecule was localized to the tegument and it was speculated that this molecule mediates the inhibition of SmTGF β RI by SmFKBP12 (Knobloch *et al.*, 2004).

Three R-Smads and one Co-Smad have been found in *S. mansoni* to date. The first two R-Smads identified were SmSmad1 and SmSmad2. Transcripts of both genes were detected in schistosomula and adult worms (Beall *et al.*, 2000). Interactions with SmTGF β RI were shown for each of the two molecules (Beall *et al.*, 2000) and confirmed for SmSmad2 by co-immunoprecipitation (Beall & Pearce, 2001). Subsequent studies found the transcript levels for SmSmad1 to be higher in mammalian-host stages than in eggs or sporocysts (Osman *et al.*, 2004). For SmSmad2 relatively constant transcript levels were found in schistosomula and couples of different ages as well as in UM and FM (Osman *et al.*, 2001). Compared to eggs and sporocysts, transcript levels were higher in mammalian host stages (Osman *et al.*, 2004). In couples, transcripts were localized to the subtegument and parenchyma as well as ovary, vitellarium, and uterus of the female. Smad2-protein detection correlated with transcript localization. By Y2H and pull-down experiments, the interaction and phosphorylation of Smad2 by SmTGF β RI were

1. Introduction

demonstrated. Additionally, SmSmad2 translocation to the nucleus following TGF β stimulation was demonstrated *in vitro* (Osman *et al.*, 2001). The last R-Smad identified in *S. mansoni* was SmSmad1b, which according to its transcript level and protein binding properties is similar to SmSmad1, and localizes to the subtegument and parenchyma of both sexes as well as to the female vitellarium and ootyp (Carlo *et al.*, 2007). Transcript levels for the Co-Smad SmSmad4 were relatively constant through all life stages (excluding cercariae and miracidia, which were not tested). The protein was localized to the tegument, vitelline cells, and the epithelium surrounding the gut. Interaction with SmSmad1 and SmSmad2 was demonstrated in a Y3H approach (Osman *et al.*, 2004). Additionally, indications were found with SmSmad2, which depends on phosphorylation of the latter molecule by SmTGF β RI. Furthermore, it was hypothesized that in the presence of SmTGF β RI SmSmad4 and SmSmad1 would not interact because of their preferred binding affinity to the receptor. Interestingly, the SmSmad4-sequence was found to contain three Erk1/2 phosphorylation motifs (Osman *et al.*, 2004), possibly indicating that SmSmad4 is a link between the TGF- β pathway and the mitogen activate protein kinase (MAPK)-pathway.

Activated Smad complexes translocate to the nucleus to interact with other co-regulators influencing gene expression (Osman *et al.*, 2001; Massague *et al.*, 2000; Massague & Wotton, 2000; Massagué & Chen, 2000; Massagué, 2000). In Search for co-regulators interacting with Smad complexes histone acetyltransferases (HATs), molecules with a function in chromatin remodeling and gene regulation, came into focus. In *S. mansoni* two HATs were identified: SmGCN5 (for *S. mansoni* 'general control nonrepressed'), (deMoraes *et al.*, 2013; de Moraes Maciel *et al.*, 2004) and SmCBP (*S. mansoni* CREB [cAMP response element-binding protein]-binding protein) (Bertin *et al.*, 2006). Both were shown to interact with SmSmads. While SmCBP showed equally strong interaction with SmSmad1 and SmSmad2, SmGCN5 showed stronger interaction with SmSmad1 or SmSmad1B compared to SmSmad2 (Carlo *et al.*, 2007). Furthermore, SmCBP was shown to interact with the nuclear receptor SmFTZ (*S. mansoni* fushi tarazu factor) (Bertin *et al.*, 2006). SmFTZ was detected in all *S. mansoni* life cycle stages. Its expression in adult male and female worms is of special interest for the male-female interaction, as FTZs are known for their participation in developmental processes, as well as sexual differentiation (De Mendonca *et al.*, 2002).

In addition to down-stream processes, ligands to schistosome TGF β Rs were sought. For a long time it was hypothesized that the TGF β -pathway was solely stimulated by host agonists until in 2007 the identification of a potential *Schistosoma* agonist was reported: SmlnAct, an ihinin/activin

like protein, was localized to the female reproductive tissue and male subtegument by *in situ* hybridization. Using western blot analyses it was shown that the protein is only expressed in paired worms and not in unisexual ones. Accordingly, the transcript level of SmInAct is reduced in unisexual males and females compared to their paired counterparts. Furthermore, knock-down of SmInAct in eggs via RNAi aborted their development (Freitas *et al.*, 2007). Later SmBMP was identified as another potential ligand of the TGF β -pathway, but belonging to a different subfamily of TGF β -associated molecules than SmInAct. The analysis of SmBMP was restricted to paired adults on the protein level, where SmBMP was detected in males and females, and to paired adults, eggs and cercariae at the transcript level, where it was detected in all these stages. Immunolocalization studies found SmBMP to the main tubules and branches of the protonephridia of males. Additional western blot analyses and immune-precipitation with culture supernatants of males revealed that SmBMP is secreted by the male (Freitas *et al.*, 2009).

The following signaling cascade was proposed by LoVerde *et al.* (2009; 2007): TGF β RII binds a TGF β /Activin or a BMP ligand, the receptor ligand complex then activates TGF β RI by phosphorylation, which again transduces the signals to R-Smad (Smad 1/2), which interacts with a Co-Smad (Smad4) translocating to the nucleus, where it regulates target gene transcription at the promoter via binding to a nuclear partner. Ultimately, the above signaling process was suggested to be a pathway essential for the male-female interaction.

1.5. Transcriptomics in schistosome research

With the start and continuance of the EST and genome projects for *S. mansoni*, *S. japonicum* and *S. haematobium* (Protasio *et al.*, 2012; Young *et al.*, 2012; Berriman *et al.*, 2009; *Schistosoma japonicum* Genome Sequencing and Functional Analysis Consortium *et al.*, 2009; Oliveira, 2007; LoVerde *et al.*, 2004; Verjovski-Almeida *et al.*, 2004; Hu *et al.*, 2003; Merrick *et al.*, 2003; Verjovski-Almeida *et al.*, 2003; Franco *et al.*, 2000) new possibilities became available to study these parasites. Microarrays and serial analysis of gene expression (SAGE), two transcriptome methods, could be applied to study the parasites. Microarrays are glass slides, which have cDNAs or oligonucleotides coupled to their surface (Causton *et al.*, 2003). SAGE is a restriction enzyme and sequencing-based method (Velculescu *et al.*, 1995), which has advanced over the years from creating short sequences (tags) of only 9 base pairs (bp) to variations that can create tags > 25 bp (Matsumura *et al.*, 2003). While microarrays can only detect transcripts represented by oligonucleotides bound to glass slides, SAGE is able to detect all mRNAs that contain the

1. Introduction

restriction site of a specific restriction enzyme. Several projects using these methods aimed at the identification of the *Schistosoma* transcriptome on a broad range including comparative analyses of the transcriptomes of different life-cycle stages including EM and UM.

Williams *et al.* (2007) compared paired adult males and females and their pairing-unexperienced counterparts as well as miracidia and sporocysts using a SAGE technique creating 21 pb tags. For EM and UM they found differential regulation for transcripts contributing to developmental processes, metabolism and the redox-system. Most studies used different schistosome-specific microarrays, beginning with cDNA-based arrays, which were later replaced by custom-designed oligonucleotide arrays. One of the first cDNA arrays used for *S. mansoni* was designed by the group of Hoffmann *et al.* (2002). In their first application they detected a tropomyosin, an actin and a dynein-light-chain to be male-specific; their transcription levels were much higher in males compared to females. Following this the same group had a larger oligonucleotide array custom-designed by Affimetrix, which containing 7,335 *S. mansoni* specific sequences. In the first study reported (Fitzpatrick *et al.*, 2005), RNA profiles of paired male and female worms were compared. A total of 197 were found to be differentially transcribed and 80 were enriched in males. Two later analyses (Waisberg *et al.*, 2007; Fitzpatrick & Hoffmann, 2006) using the same oligonucleotide array aimed to unravel differences between EM and UM. Interestingly, these two studies conducted by two different groups with the same goal, similar experimental layout, and using the same microarray already showed that data cannot necessarily be compared as both groups found dissimilar results. With regard to the expected differences between EM and UM, Fitzpatrick and Hoffmann (2006) found 30 highly expressed transcripts to be exclusive for EM, 66 for UM and concluded from their data that UM were transcriptionally more complex than EM. Waisberg *et al.* (2007) directly compared their results on highly expressed transcripts to those of Fitzpatrick and Hoffmann (2006) and found 13.3 % and no overlap for EM and UM data-sets, respectively. However, both studies postulated differences in the regulation of genes for RNA metabolism. Finally, a third microarray was designed (Fitzpatrick *et al.*, 2009) and used to study differences between life cycle stages. This resulted in the identification of several putative reference genes.

Apart from studies on *S. mansoni* several transcriptomic analyses have been performed with different *S. japonicum* strains. These studies however, did not compare EM and UM but investigated gender-associated genes (Moertel *et al.*, 2006; Fitzpatrick *et al.*, 2004). A more recent study compared different life cycle stages in *S. japonicum* (Gobert *et al.*, 2009a), but found only few genes to be enriched in UM. In 2009 Gobert and colleagues (Gobert *et al.*, 2009b) combined

microarray studies with laser microdissection. Unfortunately with regard to our study only female organs were analyzed.

Even with the past usage of large-scale transcriptomics, the question is still unanswered how males reach a status of competence and/or become able to initiate and maintain female sexual maturation.

1.6 Aims of the study

Male schistosomes are essential for female sexual maturation and thus ultimately for egg production, which causes the pathology of schistosomiasis. While the existence of a stimulus originating from the male and inducing developmental processes in the female was proposed, no conclusive evidence on the nature of such a stimulus was obtained so far (reviewed in chapter 1.2.). Since it was demonstrated that EM need less time than UM to induce stimulation of mitotic activity in females (Den Hollander & Erasmus, 1985), it was hypothesized that males have to reach a status of competence before they are able to influence the female. Thus it became of interest to study differences between EM and UM to reveal mechanisms leading to male competence and the production of a stimulus inducing female sexual maturation. Though previous studies have used microarrays and SAGE to approach this question (Waisberg *et al.*, 2007; Williams *et al.*, 2007; Fitzpatrick & Hoffmann, 2006), they provided no candidate genes encouraging more specific research concerning their involvement in these processes.

This study took on the still unanswered question, which yet unknown processes are responsible for the male maturation from UM to EM or are possibly involved in the production of a stimulus towards the female. First steps to answer this question included experiments on the effects of pairing or TNF α on male mitotic activity and a cGMP-dependent protein kinase previously reported to be differentially expressed between EM and UM (Schulze, 1997). Finally, a transcriptome analysis surmounting earlier efforts was conducted. To this end two methods, microarray and SuperSAGE, were applied and the detected transcripts annotated to the first version of the *S. mansoni* genome (Berriman *et al.*, 2009). The advantages of this approach compared to previous studies was i) the size of the microarray containing 39,342 *Schistosoma*-specific sequences representing all *S. mansoni* genes as estimated at the time of the microarrays construction, and ii) the use of SuperSAGE. Other microarrays contained only a maximum of 7,335 sequences (Fitzpatrick *et al.*, 2005), representing approximately 50 % of the estimated genes. Only one study previously used a SAGE technique, creating 21 pb tags, on schistosomes (Williams *et al.*,

1. Introduction

2007), compared to this study SuperSAGE with tags > 25 bp provides a technical advancement. Also, all earlier studies could only refer to EST projects or preliminary data of the genome project. By the combination of both methods the detection of all transcripts present in UM and EM was ensured, leading to the most complete data-set available to date. To narrow down the number of interesting genes bioinformatic tools were applied. Real-time PCR experiments were additionally used to confirm the results of microarray and SuperSAGE.

A number of genes of interest for further research were identified. Detailed experiments are needed to substantiate the role of chosen candidate genes in the development from UM to EM or possibly the nature of the stimulus important for female maturation. The discovery of genes related to these male processes is of importance for the understanding of the male-female interaction and may contribute to the discovery of new drug targets or vaccines. First characterization studies on one candidate gene were conducted.

2. Materials and methods

2.1. Materials

2.1.1. Buffers and solutions

All buffers and solutions were prepared with chemicals obtained from the companies Aldrich, Fluka, Merck, Roth, Serva and Sigma, and had p.A. quality.

Buffer or solution	Components	Application
AFA-Fixative	2 % acetic acid; 3 % formaldehyde; 70 % ethanol	fixation of <i>S. mansoni</i>
Blocking solution	4 % blocking reagent (Roche) in maleic acid buffer	<i>in situ</i> hybridization
Bouin-fixative (Sigma)	15 % saturated picric acid, 5 % formaldehyde; 1 % acetic acid; in DEPC-dH ₂ O	<i>in situ</i> hybridization
Denhardt's (100×)	2× SSC; 2 % ficoll; 2 % polyvinylpyrrolidon; 2 % BSA; in dH ₂ O; filtrated	<i>in situ</i> hybridization
H₂O_{DEPC}	0.1 % diethylpyrocarbonate in dH ₂ O; autoclaved	RNA-isolation; <i>in situ</i> hybridization
10 x DIG-rNTP Labeling Mix (Roche)	10 mM ATP, 10 mM CTP, 10 mM GTP, 6.5 mM UTP, 3.5 mM DIG-11-UTP, pH 7.5	<i>in situ</i> hybridization
DMSO	100% dimethyl sulfoxide	solvent
DNA-extraction buffer	20 mM Tris, 100 mM EDTA, pH 8.0	DNA-isolation
Ethidium bromide	0.5 µg/ml in TAE-buffer	nucleic acid staining
Fast Red TR	4-Chlor-2-methylbenzendiazonium (Sigma); 5 mg in 5 ml substrate buffer (see below)	<i>in situ</i> hybridization
Hybridization buffer	2.5 ml deionised formamide; 1.25 ml 20× SSC; 5 µl Tween 20; 50 µl 100× Denhardt's; 1 ml H ₂ O _{DEPC}	<i>in situ</i> hybridization
LiAc-solution (10×)	1 M LiAc; pH 7.5; autoclaved	yeast transformation
Maleic acid buffer	0.1 M maleic acid; 0.15 M NaCl; pH 7.5; in H ₂ O _{DEPC}	<i>in situ</i> hybridization
Maleic acid washing-buffer	0.3 % Tween 20 in maleic acid buffer	<i>in situ</i> hybridization
MOPS-buffer (10×)	200 mM morpholino propanesulfonic acid (MOPS); 50 mM sodium acetate; 10 mM EDTA; all in H ₂ O _{DEPC} ; pH 7.0; autoclaved	RNA gel- electrophoresis

2. Materials & Methods

Naphthol-AS-phosphate	C ₁₇ H ₁₃ ClNO ₅ P (Sigma); 1 mg in 20 µl DMSO	<i>in situ</i> hybridization
ONPG solution	ortho-Nitrophenyl-β-galactoside (ONPG); 4 mg/ml in Z-buffer	β-galactosidase liquid-assay
PBS (1x)	137 mM NaCl, 2.7 mM KCl, 1.5 mM KH ₂ PO ₄ , 6.5 mM Na ₂ HPO ₄ , pH 7.5	washing-buffer
PEG/LiAc-solution	40 % PEG 4000 in 1× TE- and 1× LiAc-solution	yeast transformation
PEG-solution	50 % PEG 3350 (Polyethylene glycol)	yeast transformation
PeqGold Trifast	guanidinisothiocyanat and phenol (Peqlab)	RNA isolation
Phenol	phenol (Roth)	nucleic acid extraction
Proteinase K	1 µg/ml in proteinase K buffer	<i>in situ</i> hybridization; nucleic acid extraction
Proteinase K buffer	100 mM Tris, 50 mM EDTA, pH 8.0	proteinase K reactions
RNA loading-buffer	95 % formamide, 0.025 % SDS, 0.025 % bromophenol blue, 0.025 % xylene cyanol FF, 0.025 % ethidium bromide, 0.5 mM EDTA (Fermentas)	RNA gel electrophoresis
10 x sample buffer (orange)	50 % sucrose, 0.6 % orange G in 1x TAE buffer	DNA gel- electrophoresis
Solution I	0.2 M Tris, pH 7.5	mitotic activity assay
Solution II	0.2 M Tris, 0.1 M sodium sulfate, pH 7.5	mitotic activity assay
SSC (20x)	3 M NaCl; 0.3 M Na ₃ -Citrat; pH 7.0	<i>in situ</i> hybridization
Substrate buffer	100 mM Tris/Cl; pH 8.0	<i>in situ</i> - hybridization
TAE-buffer (50x)	242 g Tris; 57.1 ml acetic acid; 100 ml 0.5 M EDTA; pH 8.0; dH ₂ O ad 1 l	DNA gel- electrophoresis
TE-buffer (10x)	0.1 M Tris-HCl; 10 mM EDTA; pH 7.5; autoclaved	yeast transformation
TESPA	3-amino-propyltriethoxysilan (Sigma)	glass slide siliconization

TFB1-buffer	12.1 g RbCl; 9.9 g MnCl ₂ · 4H ₂ O; 2.9 g potassium acetat; 1.1 g CaCl ₂ ; 50 ml glycerol; dH ₂ O ad 1 l; pH 5.8; sterile filtered	production of heat-shock competent cells
TFB2-buffer	2.1 g MOPS; 1.2 g RbCl; 8.3 g CaCl ₂ ; 150 ml glycerol; dH ₂ O ad 1 l; pH 6.8 (KOH); sterile filtered	production of heat-shock competent cells
Transcription buffer (10x) (Roche)	0.4 M Tris/Cl pH 8; 60 mM Mg ₂ Cl, 100 mM DTT, 20 mM spermidin	<i>in situ</i> hybridization
X-Gal stock solution	5-bromo-4-chloro-3-indolyl-β-D-galaktopyranosid (X-gal) in N,N-dimethyl-formamid (DMF); 20 mg/ml	β-galactosidase liquid-assay
Z-buffer/X-Gal-solution	100 ml Z-Puffer; 0.27 ml β-mercaptoethanol; 1.67 ml X-Gal stock solution	β-galactosidase liquid-assay
Z-buffer	16.1 g Na ₂ HPO ₄ · 7H ₂ O; 5.5 g NaH ₂ PO ₄ · H ₂ O; 0.75 g KCl; 0.246 g MgSO ₄ · 7H ₂ O; dH ₂ O ad 1 l; pH 7.0; autoclaved	β-galactosidase liquid-assay
Carmine red	500 mg carmine red (Certistain, Merck); 500 µl conc. HCl; 500 µl dH ₂ O; 90 % ethanol ad 20 ml	staining of <i>S. mansoni</i>

2.1.2. Media and additives

Media and additives	Components	Application
ABAM	antibiotic / antimycotic solution (Sigma)	<i>Schistosoma in vitro</i> -culture
Amino acids (Merck; Sigma)	adenin (20 mg/l), L-histidin (20 mg/l), L-leucin (100 mg/l), L-lysin (30 mg/l), L-methionin (20 mg/l), L-tryptophan (20 mg/l), uracil (20 mg/l);	additives to minimal SD-media and plates
Ampicillin (Sigma)	Ampicillin-trihydrat [D(-)-α-aminobenzyl-penicillin]; stock: 100 mg/ml in dH ₂ O; steril filtered; (final concentration: 100 µg/ml)	additive to LB-medium and –plates for growth selection
HEPES	1 M 2-[4-(2-hydroxyethyl)-1-piperazinyl]-ethan-sulfonic acid; pH 7.4; steril filtered	<i>Schistosoma in vitro</i> -culture
IPTG (Roth)	isopropylthiogalactosid; 0.1 M in dH ₂ O	blue-white selection

2. Materials & Methods

LB-agar	LB-Medium with 18 g/l agar-agar; autoclaved	<i>E. coli</i> -medium
LB-medium	10 g Bacto-Trypton; 5 g yeast extract; 5 g NaCl; ad 1 l with dH ₂ O; pH 7.5; autoclaved	<i>E. coli</i> -medium
NCS	newborn calf serum (Sigma-Aldrich)	<i>Schistosoma in vitro</i> -culture
Perfusion medium	1 % M199 powder; 2 % (v/v) 1 M Tris/HCl (pH 7.4); 0.1 % glucose; 1.25 % (v/v) M HEPES (pH 7.4) dH ₂ O ad 1000 ml before use: 10 mg/l heparin (197 U/mg, Serva)	hamster perfusion
M199-medium	M199 (Gibco); 1% HEPES; 1% ABAM; 10% NCS	<i>Schistosoma in vitro</i> -culture
Snail-solution 1	11 g CaCl ₂ ; 7 g MgCl ₂ ·6H ₂ O; dH ₂ O ad 200 ml	breeding and husbandry of <i>Biomphalaria glabrata</i>
Snail-solution 2	0.6 g K ₂ CO ₃ ; 4.6 g NaHCO ₃ ; dH ₂ O ad 200 ml	breeding and husbandry of <i>Biomphalaria glabrata</i>
Snail-solution 3	0.6 M NaOH	breeding and husbandry of <i>Biomphalaria glabrata</i>
Snail water	3 ml solution 1; 2 ml solution 2; 0.4 ml solution 3; dH ₂ O ad 1l	breeding and husbandry of <i>Biomphalaria glabrata</i>
SD-agar	SD-medium with 20 g/l agar; autoclaved; supplemented with 50 ml sterile 40 % glucose-solution (final 2% glucose)	minimal media yeast culture plates
SD-medium	6.7 g/l yeast nitrogen base; 950 ml dH ₂ O; autoclave supplemented with 50 ml sterile 40 % glucose-solution	liquid minimal yeast medium
X-Gal	stock: 2 % in dimethylformamide	blue-white selection
YPD-medium	20 g/l peptone; 10 g/l yeast extract; 950 ml dH ₂ O; autoclaved; supplemented with 50 ml sterile 40 % glucose-solution	liquid yeast full-medium
YPD-plates	YPD-medium with 20 g/l Agar; autoclaved; supplemented with 50 ml sterile 40 % glucose-solution	culture plates with yeast full-medium

YPDA-medium	YPD-Medium with 15 ml sterile 0.2 % adenine-hemisulfate-solution (final concentration: 0.003 %)	liquid yeast full-medium
Basch-medium	10 mg Basal Medium Eagle with Earle's Balanced Salt Solution; 1 g glucose; 2.4 g glucose; 1 g lacatalbumin; 2.2 g sodium bicarbonate; 5 ml hypoxanthine (1 mM); 1 ml serotonin (1 mM); 1 ml hydrocortisone (1 mM); 1 ml triiodothyronine (0.2 mM); 1 ml insulin (8 mg/ml); ad 1000 ml (pH 7.3 – 7.4). complemented with 50 ml Schneider's medium (1x); 5 ml MEM vitamins (100x) and re-adjust pH. added before use: ABAM (1:100)	<i>S. mansoni in vitro</i> -culture
SOC-medium	20 g tryptone, 5 g yeast-extract; 0.5 g NaCl; 10 ml KCl (250 mM); 5 ml MgCl ₂ (2 M) ; dH ₂ O ad 1 l; autoclaved and supplemented with 20 ml sterile glucose-solution (1 M)	<i>E. coli</i> - medium (after heat shock, during generation of competence)
Kanamycin	kanamycin-disulfate 25 mg/ml (in dH ₂ O) (final concentration 25 µg/ml)	additive to LB-medium and LB selection plates
SG-medium	6.7 g/l yeast nitrogen base (YNB, without amino acids); 20 g galactose; dH ₂ O ad 1 l; autoclaved	yeast liquid culture (minimal medium)

2.1.3. Enzymes

The following enzymes were used in this work:

Enzyme	Company	Details
DNase	Fermentas	RNase free
FirePol	Solis Biodyne	standard Taq-Polymerase
<i>Pfu</i>	Promega	DNA-Polymerase with proof reading activity
Proteinase K	Merck	cystein protease
Restriction enzymes	New England Biolabs, Fermentas	restriction endonucleases typ II
Standard reverse transcriptase	Qiagen	Quantitect (reverse transcription kit)
RNaseA	Sigma	DNase free

2. Materials & Methods

RNasin	Promega	RNase inhibitor
T4-DNA-Ligase	Fermentas	ligation of DNA
T7- and SP6 RNA-Polymerase	Roche	DNA dependent RNA-polymerases

2.1.4. Molecular weight standards

During gel electrophoresis the following molecular weight standards were used for determination of sizes and amounts of nucleic acids: HyperLadder I or II (Bioline) for DNA and RiboRuler RNA Ladder High Range (Fermentas) for RNA.

Sizes (and amounts) for HyperLadder I:

10,000 bp (100 ng); 8,000 bp (80 ng); 6,000 bp (60 ng); 5,000 bp (50 ng); 4,000 bp (40 ng); 3,000 bp (30 ng); 2,500 bp (25 ng); 2,000 bp (20 ng); 1,500 bp (15 ng); 1,000 bp (100 ng); 800 bp (80 ng); 600 bp (60 ng); 400 bp (40 ng); 200 bp (20 ng).

Sizes (and amounts) for HyperLadder II:

2,000 bp (50 ng); 1,800 bp (20 ng); 1,600 bp (20 ng); 1,400 bp (20 ng); 1,200 bp (20 ng); 1,000 bp (100 ng); 800 bp (30 ng); 700 bp (30 ng); 600 bp (30 ng); 500 bp (30 ng); 400 bp (30 ng); 300 bp (100 ng); 200 bp (40 ng); 100 bp (40 ng); 50 bp (40 ng).

Sizes (and amount) for Ribo Ruler RNA Ladder High Range:

6,000 bp; 4,000 bp; 3,000 bp; 2,000 bp; 1,500 bp; 1,000 bp; 500 bp; 200 bp; (all 120 ng).

2.1.5. Primers

Primers were commercially obtained from Biolegio or Sigma-Aldrich. The Sigma-Aldrich oligonucleotide design tool (http://www.sigmaaldrich.com/configurator/servlet/DesignTool?prod_type=STANDARD) was used routinely for calculation of annealing temperatures.

Sequences added to generate restriction enzyme sites are given in italics. Added bases (to ensure the correct reading frame in cloning procedures for yeast two-hybrid experiments) are marked in grey. Binding sites for the T7 DNA-dependent RNA-polymerase are underlined.

Primers for cGKI bear the name PKG in all primer lists. Annealing temperatures are given as they were used for the respective primer combination.

Primers for general applications:

Method	Primer name	Sequence [5'-3']	AT
Colony PCR	T7	GTAATACGACTCACTATAG	45 °C
	SP6	CATTTAGGTGACACTATAG	
Full-length sequencing	SmlnAct-5'	AATCTTGTTGTCATCCAACCTCAA	60 °C
	SmlnAct-3'	AACTACAAGCACATCCTAAAACAA	
cGKI-3' sequencing	PKG fwd 1	GGTTACATTAAATTATGCGAT	60 °C
	PKG ges R (3'utr)	GAGAGAAAGAGGGGGAAATGG	
cGKI-middle sequencing	PKG-fwd-01.09	ACCTCAACAGGCCATAGACG	60 °C
	PKG-3'-09.02	TTTTGACCAATTCCAATGTATTTAGC	
cGKI--5' sequencing	PKG ges F (5'utr)	TTACTGAAGACGATAGCGTTTGG	60 °C
	PKG-3' 01-09	TTTTATATTGGTTGCATTCTTGGT	
cGKI stage-specific transcription	PKG RNA F	GTTACATTAAATTATGCGATTT	60 °C
	PKG RNA R	CAATGGTCCATTCAATTTAACT	
Sexing-PCR	W1A	ACTGATGTGACAGGAATGAGG	65 °C
	W1B	GTGTGTTATTTGTGGTGGTCC	
	PDI-sexA-5'	TGGGGGTGAAAGAGACTCC	
	PDI-sexA-3'	ACTCCAGCGGTTTTCTGGG	

AT: annealing temperature

Primers for the generation of *in situ*-probes:

Primer name	Sequence [5'-3']	AT
Follistatin_insitu1_5'	GAACCAAAATGCAAATGTCG	60 °C
Follistatin_insitu1_3'	GCCATGATTGTTCAATCCA	
Follistatin_insitu1_T7-5'	<u>ATGTAATACGACTCACTATAGGAACCAAAATGCAAATGTCG</u>	60 °C
Follistatin_insitu1_T7-3'	<u>ATGTAATACGACTCACTATAGGCCATGATTGTTCAATCCA</u>	
Follistatin_insitu2_5'	GTGAATGTCGAAGCAAGGT	60 °C

2. Materials & Methods

Follistatin_insitu2_3'	TCCCATTTGATCCACAAAC	
Follistatin_insitu2_T7-5'	<u>ATGTAATACGACTCACTATAGGTGAATGTCTGAAGCAAGGT</u>	60 °C
Follistatin_insitu2_T7-3'	<u>ATGTAATACGACTCACTATAGTCCCATTTGATCCACAAAC</u>	
O/F-anti_in-situ_5'	CAAGTCAACATACCGCCTAAG	60 °C
O/F-anti_in-situ_3'	CAATCCAAATCGCAAACAG	
PKGI - PKG fwd 1	GGTTACATTAAATTATGCGAT	52 °C
PKGI - PKG rev	TCCTGATAATTCATCTGG	
PKGII - PKG 08-03-11 fwd	GCTGTTGGTCCTGGTGGTG	62 °C
PKGII - PKG 08-03-11 rev	AGGATAGTCCATAATTCACCGCC	
PKG_insitu-III	TCACAATCAATTAACAGTAG	50 °C
PKG_insitu-III	CTGAACTGCATCTAAATTCTTGATTAATC	
SmBMP_insitu-1-5'	GTCGTCATAATCGTGCAAG	55 °C
SmBMP_insitu-1-3'	TGGTACACAACACGGACC	
SmBMP_insitu-2-5'	TGAACGTCATATGAATGATTGG	60 °C
SmBMP_insitu-2-3'	AAAAATGGCTGCGGTTTG	
SmInAct_insitu-5'	TGATCCAAAAAAGGTTGTTATGG	60 °C
SmInAct-T7-3'	<u>GTAATACGACTCACTATAGGGA</u> ACTACAAGCACATCCTAAAACAA	
SmInAct_insitu-T7-5'	<u>GTAATACGACTCACTATAGGGT</u> GATCCAAAAAAGGTTGTTATGG	60 °C
SmInAct-3'	AACTACAAGCACATCCTAAAACAA	

AT: annealing temperature

Primers for yeast two-hybrid analyses:

Primer name	Sequence [5'-3']	AT
follistatin_y2h_5'	GAATTCATGGAAGAGAGTATATCACAAATTAG	60 °C
follistatin_y2h_3'	GTCGACTTAGAATAAATTTGAATATTTTCC	
SmInAct-Y2H-5'	CCCGGGGATGAATAGAATGTTTAAATTAATAAAA	60 °C
SmInAct-Y2H-3'	CTCGAGTTAACTACAAGCACATCCTAAA	

SmInAct:mu1-s	GTTGTTGTACACAAGCATTATCTGTAAATTTTCTGATATTGGTTGGG	55 °C
SmInAct:mu1-as	TCCCAACCAATATCAGAAAATTTAACAGATAATGCTTGTGTACAACAAC	
SmBMP-Y2H-Cterm-5'	CCCGGGGAAACCAAGATCAATTAATTATCCTAAC	57 °C
SmBMP-Y2H-Cterm-3'	CTCGAGTTAACGACAAGCACAACCTTC	
SmBMP-Y2H-ncbi-5'	CCCGGGGATGAACTCAAATATTTTAACAAAATCAG	57 °C
SmBMP-Y2H-db-Nterm-3'	CTCGAGAATTGCTTACATTATTATTATTCAGAGG	
SmBMP-Y2H-ncbi-Nterm-5'	CCCGGGGATGGAAACAGAAAAGACAAAAC	57 °C
SmBMP-Y2H-ncbi-Nterm-3'	CTCGAGGTTCTTTAGATGGTTTTTCGTATATTATC	
SmBMP-Y2H-overlap-5'	CCCGGGTGAAATAAATAGTACATCATTCTACTGG	57 °C
SmBMP-Y2H-overlap-3'	CTCGAGGATGATTATTTGTTTGTAATACATTTG	
Gal4AD-5'	CTATTCGATGATGAAGATACCCC	60 °C
Gla4AD-3'	CGGGGTTTTTCAGTATCTACGA	

AT: annealing temperature

Primers for real-time PCR:

Primer name	Sequence [5'-3']	Fin. c.	AT	E
Actin_q2-5'	GGAAGTTCAAGCCCTTGTGG	400 nM	60 °C	95 %
Actin_q2-3'	TCATCACCGACGTAGCTGTC			
GAPDH	ATCTGGACCATTGAAGGGGATT	400 nM	60 °C	93 %
GAPDH	AGATCAACTACGCGGCAACTGT			
Gobert	CTTCCAAAATGGCCGTGA	400 nM	60 °C	97 %
Gobert	TGGTGAGGAAACTCGGAGAC			
G10_q2b-5'	CGTAAAGTTGAGGCTGAGTGG	400 nM	60 °C	95 %
G10_q2-3'	CATTTGGCGATTAGATTTGC			
Nip7_q1-5'	TGAACAGACCAGACGACAAG	400 nM	60 °C	89 %
Nip7_q1-3'	TGAGAAGCGACCGATACAAG			

2. Materials & Methods

PKG_q2	CGTCGACAAATACGTGAAGC			
		300 nM	60 °C	87 %
PKG_q2	ACAAATGTCCACCATCATCG			
Proteasome-beta_q1-5'	GGTCTGGTGGTTTCTCGTTC			
		400 nM	60 °C	94 %
Proteasome-beta_q1-3'	GTACCTTCTGTTGCCCGTG			
Smp_030730(tubulin)_q1-5'	AGCTGGTCAATGCGGTAAC			
		400 nM	60 °C	96 %
Smp_030730(tubulin)_q1-3'	CACCGGATGCTTCATTGTAG			
Smp_000270-fs800-F	CAGCCGAAAAAGTCAAACA			
		600 nM	60 °C	93 %
Smp_000270-fs800-R	CCCTTTTGCATCGTAAGCT			
Smp_000430-F	CCGTAAAGGTGGTGGC			
		500 nM	60 °C	96 %
Smp_000430-R	TTGAATGTTGAATAGCCTTGC			
Smp_002890_q55b-5'	CATCGCACATCAAGACAGTA			
		600 nM	60 °C	110 %
Smp_002890_q55b-3'	TACGTTCACTGGTTGACAGA			
Smp_011100-insulinase_q2-5'	GAAATACAGACTTTATGGGAACTAGG			
		600 nM	60° C	87 %
Smp_011100-insulinase_q2-3'	TCGGGATTAAGAGAAGTCAAAA			
Smp_014610-p48-F	GACAAGCATGGTCATGGA			
		700 nM	60 °C	96 %
Smp_014610-p48-R	ATGCTTATCGTGGTCTTTACG			
Smp_020540_q2-5'	GCGAAACCGGTTACTGATAC			
		600nM	60 °C	87 %
Smp_020540	TGGATTTTTGCCAGGATTT			
Smp_024290-MAPK_q2-5'	TCATTATCGAATGAATTTGGTTC			
		600 nM	60 °C	87 %
Smp_024290-MAPK_q2-3'	TCCATGGAAATGTGGAGTC			
Smp_024860-hes_q1-5'	CGGAAAGAAAACGACGTG			
		600 nM	60°C	94 %
Smp_024860-hes_q1-3'	TGTTGCTGGGAATAAGACG			
Smp_025370_TF_q2-5'	CGATTCACATTTTGCTCCT			
		900 nM	60 °C	91 %
Smp_025370_TF_q2-3'	AGACAGCAACCGAATATTCC			
Smp_033950-Smad4-f	CCTTCTGGGTCCATACTCC			
		500 nM	60 °C	93 %

Smp_033950-Smad4-r	CCGTGTAACCGTCAACAGTG			
Smp_036470-of_q2-5'	GGTAGGATTATGTGGGGTGC			
Smp_036470-of_q2-3'	TCGCGTATGCAGCTTTAAG	400 nM	60 °C	92 %
Smp_049760-TGFβR1-F	ATGATCTCACGTGTGCGA			
Smp_049760-TGFβR1-R	GATCCGAAGGGCTGTCTT	700 nM	60 °C	91 %
Smp_050520-notch_q1-5'	TGTAATCGTGGCAGCTATGG			
Smp_050520-notch_q1-3'	TAGGGCCACACGGAGTTAAT	400 nM	60 °C	100 %
Smp_053120_q1-5'	CACAACGAAGTCGACATTTTC			
Smp_053120_q1-3'	GGCTGAACGACTTCTTGGGA	600 nM	60 °C	96 %
Smp_060160-F	GGTGTCTGATGGCTGAAG			
Smp_060160-R	CGTCATCCGAGAGCTCA	600 nM	60 °C	104 %
Smp_063190-SmInAct_q1b-5'	CACAATTTGGTAATGTTCAACG			
Smp_063190-SmInAct_q1-3'	AACTACAAGCACATCCTAAAACAA	800 nM	60 °C	91 %
Smp_077310-tegP_q1-5'	CTCGTTTTTGACGCTTTT			
Smp_077310-tegP_q1-3'	CACCAGTTTTCTCAGCATCA	600 nM	60 °C	96 %
Smp_094190-CAMKL_q1-5'	AAACGTTCTGGTCGATTGG			
Smp_094190-CAMKL_q1-3'	TTGGAAAAGCCGAAATCAC	600 nM	60 °C	95 %
Smp_105200_glypican_q4-5'	TGTAATGGTCGAATAACCTGG			
Smp_105200_glypican_q4-3'	ATCCAACCTCTCATTTGTCG	1 μM	60 °C	92 %
Smp_123300_follistatin-q1-5'	TGTTGTAAACGTGGTGGATTC			
Smp_123300_follistatin-q1-3'	CGACATTTGCATTTTGGTTC	350 nM	60 °C	92 %
Smp_126530-ets_q2-5'	TGGATGCAGATCATTTTGATG			
Smp_126530-ets_q2-3'	AGTTGCCATCATTGTTGTCG	600 nM	60 °C	89 %
Smp_130690_ZFP_q2-5'	TGTGGTTGGACATGGAGAG			
Smp_130690_ZFP_q2-3'	TCCAGGACCAAGTCGATG	600 nM	60 °C	97 %

2. Materials & Methods

Smp_131110-p14-F	CCTATGGCGGTGATTATGG			
Smp_131110-p14-R	GGCTGGGTTTGTAAAGTGC	800 nM	60 °C	96 %
Smp_133660_lin9_q1-5'	TGTTGCAACATGTTCAACCAC			
Smp_133660_lin9_q1-3'	AGTTGACCAATGAGCTCGAC	600 nM	60 °C	97 %
Smp_135020-of_q2-5'	GATTGGGCTCCCTAATTTTTAC			
Smp_135020-of_q2-3'	GCCAATATTGAACCCATCAC	600 nM	60 °C	97 %
Smp_135520-dock-q2-5'	CGTTTGCCACGAGAACTT			
Smp_135520-dock_q2-3'	GATGAACCTATTCGAGCGAG	600 nM	60 °C	101 %
Smp_139190_q4-5'	ATCCACAATTATCGCTTCTCA			
Smp_139190_q4-3'	TAAATTCCATAATGTTCCGCA	600 nM	60 °C	87 %
Smp_141410_q5-5'	ATCGTACAAGCCCATAATGG			
Smp_141410_q5-3'	GGCCAATGAGCCAATATTC	800 nM	60 °C	89 %
Smp_143350-elong_q2-5'	TATCCCACTTCGGCCTTC			
Smp_143350-elong_q2-3'	CGATGAACGGTTTTGTTTTG	600 nM	60 °C	102 %
Smp_144390-TGFβR2-F	GGCAGAAAATTCACCCA			
Smp_144390-TGFβR2-F	GGGGCCTGATATCGTAAAG	600 nM	60 °C	88 %
Smp_145150_wnt_q2-5'	AGCTCGACGTAGTCTTGTTCC			
Smp_145150_wnt_q2-3'	ATGGTGTTTCTGGATCATGC	400 nM	60 °C	98 %
Smp_146790_SmBMP_q51-5'	GTCAAAATGAACAAAATCA			
Smp_146790_SmBMP_q51-3'	GTTACGTGGAACACTTTG	600 nM	51 °C	94 %
Smp_152580-MEG5_q1-5'	GCTAGTGGAAGACAACCAAAG			
Smp_152580-MEG5_q1-3'	ATGGTAACCCCAATGATTG	1 μM	60 °C	85 %
Smp_155340-frizzled-5'	ATATGGCAGCATCAATTTGG			
Smp_155340-frizzled-3'	GGCTGTTTGACTTGCTGG	1 μM	60 °C	99 %
Smp_157540_q1-5'	TGTTGTCAAAGTCCCACCA	600 nM	60 °C	95 %

Smp_157540_q1-3'	CTGCTCCCCAACCTTTTAC			
Smp_157750-musashi-5'	ATCGTCGTAGCCTCAAGGT	600 nM	60 °C	96 %
Smp_157750-musashi-3'	GCAAAGCCTCTATGACGTG			
Smp158480_AMPlig_q3b-5'	ACTGCATCAATACCAATTAGAGTTTG	400 nM	60°C	87%
Smp158480_AMPlig_q3-3	GCCACTCTAGGCGATTGAAC			
Smp_161500_q2_GPCR-5'	CCAAACATGAATGCAACTGAA	600 nM	60 °C	99 %
Smp_161500_q2_GPCR-3'	CGTTGACGAAAATTACATCCAG			
Smp_161890(innexin)_q55-5'	AATTCGGCAATATGTTG	600 nM	55 °C	96 %
Smp_161890(innexin)_q55-3'	GCTGGAGGTAAACTGTG			
Smp_169190-tegP_q3-5'	GGCAAGCACTATTCGATCC	600 nM	60 °C	92 %
Smp_169190-tegP_q3-3'	CAGGTCGTAGACCCGTTG			
Smp_170020-GPCR_q3-5'	TGCGGATTAAAGAAAAGAAAC	600 nM	60 °C	98 %
Smp_170020-GPCR_q3-3'	TGGTTGTATGTTTCAGGCATA			
Smp_172600_hedgehog_q1-5'	TTAGAAGCAAGCGGACCAT	400 nM	60 °C	93 %
Smp_172600_hedgehog_q1-3'	TTGCCCATGTATTATGTATCTGTG			
Smp_175160-PAK-5'	GGAAATGCTAGAAGGTGAACC	600 nM	60 °C	99 %
Smp_175160-PAK-3'	GCACGAGATTGAGCATCC			
Smp_176350-contactin_q2-5'	AACGTTAGTTGGGCTGTTGG	600 nM	60 °C	98 %
Smp_176350-contactin_q2-3'	CAGCTAAATTGCGAACGACA			
Smp_177050-GCP-F	AATGTTCCACCCGACTTC	600 nM	60 °C	93 %
Smp_177050-GCP-R	CCAACCATTATCCGTGG			
Smp_194740(GPCR)_q55-5'	CAGTACAAGTGATATTTATCTATTAATC	600 nM	55 °C	85 %
Smp_194740(GPCR)_q55-3'	AACAATAGGACATTAATGATGTAC			
Smp_195010-HMG-CoA_q2-5'	CAGGCGTATAAATCTTGACCTG	600 nM	60 °C	102 %
Smp_195010-HMG-CoA_q2-3'	TTGTATCCGTCCCTTCGAC			

AT: annealing temperature, E: efficiency, Fin. c.: final concentration

2. Materials & Methods

2.1.6. Plasmids

The following commercially available vectors were used for standard cloning procedures:

Name	Description	Supplier
pDrive	Standard cloning vector	Qiagen
pBridge	Yeast two-hybrid Gal4-BD vector	Clontech
pACT2	Yeast two-hybrid Gal4-AD vector	Clontech

Based on these vectors, the following plasmid-constructs were generated:

Name	Description		c.n.
Follistatin-Y2H	vector: pBridge	insert: full-length follistatin	1371
Follistatin_in_situ-1	vector: pDrive	insert: bp 208 - 778	-
Follistatin_in_situ-2	vector: pDrive	insert: bp 914 - 1219	-
O-F-anti_in_situ	vector: pDrive	insert: bp 106 - 685	1372
PKG-3'	vector: pDrive	insert: bp 2572 - +405	1303
PKG-middle	vector: pDrive	insert: bp 402 - 2627	1307
PKG-5'	vector: pDrive	insert: bp -129 - 529	1304
PKG_in_situ-1	vector: pDrive	insert: bp 2572 - 3087	1160
PKG_in_situ-2	vector: pDrive	insert: bp 1852 - 2435	1161
PKG_in_situ-3	vector: pDrive	insert: bp 658 - 1254	1162
SmBMP-C-term	vector: pACT2	insert: bp 1981 - 2793	1373
SmBMP-middle	vector: pACT2	insert: bp 778 - 2082	1374
SmBMP-overlap	vector: pACT2	insert: bp 1505 – 2469	1375
SmBMP-N-term	vector: pACT2	insert: bp 1 - 999	1376
SmBMP_in_situ-1	vector: pDrive	insert: bp 2240 - 2694	1377
SmBMP_in_situ-2	vector: pDrive	insert: bp 1041 - 1605	1378
SmInAct-Y2H	vector: pACT2	insert: full-length SmInAct	1379

c.n.: clone numbers according to the AG-Grevelding clone-book; bp: base pair

2.1.7. Bacteria and yeasts

Heat shock-competent *E. coli* cells were used for standard cloning procedures:

NEB 10-beta: (New England Biolabs, 2008)

[*araD139*, Δ (*ara-leu*)7697, *fhuA*, *lacX74*, *galK* (Φ 80 Δ (*lacZ*) M15), *mrcA*, *galU*, *recA1*, *endA1*, *nupG*, *rpsL*(Str^R), Δ (*mrr-hsdRMS-mcrBC*)

DH5 α : (Hanahan, 1983)

[F⁻, *endA1*, *hsdR17* (*r_k⁻*, *m_k⁺*), *supE44*, *thi-1*, λ ⁻, *recA1*, *gyrA96*, *relA1*, Δ (*argF-lacZYA*), U196, Φ 80d, *lacZ* Δ M15]

The following yeast strain was employed:

AH109: MATa, *trp1-901*, *leu2-3, 112*, *ura3-52*, *his3-200*, *gal4 Δ* , *gal80 Δ* ,

LYS2::*Gal1 UAS - Gal1 TATA -HIS3*, MEL1, GAL2 UAS -GAL2 TATA -ADE2,

URA3::*MEL1 UAS -MEL1 TATA -lacZ* (James *et al.*, 1996)

2.1.8. Antibodies

During *in situ* hybridization, a digoxigenin labeled (fab-fragment) antibody coupled to alkaline phosphatase (Roche) was used. An anti-BrdU (Sigma) primary antibody and a sheep anti-mouse Ig (Amersham International, UK) secondary antibody, coupled to horseradish peroxidase, were used for determination of mitotic activity.

2.1.9. Databases and online software-tools

Database / software-tool	Special use	Internet address
SchistoDB ¹ – <i>Schistosoma mansoni</i> database	homology searches	http://beta.schistodb.net/schistodb25/
GeneDB ²	homology searches	http://www.genedb.org/Homepage/Smansoni
PubMed - U.S. National Library of Medicine National Institutes of Health	homology searches	http://www.ncbi.nlm.nih.gov/pubmed/
NCBI – national center for biotechnology information	homology searches	http://www.ncbi.nlm.nih.gov/
NCBI-blast	blast analyses	http://blast.ncbi.nlm.nih.gov/Blast.cgi

2. Materials & Methods

The sequence manipulation site	reverse complement	http://www.bioinformatics.org/sms/
ExPASy Proteomics server	translation of nucleic acid sequences into amino acid sequences	http://us.expasy.org/tools/dna.html
NPS@ - network protein sequence @nalysis	multiple alignments	http://npsa-pbil.ibcp.fr/cgi-bin/npsa_automat.pl?page=/NPSA/npsa_server.html
SMART – simple modular architecture research tool⁴	domain prediction	http://smart.embl-heidelberg.de/smart/set_mode.cgi?NORMAL=1
RestrictionMapper	restriction site finder	http://www.restrictionmapper.org/
ImageJ – Image Processing and Analysis in Java	densitometric analyses	http://rsbweb.nih.gov/ij/
R - The R Project for Statistical Computing	analysis of transcriptome data	http://www.r-project.org/
Primer3Plus	primer design	http://www.bioinformatics.nl/cgi-bin/primer3plus/primer3plus.cgi
Oligo Calc - Oligonucleotide Properties Calculator	primer design	http://www.basic.northwestern.edu/biotools/oligocalc.html
OligoAnalyzer 3.1	primer design	http://eu.idtdna.com/analyzer/Applications/OligoAnalyzer/Default.aspx
Sigma-Aldrich oligo design tool	primer design	http://www.sigmaaldrich.com/configurator/servlet/DesignTool?prod_type=STANDARD

¹Zerlotini *et al.* (2009), ²Hertz-Fowler *et al.* (2004), ³Berrimen *et al.* (2009), ⁴Schultz *et al.* (1998) & Letunic *et al.* (2012)

2.1.10. Sequencing

All sequencing was done commercially by LGC Genomics (Berlin) applying classical SANGER sequencing (Sanger *et al.*, 1977).

2. 2. Methods

2.2.1. *Schistosoma mansoni* laboratory cycle

For maintenance of the parasite life cycle under laboratory conditions, *Biomphalaria glabrata* snails were used as intermediate hosts, and Syrian hamsters (*Mesocricetus auratus*) as final hosts. The laboratory-strain of *S. mansoni* originates from a Liberian isolate obtained from Bayer AG, Monheim (Grevelding, 1995).

2.2.1.1. Infection of hamsters

Six to eight weeks old hamsters were obtained from the institute's own breeding facility or from Janvier. To soften the skin, hamsters were bathed in warm snail-water (see media and additives) without cercariae for 45 to 60 min previous to infection. Each hamster was exposed to 1,500 – 2,000 cercariae for 45 min (Dettman *et al.*, 1989). For infection, cercariae were added to the water in which hamsters were already bathing.

2.2.1.2. Hamster perfusion and *Schistosoma in vitro* culture

Hamsters were perfused seven weeks p.i. to obtain adult schistosomes. They were first anesthetized with isoflurane in a glass chamber and then euthanized using an overdose (2.5 - 3 ml) of anesthetic and muscle relaxant (Xylarium 3.1 %, Ketamine 0.19 %, in 0.9 % NaCl). Before abdomen and thorax were opened to expose intestines and heart, hamsters were sprayed with 70 % ethanol for semi-sterilization to counteract possible contaminations in the following *in vitro* culture of the recovered worms.

For perfusion (modified after: Duvall & DeWitt, 1967; Smithers & Terry, 1965), hamsters were fixed vertically on their right extremities. The portal vein was opened with a canula, connected to a flexible tube and filled with 37 °C warm perfusion medium from a 1 l flask. The canula was subsequently used to penetrate into the left heart chamber to pump perfusion medium through the vein system, flushing the worms out of the portal vein system. Worms were collected in a net beneath the hamster and transferred to a petri dish with a paint brush. If worms had already migrated to the mesenteric vein system, they were extracted by opening the veins separately.

Following perfusion, worms were transferred to culture-medium and kept at 37 °C and 5 % CO₂. Alternatively, worms were washed in 1x phosphate buffered saline (PBS) and frozen at -80 °C, either directly for protein or DNA extraction or, after an over-night treatment with RNeasy Lysis Buffer (Qiagen), for RNA extraction.

2.2.1.3. Snails

Maintenance

Snails were kept in aerated snail-water at 26 °C and a day-night rhythm of 16/8 h. They were fed every second day with cucumber slices and once a week with frozen spinach.

Infection

Snail-infection was done overnight in 12-well microtiter-plates containing 2 ml snail-water per well. Snails were placed separately into single wells and exposed to 10 - 15 miracidia each for polymiracidial infections, or one miracidium only for monomiracidial infection. Subsequently, snails were placed back into larger aquaria, which were shaded three weeks after infection to prevent early egression of cercariae, which regularly took place five weeks after polymiracidial infection or ten weeks after monomiracidial infection.

2.2.1.4. Obtaining *Schistosoma* larval stages

Miracidia

Miracida hatched from eggs extracted from livers of infected hamsters. To obtain the eggs, livers were cut into pieces and homogenized in 1x PBS. Following a 10 min centrifugation step at 400 g and 4 °C, the supernatant was discarded and the pellet resuspended in 0.9 % NaCl. This washing step was repeated twice. After the last repetition, the pellet was resuspended in 25 ml warm snail-water and collected in a 500 ml volumetric flask. Subsequently, the flask was filled with water to the brim, the main body of the flask was shaded and the upper two centimeters of the neck were exposed to bright light. Phototactically induced, the miracidia hatched from eggs in the liver homogenate and accumulated in the light-exposed area of the flask, from which they were harvested with Pasteur pipettes.

Cercariae

Five weeks after polymiracidial snail-infection or ten weeks after monomiracidial snail-infection, the snails were transferred to 12-well microtiter-plates containing snail-water. Exposure to a light-source resulted in migration of the cercariae through the snail skin within hours. Cercariae originating from monomiracidial snail-infections were collected separately and tested for their gender in a specialized PCR-reaction (2.2.4.3). They were used to generate unisexual (pairing-unexperienced) worm-populations. After determination of the titer, cercariae were used for infection.

2.2.2. Isolation of nucleic acids

2.2.2.1. Isolation of RNA from *Schistosoma mansoni*

Material used for RNA extraction had been previously treated with RNAlater (Ambion) to increase nucleic acid stability. Batches of 50 - 100 worms were supplemented with 100 μ l Trifast (Peqlab) and crushed with a sterile mortar (three times 15 s) at room temperature (RTC). Subsequently, more Trifast was added to reach a total volume of 1 ml. Thereafter, the suspension was incubated at RTC for 5 min to allow dissociation of nucleic acid-protein complexes. In a further step, 200 μ l chloroform were added, samples shaken thoroughly for 15 s and incubated at RTC for 3 - 10 min to induce phase separation. The different phases were separated through centrifugation for 5 min at 12,000 g and RTC in a table top centrifuge. Subsequently, the upper phase was transferred to another tube and supplemented with 500 μ l isopropanole, mixed and incubated 5 - 15 min on ice to induce precipitation. The precipitate was pelletized at 12,000 g and 4 °C for 10 min. The pellet was washed once with 75 % ethanol_{DEPC} and the centrifugation step repeated. RNA was dried at RTC and resuspended in 20 – 40 μ l H₂O_{DEPC}.

2.2.2.2. Isolation of DNA from *S. mansoni*

Worms were amended with 100 μ l extraction buffer and crushed with a sterile mortar (approximately three times for 15 s each). Subsequently, more extraction buffer was added to a final volume of 675 μ l and supplemented with 75 μ l 10 % SDS and 18.75 μ l 20 mg/ml proteinase K. The homogenate was incubated at 37 °C overnight.

A phenol/chloroform purification was performed the following day. Half a volume phenol was added to the now clear homogenate, vortexed vigorously and centrifuged in a table centrifuge at full speed for 5 min. The upper phase was transferred to a new tube and 1 vol phenol:chloroform (1:1) was added. The mixture was again vortexed, centrifuged and the upper phase transferred to a new tube. Chloroform ($\frac{1}{2}$ vol) was added and vortexing as well as centrifugation were performed as above.

The resulting upper phase containing DNA was transferred to a new tube and subjected to ethanol precipitation. Ammonium acetate (7.5 M, $\frac{1}{2}$ vol) and ethanol (96 %, cold, 2.5 vol) were added and the mixture incubated overnight at -20 °C. The following day, the sample was centrifuged for 40 min at 4 °C in a table centrifuge at maximum speed. The supernatant was discarded and the pellet washed with 1 ml 70 % ethanol followed by a 20 min centrifugation step as above. Again, the supernatant was discarded and the pellet left to dry for at least 30 min at RTC. The pellet was resuspended in 40 μ l dH₂O.

2.2.2.3. Isolation of plasmid DNA from bacteria

Plasmid DNA was isolated from bacteria using the „peqGOLD Plasmid Miniprep Kit I“ (PeqLab) according to the manufacturer’s protocol. The kit combines alkaline lysis, reversible binding of DNA to silica-membranes and column centrifugation.

2.2.2.4. Determination of nucleic acid concentration

Concentrations of DNA or RNA were determined using a spectral photometer (Eppendorf) or by measuring the optical density in comparison to a molecular weight standard following gel electrophoresis.

The photometer measures the concentration of RNA at a wavelength of 260 nm, the absorption maximum of nucleic acids. Purity of the sample can be determined through the extinction ratio of wavelengths 260 nm and 280 nm (absorption maximum of proteins) (E₂₆₀/E₂₈₀), which should be between 1.8 and 2.0. Lower values indicate a contamination with proteins. The determination of the nucleic acid concentration is based on the Beer-Lambert law:

$$(1) \quad c = E \times \epsilon^{-1} \times d^{-1}$$

with c: nucleic acid concentration, E: extinction, ϵ : specific extinction coefficient, d: width of cuvette.

With a width $d = 1$ cm and a wavelength $\lambda = 260$ nm, the following values can be assumed for ϵ : $1 \text{ OD}_{260} = 50 \text{ } \mu\text{g/ml}$ for double stranded DNA and $1 \text{ OD}_{260} = 40 \text{ } \mu\text{g/ml}$ for single stranded DNA or RNA.

The concentration of double stranded DNA is thus calculated with the formula:

$$(2) \quad c \left[\frac{\mu\text{g}}{\text{ml}} \right] = \text{OD}_{260} \times 50 \left[\frac{\mu\text{g}}{\text{ml}} \right] \times \text{dilution-factor}$$

Estimation of nucleic acid concentration via gel electrophoresis was done relative to a standard with known concentration. Standard and sample were separated by gel electrophoresis in an ethidium bromide stained agarose gel. The fluorescence signal of ethidium bromide (312 nm), intercalated into nucleic acids, was measured and values for sample and standard comparatively analyzed. Densitometry analyses were performed with the software ImageJ (Rasband, 2012; Schneider *et al.*, 2012; Abràmoff *et al.*, 2004).

2.2.3. Gel electrophoresis of nucleic acids

During gel electrophoresis, nucleic acids are separated according to size in agarose gels (Sambrook *et al.*, 1989). Due to the negatively charged sugar phosphate backbone, nucleic acids move towards the anode in an electric field. Movement through a gel matrix (usually agarose gels)

depends on conformation and molecular weight. Thus small nucleic acids move faster through the pores of the gel matrix than larger molecules, leading to size dependent separation.

2.2.3.1. DNA

In this thesis 1 - 2 % horizontal agarose gels, applicable to separate DNA fragments from 100 bp to 60 kb, were used. Gels were generated by dissolving the appropriate amount of agarose in TAE-buffer and this solution was supplemented with 0.5 µg/ml ethidium bromide. Electrophoresis was performed in TAE-buffer, also supplemented with ethidium bromide (0.5 µg/ml). Ethidium bromide intercalates into the DNA allowing detection by UV-light (312 nm).

Samples for DNA gel-electrophoresis were supplemented with a blue marker (Bioline) or an orange marker (self made, see 2.1.1.). The blue marker contained glycerol, which increases the density of the sample and facilitates pipetting into gel pockets. Additionally, these markers served as indicators for DNA movement during gel electrophoresis. For size determination of DNA, appropriate size standards were also separated on each gel (2.1.4.). Gel electrophoresis was performed at 90 - 170 Volt and maximal Ampere.

2.2.3.2. RNA

For separation of RNA, denaturing formaldehyde agarose-gels were used. Formaldehyde reduces secondary structures formed by single stranded RNAs. This ensures that movement of RNAs in the gel correlates with their actual size.

Gels contained 1.2 % agarose, 10 % MOPS-buffer (10x) and 16.6 % of a 37 % formaldehyde solution (which was added after dissolving the agarose and cooling the solution to approximately 50 °C).

RNAs were supplemented with a formamide and ethidium bromide-containing sample-buffer. To denature RNA secondary structures, the mixture was heated to 95 °C before gel electrophoresis. Remaining, weak secondary structures allow the intercalation of ethidium bromide and thus the fluorescence detection of RNAs by excitation with UV light (312 nm).

2.2.4.2. Gel-elution

To elute DNA from excised agarose-gel pieces, two different kits were used depending on the subsequent procedures. If DNA fragments were intended for cloning, gel extraction was performed applying the "GeneJet Gel extraction Kit" (Fermentas). The „peqGOLD Gel Extraction Kit" (PeqLab) was used to purify DNA subsequently employed as template for real-time PCR standard-curves. Each kit was used according to the manufacturer's protocols.

2.2.4. Polymerase chain reactions

The polymerase chain reaction (PCR) is a method employed to amplify specific DNA sequences (White *et al.*, 1989; Mullis *et al.*, 1986). PCR-reactions contain template DNA, two oligonucleotide primers, a thermostable DNA-polymerase, buffer and nucleotides. In a first step, the samples are heated to 95 °C to denature DNA into single strands. In a second step, the reaction is cooled down to a specific temperature at which primers anneal to their complementary DNA sequences, thus forming a starting position for DNA polymerization. The primers-annealing temperature can be calculated as $T_m = [2 \times (A + T) + (4 \times (G + C))]$. The polymerase replicates the sequence in a third step, usually at 72 °C for standard Taq-polymerases (elongation). The elongation time depends on the synthesis rate of the polymerase and the length of the sequence to be amplified (standard Taq approximately 1000 bp/min). The cycle of denaturation, primer-annealing and elongation is repeated 30 - 40 times. As DNA amounts are doubled in each cycle, an exponential amplification of the initial DNA content is achieved. The usual amplification rate is between 10^5 and 10^9 copies (Mühlhardt, 2000).

2.2.4.1. Standard PCR

The standard PCR-reaction is set up as follows:

10 - 100 ng	template-DNA
2.0 µl	5' primer (10 µM)
2.0 µl	3' primer (10 µM)
0.5 µl	dNTPs (10 mM)
2.5 µl	10 x reaction buffer
0.5 µl	FirePol <i>Taq</i> polymerase (5 U/µl)
ad 25 µl	dH ₂ O

Amplification reactions were run in a thermo-cycler programmed with specific thermo/time profiles.

Specific amplification was confirmed by gel electrophoresis using a minimum of 1/5 of the reaction volume.

2.2.4.2. Colony-PCR

One way to confirm the successful transformation of bacteria with plasmids (see 2.2.6.2.) is to perform colony PCRs. To this end, bacterial clones were picked with pipette tips and transferred to a replicate plate before the rest of the colony was suspended in a 25 µl standard PCR sample (see 2.2.4.1.). Primers were specific for the respective plasmid or the insert itself.

2.2.4.3. Sexing-PCR

To determine the gender of cercariae from monomiracidial infections, a sexing PCR modified from Grevelding *et al.* (1997b) was performed according to the following protocol:

10-50 ng	template-DNA
0.75 μ l	W1A (1 μ M)
0.75 μ l	W1B (1 μ M)
3 μ l	PDI-sexA-5' (1 μ M)
3 μ l	PDI-sexA-3' (1 μ M)
0.8 μ l	dNTPs (5 mM)
2 μ l	10x reaction buffer
2 μ l	MgCl ₂ (25 mM)
0.5 μ l	FirePol <i>Taq</i> polymerase (5 U/ μ l)
ad 20 μ l	dH ₂ O

5 min 95 °C – 30 s 93 °C – 30 s 65 °C – 15 s 72 °C – 1 min 72 °C

x40

2.2.4.4. Reverse transcriptase reactions

For studies on RNA e.g. to obtain a specific sequence or to estimate its amount within a certain life cycle stage, copy(c)DNA was generated by reverse transcription (RT) of RNA, generally with the Quantitect RT-Kit (Qiagen). A major advantage of this kit is that potential DNA contaminations do not have to be removed by DNase reactions, as the kit contains a non-enzymatic DNA wipeout step. A mixture of random hexamers as well as oligo-dT primers is included in the kit. Binding to their complementary RNA sequences, primers serve as starting positions for the reverse transcriptase. Adequate controls for contamination of reagents, as well as residual DNA were included. Reactions were performed at 42 °C for 30 min, with a final step at 95 °C for 5 min to inactivate the reverse transcriptase. A dilution of the respective cDNA (1:4 or higher) was used for subsequent PCR reactions.

Strand-specific RT-reactions

For detection of strand-specific transcription, RT-reactions were set up with Thermoscript reverse transcriptase (Invitrogen). This enzyme is advantageous for reactions with transcript-specific primers, as reverse transcription can be performed at 60 °C. A disadvantage compared to the Quantitect RT-Kit (Qiagen) is the need to remove DNA-contaminations within the RNA samples prior to the RT-reaction. Therefore, RNAs were treated with 1 U DNase for 20 min and precipitated

2. Materials & Methods

with LiCl₂ (see 2.2.8.4). Subsequently, 400 ng RNA were analyzed for residual DNA contamination using the protocol for sexing-PCR (see 2.2.4.3.). Once DNA contamination was removed, cDNA was synthesized from 200 ng RNA according to the ThermoScript user-handbook.

2.2.4.5. Real-time PCR

Compared to standard PCRs, real-time PCRs are able to monitor the amplification process in each cycle, hence allowing for exact quantification. This is achieved by the use of fluorescent dyes that intercalate into double stranded DNA or are linked to a template specific probe. A threshold is defined for the fluorescence signal (equivalent to a certain amount of amplification product) when all reactions are still in their exponential amplification phase. Modern computer programs for real-time PCR employ optimized algorithms determining this threshold, which is subsequently used to define at which cycle (ct) each sample reaches the according fluorescence signal. The obtained ct-value is then used to calculate differences in the original template amount between samples.

Though more specific in signal, probe based real-time PCR is often not practicable due to its cost intensity. Use of DNA intercalating dyes is far more cost efficient, especially if a multitude of genes are to be analyzed. Most available kits use the fluorescent dye SYBRGreen (excitation: 497 nm, emission: 520 nm) which binds to the minor groove of double stranded DNA. Within the DNA-dye-complex, SYBRGreen emits fluorescence signals, which are detected by the real-time PCR cycler. One major disadvantage of this dye is its binding to primer-dimers - which may form during the PCR reaction - thus distorting the specific signal. Therefore, amplification products for SYBR-green real-time PCR reactions should be larger (150 - 200 bp) than those in probe-based assays (50 - 100 bp) to allow differentiation between the real amplification product and primer dimers. Differentiation is achieved by classical agarose gel electrophoresis or by generation of a dissociation curve at the end of a real-time PCR reaction. The dissociation curve indicates the T_m of the sample. If the dissociation curve exhibits more than one peak, unspecific products are present within the sample.

One factor important for correct quantification is the primer efficiency. It is an indicator for the accuracy of the performed reaction with respect to the theoretical doubling of DNA amounts during each PCR cycling:

$$(3) \quad f(n) = x 2^n$$

With x = template amount and n = number of cycles.

Primer efficiencies are calculated with the help of standard curves (Adams, 2013) giving the ct as function of the log₁₀ template amount:

$$(4) \quad y = mx + b$$

with $y = ct$, $m = \text{slope}$, $x = \log_{10} \text{template amount}$, $b = y\text{-intercept}$.

To obtain standard curves, a 10-fold dilution series of a standard (e.g. gel eluate) is used as template for real-time PCR. The curve's slope is used to calculate the primer efficiency:

$$(5) \quad E = \left[10^{\left(\frac{-1}{m}\right)} \right] - 1$$

where E is the primer efficiency and m the slope.

Primer efficiencies between 0.9 and 1.1 (correspondingly 90 % and 110 %) indicate optimal amplification.

In addition to the different chemical approaches, several options for quantitation exist. Quantitation relative to a reference gene is based on the hypothesis that expression of certain genes is independent of external or internal stimuli, like e.g. inhibitor treatment. The reaction setup is more sample intensive, as each sample has to be analyzed for the gene of interest (GOI) and the reference gene. Additionally, identification and verification of a reliable reference gene is tedious. Furthermore, the amplification efficiency of primers for GOI and reference gene amplification has to be similar (10 % difference may be allowed).

Quantitation relative to a standard curve is independent of reference genes. The same standard curve used for calculation of primer efficiencies is used as a reference to calculate initial template concentrations of a sample, relative to its standard, via the ct .

Executing real-time PCR

Real-time PCRs were performed on a Rotor Gene Q (Qiagen). SYBR-Green MasterMixes used were either PerfeCTa SYBR Green SuperMix (Quanta) or RotorGene SYBR Green PCR Kit (Qiagen). Reactions were performed in a total volume of 20 μl , with a three step thermal profile and a final melt curve analysis. Measurements were quantified relative to a standard-curve. Reaction efficiencies were normally between 90 - 100 %, but never below 85 %. Additionally, efficiencies were checked on a dilution series (1:4) of pooled sample-cDNAs to exclude inhibitory effects of residual RT-components. RNAs from EM and UM were evaluated for similar quality on a denaturing formaldehyde agarose (1.2 %) gel (see 2.2.3.2.). cDNAs (see 2.2.4.4.) were diluted 80-fold for use and added 1:4 to the final reaction. Primers, primer concentrations used for real-time PCR, annealing temperatures and amplification efficiencies are described in chapter 2.1.5. Standard-curves were run in duplicate after initial tests determining primer-efficiencies. Reactions on cDNA-samples were performed in triplicates. Ct-values of runs were exported and analyzed in

2. Materials & Methods

Excel. For standard curves, the number of template molecules within each dilution was calculated using the formula:

$$(6) \quad \frac{v \times co \times Ac}{s \times 660 \frac{g}{mol}}$$

with v = template-volume added to the reaction, co = concentration, Ac = Avogadro constant, s = product size, where 660 g/mol is the molecular weight of a base pair.

The most concentrated dilution contained template amounts in a picomolar range. Ct-values for standard curves were plotted against \log_{10} -values of template molecules. The function of the line of best fit was calculated (see formula (4)). This formula was used to estimate the primer-efficiency and also to calculate \log_{10} -template amounts for samples, entering according ct-values into the function. Subsequently, the exponential function of \log_{10} -template amounts was computed. These values were finally used to calculate \log_2 ratios(EM/UM). The Wilcoxon rank sum test package (Mehta & Patel, 2013; Hollander & Wolfe, 1973; Bauer, 1972) for the open source software R (<http://www.R-project.org/>, R Development Core Team, 2013) was used to determine, if differences between EM and UM were significant.

2.2.4.6. Mutagenesis

To correct for mutations accidentally generated during PCRs or cloning procedures (see 2.2.5), site directed mutagenesis was performed. Specific primers were designed according to the instruction manual of the “QuikChange® Site-Directed Mutagenesis Kit” (Stratagene). To prevent introduction of further mutations, a proof-reading polymerase was used. The mutagenesis reaction contained the following reagents:

5.0 μl	plasmid-DNA (5 ng/ μl)
5.0 μl	5'-primer (5 μM)
5.0 μl	3'-primer (5 μM)
5.0 μl	dNTPs (2 mM)
5.0 μl	10x reaction buffer
1.0 μl	<i>Pfu</i> polymerase (3 U/ μl)
24.0 μl	dH ₂ O

30 s 95 °C – 30 s 95 °C – 1 min 55 °C – 20 min 68 °C – 20 min 72 °C

x 35

Following mutagenesis, 10 μl of the reaction were separated on an agarose gel in comparison to the original plasmid (50 ng). Due to methylation, plasmid-DNA moves slower through agarose than

PCR amplification products. Thus, success of mutagenesis can be confirmed by comparative analysis of plasmid DNA and mutagenesis product.

Subsequently, the residual 40 µl of the reaction were supplemented with 1 µl *DpnI* (20 U/µl) and incubated for one hour at 37 °C. *DpnI* specifically degrades the methylated, plasmid-derived template DNA. Finally, 1 µl of this reaction was used for bacterial transformation (2.2.6.2.). To confirm the successful mutagenesis, the resulting products were sequenced (see 2.1.10).

2.2.5. Cloning of DNA into plasmid vectors

For specific applications, like yeast two-hybrid interaction studies (see 2.2.7.) or bacterial multiplication of specific DNA-fragments previous to sequencing, DNAs were cloned into plasmid vectors.

2.2.5.1. Restriction enzyme digestions

Type II restriction endonucleases (restriction enzymes) are commonly employed to generate fragments with specific overhangs in cloning procedures. Usually, a 20 µl reaction is prepared, containing 10 - 20 U of the enzyme (never more than 10 % of the reaction volume), 2 µl of the enzyme-specific 10x buffer, 1 µg DNA and dH₂O. Reactions are incubated for 2 - 4 h at an enzyme specific temperature (usually 37 °C). Subsequently, the complete reaction is separated by agarose gel electrophoresis and gel-eluted after validation of correct size of cleavage-products.

2.2.5.2. Ligation

During standard cloning procedures, PCR amplification products are ligated into vectors such as pDrive (Qiagen) according to the manufacturer's protocol. The procedure takes advantage of the A-overhangs at the end of PCR-amplification products generated by *Taq*-polymerases.

For specific cloning approaches, DNAs (inserts) and plasmid vectors are cleaved with the same restriction endonucleases to generate complementary sticky ends. They are then ligated with T4 DNA-ligase (Fermentas). The enzyme catalyzes binding of neighboring 3'-OH and 5'-phosphate ends. The ratio insert:vector should approximately be 5:1. A standard 20 µl ligation-reaction contained 2 µl reaction buffer, 1 µl T4-ligase (5 U/µl), 50 ng vector-DNA and dH₂O. Required DNA amounts of the insert were calculated by the formula (Mühlhardt, 2000):

$$(7) \quad mi = \frac{5 \times mv \times si}{sv}$$

with mi = ng insert DNA, mv = ng vector DNA, si = insert size, sv = vector.

2. Materials & Methods

Ligation reactions were incubated 2 h – over night at 16 – 20 °C and subsequently used for transformation into competent bacteria (2.2.6.2.).

2.2.6. Bacteria

2.2.6.1. Production of heat-shock competent bacteria

To obtain heat-shock competent bacteria, a 10 ml culture of an appropriate strain of *E. coli* (here NEB10 β [New England Biolabs]) was incubated overnight at 37 °C at 225 rpm in a sterile volumetric flask. 1 ml of the culture was transferred to warm LB-medium (100 ml) and incubated again at 37 °C and 200 rpm until an OD₆₀₀ of 0.5 was detected with a photometer. Once the according density of the bacteria was reached, the volumetric flask was placed on ice for 5 min and bacteria were subsequently pelleted by centrifugation at 4000 g and 4 °C. After discarding the supernatant, the pellet was resuspended in precooled TFB1-buffer and incubated on ice for 90 min. The centrifugation step was repeated and the pellet resuspended in precooled TFB2-buffer. Subsequently, 100 μ l aliquots are frozen in liquid nitrogen and stored at -80 °C.

2.2.6.2. Transformation of heat-shock competent bacteria

For transformation of bacteria with a plasmid-construct, an aliquot of heat-shock competent cells was thawed on ice, 5 – 10 μ l plasmid DNA were added and mixed with the bacterial suspension and subsequently incubated on ice for 30 min. This is followed by a heat shock for 1 min at 42 °C and 3 min on ice. After addition of 800 μ l antibiotic-free LB-medium, the cells were incubated for 40 min at 37 °C and 200 rpm. Finally, bacteria were plated onto the appropriate selection agar.

2.2.6.3. Blue-white selection

In standard cloning procedures, sequences of interest are cloned into vectors, such as pDrive, which contain a coding region for a β -galactosidase (β -gal) subunit in addition to an antibiotic resistance gene. As the multiple cloning site of pDrive disrupts the β -gal coding region, β -gal activity can be used for the selection of bacteria transformed with insert-containing plasmids. To this end, bacteria were plated on LB-agar plates supplemented with 100 μ g/ml ampicillin, 0.2 mM isopropyl thiogalactoside (IPTG), and 0.004% 5-Brom-4-Chlor-3-indoyl- β -D-galactosid (X-Gal). IPTG induces the LacZ gene and thus β -gal expression. β -gal cleaves X-Gal and the cleavage product reacts with oxygen to the blue color indigo.

2.2.6.4. Liquid culture

For multiplication of bacteria in liquid culture, one colony from an agar-plate or approximately 10 μ l from a glycerol stock were added to 5 – 30 ml of LB-medium, supplemented with the appropriate antibiotic and incubated over night at 37 °C and 200 rpm.

2.2.6.5. Glycerin-stocks

For long-term storage of bacteria, 1 ml of a well grown over-night culture was mixed with 500 μ l sterile glycerol (99%) and frozen at -80 °C.

2.2.7. Yeasts

Experiments with yeasts were conducted together with Dr. Svenja Beckmann.

2.2.7.1. Liquid culture

To obtain enough yeast material to start a liquid culture, a pre-culture (Yeast Protocols Handbook, 2001) with 5ml YPD (or other appropriate medium) and one yeast culture from a stem-plate was incubated overnight (16 – 18 h) at 30 °C and 200 rpm. After this incubation period, the culture should have reached an OD₆₀₀ exceeding 1.5 (indicating stationary growth). In case a log-phase culture was needed the over-night culture was diluted in fresh medium to an OD₆₀₀ of 0.2 - 0.3 and grown further (30 °C, 200 rpm) to an OD₆₀₀ of 0.4 - 0.6.

2.2.7.2. Glycerin-stocks

For long-term conservation of yeasts, glycerin-stocks were generated (Yeast Protocols Handbook, 2001). Single yeast colonies were picked from an agar-plate and mixed into 200 – 500 μ l YPD (or appropriate) medium. Glycerol was added to an end-concentration of 25 % and the suspension was stored at -80 °C after mixing. Transformed yeasts should be stored in the according SD-minimal medium. For re-use a small part of the glycerin stock was plated on YPD agar plates or on an appropriate selection plate and incubated at 30 °C. Such a yeast stem-plate can be stored at 4°C for approximately 2 months.

2.2.7.3. Production of yeast cells competent for transformation

Transformation competent yeast cells were prepared according to the following procedure: 30 ml of a 50 ml overnight culture were mixed into 300 ml YPD-medium to an OD₆₀₀ of 0.2 – 0.3. This culture was incubated at 30 °C and 200 rpm to obtain an OD₆₀₀ of 0.4 - 0.6. Yeasts were pelleted by centrifugation at RTC for 5 min at 1,000 g and resuspended in sterile TE-buffer or dH₂O. This

was followed by another centrifugation step under the same conditions as before and this pellet was resuspended in 1.5 ml of fresh and sterile 1x TE / 1x LiAc (1x TE-buffer, 1x LiAc; 0.1 M).

2.2.7.4. Transformation of yeast – lithium acetate method

Yeasts were transformed by the lithium-acetate-method (Yeast Protocols Handbook, 2001). Depending on the experimental set up, one or two plasmids were transformed. The protocol was the same in both cases. Plasmid DNA (0.1 µg) was mixed with 0.1 mg herring-sperm DNA, which served as carrier-DNA, and 0.1 ml transformation-competent yeast-cells were added. The suspension was vortexed and 0.6 ml sterile PEG/LiAc-solution (polyethyleneglycole-lithium-acetate-solution) were added, followed by 10 s of vortexing and a 30 min incubation at 30 °C and 200 rpm. Before the heat-shock, 70 µl dimethyl sulfoxide (DMSO) were added to the sample. Heat-shock was performed at 42 °C for 15 min in a water bath followed by another 2 min incubation on ice. Cells were pelletized by centrifugation for 5 s and 13,000 rpm at room temperature. The pellet was resuspended in 500 µl sterile 1x TE buffer and 100 – 500 µl of the suspension were plated onto SD-plates, selecting for the according plasmid or plasmids. Plates were incubated at 30 °C for 2 - 4 days until yeast colonies were visible.

2.2.7.5. Yeast two-hybrid system

The yeast two-hybrid (Y2H) system is used to investigate protein-protein interactions (Chien *et al.*, 1991). In this work, the employed Y2h system (Matchmarker II, Clontech) is based on the yeast transcription factor GAL4, which contains two domains with separate functions: the DNA-binding domain (BD) and the transcription activation domain (AD). Both domains are integrated into different plasmid vectors. Neither of the two domains alone is able to activate transcription. Only if they get into physical contact, an active transcription factor is formed. To test direct protein-protein interaction, the sequence of one of the proteins to be tested, or an appropriate partial sequence, is cloned into the vector containing the AD domain, while the sequence of the other protein is cloned into the vector containing the BD domain. In case the chimeric proteins are expressed and the proteins interact, the AD and BD domains come into physical contact, restoring the active transcription factor and its ability to bind to the GAL4-UAS (up-stream activating sequence) to initiate transcription of down-stream genes. For selection, auxotrophy genes (ADE2, HIS3) or reporter genes for color-selection (LacZ) are used.

2.2.7.6. Colony lift filter assay

The β -gal filter-assay is used to verify the interaction of clones which survived HIS3-/ADE2-selection. Interaction of gene-products from plasmids transformed into yeast results in β -gal expression. Thus, interaction of positive clones can be identified by blue color of the respective colonies.

To perform filter-assays, a Whatman filter-paper was soaked in Z-buffer/X-Gal solution and placed into a 20 mm plastic dish. Sterile Whatman filter-paper strips were softly pressed onto plates containing the yeast colonies to be analyzed. After transfer of the yeast colonies to the filter-paper strips, they were frozen in liquid nitrogen for 10 s and subsequently thawed at RT to destroy the yeast cell walls. Finally, the filter-paper strips were placed onto the Z-buffer/X-Gal solution soaked Whatman filter-papers and incubated at 30 °C. Filters were checked regularly for blue coloring.

2.2.7.7. β -galaktosidase-liquid assay

To quantify the relative interaction-strength of binding partners, a β -gal liquid assay was applied (Yeast Protocols Handbook, 2001). In this assay ONPG, which is converted by β -gal to o-nitrophenol and D-galactosidase, is used as substrate for β -gal. The intensity of the resulting yellow color, can be determined photometrically. To perform the liquid assay, a 5 ml over-night culture was grown in selection medium and 2 ml were added to 8 ml fresh YPD medium. The culture was incubated at 30 °C and 200 rpm until an OD₆₀₀ of 0.5 - 0.8 was reached. Subsequently, the yeast culture was subdivided into three tubes of 1.5 ml each and centrifuged for 30 s at 13,000 rpm. The supernatants were discarded and the pellets resuspended in 1.5 ml Z-buffer. Following another centrifugation step (1 min, 13,000 rpm), the pellets were resuspended in 300 μ l Z-buffer (equaling a 5x concentration factor). Thereafter, the suspensions were again divided into new tubes at 0.1 ml each, incubated in liquid nitrogen for 1 min and thawed in a 37 °C water bath. This freeze and thaw cycle was repeated twice. For subsequent use as reference during photometric measurements, a 100 μ l aliquot of Z-buffer was treated in the same way as the samples during the following procedure. After addition of 700 μ l Z-buffer containing 0.27 % β -mercaptoethanol, the enzymatic reaction was started through immediate addition of the substrate (160 μ l ONPG 4 mg/ml in Z-buffer, mixed for 1 – 2 h). Samples were incubated at 30 °C. When yellow coloring was observed (minutes to 24 h), the reaction was stopped by addition of 400 μ l Na₂CO₃ (1 M). The incubation time was noted and samples centrifuged for 10 min at 13,000 rpm. Supernatants were transferred into clean cuvettes and measured at OD₄₂₀ (Buro *et al.*, 2010). Photometric values should be between 0.02 and 0.1 to be in the linear measurement

2. Materials & Methods

area of the assay. In case of higher ODs the samples were diluted accordingly. The following formula was used to calculate the β -gal-units from the photometric measurements:

$$(8) \quad \beta - galactosidase - units = \frac{1000 \times OD_{420}}{t \times V \times OD_{600}}$$

[t = sample incubation time in min, V = 0.1 ml x concentration factor (here: 5),

OD₄₂₀ = sample-absorption, OD₆₀₀ = absorption of initial 8 ml culture]

One unit of β -gal is defined as the amount of enzyme that hydrolyzes 1 μ mol ONPG per min and cell (Miller, 1992; Miller, 1972).

2.2.8. *In situ* hybridization

To investigate the localization of specific transcripts in worm tissues, *in situ* hybridizations were performed. Labeled RNA probes were used to detect mRNAs within *S. mansoni* tissue slices (Köster *et al.*, 1988)

2.2.8.1. Fixation

Worms were fixed directly after perfusion by incubation in Bouin's fixative for 90 min at RT. Subsequently, they were dehydrated by an ascending alcohol series for 45 min each in: 30 % ethanol_{DEPC}, 50 % ethanol_{DEPC}, 70 % ethanol_{DEPC}, 90 % ethanol_{DEPC}, 96 % ethanol_{DEPC}, 96 % ethanol_{DEPC} supplemented with two drops chromotrop 2R and finally, methyl benzoate (at ethanol concentrations > 90 %, incubation can be done overnight). After the methyl benzoate step, worms were washed twice for 5 min in benzol and afterwards kept in pre-warmed (60 °C) paraffin (Histowax, Reichert-Jung, Germany) overnight. Finally, worms were transferred into paraffin filled ice-cube trays (at 60 °C). After proper placement of worms (approx. 3 per well) at the bottom of the well, the ice-cube trays were cooled down and finally frozen at -20°C.

2.2.8.2. Preparation of glass slides

Microscope slides were degreased in ethanol and acetone (1:1) overnight and subsequently siliconized once for 2 min in 10 ml TESPA (3-Amino-propyltriethoxysilan, Sigma) / 500 ml acetone. Afterwards, slides were washed once in dH₂O and dried at 37 °C.

2.2.8.3. Tissue sections

Paraffin blocks were trimmed to reduce the sectional area containing worms as far as possible. 5 μ m sections were cut with a microtome (Leica, Histoslide 2000 R) and transferred to the surface of a 42 °C water bath (dH₂O) with a small brush to stretch the paraffin slices before their transfer

to siliconized slides and drying. After microscopic evaluation, slides were incubated at 60°C overnight and stored at RT in a dry environment.

2.2.8.4. Probe synthesis

For the detection of mRNAs in tissue, sequence-specific, labeled RNA-probes were used. To be able to produce template for probe generation by *in vitro* transcription, the according sequence was cloned into the vector pDrive. Thereafter, the sequence was amplified from pDrive with the vector specific primers T7 and SP6. Alternatively, T7-tagged gene-specific primers were designed and used for amplification from cDNA. The amplification product was used as template in the *in vitro* transcription reaction, which contained Dig-labeled UTP to label the newly synthesized RNA. Sense and anti-sense probes were generated from pDrive derived transcription templates by employing either T7 or SP6 RNA polymerase. If T7-tagged primers were used, a 5'-T7 fragment as well as a 3'-T7 fragment had to be amplified as template for transcription. The transcription reaction was prepared as follows and incubated for at least 2 h at 37 °C:

2 µl	10x transcription-buffer
2 µl	10x DIG-rNTP Labeling Mix
0.5 µl	RNasin (Promega)
x µl	1 µg PCR-product
2 µl	RNA Polymerase (20 U)
x µl	H ₂ O _{DEPC}
total volume: 20 µl	

Thereafter, the template was removed from the reaction by addition of 1 U DNaseI (Fermentas) and incubation for 20 min at RTC. The enzymatic reaction was stopped with 2 µl ethylene diamine tetra acetic acid (EDTA) (per 20 µl reaction volume) and the RNA-probe precipitated with 1/10 vol 4 M LiCl₂ and 2.5 vol ethanol (96%) overnight at -80 °C. Probes were pelletized by centrifugation at 13,000 rpm for 30 min at 4 °C. After one washing step with 70 % ethanol_{DEPC} and centrifugation for 10 min, pellets were dried and resuspended in 20 µl H₂O_{DEPC}. Probe synthesis was checked by gel electrophoresis (1µl/probe).

Transcript blot

The incorporation of Dig-UTP into the probes was verified by a transcript blot (similar to a capillary northern blot).

RNA gels with probes were washed thrice in H₂O_{DEPC} and incubated for 45 min in 10x SSC_{DEPC} before blotting (Fig. 2.1). After overnight transfer of probes to a nitrocellulose membrane, the

2. Materials & Methods

latter was dried and crosslinked. After 30 min incubation in 2 % blocking solution (Roche) (slight rotation), the membrane was exposed to an anti-Dig antibody (Roche) conjugated to alkaline phosphatase (1:2500 in 2 % blocking solution) for 2 h (slight rotation). Subsequently, the membrane was washed twice for 15 min at RT in 1x maleic acid buffer supplemented with 0.3 % Tween 20, followed by an equilibration step in substrate buffer for 5 min. The Dig-signal was detected with 50 mg Fast Red TR, dissolved in 50 ml substrate buffer and 10 mg Naphthol-AS-Phosphate, dissolved in 200 μ l DMSO, the two solutions were mixed and filtered before application on the membrane. Naphthol-AS-Phosphate acts as substrate for alkaline phosphatase. The dephosphorylated reaction product forms an insoluble red azo-dye together with Fast Red TR. Reactions were stopped by rinsing the membrane in dH₂O.

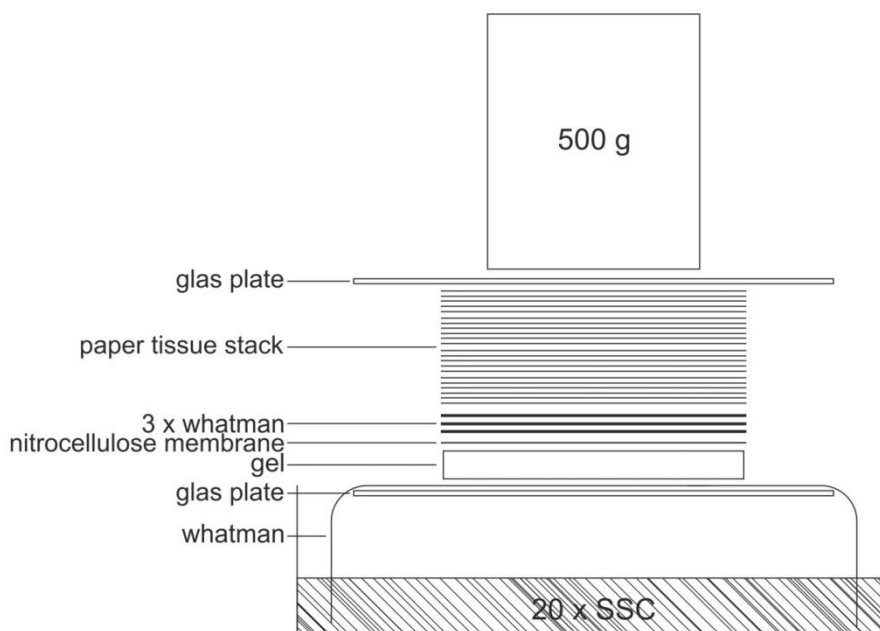


Figure 2.1: Transcript blot setup.

Schematic presentation of a transcript blot (equals a capillary northern blot). RNA is transferred from an agarose-gel onto a nitrocellulose membrane.

2.2.8.5. *In situ* hybridization protocol

For *in situ* hybridization, the tissue slides have to be deparaffinized and rehydrated. To this end they were incubated twice in xylene (5 min) and subsequently - for 5 min each - in ethanol_{absolute}, 96 % ethanol, 70 % ethanol and H₂O_{DEPC}. To enhance permeability of tissues, an additional incubation for 20 min was performed each in 0.2 N HCl and proteinase K (1 μ g/ml, 37 °C), with an intermediated equilibration for 5 min at 37 °C in proteinase K buffer (without proteinase K). Subsequently slides were incubation for 5 min each in 0.2 % Glycin, 15 s and 20 % acetic acid (4 °C). Glycin stops the proteinase reaction, while the acetic acid reduces the background in the

following color reaction by blocking the alkaline phosphatase within the tissue. Incubation for 5 min 1x PBS_{DEPC} and 15 min 20 % Glycerol followed. Slides were shortly rinsed in 2x SSC and put on a heated plate (70 °C) for 10 – 12 min. Before addition of the hybridization mixture, they were cooled down on a metal plate previously cooled to -80 °C.

While the slides were washed, the probe-mixture was prepared as follows:

4 - 8 µl	probe
2 µl	herring-sperm DNA (10 mg/ml)
4 µl	tRNA (33 mg/ml)
ad 20 µl	H ₂ O _{DEPC}

The probe mixture was heated to 70 °C for 10 - 12 min and then supplemented with 180 µl hybridization buffer (per 20 µl probe mixture). Of this hybridization mixture 200 µl were applied onto the cooled slides. The hybridization reaction took place overnight at 42 °C in a humid chamber.

Subsequently, slides were washed for 15 min each in 2x SSC with 0.1 % Tween 20 at 42 °C and 1x SSC at RTC. Within the salt solution excessive probe diffuses from the slides and is washed off. Thereafter, they were equilibrated for 5 min in maleic acid buffer and incubated for 30 min in 4 % blocking solution at RT in a humid chamber (~200 µl per slide). Dig-UTP was detected with an anti-dig antibody (1:500, in 2 % blocking) by incubation for 2 h at room temperature. After two times 20 min washing in maleic acid buffer at RTC and 5 min equilibration in substrate buffer, the color reaction was performed as described for the transcript blot, but in variation to this for up to 2 h. Finally, slices were shortly rinsed in water to terminate the color reaction and sealed off with Aquatex (Merck) and a coverslip.

2.2.9. Determination of mitotic activity

For determination of mitotic activity the method of Knobloch *et al.* (2002a) was adapted. About 30 couples were treated with 5'-bromo-2'-deoxyuridine (BrdU; Sigma), a thymidine analogue, which is incorporated into DNA during synthesis processes. The incubation time depended on the experiment (see 2.2.11., 2.2.12). DNA was extracted (see 2.2.2.2) and resuspended in 55 µl dH₂O. Concentration was determined by densitometry (see 2.2.2.4.). Therefore, 5 µl of each sample were loaded onto a 1 % agarose gel and compared to 100 ng and 200 ng λ-DNA. If gel electrophoresis revealed RNA contamination, a RNase step was performed additionally.

2. Materials & Methods

To determine BrdU incorporation into DNA, 800 ng of DNA in a volume of 50 μ l were slot blotted onto a nitrocellulose membrane (Whatman) with a slot blotting machine (SRC 072/0 Minifold II, Schleicher & Schnell, Dassel, D), according to the manufacturer's protocol. After drying (approximately 30 min), RTC the membrane was cross linked (Stratalinker 2400; Stratagene, Amsterdam, NL) and washed in solution I (see 2.1.1) for 5 min. To determine the amount of DNA successfully transferred to the membrane, the latter was stained with 10 μ g/ml 4',6-diamidino-2-phenylindole (DAPI, Sigma) diluted in solution II (see 2.1.1) for 40 min at RTC on a shaker, protected from light. To minimize background staining, the membrane was rinsed in solution I for 5 min and afterwards for another 1 – 8 h. Intensity of staining was detected on a UV-table (Intas). Subsequently, the membrane was blocked with 1x Roti Block (Roth) for at least 45 min at RTC on a shaker (60 rpm). For BrdU detection, the membrane was incubated with anti-BrdU-antibody (Sigma) diluted 1:1,000 in $\frac{1}{2}$ x Roti Block for 2 – 3 h at RTC. This was followed by 3 washing steps (10 min each) with 1x PBS containing 0.05 % Tween 20 (Roth), and incubation with a secondary antibody coupled to horse radish peroxidase (anti-mouse Ig from sheep; Amersham International, UK) used in a 1:12,000 dilution in $\frac{1}{2}$ x RotiBlock. Incubation was done for 2 - 3 h at RT under slight rotation. Subsequently, the blot was washed thrice for 10 min with 1x PBS containing 0.05 % Tween 20. Chemiluminescence detection of BrdU-incorporation was performed with Pierce ECL western blotting substrate (Pierce). Densitometry was performed as described in chapter 2.2.2.4. by setting chemiluminescence signals for BrdU into relation to DAPI-signals.

2.2.10. Carmine-red staining of adult schistosomes

Adult worms were fixed in AFA-fixative (a mixture of acetic acid, formaldehyde and ethanol) for at least 24 h at RTC in the dark and stored for later use. For confocal laser scanning microscopy (CLSM), the fixed worms were stained with carmine red according to the following procedure: Worms were incubated in carmine red for 30 min with slight rotation. Thereafter, they were destained in acidic ethanol (70 % ethanol + 2.5 % HCl) until no more stain diffused from the worms. Dehydration was done by a short incubation in 90 % ethanol, and, subsequently, 100 % ethanol. Finally, worms were embedded in Canada balsam (2:1 with xylene; Merck) and covered with a cover slip (Beckmann *et al.*, 2010b; Neves *et al.*, 2005; Machado-Silva *et al.*, 1997).

CLSM analysis (Leica TSC SP2) was done, using the reflection-mode with a He/Ne-Laser and an Ar/Ar/Kr-laser. Excitation was set to 48% at 488 nm and a 470 nm long pass filter was used for detection.

2.2.11. Pairing experiments

For analysis of pairing-dependent mitotic activity (MA), separated females from mixed-sex infections were collected from perfusions and cultured for one week to reset mitotic activity and induce a pseudo-juvenile developmental state. Males were collected from another perfusion the following week and kept in culture for 2 days before the start of the experiment. EM were separated at the day of perfusion and kept “single” for 2 days. For pairing, males were co-cultured with the pseudo-juvenile females and it took several hours for the couples to form. Re-mated pairs, as well as controls, were transferred to fresh medium containing 1 mM BrdU and incubated for 12 h, 24 h or 48 h. Pairing was checked at least every 12 h. Subsequent to the incubation in BrdU, worms were separated and collected in 1.5 ml tubes, medium was removed, and samples were stored at -80°C.

2.2.12. TNF α treatment

To analyze the influence of human TNF α on *S. mansoni* mitotic activity, couples were treated with 0.2 / 1 / 5 / 20 or 50 ng/ml TNF α (Biomol or Cell Signaling) in the presence of 1 mM BrdU. For each experiment, 30 – 40 couples were used. To ensure that worms were adapted to culture conditions, treatment was started two days after perfusion and continued for three days. Medium with TNF α and BrdU was changed daily. After the treatment period, couples were separated, collected in 1.5 ml tubes without medium and stored at -80 °C.

2.2.13. Inhibitor treatment

To investigate the role of *S. mansoni* cGKs, couples were treated with 1 μ M of the cGK-inhibitor Rp-8-pCPT-cGMPs (Biolog) dissolved in culture medium (see 2.1.1.). Worms were treated for up to 6 days. Each day the medium was changed, eggs counted, and couples monitored for behavioral or physiological abnormalities. After treatment, worms were fixed in AFA, stained with carmine red and analyzed by CLSM (see 2.2.10.).

2.2.14. Transcriptome studies

To identify differences in the transcriptomes of EM and UM, microarray analyses and SuperSAGE were performed. The microarray is a platform-based method. Short single-strand DNA probes attached to fixed ‘spots’ on a glass slide are used to detect fluorescence marked RNAs from a sample (Causton *et al.*, 2003). Thus, detection of transcripts is fluorescence-intensity based.

2. Materials & Methods

SuperSAGE on the other hand is platform-independent. A series of restriction enzyme digestion steps leads to the generation of short sequence ‘tags’ of 27 nt. Thus, final transcript detection is achieved by sequencing of the obtained tags, even allowing for quantification of transcript numbers (Matsumura *et al.*, 2010; Molina *et al.*, 2008; Matsumura *et al.*, 2003; Figure 2.2.).

For both transcriptome analyses, males from unisexual or bisexual infections were collected. Batches of 50 flukes were treated with 200 µl RNeasy lysis buffer (Qiagen) to stabilize RNA. After incubation at 4 °C overnight, the liquid was removed and worms were frozen at -80 °C. Depending on the applied method, subsequent procedures differed as described in the respective chapters (2.2.14.1, 2.2.14.2, Fig. 2.2).

It should be noted that during this thesis, methods for selecting male worms became more sophisticated. In the beginning all male worms from perfusions of hamsters infected with mixed-sex cercariae were defined as EM (this applies to the first two biological replicas for the microarrays). Later, males that were in copulation with a female at the time of perfusion and subsequently separated were defined as EM. This ensured their status of pairing-experience as well as excluding female contamination. Additionally, all males were more carefully selected with regard to their “fitness”: only worms sucked to the petri dish were defined as physically fit enough to show representative transcription.

2.2.14.1. Microarrays

Microarray experiments took place in the laboratory of Sergio Verjovski-Almeida at the department for Biochemistry of the University of Sao Paulo, using a 44k oligonucleotide array designed by the same group (Verjovski-Almeida *et al.*, 2007) in collaboration with Agilent Technologies. RNeasy lysis buffer (Qiagen) treated samples were sent to Sao Paulo on dry ice.

Experimental procedure:

For total RNA isolation, approximately 25 worms from each batch were washed twice in 500 µl H₂O_{DEPC}, followed by addition of 1 ml TRIzol reagent (Invitrogen). Subsequently, the worms were homogenized mechanically and incubated for 5 min at RTC before 200 µl chloroform were added, mixed for 15 s, and incubated for 2 - 3 min. Following centrifugation for 15 min at 12,000 g and 4 °C, the upper phase was transferred to a new tube and mixed with 500 µl isopropanol for precipitation of the RNA. After incubation for 10 min at RTC, the RNA was pelletized for 10 min at 12,000 g and 4 °C. The pellet was washed with 1 ml 75 % ethanol and centrifuged again for 5 min at 7,500 g and 4 °C. The supernatant was discarded, the pellet dried and resuspended in 25 µl H₂O_{DEPC}. Before concentration determination employing a spectrophotometer (Nanodrop), the

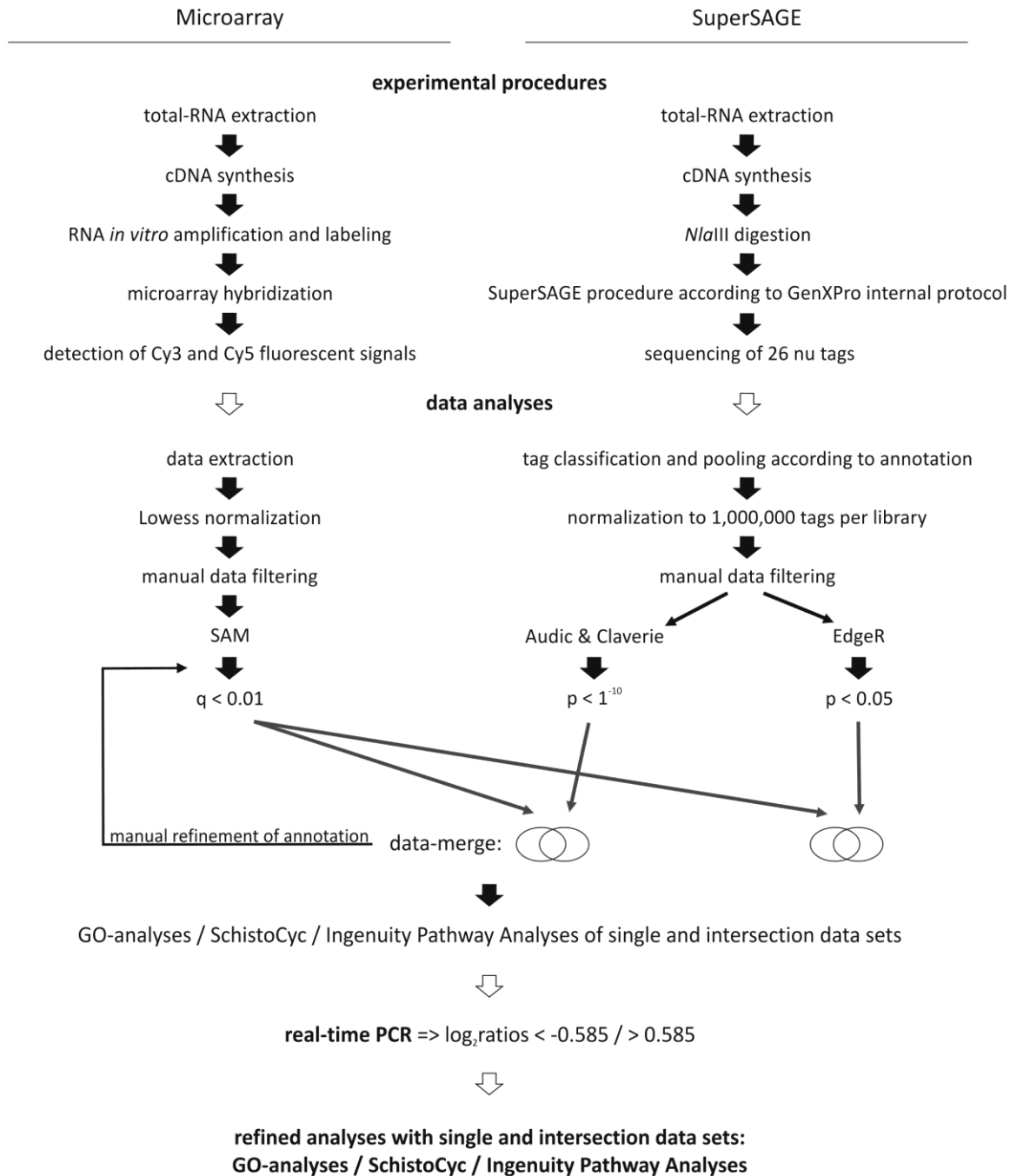


Figure 2.2: Flowchart of microarray and SuperSAGE experimental procedures and analyses.

Schematic representation of the workflow for both transcriptome detecting methods and subsequent data analyses.

RNA was shortly heated to 65 °C. RNA was further purified using the Qiagen RNeasy Mini kit, applying the animal tissue protocol with the following modifications: samples were supplemented to a volume of 100 µl, and 350 µl RLT buffer as well as 250 µl ethanol (70 %) were added before the suspension was transferred onto a kit column. An on column DNase digestion step was included (see appendix D of the user handbook). RNA was eluted with 30 µl H₂O_{DEPC} and the flow-through was again applied to the column for a second elution step. Concentration of RNA was

2. Materials & Methods

determined again (see above) and its quality checked on a Bioanalyzer (Agilent 2100 Bioanalyzer, Agilent Technologies) according to the manufacturer's protocol.

For all subsequent procedures, the Agilent 'Two Color Microarray-Based Gene Expression Analysis' protocol was followed; in short: Two aliquots of 300 ng RNA per sample were used. Previously prepared spike-in controls were added to the RNAs, which were reverse transcribed, *in vitro* amplified and labeled with Cy3 or Cy5. Labeled RNA was purified using the Qiagen RNeasy Mini Kit components following the Agilent protocol except for one modification: the eluate was passed over the column a second time. Concentration and labeling efficiency were determined on a Nanodrop spectrophotometer. The 17 h overnight hybridization was done according to the Agilent protocol.

The custom designed array (GEO accession number GPL8606; Agilent Technology; Verjovski-Almeida *et al.*, 2007) used in this analysis contained 60mer oligonucleotides and was re-annotated (Oliveira *et al.*, 2011) after publication of the genome project (Berriman *et al.*, 2009). Three biological replicas for EM and UM each were used during microarray analysis, each with four technical replicas including dye swaps.

Data analysis:

After data extraction (Agilent feature extraction software) three data files were generated using the open source software R (R Development Core Team, 2013): First, a file was generated, containing average intensities of all oligonucleotides for each experiment and dye (supplementary-file1). Secondly, \log_2 ratios for each oligonucleotide in each experiment were calculated (Causton *et al.*, 2003), using EM-values as controls ($\log_2 \frac{\text{intensity}_{-UM}}{\text{intensity}_{-EM}}$) (supplementary-file2). The third file contained information on signal detection for each oligonucleotide (supplementary-file3).

Subsequently, calculated \log_2 ratios (supplementary-file2), information on signal detection (supplementary-file3) and definitions on oligonucleotides use in analysis (column "to be used in analysis" in supplementary-file4 from Oliveira *et al.*, 2011) were combined using Spotfire (Kaushal & Naeve, 2004). A manual filtering process was applied, whereby oligonucleotides and respective \log_2 ratios were kept for analysis according to the following criteria: 1. Oligonucleotides had to be marked for use in analysis 2. Signal detection for oligonucleotides had to be positive in at least three technical replicas of one biological replica and in all three biological replicas of EM and/or UM. With these pre-selected \log_2 ratios a statistical analysis for microarrays (SAM) (Tusher *et al.*, 2001) was performed using a 'one class analysis'. Subsequently \log_2 ratios and results from the

significance analysis were combined with transcript-annotations from supplementary-file4 in one excel-file (supplementary-file5). For further data analyses a set of transcripts was created from sense transcripts significantly regulated with $q < 1\%$.

2.2.14.2. Super-SAGE

SuperSAGE experiments were performed by the company GenXPro (Frankfurt). Total RNA was extracted from 50 worms using three biological replicas for each group (EM or UM) as described in 2.2.2.1., RNA-quality was checked on a denaturing formaldehyde gel as well as with the Agilent Bioanalyzer 2100. Samples were sent to GenXPro on dry ice. The experimental procedure followed the one described by Matsumura *et al.* 2003, with minor changes as given in Molina *et al.* 2008 (Fig. 2.3). Six libraries were generated containing sequence-tags detected in the according one of the six samples.

Data analysis:

Sequence-tags were annotated applying the same procedure as for the re-annotation of the microarray (Oliveira *et al.*, 2011). Likewise, transcripts were classified into sense- and anti-sense. Additionally, SuperSAGE transcripts were further distinguished into predicted intron- or exon-sequences. Transcripts with the same annotation, strand- and coding region-prediction were summed up. Counts were normalized to a library size of 1,000,000 and a filtering process was applied keeping only those transcripts that were detected in two out of three biological replicas in at least EM or UM. Subsequently, two different statistical tests were applied, the R implementation Edge R (Robinson *et al.*, 2010) and a GenXPro internal program based on the method of Audic and Claverie (A&C) (Audic & Claverie, 1997). While both methods are well adapted for statistical evaluation of SuperSAGE data, the EdgeR method is more stringent resulting in a very low number of significantly regulated transcripts. For successive analyses two subsets of sense transcripts were used, depending on the statistical method (EdgeR: $p < 0.05$, A&C: $p < 1^{-10}$). Also, transcripts without annotation were excluded from further analyses.

2.2.14.3 Merging data from microarray and SuperSAGE experiments

Microarray and SuperSAGE data were compared by their Smp_numbers (*S. mansoni* specific gene code or equivalent), using the programs Spotfire and Excel. Smp_numbers which did not show a match were manually checked. During this process it was found, that a number of 1006 oligonucleotides without gene predictions according to the latest array annotation (Oliveira *et al.*,

2. Materials & Methods

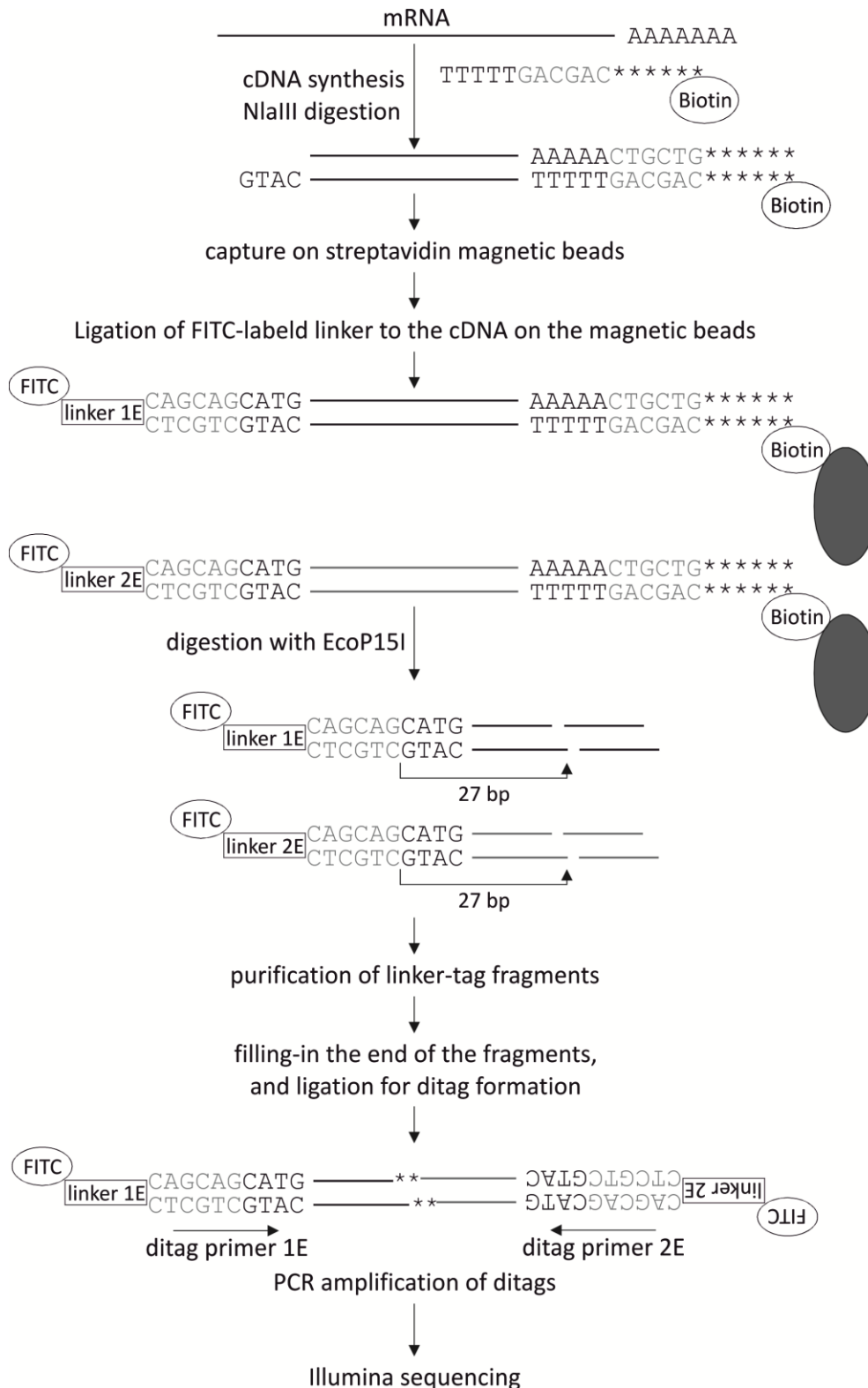


Figure 2.3: Flowchart of the SuperSAGE experimental procedure modified from Matsumura *et al.* (2003). From a given RNA double-stranded cDNA is synthesized with a biotinylated oligo-dT primer containing the recognition site of the restriction enzyme *EcoP15I* (CAGCAG). Subsequently, cDNAs are digested with *NlaIII* and captured on streptavidin magnetic beads at the 3'-end. After washing, the cDNAs are divided into two separate groups and ligated to linker-fragments containing an *EcoP15I* recognition site. Following digestion with *EcoP15I* fragments are separated on PAGE, visualized and collected from the gel. The two different linker groups are mixed, blunt ended and ligated to each other. Resulting ditags are amplified and subsequently sequenced using an Illumina (Solexa) sequencer.

2011) could be annotated to gene predictions in SchistoDB 2.0 manually, after all. These annotations were integrated into the existing microarray data, excluding redundancies.

From the comparison three data-sets were derived. One intersection-set, which contained transcripts detected with both methods and two method-only sets, containing transcripts detected only with microarrays or SuperSAGE.

2.2.14.4. Gene ontology and network analysis

To ease interpretation, three different analyses were performed with each data-set obtained from microarray, SuperSAGE or intersection. The ontologizer (Robinson *et al.*, 2004) was used to detect significantly enriched gene ontology (GO) categories for selected data-sets. The tool compares a study count, e.g. all significantly regulated transcripts, to a population count, e.g. all transcripts detected. Through a GO-specific reference file, transcripts within each of these data-sets are allocated to GO categories. The composition of categories and the number of transcripts per category are compared between the two data-sets. GO categories used in this thesis, were originally linked to contigs used for the design of the microarray. Thus all sense transcripts from the array analysis had a GO annotation, while only those SuperSAGE-detected transcripts could be used for the analysis that had representatives on the microarray. According comparisons were done as for the data- intersection (2.2.14.3). Text-files containing the respective contig annotations of a data-set were uploaded into the tool. Analyses were done applying the statistical functions 'parent-child-intersection' and 'Benjamini-Hochberg' corrections.

In addition to GO analyses the *S. mansoni* specific non statistical online pathway tool 'SchistoCyc' (available at SchistoDB 2.0) (Zerlotini *et al.*, 2009) and the 'ingenuity pathway analysis' (IPA) tool (<http://www.ingenuity.co>; Thomas & Bonchev, 2010) were used to facilitate data-interpretation.

SchistoCyc allocates a given set of Smp_numbers to *S. mansoni* metabolic pathways. To perform the data allocation the application 'omics viewer' on the SchistoCyc web-page (<http://schistocyc.schistodb.net/SM/expression.html>) was selected. A text-file containing Smp_numbers and log₂ratios of the respective data-set was up-loaded, and the following settings chosen: display of 'absolute' results, 'a single data column', '0-centered scale', 'Gene names and/or identifiers', 'Data column' = 1. Allocation results were extracted through a software-created table and/or manually. For Smp_numbers ending on ".x", the latter was replaced with ".1".

IPA was used to detect significantly enriched canonical pathways, transcription factors of significantly regulated transcripts, and significantly enriched potential networks. As the IPA tool

contains no *Schistosoma* specific information, only those transcripts could be used for the analysis, which had a homology to the human molecule > 60 %. Transcripts from the microarray analysis were selected using the column 'to be used in IPA' given in the annotation table (Oliveira *et al.*, 2011). As no comparable information had been generated during the annotation of SuperSAGE tags, detected transcripts were again compared to the information given for the microarray as described in 2.2.14.3. Information on significances, log₂ratios and gene-annotations was up-loaded into IPA. For the core analysis the user data-set served as reference, significance value and log₂ratio thresholds were chosen depending on the data-set (Fig. 2.2). Statistical tests for canonical pathways were always 'P-H Multiple testing' corrected.

2.2.14.5. Comparative analysis to previous studies

To obtain further evidence on the reliability of the data obtained in this thesis and the importance of specific genes for the difference between EM and UM, data previously generated by other studies were compared to those described in this thesis. The three largest data-sets checked for similarities were those generated in the studies of Fitzpatrick *et al.* (2006), Nawaratna *et al.* (2011) and Waisberg *et al.* (2008). Generally, comparisons between the data-sets were done by Smp_annotation comparison via Spotfire and subsequent manual correction. However, the studies of Fitzpatrick *et al.* (2006) and Waisberg *et al.* (2008) were generated previous to the publication of the *S. mansoni* genome. Thus data had to be processed previous to the comparison: As it seemed disproportionate to re-annotate the complete microarray used by Fitzpatrick *et al.* (2006), oligonucleotides for significantly regulated transcripts (in EM and/or UM) were blasted at SchistoDB 2.0 to obtain Smp_annotations. For the comparison to the data of Waisberg *et al.* (2008) served a 'list of the top 30 most differentially expressed genes in male worms due to host sex effect' (table 2 in the publication). Accession numbers given in the table were used to obtain sequences, which were then blasted at SchistoDB 2.0 to obtain Smp_numbers.

3. Results

3.1. Analyses on mitotic activity in male worms

3.1.1. Pairing inconsistently stimulates male mitotic activity

Several former studies have been concerned with the effect of EM on females and the understanding of the nature of the male-induced maturation of the female (Basch & Nicolas, 1989; Gupta & Basch, 1987; Popiel, 1986; Den Hollander & Erasmus, 1985; Basch & Basch, 1984; Popiel & Basch, 1984a; Atkinson & Atkinson, 1980; Ruppel & Cioli, 1977; Shaw *et al.*, 1977; Michaels, 1969; Armstrong, 1965; Moore *et al.*, 1954). DenHollander and Erasmus showed already in 1985 that UM take approximately 24 h longer than EM to stimulate MA in females. From this and other lines of evidence it was hypothesized that genes are differentially expressed between EM and UM. Because the data obtained by DenHollander and Erasmus (1985) were based on the measurement of mitotic activity by incorporation of [3H]thymidine into DNA, a method established in our laboratory and based on BrdU incorporation together with DNA slot-blot analysis (Knobloch *et al.*, 2002a) was used to perform similar experiments under non-radioactive conditions (2.2.11). The original experiments were done using females from unisexual infections, which could not be generated in sufficient amounts during this thesis. However, it is known that females, separated from their male partners de-differentiate into an immature-like state and also reduce mitotic activity within one week (Knobloch *et al.*, 2006). Therefore, females were separated from males after hamster perfusions and kept in culture for at least one week. After this separation period females were re-paired with either EM or UM *in vitro*. Re-paired worms were incubated with 1 mM BrdU for 12 h / 24 h / 48 h (2.2.11). To estimate MA in male and female worms DNA was extracted and the amount of incorporated BrdU determined (2.2.9).

First experiments, providing one data-set for 12 h, one for 24 h and three for 48 h of re-pairing, did not completely confirm the effect observed by DenHollander and Erasmus (1985) (Figure I., see appendix), as results were very inhomogeneous for females (Figure II., see appendix). After 12 h the MA for both groups of re-paired females was above that of the control but higher in females paired with UM. After 24 h no difference was found between the MA of females paired to EM or UM, but both showed lower MA than the according control. For 48 h re-pairing one experiment indicated higher MA in females paired with EM, while the value for females paired with UM was only slightly lower than that of the control. The second experiment showed the opposite result, while the third showed only minor differences between all three groups (control, paired with EM, paired with UM) (Figure II., see appendix).

3. Results

For males these initial experiments indicated that pairing has a stimulatory effect on MA, especially for UM (Figure III., see appendix). After 12 h of re-pairing two independent experiments showed a higher MA in paired males, EM as well as UM, compared to their respective unpaired controls. For 24 h of re-pairing two independent experiments provided contradictory results; one showing up-regulation of MA in re-paired EM, while showing down-regulation for paired UM compared to the respective controls; the other one gave opposite results, with enhancement of MA in UM and reduction in EM. For 48 h of re-pairing four experiments were done. Two showed lower MA in EM and higher MA in UM compared to controls, one showed up-regulation for both male groups and one showed down-regulation for both male groups. Technical replicas for two of the 48 h experiments confirmed the results of the first technical replica for UM but exhibited contradictory results for EM (Figure IV., see appendix).

As the male worms for these initial experiments were selected only with regard to their perfusion-origin - unisexually or bisexually infected hamsters – further experiments were performed with worms selected by stronger criteria: only EM with a definite pairing status were used; as an indicator for viability, only worms sucked to the culture dish were used; additionally, males were allowed to stay in culture for two days before the start of the experiment to regenerate (i) from perfusion stress, and (ii) in case of EM, from the stress induced by separation from females. Initial experiments had shown that higher re-pairing rates can be obtained with this procedure, an observation also supported by earlier results from other groups (Michaels, 1969).

Repetition of pairing experiments under the refined conditions, using four biological replicas for each BrdU incubation period (12 h / 24 h / 48 h) and evaluating all of them at the same time, still led to inhomogeneous, non-conclusive results (Figures V. and VI., see appendix). After 12 h of re-pairing no stimulation of MA in females was found for the first biological replica, compared to the respective controls. Stimulation of MA in females paired to EM and UM was found in two cases, but it was not possible to conclude without doubt if one was stronger than the other. Only in one case MA was stronger than the respective control for females paired to EM and lower in females paired to UM, however, in this case the MA value was extraordinarily high in the control. At 24 h of re-pairing, up-regulation of MA in females was found twice, independent of their pairing partner. However, down-regulation of MA in females was also found twice and independent of the male partners' experience state. After 48 h of re-pairing one replica showed reduced MA compared to controls for both female groups, independent of the pairing partner. Twice MA was enhanced in females paired to EM, while being reduced in females paired to UM and once MA was

enhanced in females paired to UM while it was at the level of control for females paired to EM (Figure V., see appendix). It has to be noted that DAPI-signals for female DNAs were generally weak. As final MA-values were calculated by setting BrdU signals into relation to DAPI-signals, the latter have a strong influence on the overall results.

Concerning MA in males a similar data distribution was found. After 12 h of pairing one replica showed down-regulation of MA in EM but up-regulation in UM, while another replica gave the opposite result. Of the others, two exhibited reduced values for MA in both groups of re-paired males, while the fourth one detected enhanced MA in both groups. For 24 h of pairing data from one replica showed MA to be down-regulated in both EM and UM after pairing while data from another replica detected up-regulation in both cases. The other two replicas showed decreased MA in EM and increased MA in UM. After 48 h down-regulation for both groups was found twice, while in two cases MA was enhanced in EM and reduced in UM (Figure VI., see appendix).

Thus the data of Den Hollander and Erasmus could not be confirmed, and no conclusive result was obtained concerning a stimulatory effect of pairing on mitosis in males.

3.1.2. TNF α treatment has a dose-dependent effect on mitotic activity in males

In parallel to the pairing experiments the effect of TNF α on the MA of male and female worms was analyzed. A previous publication had linked enhanced egg production to a stimulatory effect of TNF α (Amiri *et al.*, 1992). First experiments performed in our laboratory to detect a possible effect on MA in females indicated a stimulatory effect of TNF α on MA in males, an effect further investigated in this thesis. Initially, three experiments were performed testing TNF α at concentrations of 5 ng/ml, 20 ng/ml and 50 ng/ml, showing a stimulatory effect on MA in males for all these concentrations in two out of three experiments. MA was concentration-dependently enhanced with lower amounts of TNF α . In the third experiment the same concentration-dependency could be observed, however, only 5 ng/ml led to an enhanced MA. Values for the other two concentrations were below that of control (Figure VII., A-C, see appendix). To investigate whether this effect could be further increased by even lower concentrations one further experiment was done testing 0.2 ng/ml, 1 ng/ml and 5 ng/ml. Additionally, a medium test was included with the standard culture medium used in our laboratory, and Basch medium. The latter was previously used for *in vitro* experiments, which provided evidence for a role of TNF α in schistosome biology (Amiri *et al.*, 1992). Results obtained from the experiment with lower TNF α concentrations contradicted those of the previous experimental series, as a concentration-

dependent reduction of MA in males was observed in response to TNF α treatment. Also the concentration-dependent effect was influenced by the medium. Using M199 higher concentrations of TNF α led to a stronger reduction of MA, while in Basch medium lower concentrations led to a stronger reduction (Figure VII., M199 + Basch, see appendix).

The effect on females in all these experiments was inhomogeneous, showing great biological variance but also an influence of the medium, as indicated by the male data (Figure VIII., see appendix.).

In conclusion, the above described data show that TNF α exerts a concentration-dependent effect on schistosome MA, especially in male worms. However, this effect is strongly dependent on the culture medium, or rather individual components thereof, concerning strength and direction of the observed MA regulation.

3.2. The cGMP-dependent protein kinase SmcGKI may have a function in schistosome gonads

Previous results from a Diploma thesis in our group indicated a possible differential expression between EM and UM for a *S. mansoni* cGMP-dependent protein kinase (SmcGKI) (Schulze, 1997). Differentially transcribed genes were identified by RAP-PCR (RNA-fingerprinting by arbitrarily primed PCR), a method applying random 20mers during reverse transcription and subsequent amplification. Amplification products were separated on poly-acrylamide gels and differences between the used samples noted. To confirm these observations RNA slot blots and Northern blots were performed leading to contradictory results. While the first indicated stronger transcription of cGK in EM, the latter indicated no transcription in EM and some transcription in UM; the size of the detected transcript was 1.5 kb. Sequencing and data base comparison of the respective clone revealed a 189 nucleotide fragment that showed similarity to the published sequence AF009659 (Neto *et al.*, 1997) which represents a 599 bp fragment annotated as “cGMP-dependent protein kinase”. To clarify the above results the full-length coding sequence (CDS) of the cGK was identified, and first characterization studies performed (parts of these results were published in Leutner *et al.*, 2011).

3.2.1. SmcGK1 sequence identification

The full-length CDS of SmcGK1 is 3,105 nt long (accession number FR749994), encoding a protein of 1035 amino acids. From position 2,563 – 3,093 the nucleotide sequence is identical to the one previously identified in our laboratory (Schulze, 1997). Comparison of the full-length sequence to its prediction in the *S. mansoni* genome data base SchistoDB 2.0 (Smp_123290) revealed additional 165 nucleotides in the amplified sequence, at position 1,896-2,060 (Figure IX., see appendix). BlastX analyses with the complete amino acid sequence of SmcGK1 annotated the molecule to the group of membrane-bound type II cGKs. As the amino acid sequence of SmcGK1 lacks a myristoylation motive (Zhang & Rudnick, 2011; Vaandrager *et al.*, 1996) phylogenetic analyses were performed with different parts (full-length or kinase domain only) applying the software ClustalX (Larkin *et al.*, 2007). These indicated that the homology to mammalian cGKII is based on similarities within the kinase domains (Figure X. A, see appendix), while a full-length comparison placed SmcGK1 closer to the *Drosophila* cGKI and *C. elegans* cGK (Figure X. B, see appendix), giving the molecule an altogether intermediate position in cGK classification.

3.3.2. Other *S. mansoni* cGKs

Five further cGK predictions were found in the *S. mansoni* genome (SchistoDB 2.0): Smp_168670, Smp_174820, Smp_151100, Smp_080860, Smp_078230. The latter three could be amplified by RT-PCRs resulting in products of expected sizes (Figure 3.1.). The amplification product for Smp_174820 was smaller than expected (1,044 bp) (Figure 3.1.), and Smp_168670 could not be amplified at all. As the open source software SMART (http://smart.embl-heidelberg.de/smart/set_mode.cgi?NORMAL=1, Letunic *et al.*, 2012; Schultz *et al.*, 1998) predicted only a kinase domain for Smp_080860 and only cGMP-binding sites for Smp_078230 it was hypothesized that the two predictions are part of the same gene. Combination of the 5'-primer for Smp_078230 and 3'-primer for Smp_080860 resulted in a PCR product of expected size (2,123 bp) (Figure 3.1.). Since previous results had indicated differential transcription for Smp_123290 / SmcGK1 the experimental focus remained on this cGK.

3. Results

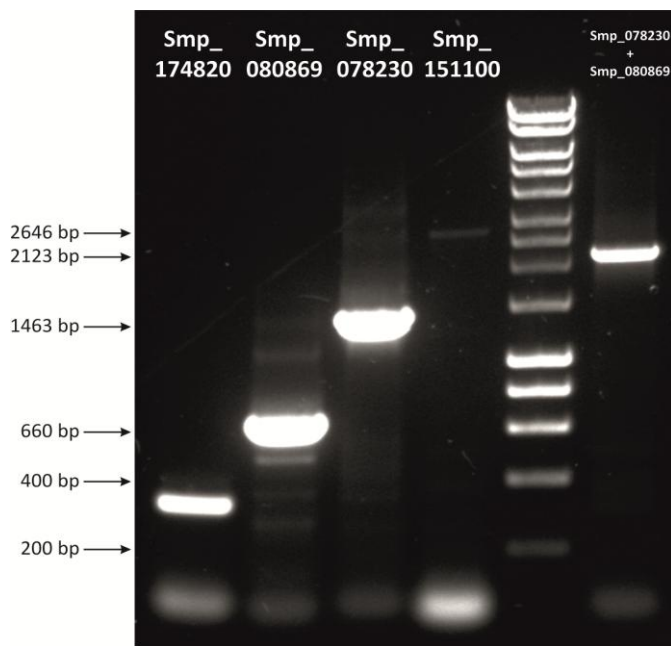


Figure 3.1: Amplification products from RT-PCR reactions for different *Schistosoma* cGKs.

Of the five *Schistosoma* cGKs other than cGKI, predicted by the genome project, four could be amplified. For Smp_151100, Smp_080860 and Smp_078230 products of the expected sizes (2,646 bp, 660 bp and 14,63 bp respectively) were obtained, while the product for Smp_174820 was much shorter (~350 bp instead of 1,044). Also a combination of the 5'-primer for Smp_078230 and 3'-primer for Smp_080860 resulted in a product, indicating that the two predictions are parts of the same gene. (marker: Hyperladder I)

3.2.3. SmcGK1 action in *S. mansoni* reproductive organs

To obtain first evidences for a functional role of cGKs in schistosomes worm couples were treated with the cGMP analog (PR)-8-pCPT-cGMPS, aiming at the inhibition of SmcGKs. Treatment with 1 mM (PR)-8-pCPT-cGMPS resulted in a reduction of egg production (Figure 3.2.) already after one day. Carmine Red staining and subsequent analysis of treated worms by confocal microscopy showed morphological changes in females but not in males (compared to respective controls). In treated females (Figure 3.2., A 1-3) a large number of mature oocytes was found in the oviduct, ovaries were disarranged, and all tissues showed disintegration, which may be a sign of apoptosis. These effects increased time-dependently (Figure 3.2.). However, two subsequent experiments (Figure XII., see appendix) lacked the immediate effect on the morphology observed during the initial assay; a slight increase of the number of oocytes within the oviduct was found only after 6 d of treatment. The reduction in egg production on the other hand was similar.

In addition to the effects on females described above, both genders were affected in their motility by the inhibitor during the initial experiment (supplementary-file6). Compared to controls the movement of treated worms became choppy over time, slowed down, and was finally reduced to near immobility. Also separation of couples occurred more often in treated worms, compared to controls.

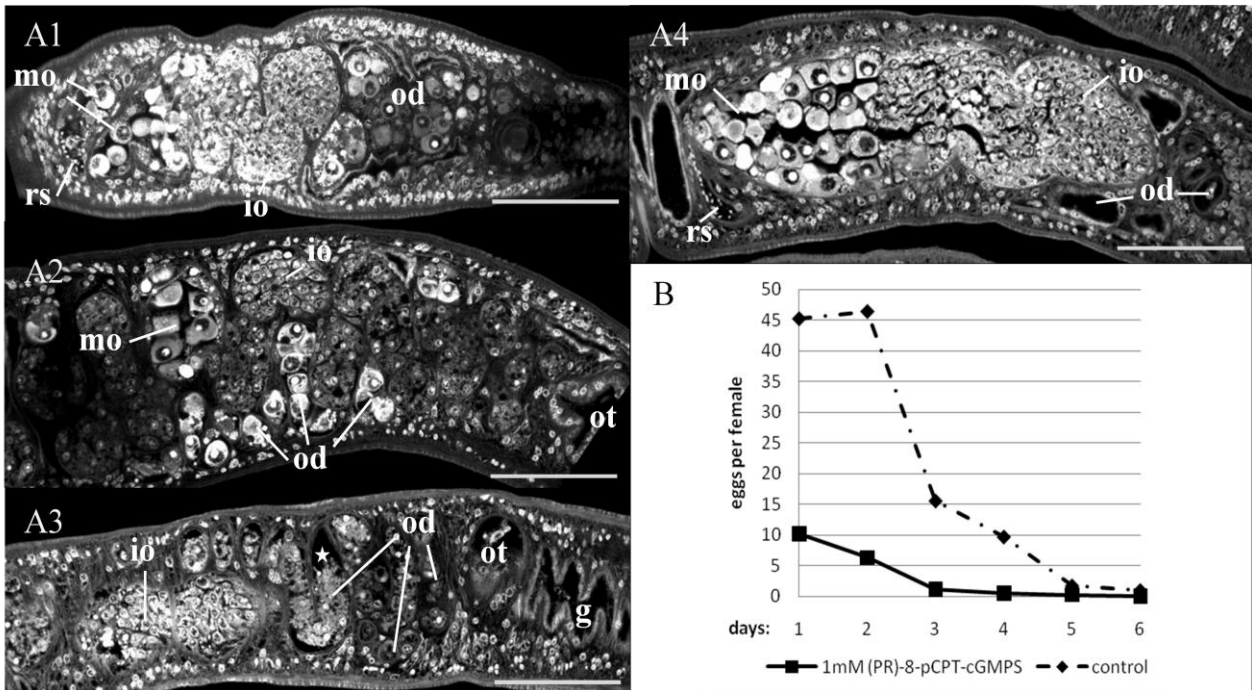


Figure 3.2: Effects of the treatment of *S. mansoni* couples with a cGK inhibitor (Leutner *et al.*, 2011).

Pictures from confocal laser scanning microscopy demonstrate the effect of the cGK inhibitor (PR)-8-pCPT-cGMPs on female morphology. Additionally *in vitro* egg production under the influence of the inhibitor is shown. **A**, influence of inhibitor treatment on the ovary and oviduct of a female worm treated with inhibitor for A1: two days, A2: four days, A3: six days; A4: untreated control after two days, which is representative for days 4-6 (scale bar: 75 μ m; g: gut; io: immature oocytes; mo: mature oocytes; od: oviduct; ot: ootype; rs: receptaculum seminis). **B**, comparison of egg production of inhibitor treated (1 mM) versus control females, showing eggs per day and female.

In situ hybridization experiments with couples and UM substantiated the results from inhibitor studies, indicating a role of SmcGK1 in the reproductive organs of schistosomes. The localization studies gave evidence for the transcription of SmcGK1 in the testes of both male groups, ovary (and vitellarium) of paired females, and the gut (at least in UM) with sense as well as anti-sense probes (Figure 3.3.).

3. Results

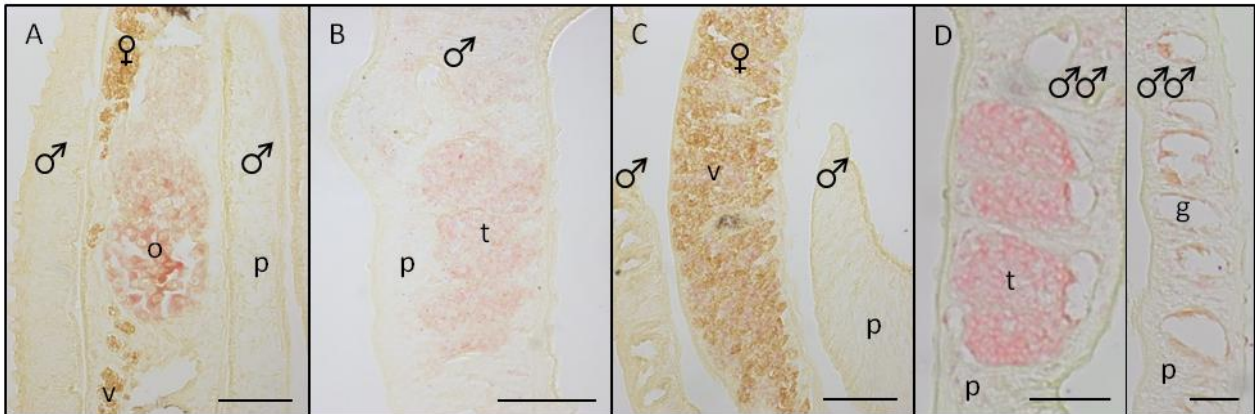


Figure 3.3: *In situ* hybridization with SmcGKI-specific anti-sense probes (modified from: Leutner *et al.*, 2011).

Pictures are representative for three different probes as well as for the detection of anti-sense RNAs. SmcGKI transcripts were detected in **A**, ovary (o), **B**, testes (t) of EM, **C**, weakly within the vitellarium (v); **D**, testes (t) of UM, gut (g) of UM. (scale bar: 50 μ m; p: parenchyma)

3.2.4. SmcGK1 anti-sense transcription

Because SmcGKI anti-sense transcription was indicated by *in situ* hybridization experiments as well as in preliminary SuperSAGE results, strand specific RT-PCR experiments were conducted aiming at the detection of the according transcripts. Specific products for both strands were found using RNAs from EM, UM, pairing-experienced females, and pairing-unexperienced females, while control reactions remained without a specific product (Figure 3.4.).

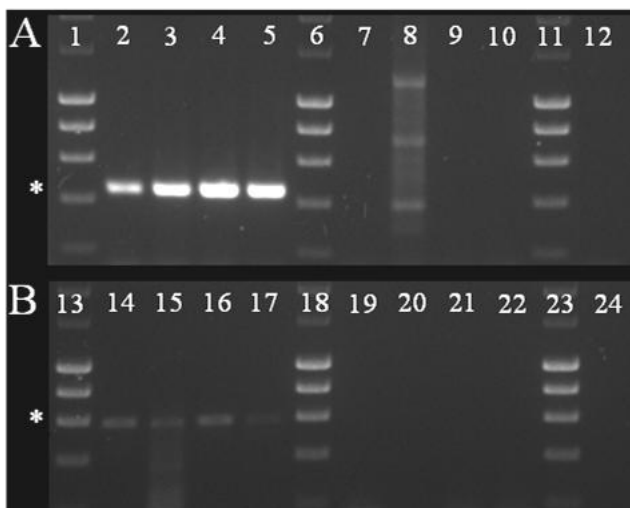


Figure 3.4: Strand-specific RT-PCRs for SmcGK1 (modified from: Leutner *et al.*, 2011)

Strand-specific RT-PCRs detected SmcGK1 sense-transcripts (A) of the expected size (452 bp; see star) in EF (2); UF (3); EM (4); UM (5). Controls: EF RT⁻ (7); UF RT⁻ (8); without template (9); EM RT⁻(10); UM RT⁻ (12). Also, SmcGK1 anti-sense transcripts (B) were detected (609 bp, see star) in EF (14), UF (15), EM (16), and UM (17). Controls (lanes 19-22, 24) as in A. Marker: Hyperladder I, lanes 1, 6, 11, 13, 18, 23.

3.2.5. Differential transcription of SmcGK1 between male stages was not confirmed

While first results from semi-quantitative RT-PCRs did not confirm differential transcription of SmcGK1 between EM and UM (Figure XI., see appendix) preliminary results from microarrays and SuperSAGE performed in this thesis indicated a possible differential transcription between the two stages. In preliminary analyses signals for one microarray oligonucleotide Q2_P04382 ($q = 0.003$, $\log_2(\text{UM}/\text{EM}) = -0.683$) and a SuperSAGE tag with the annotation Smp_123290 ($p = 1.080$, $\text{foldchange}(\text{UM}/\text{EM}) = -1.085$) indicated a significant down-regulation of SmcGK1 transcripts in UM. After establishment of real-time PCR in our laboratory (see 3.4.), differential transcription between EM and UM was tested quantitatively for three biological replicas (Figure 3.5.). Results were very variable and thus did not indicate differential transcription of SmcGK1 between EM and UM. The latter result was confirmed by the final analyses of microarray and SuperSAGE data-sets (Table I., see appendix), which indicated significant differences of transcripts between EM and UM for Smp_151100, but none of the other *S. mansoni* cGKs (Table I., see appendix).

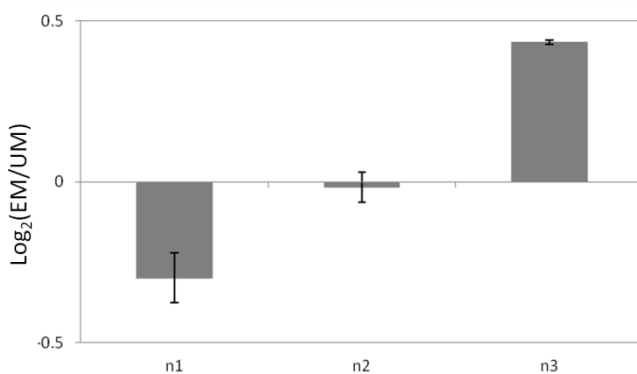


Figure 3.5 Real-time PCR for SmcGK1.

Three different biological samples (n1-n3) for EM and UM were compared *via* real-time PCR; the \log_2 ratio is depicted. Differences in SmcGK1 transcription between EM and UM varied largely, with each biological sample. Thus differential regulation for this gene between EM and UM is unlikely.

In summary, four different cGKs were amplified from *S. mansoni* by PCR. One of these, SmcGK1, was further analyzed as it had been described previously as being differentially expressed between EM and UM (Schulze, 1997). The results detailed above indicated a role for SmcGKs, and especially SmcGK1, in the reproductive organs of schistosomes, as transcripts for SmcGK1 were detected in the reproductive organs and inhibitor experiments led to a phenotype in the ovary. However, transcriptional analyses of SmcGK1 did not give sufficient evidence for differential regulation of the molecule between EM and UM. The role of an anti-sense transcript detected by *in situ* hybridization experiments as well as RT-PCR has to be further analyzed.

3.3. Transcriptome analyses comparing EM and UM

To allow a large scale detection of genes that are differentially transcribed between EM and UM, two different approaches were chosen. The platform-based microarray detects transcripts represented by oligonucleotides bound to glass slides, while the platform-independent SuperSAGE is able to detect all mRNAs with an *Nla*III restriction site, represented by short sequence tags of 27 nucleotides. By combining both methods it was intended to ensure the detection of all transcripts and to provide two independent indications for their presence. Furthermore, it was expected that each of the methods is able to detect transcripts that for technical reasons are not detectable by the other method.

Each data-set was analyzed for general transcript detection, composition of sense and anti-sense RNAs, statistical significance of detected differences between EM and UM, and distribution of elevated transcripts in either EM or UM (which implicates reduction of transcripts in the opposite pairing status). In order to facilitate the interpretation of the large scale transcriptome data and selection of molecules for first characterization studies a GO- as well as two network-analysis tools were applied.

GO analyses classify molecules within a given data-set into functional categories with the three major categories biological process, cellular component, and molecular function. A study set of genes (in this case all transcripts significantly differing between EM and UM) is compared to a population set (in this case all transcripts detected), and categories significantly enriched in the study set are detected. Those enriched categories and the genes they contain are of special interest as they indicate functions important or even specific to the studied object.

Of the two network analysis tools one – SchistoCyc - is *S. mansoni*-specific (Zerlotini *et al.*, 2009), allowing the interpretation of obtained data with regard to the detection and regulation of transcripts for metabolism-associated enzymes. The second tool, “ingenuity pathway analysis” (IPA) (Thomas & Bonchev, 2010) can be applied for transcripts with a strong homology to a human molecule (>60 %; 3,779 of 11,132 represented on the microarray). The program searches within a given data-set for potential molecular networks and canonical pathways enriched for significantly regulated transcripts as well as activated transcription factors based on the differential transcription of their targets.

3.3.1. Microarray analyses detected 1,572 significantly regulated transcripts

Microarray analyses were conducted in cooperation with Prof. Sergio Verjovski-Almeida and Dr. Katia Oliveira at the University of Sao Paulo. Three samples of EM and UM were used, each generated by infections of hamsters with unisexual or bisexual cercariae. RNA was extracted from approximately 25 worms per sample. After reverse transcription to cDNA and *in vitro* amplification, during which Cy3 or Cy5 labeling dyes were incorporated, RNAs were hybridized to the microarrays in technical quadruplicates (including dye swap) (2.2.14.1). Hybridization results were evaluated with Agilent feature extraction software. Subsequent data processing included calculation of \log_2 ratios, data filtering for consistency of transcript detection and annotation of detected transcripts.

After re-annotation of the 44k oligonucleotide array (Verjovski-Almeida *et al.*, 2007) in 2011 (Oliveira *et al.*, 2011) 19,197 oligonucleotides were selected as gene representatives: 11,132 detecting RNAs in orientation of predicted transcripts, and 8,065 detecting RNAs complementary to predicted transcripts. Of these 19,197 representatives, 10,115 were detected as defined in 2.2.14.1; 1,966 representing anti-sense and 8,149 representing sense-detecting oligonucleotides.

During the process of merging microarray and SuperSAGE data (see chapter 3.3.3.) a number of 1,006 oligonucleotides without gene predictions according to the latest microarray annotation (Oliveira *et al.*, 2011) could be annotated to gene predictions in SchistoDB 2.0 manually. This changed the number of detected sense transcripts from 8,149 to 7,494.

Significance analysis for microarrays (SAM) (Tusher *et al.*, 2001) was performed (see 2.2.14.1.), and afterwards only sense transcripts were further analyzed. Figure 3.6. shows a hierarchical clustering of the 1,571 sense transcripts that were significant ($q < 0.01$) after statistical analysis, of these 629 transcripts were up-regulated in EM and 942 transcripts were up-regulated in UM (supplementary-file5). The figure shows, that technical replicas cluster according to their biological origin but also emphasizes differences between technical replicas.

Gene Ontology of data obtained by microarray analyses

A Gene Ontology analysis of the 1,571 significantly regulated transcripts identified 22 categories to be significantly enriched ($p < 0.05$) in study sets representing genes with enhanced transcripts in either EM or UM. Only one of these enrichments, the category membrane, was detected for the transcripts enhanced in EM (Figure 3.7.; Table II., see appendix), while all others were found for transcripts enhanced in UM. Most enriched categories belonged to the super-ontology biological process.

3. Results

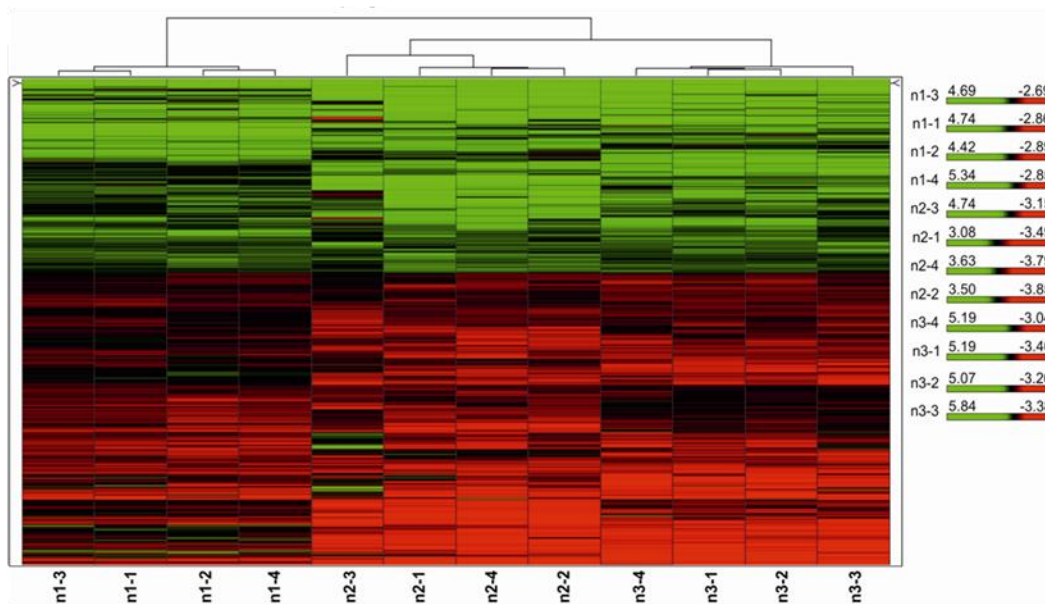


Figure 3.6: Hierarchical clustering of transcripts significant after SAM.

A hierarchical clustering (Ward's method) for significantly ($q < 0.01$) regulated transcripts from all technical replicas, tested in the microarray analyses is shown. Colors and color intensities indicate the strength and direction of regulation for each transcript. Green: genes with higher transcript levels in EM. Red: genes with higher transcript levels in UM. The dendrogram at the top indicates that technical replicas cluster according to their biological origin (n1-n3).

SchistoCyc – metabolic analysis of the data obtained by microarrays

Of the 1,571 genes with transcript levels significantly different between EM and UM in the microarray analyses 1,263 had Smp_numbers, which were used to continue the analysis. The SchistoCyc tool (Zerlotini *et al.*, 2009) recognized 1,227 Smp_numbers but only 125 could be matched to metabolic processes (Table III., see appendix):

- **Carbohydrates:** For a number of enzymes involved in carbohydrate biosynthesis processes, transcripts were found to be significantly up-regulated in UM. They belong to the pathways glycogen biosynthesis, UDP-galactose biosynthesis, galactose degradation, UDP-N-acetyl-D-galactosamine biosynthesis and GDP-mannose biosynthesis. Also several transcripts were significantly up-regulated in EM, belonging to the pathways UDP-galactose biosynthesis, galactose degradation, GDP-L-fucose biosynthesis I and GDP- α -D-perosamine biosynthesis.
- **Pentose-phosphate cycle:** No transcripts associated with pentose-phosphate cycle were detected to be significantly regulated.
- **Glycolysis, citrate cycle, aerobic respiration and amino acids:** Transcripts detected as significantly regulated and coding for enzymes involved in glycolysis, citrate cycle, aerobic respiration or amino acid associated pathways were enhanced in UM, apart from one exemption for amino acid biosynthesis.

- **Lipids and fatty acids:** Significantly up-regulated transcripts in EM were detected for enzymes involved in the mevalonate pathway, fatty acid β -oxidation, phospholipid biosynthesis, di- and triacylglycerol biosynthesis. Significant up-regulation in UM was detected for transcripts of other enzyme of the mevalonate pathway, di- and triacylglycerol biosynthesis and additionally of glycerol degradation processes.
- **Bases:** Transcripts for enzymes involved in degradation of purine ribonucleosides, salvage pathways of guanine, xanthine and their nucleosides, salvage pathways of pyrimidine ribonucleotides and salvage pathways of adenine, hypoxanthine and their nucleosides were significantly up-regulated in EM. While transcripts for enzymes associated to formyltetrahydrofolate biosynthesis, de novo synthesis of uridine-5'-monophosphate, de novo biosynthesis of pyrimidine deoxyribonucleotides and salvage pathways of adenine, hypoxanthine and their nucleosides were significantly up-regulated in UM.
- **Other:** Other pathways, for which transcripts of enzymes were detected as significantly regulated between EM and UM, were: betaxanthin biosynthesis, betacyanin biosynthesis, phenylethanol biosynthesis, catecholamine biosynthesis, and glutathione biosynthesis (up-regulated in EM), and sulfide oxidation, catecholamine biosynthesis, colonic acid building block biosynthesis, heme biosynthesis, geranyldiphosphate biosynthesis and geranylgeranyldiphosphate biosynthesis for transcripts up-regulated in UM.

Ingenuity pathway analysis of the data obtained by microarrays

IPA detected two canonical pathways enriched for significantly regulated transcripts - citrate cycle and mitochondrial dysfunction. No transcription factors were predicted to be activated. However, a large number of possible networks was found within the significantly regulated transcripts, combining functional categories as follows (given are networks with more than 10 molecules):

1. Cardiovascular Disease, Genetic Disorder, Metabolic Disease.
This network contains a noticeable number of NADH-dehydrogenases and other molecules related to metabolism, all according transcripts were significantly up-regulated in UM.
2. Cancer, Genetic Disorder, Neurological Disease.
3. Cell-To-Cell Signaling and Interaction, Nervous System Development and Function, Cell Morphology.
Within this network were several potassium channels and glutamate receptors, all transcripts were significantly up-regulated in UM.
4. Post-Translational Modification, Protein Folding, Nucleic Acid Metabolism.
5. Cellular Growth and Proliferation, Cellular Development, Nervous System Development and Function.
6. Cell Death, Carbohydrate Metabolism, Small Molecule Biochemistry.

3. Results

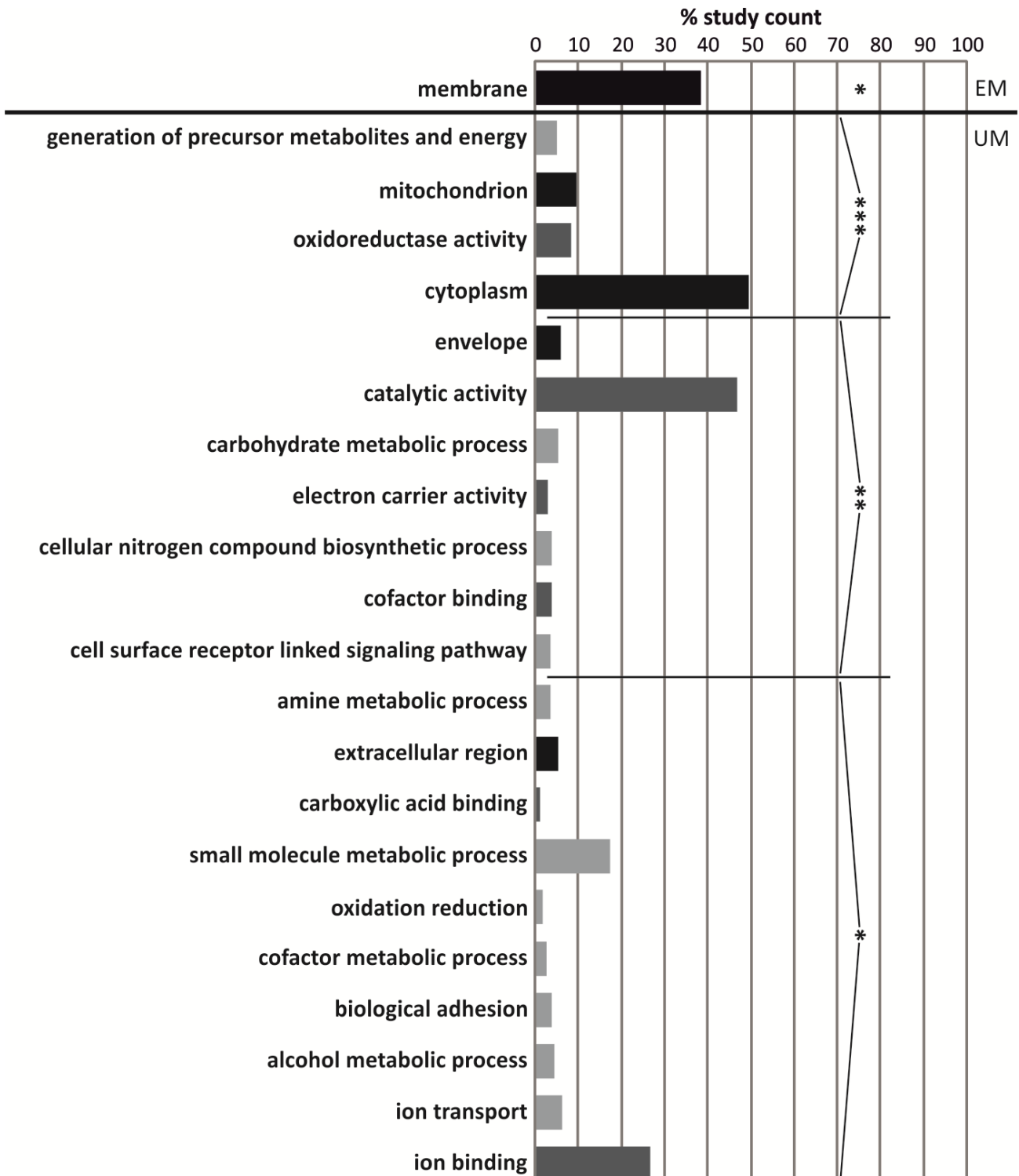


Figure 3.7: Gene Ontology - enriched categories for transcripts significantly regulated between EM and UM according to the microarray analyses.

A gene ontology analysis was performed for transcripts significantly regulated according to the microarray experiments. Only one category was significantly enriched for genes with higher transcript levels in EM, while 21 were significantly enriched for genes with a higher transcript levels in UM. Light grey: biological process; grey: molecular function; black: cellular component; p-values for the GO analysis: * $p < 0.05$, ** $p < 0.005$, *** $p < 0.0001$.

7. Cellular Assembly and Organization, Cellular Function and Maintenance, DNA Replication, Recombination, and Repair.
8. DNA Replication, Recombination, and Repair, Energy Production, Nucleic Acid Metabolism.
This network contains a number of ATPsynthases and ATPases, for which transcripts were significantly up-regulated in UM.
9. Cell Death, Cellular Development, Hematopoiesis.
Several DNAJ transcripts were significantly up-regulated in UM within this network.
10. Small Molecule Biochemistry, Drug Metabolism, Endocrine System Development and Function.
11. Cell-To-Cell Signaling and Interaction, Nervous System Development and Function, Amino Acid Metabolism.
12. Lipid Metabolism, Small Molecule Biochemistry, Vitamin and Mineral Metabolism.
13. Cellular Assembly and Organization, Cellular Function and Maintenance, Protein Synthesis.
This network contains a number of cytoskeleton related proteins, for most of which transcripts were up-regulated in EM.
14. Cellular Function and Maintenance, Cellular Compromise, Cellular Assembly and Organization.
15. Cellular Function and Maintenance, Drug Metabolism, Molecular Transport.
16. Embryonic Development, Organismal Development, Biliary Hyperplasia.
17. Cell Cycle, Hair and Skin Development and Function, Antigen Presentation.
18. Molecular Transport, Carbohydrate Metabolism, Cellular Growth and Proliferation.
19. Cellular Movement, Cell-To-Cell Signaling and Interaction, Cell Morphology.
20. Cellular Function and Maintenance, Nucleic Acid Metabolism, Small Molecule Biochemistry.
21. Hepatic System Development and Function, Liver Proliferation, Tissue Morphology.
22. Genetic Disorder, Metabolic Disease, Cellular Function and Maintenance.
23. Cellular Movement, Cellular Development, Cellular Growth and Proliferation.
Within this network the molecule follistatin stands out for the strong, significant up-regulation of its transcripts in UM. Follistatin is a potential inhibitor of TGF β -pathways (Moustakas & Heldin, 2009; Massagué & Chen, 2000).
24. DNA Replication, Recombination, and Repair, Nucleic Acid Metabolism, Small Molecule Biochemistry.
This network includes molecules like wnt5A, several G-protein coupled receptors (GPCRs) and G-proteins, as well as the signal transduction molecule lin-9, for which transcript were significantly regulated between EM and UM.
25. Cell Cycle, DNA Replication, Recombination, and Repair, Cancer.

The comparative analysis of the transcriptomes of EM and UM by microarray experiments detected a large number of transcripts significantly regulated between these two stages. GO and network analyses revealed an overall bias towards transcript up-regulation in UM, when searching for any kind of enriched categories or networks. Within this group of transcripts up-regulated in UM was follistatin (Smp_123300), belonging to the GO category extracellular region and the IPA networks 18 and 23. This transcript came into focus, as it codes for a potential inhibitor of TGF β -

pathways (Moustakas & Heldin, 2009; Massagué & Chen, 2000). Previous studies (Knobloch *et al.*, 2007; LoVerde *et al.*, 2007) have linked these pathways to *S. mansoni* female developmental processes. Furthermore TGF β -pathways were postulated to be involved in male-female interaction (LoVerde *et al.*, 2009; LoVerde *et al.*, 2007).

3.3.2. SuperSAGE detected 53 or 815 significantly regulated transcripts depending on the applied statistics

SuperSAGE experiments were performed in cooperation with the company GenXPro (Frankfurt, Germany). Similar to the microarray experiments three samples of EM and UM each were collected, independently from each other as well as from the microarray samples. A minor change was executed concerning worm-selection: EM not only had to originate from bisexual hamster infection as for the microarray experiments, but were additionally collected from freshly separated couples. Worms for both groups had to be physically vital, the according indicator being their adhesion to culture dishes with the ventral sucker and their regular wave-like movement. RNA was extracted from 50 worms per sample. The further experimental procedure was performed by GenXPro according to an internal protocol (Matsumura *et al.*, 2010; Molina *et al.*, 2008; Matsumura *et al.*, 2003).

SuperSAGE tags were annotated with the same procedure used for the revised version of the 44k oligonucleotide array, and counts for different tags were summed up, if they showed the same annotation. As for the microarrays, transcripts were classified into sense and anti-sense. Additionally, SuperSAGE transcripts were further distinguished into predicted intron- or exon-sequences. Thus 25,597 transcripts were detected with SuperSAGE (wherein up to four transcripts according to the annotated category represented one gene).

Two different significance analyses were performed for SuperSAGE. Initially the R implementation EdgeR (Robinson *et al.*, 2010) was used. Based on this statistics most genes were selected for real-time PCR verification. However, performing EdgeR resulted in a very low number of transcripts recognized as significantly regulated between the two stages. Since the microarrays in comparison detected a vast number of significantly regulated transcripts a meaningful comparison of the two data-sets seemed impossible, and a bias towards the microarray results inevitable. Therefore a second statistical analysis was performed for the SuperSAGE data, according to the method of A&C (Audic & Claverie, 1997).

Subsequent to each of the significance analyses (with all 25,597 transcripts) 5,987 transcripts without annotation as well as 7,124 transcripts classified as anti-sense were excluded from further analyses. Of the remaining 12,486 sense transcripts 8,969 were classified as representing exons and 3,517 were classified as representing introns. Altogether, sense transcripts were found for a number of 9,344 unique genes. Of these, 5,601 genes had representatives in both groups classified, exons as well as introns. For 2,581 genes only exon representing sense transcripts were detected, and for 219 genes only intron representing sense transcripts were detected.

3.3.2.1 SuperSAGE – EdgeR statistical analysis of SuperSAGE data

Using EdgeR statistics to analyze SuperSAGE data for significant ($p < 0.05$) regulation between EM and UM, resulted in the identification of 53 transcripts (supplementary-file7, sheet “unique-sense-transcripts signif”): 26 up-regulated in UM, 27 up-regulated in EM. The hierarchical clustering and list of the respective genes are presented in figure XIII. and table IV. (see appendix). A GO analysis with these gene-representatives did not result in any significantly enriched categories, which can be explained by the low number of significantly regulated transcripts. 47 transcripts were uploaded into the SchistoCyc omics viewer tool (Zerlotini *et al.*, 2009), which were all recognized but only one was associated to metabolic processes: aromatic-L-amino-acid decarboxylase/ dopa-decarboxylase (DDC) (Smp_135230), up-regulated in EM, belonging to the pathways phenylethanol biosynthesis and catecholamine biosynthesis. Using EdgeR SuperSAGE data in IPA no canonical pathways enriched for significantly regulated transcripts and no activated transcription factors were detected; just one network was found: “Amino Acid Metabolism, Molecular transport, Small Molecule Biochemistry”. The network contained five significantly regulated transcripts. One, follistatin (Smp_123300), was up-regulated in UM, the four others, a signal peptidase (Smp_024390.x, significant), a solute carrier (Smp_145980.x; significant), an ATPase (gi|60692940, significant), a glutamate transporter (Smp_147390; not significant), and a RNA polymerase (Smp_165980) were up-regulated in EM.

3.3.2.2 SuperSAGE – Audic & Claverie statistical analysis of SuperSAGE data

Due to the low amount of significantly regulated transcripts found by EdgeR statistics, which complicated the comparison to the microarray data, a second significance analysis using the method of A&C (Audic & Claverie, 1997) was executed for the SuperSAGE data. According to this statistical evaluation (supplementary-file8) sense-transcripts for 815 genes were significantly ($p < 10^{-10}$) regulated between EM and UM. Of these, 393 were up-regulated in EM and 422 up-regulated in UM (Figure 3.8.; supplementary-file8,sheet: „unique-sage-sense-sig”).

3. Results

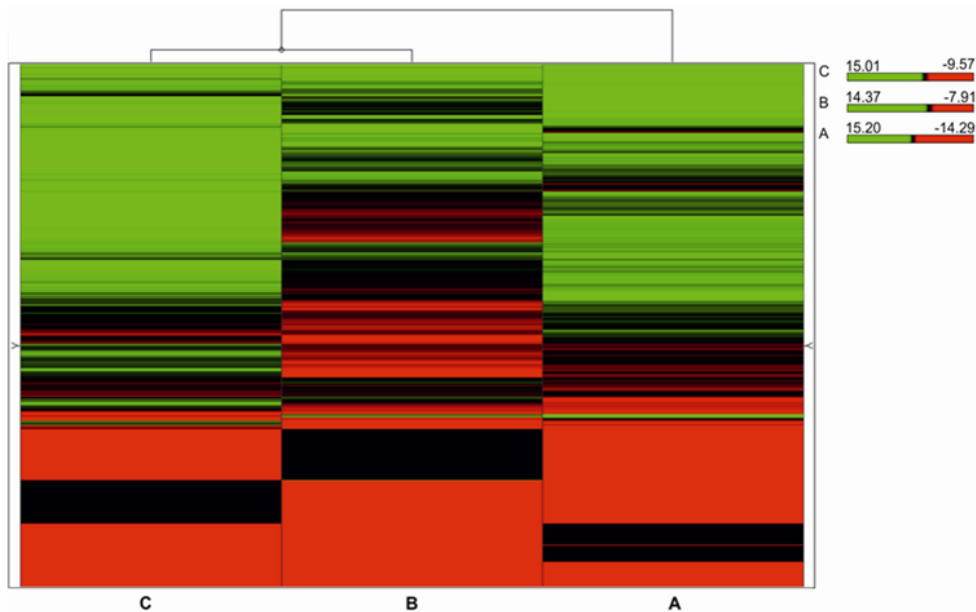


Figure 3.8: Hierarchical clustering of transcripts significantly regulated in SuperSAGE data according the statistics of Audic and Claverie.

Hierarchical clustering (Ward's method) of significantly regulated transcripts from all replicas tested in SuperSAGE. Colors and color intensities indicate the strength and direction of regulation for each transcript. Green: genes with higher transcription in EM. Red: genes with higher transcription in UM. A, B, C: biological replicas 1-3.

Gene Ontology of SuperSAGE data analyzed with the A&C statistics

For each set of up-regulated transcripts a GO analysis was performed. However, only 368 of the EM up-regulated transcripts and 343 of the UM up-regulated transcripts could be used for GO as the reference files for the tool were adapted to the contigs used in the design of the microarray, on which some of the transcripts detected by SuperSAGE were not represented. For the same reasons the reference population (=population count), which should consist of all detected genes, contained only 6,821 of 9,344 transcripts. No significantly enriched categories were found for the transcripts up-regulated in EM, but seven significantly enriched categories ($p < 0.05$) were detected for transcripts up-regulated in UM (Figure 3.9.; Table V., see appendix) with the super-ontology 'cellular component' dominating.

SchistoCyc – metabolic analysis of SuperSAGE data significant according to the A&C statistics

Of the 815 transcripts that were significantly regulated between EM and UM according to SuperSAGE those that had Smp_numbers were uploaded into the software tool, which recognized 782 of the genes and associated 60 to metabolic pathways (Table VI., see appendix):

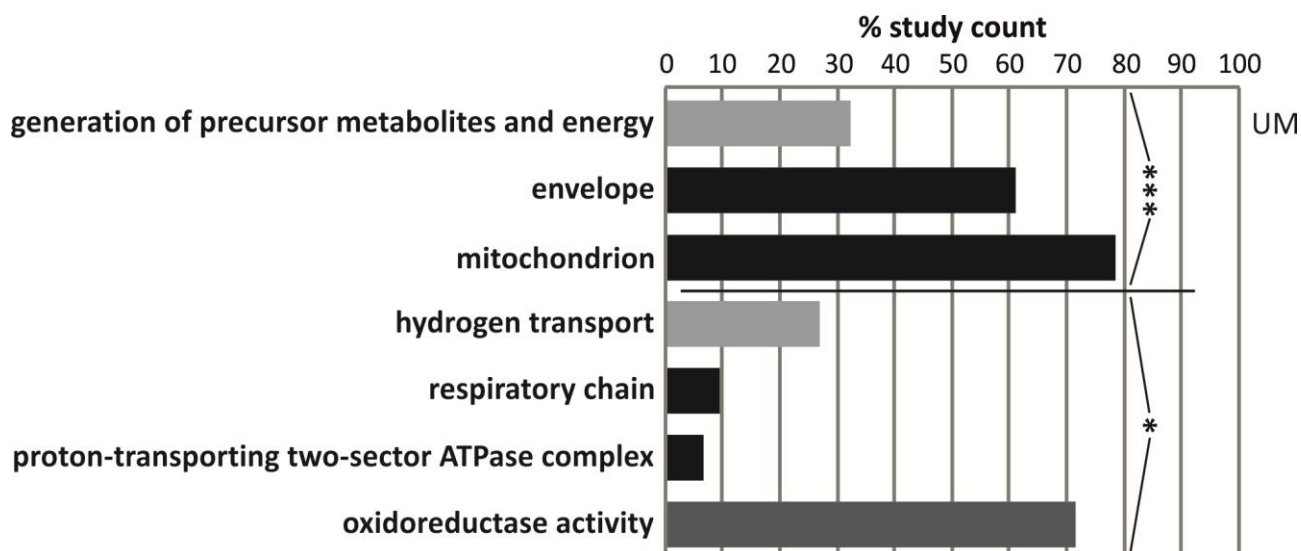


Figure 3.9: Gene Ontology - enriched categories for transcripts significantly regulated between EM and UM according to SuperSAGE.

Categories significantly enriched for genes with higher transcription in UM are shown. No categories were found to be significantly enriched within the transcripts up-regulated in EM. light grey: biological process; grey: molecular function; black: cellular component; p-values for the GO analysis: * $p < 0.05$, *** $p < 0.0001$.

- **Carbohydrates:** For enzymes participating in carbohydrate biosynthesis processes, one transcript was significantly up-regulated in UM (GDP-mannose biosynthesis) and one up-regulated in EM (D-mannose degradation).
- **Pentose-phosphate cycle:** One transcript coding for an enzyme associated to the pentose-phosphate cycle was found. Transcripts for 6-phosphogluconolactonase were significantly up-regulated in EM.
- **Glycolysis:** Of 6 transcripts for enzymes involved in glycolysis, detected as significantly regulated between EM and UM, 4 were up-regulated in UM and 2 in EM.
- **Citrate cycle:** One transcript coding for an enzyme involved in the citrate cycle was detected to be significantly up-regulated in UM.
- **Aerobic respiration:** Apart from one transcript all significantly regulated transcripts for enzymes involved in aerobic respiration were up-regulated in UM.
- **Lipids and fatty acids:** Several transcripts for members of di- and triacylglycerol biosynthesis, glycerol degradation, fatty acid biosynthesis, elongation and β -oxidation were significantly up-regulated in EM. Transcripts significantly up-regulated in UM were found for trans,trans-farnesyl diphosphate biosynthesis, CDP-diacylglycerol biosynthesis, mevalonate pathway, di- and triacylglycerol biosynthesis as well as glycerol degradation. Apart from a putative glycerol-3-phosphate dehydrogenase (Smp_030500.x) involved in CDP-diacylglycerol biosynthesis none

3. Results

of the transcripts were the same as found for this category within the significantly regulated genes from the microarray experiments.

- **Amino acids:** Enzymes associated with amino acid biosynthesis-processes, for which transcripts were detected to be significantly regulated between the two male stages, are involved in arginine degradation, alanine biosynthesis, alanin degradation, thioredoxin biosynthesis (up in UM), glutathione biosynthesis and S-adenosyl-L-methionine cycle (up in EM).
- **Bases:** All transcripts for enzymes involved in base synthesis detected as significantly regulated between EM and UM were enhanced in the unexperienced stage.
- **Other:** Transcripts for one enzyme involved in either catecholamine biosynthesis or phenylethanol biosynthesis were significantly up-regulated in EM.

Comparing the metabolomic analyses of SuperSAGE and microarray data the most evident difference was found for transcripts representing enzymes involved in base biosynthesis, which were significantly up-regulated in UM in the SuperSAGE data. Other transcripts significantly up-regulated in EM in the microarray data code for enzymes involved in according salvage or degradation processes.

Ingenuity pathway analysis of SuperSAGE data analyzed with A&C statistics

Analyzing the obtained SuperSAGE data with the IPA tool, one canonical pathway was found to be enriched for significantly regulated transcripts: Oxidative phosphorylation. Furthermore, three transcription factors were predicted to be activated (supplementary-file9): ‘peroxisome proliferator-activator receptor gamma, coactivator 1 alpha’ (PPARGC1A), ‘estrogen-related receptor alpha’ (ESRRA), ‘CCAAT/enhancer binding protein (C/EBP), alpha’ (CEBPA). Compared to the microarray analyses, fewer networks enriched for significantly regulated transcripts were found (also due to the lower number of significantly regulated transcripts); these included the following categories (given are those networks with more than 10 molecules):

1. Gene Expression, Protein Synthesis, Cell Death.
2. DNA Replication, Recombination, and Repair, Energy Production, Nucleic Acid Metabolism.
The network contains many ATP synthases, for which transcripts were up-regulated in UM and ATPases for which transcripts were up-regulated in EM.
3. Drug Metabolism, Endocrine System Development and Function, Lipid Metabolism.
4. Cellular Development, Hematopoiesis, Cell Death.
Within this network are a number of heat shock proteins and several DNAs for which transcripts were up-regulated in EM.
5. Cell Cycle, Cancer, Cell Morphology.

Like network 1 found in the array by IPA, this network contains several NADH-dehydrogenases for which transcripts were up-regulated in UM.

6. Infectious Disease, Cellular Assembly and Organization, Cellular Function and Maintenance.
7. Dermatological Diseases and Conditions, Infectious Disease, Organismal Injury and Abnormalities.
8. Cellular Movement, Drug Metabolism, Endocrine System Development and Function.
9. Cancer, Reproductive System Disease, Renal and Urological Disease.
10. Cell-To-Cell Signaling and Interaction, Cellular Movement, Infectious Disease.
11. Gene Expression, Cell Cycle, Cellular Growth and Proliferation.
12. Cell Cycle, Cellular Development, Cellular Growth and Proliferation.

SuperSAGE detected fewer transcripts to be significantly regulated between EM and UM than the microarrays. Similar to the microarrays, GO and network analyses indicated a bias of enriched groups towards UM up-regulated transcripts. Corresponding to the microarray analyses, SuperSAGE also detected transcripts of the TGF β -pathway inhibitor follistatin as significantly up-regulated in UM.

3.3.3. Combinatory analysis of microarray and SuperSAGE data

To facilitate the discovery of transcripts significantly regulated in both analyses, respective results were compared. Additionally, the impact of biological variance and / or method-dependency of the above results was evaluated. To this end sense data from both approaches were compared applying the software Spotfire, or manually, if necessary.

A number of 6,326 transcripts were detected by both methods (supplementary-file10; supplementary-file11), while 3,018 were found with SuperSAGE only (supplementary-file12) and 1,168 with the microarrays only (supplementary-file13) (Figure 3.10.).

For the overlap of genes with significantly regulated transcripts between EM and UM, analyses were in agreement for 11 transcripts only, using EdgeR statistics for the SuperSAGE data (Figure 3.10.). In sum this statistical setup detected 31 transcripts in the overlap to be significantly regulated between the two male stages in SuperSAGE, while 1,341 were found for the microarrays. Any further data analyses performed with this combinatory data-set would be 'array biased'. This, in addition to the altogether low amount of genes detected as significantly transcribed between EM and UM in SuperSAGE EdgeR statistical analysis encouraged the search for another statistical approach, leading to the A&C statistics for SuperSAGE (see 3.3.2.2).

It has to be noted that among the 11 protein coding genes within the overlap of significantly

3. Results

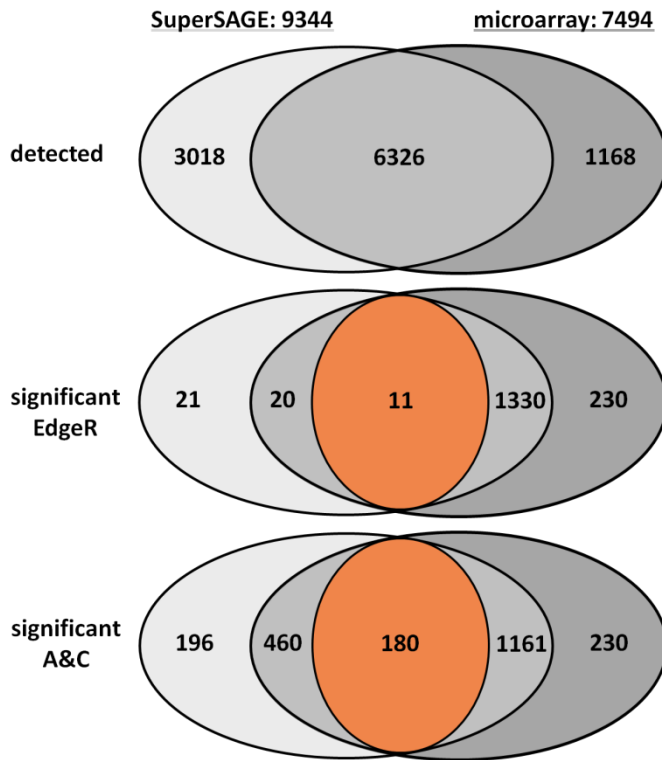


Figure 3.10: Venn diagram of SuperSAGE and microarray data.

The diagram presents counts for transcripts detected by either one or both methods, and also the amount of genes significantly regulated between EM and UM in each of the resulting groups. For these transcripts the contrast between the two SuperSAGE statistical approaches is demonstrated. Light grey: SuperSAGE; grey: transcripts detected by both analyses; dark grey: microarray; orange: genes significantly regulated between EM and UM within the overlap of both transcriptome approaches.

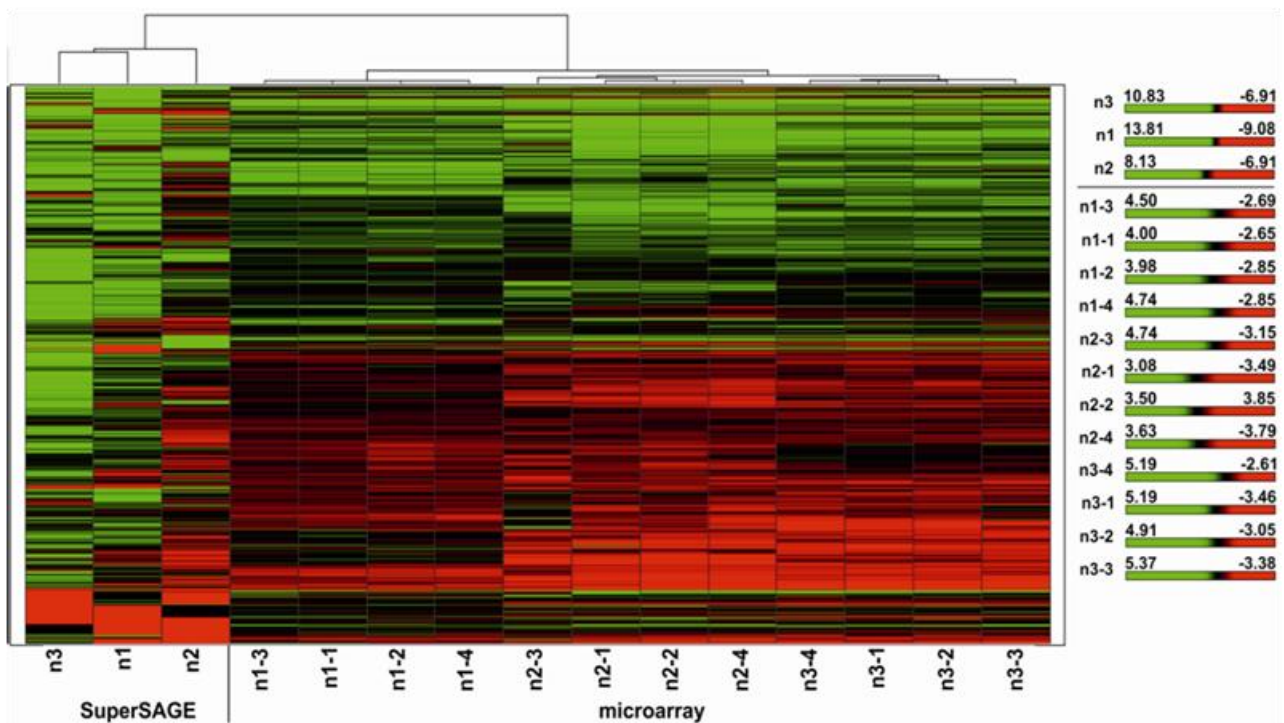


Figure 3.11 Hierarchical clustering of transcripts significantly regulated in SuperSAGE and/or microarray analyses.

A hierarchical clustering (Ward's method) is shown for transcripts significantly regulated according to microarray statistics, SuperSAGE statistics (A&C), or both. Log₂ratios from all microarray technical replicas as well as all SuperSAGE biological replicas are represented. Colors and color intensities indicate the strength and direction of regulation for each transcript.

Green: genes with higher transcript levels in EM; Red: genes with higher transcript levels in UM, the dendrogram at the top indicates that replicas cluster according to their biological (n1-n3) and methodological origin.

regulated transcripts from microarrays and SuperSAGE-EdgeR, only 4 had functional annotations and showed the same direction of regulation in both analyses. Among these, only follistatin (Smp_123300) had a functional annotation related to signal transduction. The other transcripts were: DDC (Smp_135230), oxalate-formate antiporter (OxIT) (Smp_036470) and an AMP dependent ligase (Smp_158480).

Performing the data comparison between microarray analyses and SuperSAGE with A&C-statistics, 180 transcripts were detected by both analyses to be significantly regulated, while further 460 were significantly ($p < 1^{-10}$) regulated according to the SuperSAGE statistics only, and 1,161 were significantly ($q < 0.01$) regulated according to the microarray statistics only (Figure 3.10).

This collection of transcripts significantly regulated in only one or both analyses is represented by the hierarchical clustering in figure 3.11. The figure demonstrates strong differences between the two analyses for individual transcripts. Also, the same collection of genes was used for a GO analysis (Figure XIV., see appendix). Comparing the GO for these combined data to the GOs performed for the single analyses, strong similarities between the array-GO and the combined-GO were found (as indicated in Figure XIV., see appendix). Thus a strong bias of significant genes in the overlap between the two analyses towards the microarray data was noted, even with the changed statistics for SuperSAGE data. This, in combination with the observation from preliminary real-time PCR data available at this time-point, led to the decision that further data analyses concerning transcripts detected by both analyses should be done only with those significantly regulated in both analyses (Table VII., see appendix).

Repetition of the hierarchical clustering using only the 180 transcripts significantly regulated in both analyses (Figure XV., see appendix) showed once again the strong differences in regulation between the two methodological approaches for individual transcripts.

Data differing between both analyses

Of the transcripts detected in one of the analyses only those which showed significant regulation between EM and UM were further analyzed; 175 in case of SuperSAGE-A&C and 230 in case of the microarrays (supplementary-file12; supplementary-file13). In search for an explanation as to why these transcripts were detected by only one of the two methods, significantly regulated SuperSAGE transcripts were checked against those represented on the microarray, and some of the microarray transcripts were analyzed for *Nla*III restriction enzyme recognition sites. As the microarray does not contain representatives for some transcripts and since SuperSAGE can only detect transcripts containing a *Nla*III restriction enzyme recognition site (see 2.2.14.2.) the lack of

3. Results

transcript detection by one method can be explained by the specific approach. In case of the 175 significantly regulated SuperSAGE-only transcripts 78 were not detected by the microarray, while 97 were actually newly found (Table. 3.1.). Only 54 of the 230 transcripts significantly transcribed according to the microarray-only group had Smp_ annotations, 98 transcripts had no homologies to known *Schistosoma* sequences, 62 were annotated to known contigs, and 16 to *S. japonicum* genes. The CDS of 21 genes from the list of transcripts detected by the microarrays only were subjected to a restriction site search engine (<http://www.restrictionmapper.org/>). They were chosen, because they each had a Smp_number and respective transcripts were strongly regulated. Only 3 of these 21 transcripts had no *Nla*III site (Table. 3.2.).

Gene Ontology for transcripts significantly regulated according to microarrays and SuperSAGE

Performing a GO analysis for the 180 transcripts detected as significantly regulated between EM and UM in both transcriptome analyses, the tool detected significantly ($p < 0.05$) enriched categories for transcripts up-regulated in UM, only (Figure 3.12.). Compared to the single method data analyses, altogether fewer categories were significantly enriched even within the data-set of UM up-regulated transcripts. No super-ontology was dominant.

SchistoCyc – metabolic analysis of transcripts significantly regulated in both analyses

Of the 180 genes significantly transcribed between EM and UM according to both analyses 171 had Smp_numbers and were uploaded into SchistoCyc (Zerlotini *et al.*, 2009). The software tool recognized 165 of these gene-representatives and matched 18 to metabolic pathways of which all but one were up-regulated in UM (Table IX., see appendix):

- **Carbohydrates:** Only one significantly up-regulated transcript in UM was identified as associated with carbohydrate-related metabolic reactions and the pathway GDP-mannose biosynthesis.
- **Pentose-phosphate cycle:** No transcripts associated to this metabolic cycle were found to be significantly regulated.
- **Glycolysis, citrate cycle, aerobic respiration:** All transcripts for enzymes involved in any of these processes were significantly up-regulated in UM.
- **Lipids and fatty acids:** One transcript encoding for an enzymes involved in CDP-diacylglycerol biosynthesis as well as glycerol degradation was detected to be significantly up-regulated in UM compared to EM.

Table 3.1. Selection of transcripts detected by SuperSAGE only.

ID	Gene annotation Smp	Source	Average log ₂ (EM/UM)	p-value (A&C)	Probe Name
Smp_130690	zinc finger protein, putative	Exon	8.54	1.59E-20	Q2_P01072
JAP09507.C	dynein, axonemal, heavy chain 10 [Homo sapiens]	Exon	5.57	1.98E-246	Q2_P39947
Smp_011100	M16 family peptidase, putative	Exon	4.30	5.49E-38	n.o.
Smp_157750	rna-binding protein musashi-related	Exon	3.31	8.37E-11	Q2_P20135
Smp_173350.x	egg protein CP391S-like	Exon	2.70	6.52E-23	Q2_P18640
Smp_008660.1	gelsolin isoform a precursor [Homo sapiens]	Exon	0.91	0	Q2_P18327
Smp_160360	sodium/chloride dependent neurotransmitter transporter, putative	Exon	0.89	2.08E-26	Q2_P00318
Smp_097020.4	fbxl20, putative	Exon	0.74	2.76E-11	Q2_P24759
Smp_186050	heat shock protein, putative	Exon	0.73	2.02E-141	Q2_P34228
Smp_163320.x	ank repeat-containing, putative	Exon	0.68	3.28E-28	Q2_P10446
Smp_013860	glutamate-cysteine ligase	Exon	0.63	2.63E-29	Q2_P05616
Smp_140450.1	cleavage and polyadenylation specificity factor, putative	Exon	0.60	5.33E-12	Q2_P30180
Smp_073130.2	loss of heterozygosity 11 chromosomal region 2 gene a protein homolog (mast cell surface antigen 1) (masa- 1), putative	Exon	0.59	1.75E-12	Q2_P02285
Smp_162630.1	ubiquitin-activating enzyme e1, putative	Exon	0.58	1.28E-11	Q2_P27179
Smp_195040	fimbrin, putative	Exon	0.54	4.19E-45	n.o.
Smp_129350	rab, putative	Exon	0.54	1.02E-14	Q2_P24991
Smp_130520.2	prominin (prom) protein, putative	Exon	0.52	1.22E-15	Q2_P03205
Smp_053390	histone H4, putative	Exon	0.52	1.58E-50	n.o.
Smp_017070	26S protease regulatory subunit S10b, putative	Exon	0.45	3.50E-11	Q2_P33233
Smp_145290	alkaline phosphatase, putative	Exon	0.34	1.76E-26	n.o.
Smp_054160	Glutathione S-transferase 28 kDa (GST 28) (GST class-mu), putative	Exon	0.31	8.70E-29	Q2_P04230
Smp_141490	ring finger protein 151, putative	Exon	0.30	7.85E-23	n.o.
Smp_082240	histone H3, putative	Exon	-0.01	1.52E-13	n.o.
Smp_009780.1	14-3-3 protein, putative	Exon	-0.01	1.89E-11	Q2_P22766
Smp_125320	MEG-9	Exon	-0.05	4.75E-18	n.o.
Smp_158110.2	Peroxiredoxin, Prx2	Exon	-0.06	1.08E-21	Q2_P35894
Smp_072140	Rho2 GTPase, putative	Exon	-0.07	6.71E-14	n.o.
Smp_045220.1	myosin light chain 1, putative	Exon	-0.08	8.40E-29	Q2_P23681
Smp_179950	cathepsin B-like peptidase (C01 family)	Exon	-0.09	1.63E-152	n.o.
Smp_097380	groes chaperonin, putative	Exon	-0.09	8.76E-14	Q2_P25391
Smp_175740.2	60S ribosomal protein L14, putative	Exon	-0.14	2.47E-11	Q2_P02600
Smp_009650.1	mitochondrial processing peptidase beta subunit precursor [Homo sapiens]	Exon	-0.16	1.99E-13	Q2_P23534
Smp_144000	cytochrome C oxidase polypeptide vib, putative	Exon	-0.21	1.83E-26	n.o.
Smp_062790	grpe protein, putative	Exon	-0.23	1.38E-15	Q2_P07255
Smp_036400.1	NADH-ubiquinone oxidoreductase ash1 subunit, putative	Exon	-0.25	3.69E-39	Q2_P07094
Smp_067060	cathepsin B-like peptidase (C01 family) (Exon	-0.25	3.81E-208	n.o.
Smp_134590	unc-13 (munc13), putative	Exon	-0.27	2.07E-12	Q2_P24021
Smp_082120	ATP synthase delta chain, mitochondrial, putative	Exon	-0.27	6.13E-19	Q2_P21557
Smp_196160	Isocitric dehydrogenase subunit alpha, putative	Exon	-0.27	1.41E-12	n.o.
Smp_139970	Calmodulin-3 (CaM-3), putative	Exon	-0.29	5.50E-41	n.o.

3. Results

Smp_085840.x	MEG-4 (10.3) family	Exon	-0.37	9.22E-61	n.o.
Smp_042590.1	NADH-ubiquinone oxidoreductase 1, chain, putative	Exon	-0.41	1.46E-70	Q2_P19644
Smp_131640	rna-binding protein musashi-related	Exon	-0.42	2.03E-26	Q2_P32866
Smp_152580	MEG-5	Exon	-0.44	8.41E-89	Q2_P15612
Smp_163710	MEG-6	Exon	-0.45	0	Q2_P20778
Smp_012050	bola-like protein my016	Exon	-0.53	5.45E-14	n.o.
Smp_012380	potassium channel beta, putative	Exon	-0.76	4.42E-12	Q2_P10250
Smp_164480	tubulin beta chain, putative	Exon	-0.83	1.05E-43	n.o.
Smp_124570	leucine zipper protein, putative	Exon	-0.92	2.92E-16	Q2_P05434
Smp_170020	neuropeptide receptor, putative	Intron	-0.93	3.21E-18	n.o.
Smp_152630	MEG-12	Exon	-0.96	1.79E-178	Q2_P14896
Smp_068240	zinc finger protein, putative	Exon	-1.05	7.70E-30	n.o.
Smp_105730	CAI-2 protein, putative	Exon	-1.07	1.88E-39	n.o.
Smp_000170	neurocalcin homolog (drosnca), putative	Exon	-1.15	4.11E-29	Q2_P32680
Smp_159950	neuropeptide Y precursor, putative	Exon	-1.80	2.68E-11	n.o.
Smp_022570.1	ATXN7L3-like protein	Exon	-2.88	0	Q2_P05627
Smp_043340	biogenic amine (dopamine) receptor, putative	Exon	-2.88	0	n.o.
Smp_062510.1	ral, putative	Exon	-2.88	0	Q2_P18191
Smp_118850	rho gtpase activating protein, putative	Exon	-2.88	0	Q2_P09969
Smp_120080.2	nitrilase-related	Exon	-2.88	0	Q2_P27840
Smp_129870	cement precursor protein 3B variant 1, putative	Exon	-2.88	0	n.o.
Smp_150540	histone H3, putative	Exon	-2.88	0	n.o.
Smp_160040	Abnormal long morphology protein 1 (Sp8), putative	Exon	-2.88	0	n.o.
Smp_165390	CCAAT-box DNA binding protein subunit B, putative	Intron	-2.88	0	n.o.
Smp_175630	collagen alpha chain, putative	Exon	-2.88	0	n.o.
Smp_188100	pyruvate carboxylase, putative	Exon	-2.88	0	n.o.
Smp_193630	endoglycoceramidase, putative	Exon	-2.88	0	n.o.
Smp_193880	endothelin-converting enzyme-like 1 (damage- induced neuronal endopeptidase)	Exon	-2.88	0	Q2_P30970
Smp_180330	MEG-2 (ESP15) family	Intron	-3.21	0	n.o.
Smp_043910	tubulin tyrosine ligase-related	Exon	-3.21	0	n.o.
Smp_143350	elongin A-related	Exon	-3.21	0	Q2_P33108
Smp_150370	metabotropic glutamate receptor 2, 3 (mglur group 2), putative	Exon	-3.21	0	Q2_P03124
Smp_154410	alpha(1,3)fucosyltransferase, putative	Exon	-3.21	0	n.o.
Smp_155940	protein kinase C, mu, putative	Intron	-3.21	0	n.o.
Smp_160780	voltage-gated potassium channel, putative	Intron	-3.21	0	Q2_P13612
Smp_172320	myosin xvIII, putative	Exon	-3.21	0	Q2_P06359
Smp_189850	sugar transporter, putative	Exon	-3.21	0	n.o.
Smp_163690	RNA-binding protein Nova-2 [AA 29-492], putative	Exon	-3.21	0	n.o.
Smp_151390	family S9 non-peptidase homologue (S09 family)	Intron	-3.41	0	n.o.
Smp_140070	adenylate and guanylate cyclases, putative	Intron	-3.41	0	Q2_P09452
Smp_164270	cell adhesion molecule, putative	Intron	-3.41	0	Q2_P28083
Smp_123760	krp3, putative	Exon	-3.55	0	n.o.
Smp_149320	tricarboxylate transport protein, putative	Exon	-3.55	0	n.o.
Smp_196120	Transformation/transcription domain-associated protein, putative	Exon	-3.55	0	Q2_P21243
Smp_160210	ceramide glucosyltransferase, putative	Exon	-3.66	0	n.o.
Smp_158020	heat shock protein 70 (hsp70)-interacting	Exon	-4.32	0	n.o.

	protein, putative				
Smp_098780	forkhead protein/ forkhead protein domain, putative	Exon	-4.85	0	n.o.
JAP10881.C	mucolin 2 [Homo sapiens]	Exon	-5.21	6.26E-294	Q2_P41336
Smp_180320.x	egg secreted protein ESP15-like	Intron	-5.32	0	Q2_P03546

Of the 175 transcripts significantly regulated between the two male stages and detected by SuperSAGE only, 89 are shown that have Smp_numbers, functional annotations other than hypothetical and which were checked for a representative oligonucleotide on the microarray.

Grey background: transcripts detected as low abundant according to the definition in 3.4.2.; n.o.: no oligonucleotide representing this gene is included in the microarray.

Table 3.2. Selection of transcripts detected by microarray experiments only.

NR Gene	Gene annotation	Average log ₂ ratio (EM/UM)	q-value(%)	<i>NotI</i> -site
Smp_002890	DNA-directed RNA polymerase III largest subunit, putative	-0.56007564	0.29685345	yes
Smp_016920	conserved hypothetical protein	0.59097185	0.54850698	yes
Smp_024290	MAP kinase kinase protein DdMEK1 , putative	-0.70037181	0.2282315	yes
Smp_028200.x	Troponin I (Tnl), putative	0.46993746	0.17526259	yes
Smp_033000	calcium-binding protein, putative	1.27957107	0	no
Smp_053120	S-adenosyl-methyltransferase mraW, putative	-0.69289053	0	no
Smp_055140	conserved hypothetical protein	-0.32107851	0.41247143	yes
Smp_081140	dbl related	0.78847663	0.2282315	yes
Smp_103360	protein kinase, putative	0.78848091	0.17526259	yes
Smp_127870	Neurotrimin precursor (hNT), putative	0.30154723	0.54850698	yes
Smp_133660	lin-9, putative	1.07168092	0.17526259	yes
Smp_135020	oxalate-formate antiporter, putative	1.18335533	0	yes
Smp_149500	elongation factor 2 kinase, putative	-0.37803573	0.73474424	yes
Smp_151090	cationic amino acid transporter, putative	0.57359764	0.0753035	yes
Smp_157680	U6 snrna-associated sm-like protein lsm4	0.29301676	0.54850698	no
Smp_158680	molybdopterin biosynthesis protein, putative	0.47358232	0.0753035	yes
Smp_168410	tripartite motif protein trim9, putative	-0.53872955	0.73474424	yes
Smp_169190	tegumental protein , putative	1.79677183	0	yes
Smp_173240	cement precursor protein 3B variant 3, putative	0.8522954	0.1032034	yes
Smp_178680	poly(A) polymerase, putative	-0.34831405	0.1032034	yes
Smp_195010	HMG-CoA synthase	-0.64125427	0	yes

Shown are the 21 genes detected in the microarray analyses only and which were analyzed for the presence of *NotI* restriction sites.

- **Amino acids:** Both analyses detected transcripts for members of the alanine biosynthesis or degradation process as significantly up-regulated in UM.
- **Bases:** One transcript coding for an enzyme involved in formyltetrahydrofolate biosynthesis was detected as significantly up-regulated in UM.
- **Other:** For one enzyme involved in catecholamine biosynthesis and phenylethanol biosynthesis transcripts were found to be significantly up-regulated in EM.

3. Results

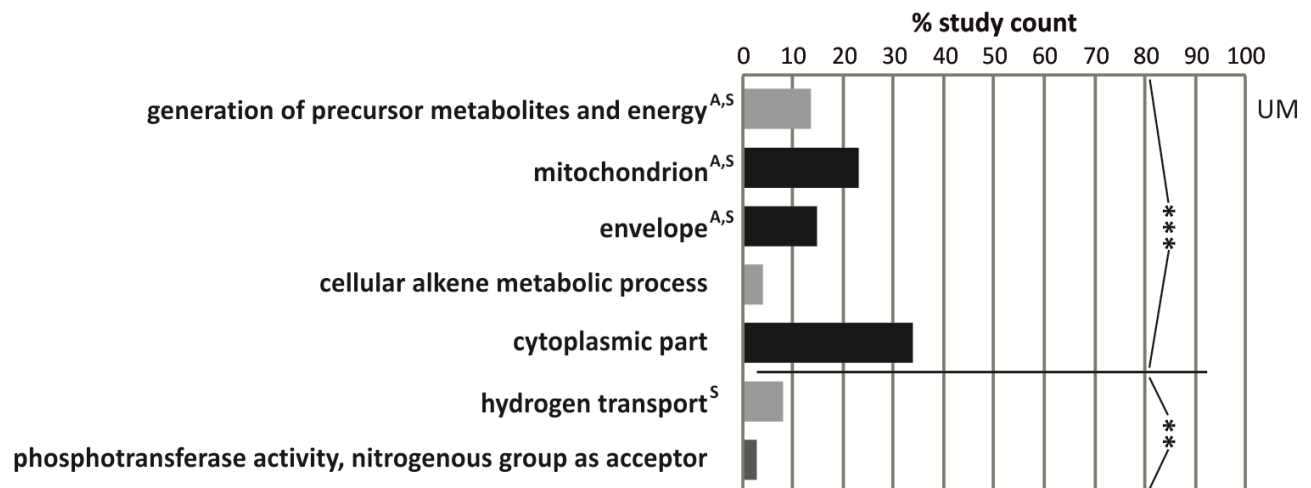


Figure 3.12: Gene Ontology - enriched categories for transcripts significantly regulated between EM and UM in both analyses.

GO was performed for transcripts significantly regulated according to the microarray experiments and SuperSAGE. No enriched categories were found for transcripts up-regulated in EM, but seven for transcripts up-regulated in UM; the latter are presented here.

Light grey: biological process; Black: cellular component; grey: molecular function; p-values for the GO analysis: ** $p < 0.005$, *** $p < 0.0001$; A: category also detected as enriched in microarray analyses; S: category also detected as enriched in SuperSAGE.

Ingenuity Pathway analysis of transcripts significantly regulated in both analyses

IPA was done with 39 of the 180 transcripts significantly regulated in both studies. They were analyzed in the context of all transcripts, detected in any analysis that could be uploaded to the IPA tool. Of the \log_2 ratio from the two analyses, the one with the higher absolute value was chosen for IPA. No canonical pathways were found to be enriched with significantly regulated transcripts, and like in the single-data analyses for the array no transcription factors were notified as activated. Five networks enriched for molecules with significantly regulated transcripts, containing more than 10 molecules, were found:

1. Post-Translational Modification, Protein Folding, Cardiac Hypertrophy
2. Lipid Metabolism, Small Molecule Biochemistry, Connective Tissue Development and Function
3. Cell Cycle, Embryonic Development, Organismal Development
4. Amino Acid Metabolism, Post-Translational Modification, Small Molecule Biochemistry
5. Embryonic Development, Hair and Skin Development and Function, Organ Development

By merging the data obtained from microarray analyses and SuperSAGE it was found that a large number of transcripts was detected in both analyses (Figure 3.10.). Regarding those transcripts detected by only one of the two methods, SuperSAGE found more transcripts than the microarrays. While the distribution of transcripts detected by SuperSAGE-only was made up relatively equal of genes with and without a representative oligonucleotide on the microarray

(107/89), few transcripts found in the microarray-only group lacked a *NlaIII* restriction enzyme recognition site.

The population of transcripts significantly regulated in both experimental groups was biased towards the microarrays, which in comparison to the SuperSAGE detected more transcripts to be significantly regulated between EM and UM. Analyzing the 180 gene-representatives that were significantly regulated in both transcriptome approaches with different software tools, this group of transcripts showed, like the microarray analyses and SuperSAGE previously, a slight bias towards transcripts up-regulated in UM. Data analyses of this reduced set of transcripts also resulted in a reduced set of enriched GO categories, metabolic pathways and IPA-networks detected, compared to the single method data analyses. Follistatin, mentioned previously in the single data analyses, stood out especially in the initial overlap between microarray- and SuperSAGE EdgeR-data, as being the only transcript with a functional annotation related to signaling cascades. It was also found in the overlap of microarray- and SuperSAGE A&C-data.

3.4. Real-time PCR

3.4.1 Establishing real-time PCR

To verify the results of the SuperSAGE and microarray analyses by real-time PCR, the method had to be established in our laboratory. Initially the EvaGreen MasterMix (MM) from SolisBidyne was used, however, the components of this mixture facilitated the formation of primer dimers. Subsequently, real-time MMs from different manufacturers were tested for their ability to inhibit the formation of primer dimers and to enhance specificity of the amplification reaction-product. After a first series of MM tests (Table X., see appendix), excluding those MMs with a strong tendency to form dimers or resulting in low primer-efficiencies, further tests, as well as cost/performance considerations, led to the final choice of PerfeCTaTM SYBR^R Green Super Mix (Quanta / VWR Germany) as standard reagent (data not shown). Whenever this MM was not available the RotorGene MM from Qiagen was used, which had performed equally well during testing (data not shown).

The initial aim was to establish a real-time PCR protocol allowing the quantification relative to a housekeeping transcript that had to be selected. To this end, a detailed analysis was performed comparing the herein presented two transcriptome data-sets and additionally two further data-sets available from our working group to a number of reference genes postulated by Fitzpatrick *et al.* (2009). This analysis led to the conclusion that the choice of reference genes could not be

generalized but had to be made with respect to the specific experiment. None of the reference genes postulated (Fitzpatrick *et al.*, 2009) was applicable for all transcriptome data-sets from our group used for the comparison. A number of potential reference genes (actin, tubulin, proteasome-beta, nip7, gapdh, 'gobert' [Smp_176580 - serin/threonin kinase], g10) was tested for EM and UM and evaluated with the Excel-implementation BestKeeper (Pfaffl, 2004). Actin seemed the most reliable reference gene (supplementary-file14). However, with respect to the comparative data analysis and initial difficulties in achieving similar primer efficiencies for different genes, an approach was finally chosen that allowed quantification relative to a standard curve (2.2.4.4.).

3.4.2. Verification of significantly transcribed genes

Real-time PCR experiments were performed to answer two different questions:

1. Can the regulation of transcripts, detected in any of the analyses, be confirmed by real-time PCR?
2. Is one of the two transcriptome analyses more reliable in the detection of differences between EM and UM?

Initially, experiments were planned based on the data-sets available from microarrays and SuperSAGE following EdgeR analyses. Later, this choice of genes was complemented with data from SuperSAGE following A&C statistics. For the selection of genes 12 technical groups were defined (Table 3.3. headers: up / down; supplementary-file15). Within these groups genes were chosen according to their functional annotation (Table 3.3. first column). Furthermore, the chosen genes represented the bias of significantly regulated transcripts towards the microarrays, only a third of the tested transcripts was significant in the SuperSAGE-A&C statistical analysis, while two thirds were significant in the microarray analyses. Thus, real-time PCR analyses are representative for the distribution of significant genes throughout the two analyses. A number of genes was chosen only for their function, independent of significance, especially when they were linked to the TGF β -pathway. During the selection and verification process it was found that a further refinement for the choice of transcripts should be done. It was defined that signals for significantly regulated transcripts had to be at least 1.5-times higher in one condition than in the other ($\log_2\text{ratio} = \pm 0.585$).

Finally, real-time PCR experiments were done for 3 transcripts found to be significant in both analyses even with EdgeR statistics (follistatin – Smp_123300, OxIT – Smp_036470, AMP-

dependent ligase – Smp_158480). After the change to A&C statistics 4 more transcripts were included into this group (dock – Smp_135520, pinch - Smp_020540.x and two egg-shell protein coding transcripts: Smp_131110.x and Smp_000430). For the group of genes detected by both analyses, but significant only in the microarray analyses, 16 were tested in real-time PCR experiments (Table 3.3.). For the according group of SuperSAGE significant transcripts only 3 were tested, one already detected by EdgeR statistics (cell adhesion molecule - Smp_141410) and two added after A&C statistics (TGF β RII - Smp_144390 and Smad4 - Smp_033950). In addition to transcripts detected by both analyses some were selected that were detected by only one analysis, 7 in case of the microarrays, 10 for SuperSAGE (Table 3.3.; Figure 3.13.).

Results from real-time PCR experiments were tested for significant differences between EM and UM by applying a Wilcoxon rank sum test (Mehta & Patel, 2013; Hollander & Wolfe, 1973; Bauer, 1972) (supplementary-file15). Furthermore, they were compared graphically to microarray and SuperSAGE data (Figure 3.13.) and correlation analyses were performed (see below). The graphical comparison of log₂ratios from biological replicas of all three transcriptome studies revealed strong biological variance for many transcripts; even within single analyses. The most stable and reproducible results obtained by real-time PCR were those for which microarray analyses and SuperSAGE were already in accordance. This applied especially to three of the transcripts originally placed in the overlap of transcripts significantly regulated in microarray and SuperSAGE-EdgeR statistical analyses: follistatin (Smp_123300), OxIT (Smp_036470), and an AMP dependent ligase (Smp_158480). For all three transcripts differences between EM and UM were significant according to the Wilcoxon rank sum test.

The strong regulation of transcripts for follistatin and its potential inhibitory role in a schistosome TGF β -pathway led to the definition of a functional group containing several members of the TGF β -pathway (Table 3.3.; Figure 3.13.). Transcripts for two Smad molecules were significantly regulated in microarray analyses or SuperSAGE. Smad4 (Smp_033950) transcripts were significantly up-regulated in EM according to SuperSAGE. Transcripts for another Smad (Smp_157540), not yet described in *S. mansoni*, were significantly down-regulated in EM according to the microarray analyses. For both Smads the respective other transcriptomic approach contradicted this result, indicating strong biological variance, which was confirmed by real-time PCR experiments. Similar results were obtained for transcripts of the *S. mansoni* bone morphogenic protein (SmBMP,

3. Results

Table 3.3: Genes selected for real-time PCR verification.

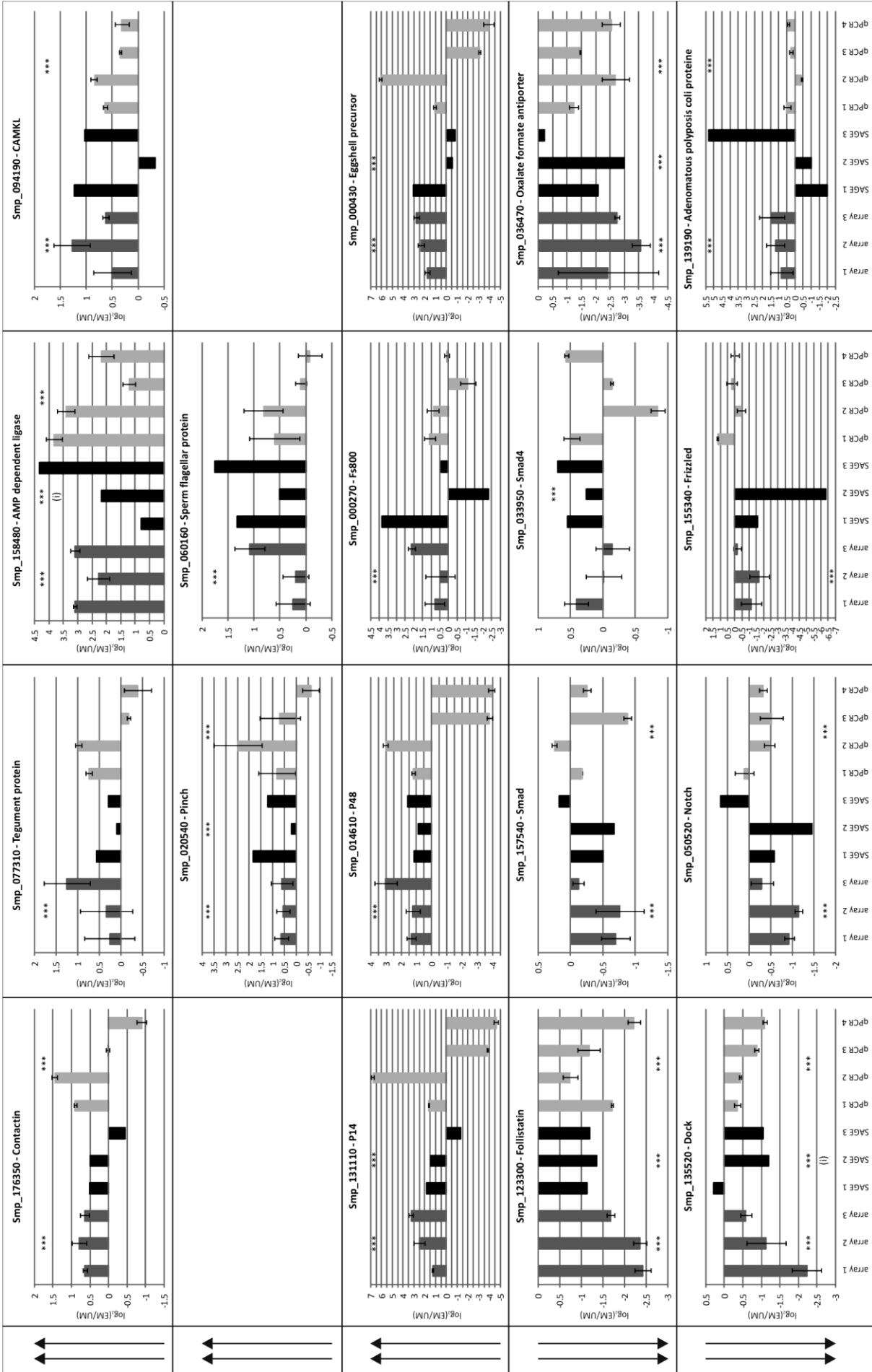
group name	Oligo	SuperSAGE-mo	SAGE-strand	GeneID	Annotation	microarray		SuperSAGE		qPCR		microarray + SuperSAGE different direction		microarray only + Niall		SuperSAGE only present on array/not present on array	
						log ₂ -ratio (EM/UM)	q-value	log ₂ -ratio (EM/UM)	P-value A&C	log ₂ -ratio (EM/UM)	Wilcoxon -rank	same direction	down-array	up-array	down	up	down
TGF-beta related	O2_P13888	11471	exon	Smp_123300	Snf5t	-2.15E+00	0.00E+00	-1.23E+00	7.06E-20	4.53E-02	-1.43E+00	1.23E-03	yes				
	O2_P40273	17328	exon	Smp_146790	SmbBMP	-8.71E-01	0.00E+00	6.91E-02	1.37E-01	1.00E+00	-2.34E-01	1.93E-01	yes				
	O2_P18901	24596	exon	Smp_177050	GCP	-4.54E-01	7.35E-01	2.50E-01	8.09E-03	1.00E+00	-5.27E-01	6.20E-01	yes				
	O2_P20876	5654	intron	Smp_063190	SmlnAct	no	3.12E-01	3.12E-01	4.90E-01	1.00E+00	1.94E-02	4.68E-01					yes
	O2_P06542	16704	intron-la	Smp_049760	TGFBRI	2.84E-01	2.45E+00	-2.56E-01	3.11E-01	1.00E+00	3.78E-01	1.93E-01	yes				
surface proteins	O2_P10970	4094	exon	Smp_144390	TGFBRII	3.99E-02	3.36E+01	0.00E+00	0.00E+00	1.00E+00	6.61E-01	1.01E-01	yes				
	O2_P18126	19954	exon	Smp_039950	Smaid4	8.36E-02	2.64E+01	5.00E-01	5.00E-12	1.00E+00	-1.05E-03	6.50E-01	yes				
	O2_P38240	15956	exon	Smp_157540	Smaid4	-5.24E-01	5.92E-02	-3.33E-01	3.43E-02	1.00E+00	-3.35E-01	4.78E-02	yes				
	O2_P36119	24413	exon	Smp_141410	cell adhesion molecule	-2.10E-01	1.86E+00	9.04E+00	0.00E+00	2.13E-26	-1.10E-01	7.78E-01	yes				
	O2_P01265	21010	exon-la	Smp_176350	contactin	6.93E-01	0.00E+00	1.88E-01	7.44E-01	1.00E+00	4.86E-01	1.92E-02	yes				
ion channels	O2_P24579	8298	exon	Smp_077310	tegument protein	6.14E-01	5.49E-01	3.13E-01	3.87E-01	1.00E+00	2.87E-01	9.21E-01	yes				
	O2_P24095	-	exon	Smp_169190	tegumental protein, putative	1.80E+00	0.00E+00	0.00E+00	-	-	2.51E+00	2.17E-03	yes				
	O2_P09465	4369	exon	Smp_105200.1	glypican, putative	-2.91E+00	0.00E+00	-1.76E+00	1.36E-25	8.80E-04	-1.92E+00	1.11E-03	yes				
	O2_P32730	-	exon	Smp_135020	oxalateformate antiporter	1.18E+00	0.00E+00	-	-	-	8.38E-01	2.42E-02	yes				
	O2_P194740	26308	exon-la	Smp_194740	G-protein coupled receptor	nd	-	4.99E+00	3.46E-01	7.79E-01	9.89E-02	2.48E-01	yes				
gPCRs	O2_P170150	20919	exon	Smp_170150	Rhodopsin-like orphan GPCR	no	-	1.48E+00	9.58E-04	4.84E-01	8.46E-01	7.78E-03				yes	
	O2_P170020	22958	intron-la	Smp_170020	G-protein coupled receptor	no	-	3.21E-18	2.41E-01	2.41E-01	-6.51E-01	2.42E-02					
	O2_P17922	14507	intron	Smp_135520	dock	6.12E-01	0.00E+00	-6.49E-01	7.51E-26	7.71E-01	-7.06E-01	1.65E-04	yes				
	O2_P36242	2823	exon	Smp_020540.x	pinch	-7.00E-01	2.28E-01	-	1.54E-18	8.25E-01	8.54E-01	4.32E-02	yes				
	O2_P14660	-	exon	Smp_024290	DoDMK1	nd	-	1.42E+00	6.34E-03	8.77E-01	-1.88E-01	3.18E-01	yes				
WNT-related	O2_P06737	9792	exon	Smp_175160	serine/threonine Kinase - PAK	nd	-	1.42E+00	6.34E-03	8.77E-01	-1.88E-01	3.18E-01	yes				
	O2_P35708	16908	exon	Smp_094190	CAMKK	7.99E-01	0.00E+00	6.43E-01	3.66E-02	1.00E+00	5.38E-01	7.88E-03	yes				
	O2_P31005	15413	exon-la	Smp_145140	wnt-5, putative	-7.54E-01	0.00E+00	9.09E-02	3.80E-01	1.00E+00	-6.32E-02	3.11E-01	yes				
	O2_P32430	19392	exon	Smp_139190	adenomatous polyposis coli protein	1.16E+00	0.00E+00	7.74E-01	2.28E-01	1.00E+00	1.78E-01	4.02E-02	yes				
	O2_P26504	5728	exon	Smp_155340	frizzled	-1.02E+00	5.92E-02	-2.64E+00	4.48E-03	6.24E-01	2.28E-01	4.87E-01	yes				
notch-related SHH	O2_P32346	23586	intron	Smp_050520	egf-like domain protein / notch sonic hedgehog, putative	-7.91E-01	0.00E+00	-4.60E-01	3.03E-01	1.00E+00	-3.25E-01	3.74E-02	yes				
	O2_P05101	3289	exon	Smp_025370	lipopolysaccharide-induced transcription factor regulating tumor necrosis factor alpha	6.16E-01	0.00E+00	2.20E-01	3.43E-03	1.00E+00	4.40E-01	3.69E-01	yes				
	O2_P04978	13346	exon	Smp_130690	zinc finger protein, putative - ZFP	nd	-	8.54E+00	1.59E-20	6.31E-14	-1.71E-01	7.00E-01				yes	
	O2_P11018	12298	exon-la	Smp_024860	lin-5, putative	1.07E+00	1.75E-01	-	3.10E-05	7.27E-01	3.58E-01	4.65E-02			yes		
	O2_P32005	20111	exon	Smp_126530	ets	-8.82E-01	0.00E+00	-6.93E-01	2.27E-01	9.52E-01	4.79E-03	5.41E-01	yes				
metabolism	O2_P18088	-	exon	Smp_143350	ma-binding protein musashi-related	nd	-	3.31E+00	8.37E-11	2.82E-04	-1.53E-01	6.71E-01	yes				
	O2_P03565	1834	exon	Smp_152580	elongin	nd	-	-3.71E+00	0.00E+00	9.52E-01	1.06E-01	7.67E-01	yes				
	O2_P37788	20186	intron	Smp_002890	MEGS	nd	-	-4.40E-01	8.41E-89	9.28E-01	1.51E-01	8.72E-01	yes				
	O2_P37959	6649	exon	Smp_002890	DNA-directed RNA polymerase III largest subunit	-5.60E-01	2.97E-01	-	-	-	1.12E-01	8.31E-01	yes				
	O2_P32005	-	exon	Smp_053120	s-adenosyl-methyltransferase mraw	-6.93E-01	0.00E+00	-	-	-	-8.55E-01	3.19E-02					yes
egg shell proteins	O2_P25403	693	exon	Smp_011100	insulinase-related	no	-	4.30E+00	5.49E-38	3.64E-02	8.67E-01	8.58E-04	yes				
	O2_P13376	13447	exon	Smp_158480	AMP dependent ligase	2.82E+00	0.00E+00	2.82E+00	4.01E-12	2.44E-03	2.65E+00	7.40E-04	yes				
	O2_P06437	2190	exon	Smp_195010	HMG-CoA Synthase	-6.41E-01	0.00E+00	-	-	-	-4.82E-01	3.42E-02	yes				
	O2_P38299	729	exon	Smp_060160	sperm flagellar protein	5.11E-01	4.12E-01	1.19E+00	3.60E-02	9.28E-01	3.63E-01	9.11E-02	yes				
	O2_P38299	729	exon	Smp_131110.x	p4800	1.14E+00	7.53E-02	6.45E-01	1.77E-02	9.28E-01	2.38E-01	6.60E-02	yes				

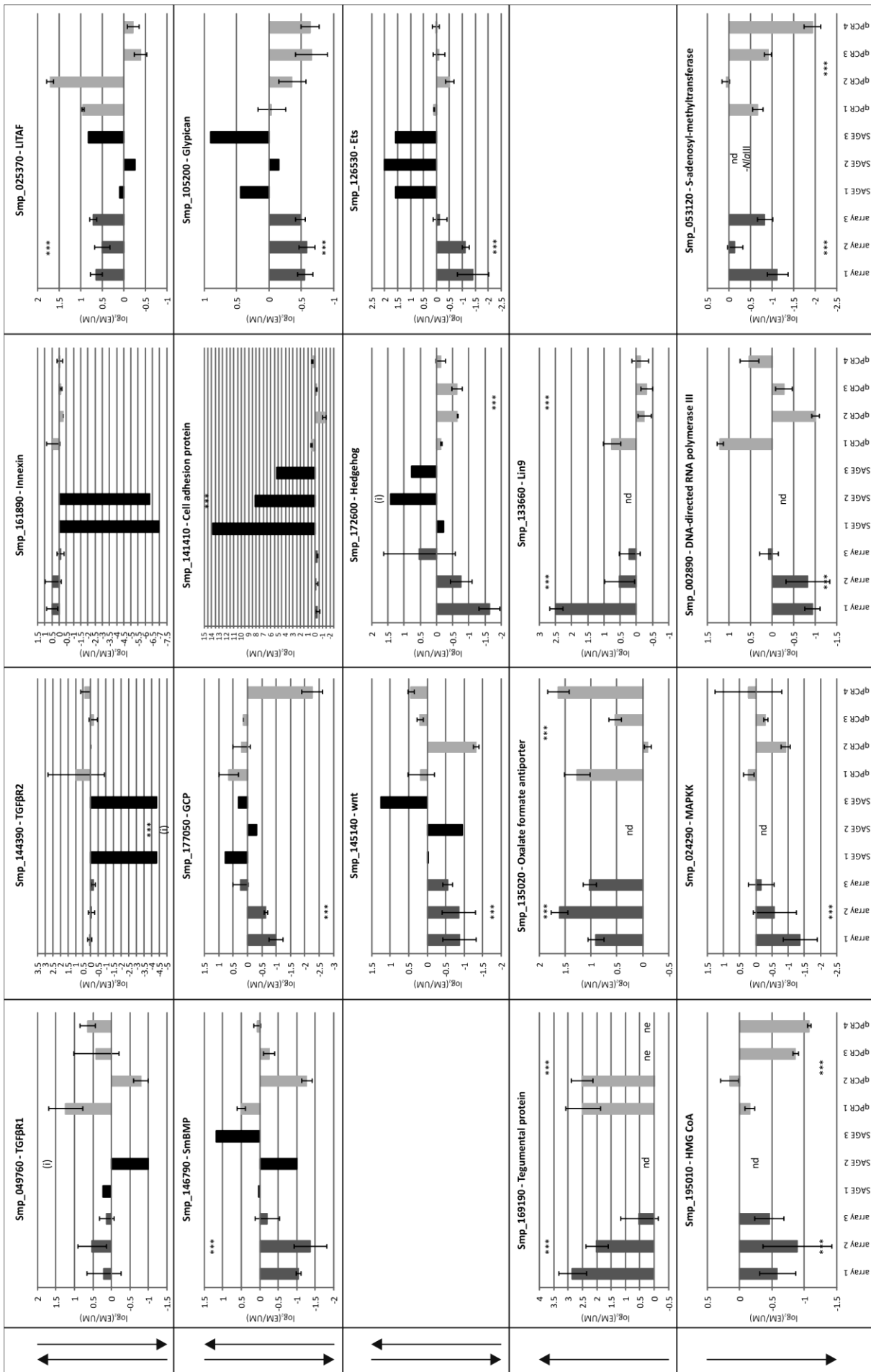
For real-time PCR verification of the transcriptome analyses-data-set 47 genes were chosen and grouped into technical and functional categories. The table shows oligonucleotides of these categories, the regulated genes with their identifiers for each analysis, log₂ratios and statistical values. no: the microarray does not contain an oligo representing this gene; nd: the analysis did not detect a transcript for this gene (according to the definition in 2.2.14.1.; la: transcripts are low abundantly detected by SuperSAGE; red: significance of 'differential' values.

Smp_146790) and the gynaecophoral canal protein (GCP, Smp_177050), both significantly down-regulated in EM according to the microarray analyses as well as for transcripts of one TGF β R (Smp_144390) significantly down-regulated in EM according to SuperSAGE (Figure 3.13.). Transcripts for another TGF β R (Smp_049760) and a possible follistatin interactor, the *S. mansoni* inhibin/activin (SmInAct, Smp_063190), were additionally checked in real-time PCR, even though they were not significant in any of the transcriptome analyses. Strong variance between biological replicas and analyses was confirmed by real-time PCR experiments (Figure 3.13.). None of the transcripts in the TGF β -related group apart from follistatin showed a significant regulation between EM and UM in real-time PCR experiments.

Another functional group was deduced from IPA-network 24 for the microarrays, which contained Wnt5A (wingless-related MMTV integration site, Smp_145140), a seven membrane receptor (frizzled –Smp_155340) and the tumor suppressor gene lin-9 (abnormal cell LINEage, Smp_133660). The transcript annotated as Wnt5A (Smp_145140) was significantly down-regulated in EM in the microarray analyses. Transcripts for the potential wnt receptor, frizzled (Smp_155340), were also significantly down-regulated in EM according to the microarray experiments. Furthermore, transcripts for adenomatous polyposis protein (Smp_139190), a down-stream signal transduction molecule in Wnt-signaling and lin-9 were significantly up-regulated in EM in the microarray analyses. As Wnt-pathways play important roles in developmental processes of other organisms (Kristiansen, 2004), the above group of molecules stood out when choosing interesting molecules from the microarray experiments for further analyses. However, all of the mentioned transcripts were not significantly regulated in the SuperSAGE data-set, and lin-9 was not even detected by this method, though the predicted sequence contains a *Nla*III restriction site. The direction of regulation of transcripts detected for Wnt5A (Smp_145140), frizzled (Smp_155340) and adenomatous polyposis (Smp_139190) protein by SuperSAGE varied strongly between biological replicas. However, according to the Wilcoxon rank sum test significant regulation for adenomatous polyposis protein (Smp_139190) and lin-9 (Smp_133660) as detected by the microarrays, was confirmed by real-time PCRs. Still, biological variation was confirmed by real-time PCR experiments for all four transcripts of the Wnt-group (Figure 3.13.).

3. Results





3. Results

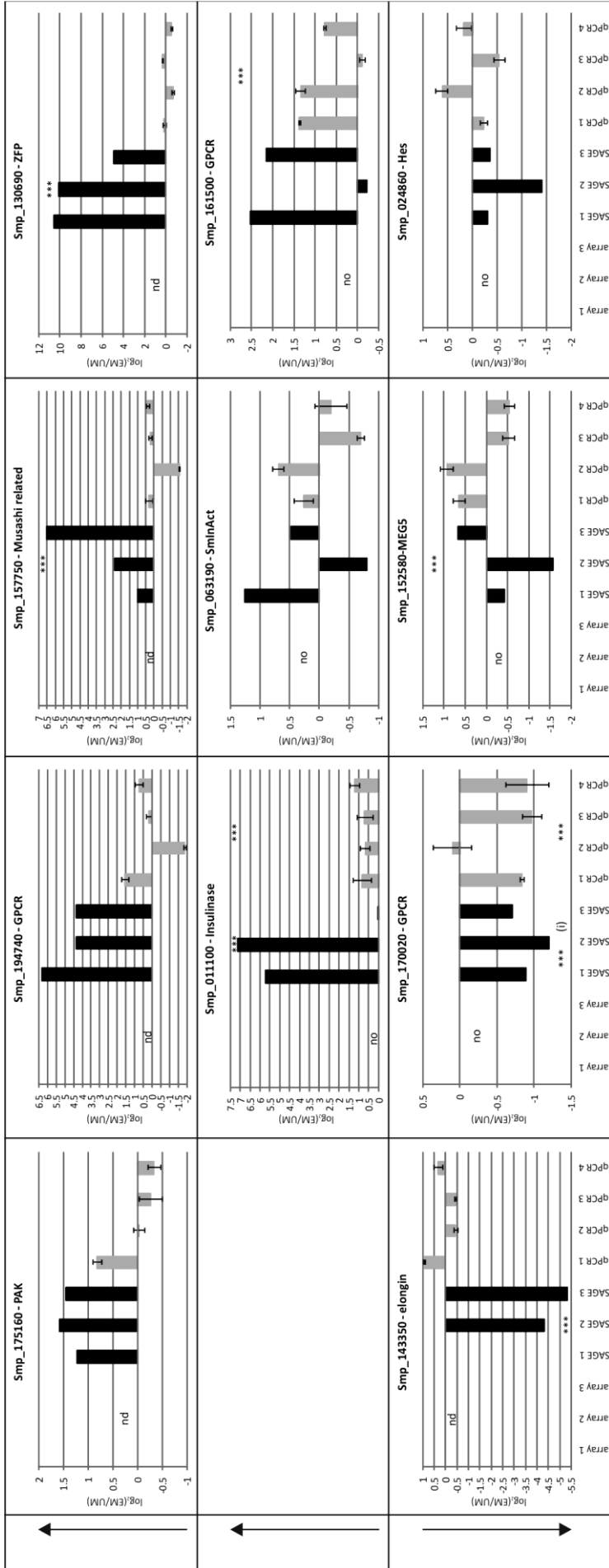


Figure 3.13: Results of real-time PCR –verification experiments for microarray and SuperSAGE data.

All genes tested in real-time PCR are shown as well as their technical classification. \log_2 ratios are given for all biological replicas tested in either microarray, SuperSAGE or real-time PCR. Many transcripts show great biological variance, even if regulation between EM and UM was detected as significant. Most reproducible were those results, for which microarray analyses and SuperSAGE were already in accordance. Arrows in the left most column represent regulation in EM according to microarray (left) and SuperSAGE (right). Grey: microarray; black: SuperSAGE; light grey: real-time PCR. Stars in graphs indicate significance in the according analysis. ne: data not evaluable; nd: no transcripts for this gene detected in this analysis; no: this gene is not represented by an oligonucleotide on the microarray; i:detected transcripts were aligned to a predicted intron. (To ease comparison between graphs all y-axis intervals were set to 0.5)

Unexpectedly transcripts for a number of egg-shell precursors genes, p14 (Smp_131110), p48 (Smp_014610), fs800 (Smp_000270) and an 'eggshell precursor protein' (Smp_000430), were significantly up-regulated in EM according to the microarray analyses, a result independently found in other studies as well (Nawaratna *et al.*, 2011). However, a critical evaluation of the \log_2 ratios for the different biological replicas in SuperSAGE showed variance in the direction of regulation (Figure 3.13.). A similar discrepancy between SuperSAGE replicas was found for the other mentioned egg-shell related transcripts, except for p48. Real-time PCR experiments confirmed this variation in the direction of regulation between replicas for all four transcripts of egg-shell genes and differences were non-significant according to the Wilcoxon rank sum test.

Of the transcripts detected in the microarray experiments 36 were tested with real-time PCR. The obtained \log_2 ratios strongly correlated according to testing with Spearman's rank correlation coefficient ($p < 0.001$, $r = 0.643$) (Myers & Well, 2003). The same test for 40 transcripts detected by SuperSAGE and analyzed by real-time PCR did not detect significant correlation between the \log_2 ratios of the two experimental groups. \log_2 ratios from SuperSAGE and real-time PCR were more different in their absolute values than those from microarrays and real-time PCR. A close observation of the SuperSAGE counts for each transcript and biological sample revealed this difference as a potential mathematical problem. The number 0 was substituted with 0.05 for calculation of \log_2 ratios; the lower such a substitution value is chosen, the higher the absolute value becomes for the calculated \log_2 ratio, which then may no longer represent true ratios. Similar to the microarray data, SuperSAGE data had been filtered for constant transcript detection (2.2.14.2). However, many transcripts remained, which may be defined as low abundant. They lack detection of transcripts in more than 3 libraries and/or show normalized transcription counts of below 10 for all biological samples. Within the 40 SuperSAGE detected transcripts tested in real-time PCR, 7 fell into this newly defined category of low abundant transcripts. Exclusion of these 7 from the calculation of Spearman's rank correlation coefficient (Myers & Well, 2003) led to the detection of significant correlation between \log_2 ratios from SuperSAGE and real-time PCR ($p < 0.05$, $r = 0.328$). Transcripts excluded from the test were: adenomatous polyposis coli protein (Smp_139190); TGF β RII (Smp_144390); two GPCRs (Smp_170020, Smp_194740); elongin (Smp_143350); innexin (Smp_161890.x), and ets (Smp_126530).

Thus, real-time PCR results supported the detection of significantly regulated transcripts found in microarray and SuperSAGE experiments, although \log_2 ratios from real-time PCR correlated more strongly to those of the microarrays. Additionally, real-time PCR experiments led to a refined data-

evaluation, wherein only those genes were defined as significantly differentially (sig. diff.) transcribed that showed a \log_2 ratio with an absolute value greater than 0.585 (equaling a 1.5 times higher transcription in one male stage compared to the other). Also, following correlation evaluation it was concluded that low abundantly transcribed genes (as defined above) should be excluded from the analyses.

With regard to functional groups real-time PCR results confirmed the strong up-regulation of follistatin transcripts in UM, while other members of the TGF β -pathway were not regulated between EM and UM. This indication for a specific differential regulation of only one molecule at the top of / as a potential regulator of the TGF β -pathway encouraged further analysis of this transcript. Additional experiments on wnt-pathway related transcripts were discouraged by the real-time PCR results, which confirmed strong variances of \log_2 ratios between biological replicas found by SuperSAGE, and contradicting the significant regulations detected by microarrays especially for wnt5A and frizzled. Furthermore, the significant up-regulation of egg-shell protein transcripts in EM found in the microarray data is questionable with regard to real-time PCR results; again a confirmation of SuperSAGE findings, in tendency.

3.5. Data-analyses with refined criteria drastically reduced the number of interesting genes

Following definition of new criteria after evaluation of the real-time PCR results, the influence of these criteria on previous data analyses was investigated. Results for GO, as well as network analyses and especially the overlapping data from microarrays and SuperSAGE were reevaluated.

Microarray analyses results with new criteria defined after real-time PCR experiments

Using the more stringent criterion for differential transcription (\log_2 ratio > 0.585 or < -0.585) in addition to significance ($q < 0.01$), only 526 transcripts from the microarray experiments fulfilled these requirements. This led to a more equal distribution between EM and UM up-regulated transcripts: 229 up in EM, 297 up in UM (Figure XVI and Table XI, see appendix). According to the lower number of transcripts, also the significantly enriched GO categories decreased drastically and no more sub-groups of the super-category molecular function could be detected. Furthermore, enriched categories were only found for UM and no longer for EM (Figure 3.14.; Table XII., see appendix).

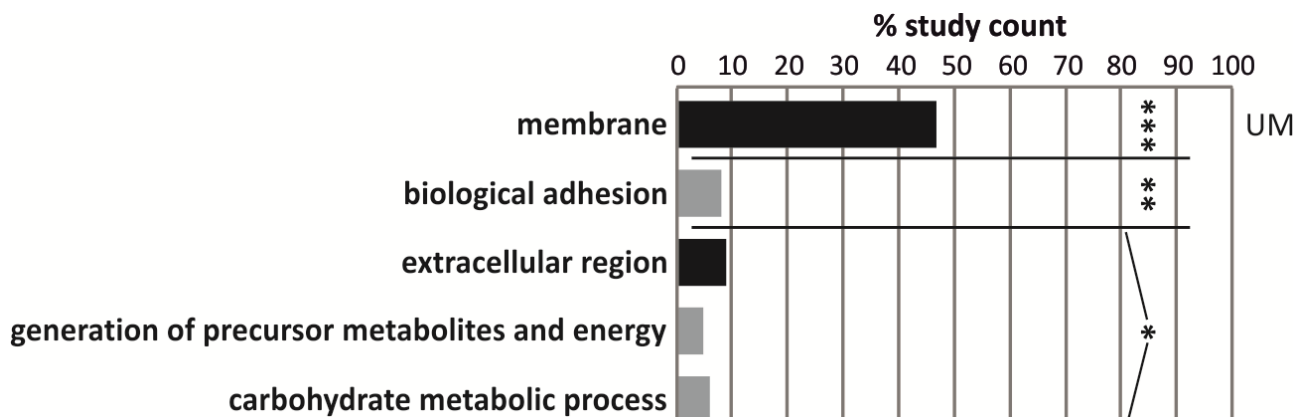


Figure 3.14: GO for transcripts significantly and differentially regulated according to the microarray analyses.

Applying the more stringent selection criteria ($\log_2\text{ratio} > 0.585$ or < -0.585) defined after evaluation of real-time PCR results no more significantly enriched categories were found for transcripts up-regulated in EM. Fewer categories were detected as enriched in UM up-regulated transcripts (represented here), but with at total lack of the super-category molecular function. Light grey: biological process; black: cellular component; p-values for the GO analysis: **p < 0.005, *p < 0.005; ***p < 0.0001

Of those transcripts already associated to metabolic pathways only 18 showed a more than 1.5 times higher ($\log_2\text{ratio} > 0.585$ or < -0.585) transcription in one male stage compared to the other (Table III underlined annotations, see appendix). Corresponding enzymes are associated with the following metabolic pathways:

- Carbohydrates, citrate cycle, aerobic respiration, amino acids: All transcripts for enzymes in these categories were up-regulated in UM.
- Pentose-phosphate cycle, glycolysis: For enzymes in these metabolic pathways no transcripts were found to be sig. diff. regulated in the microarray analyses.
- Lipids and fatty acids: Except for one, all sig. diff. regulated transcripts for enzymes involved in mevalonate pathway, fatty acid β -oxidation, phospholipid biosynthesis, di- and triacylglycerol biosynthesis were up-regulated in EM.
- Bases: All transcripts for enzymes in this category sig. diff. regulated according to the microarrays were up-regulated in EM.
- Other: Four transcripts up-regulated in EM coded for enzymes related to betaxanthin biosynthesis, betacyanin biosynthesis, phenylethanol biosynthesis, and catecholamine biosynthesis. Three transcripts significantly up-regulated in UM coded for enzymes involved in sulfide oxidation and colanic acid building block biosynthesis.

A renewed IPA for the group of sig. diff. transcribed genes found no canonical pathways enriched for such genes or transcription factors predicted to be activated. A reduced number of networks was found, including (only those with more than 10 molecules):

3. Results

1. Cell Death, Cellular Movement, Lipid Metabolism.
2. Lipid Metabolism, Small Molecule Biochemistry, Drug Metabolism.
3. Cell-To-Cell Signaling and Interaction, Nervous System Development and Function, Cell Death.
4. Cardiovascular Disease, Organismal Injury and Abnormalities, Cellular Development.
5. Cancer, Organismal Injury and Abnormalities, Cell Death.
6. Genetic Disorder, Respiratory Disease, Cardiovascular Disease.
7. Cellular Development, Inflammatory Response, Post-Translational Modification.
8. Nucleic Acid Metabolism, Small Molecule Biochemistry, Cell Signaling.
9. Free Radical Scavenging, Molecular Transport, Cellular Assembly and Organization.

Altogether a more stringent selection of transcripts for GO and network analyses resulted in fewer categories, pathways, and networks enriched within the reduced data-set. However, it is noteworthy that the GO category extracellular region, containing follistatin, was still significantly enriched within the UM up-regulated data-set ($p < 0.05$).

SuperSAGE results with new criteria defined after real-time PCR experiments

Applying the refined criteria (sig. diff.: $p < 1^{-10}$ and $\log_2\text{ratio} > 0.585$ or > -0.585 ; abundant: transcript-counts ≥ 10 in at least one library) to the SuperSAGE data, 253 transcripts were found. Of these 218 were up-regulated in EM and 35 in UM (Figure XVII.; see supplementary-file8, sheet: 'unique-sage-abundant-sense-sig'). Also \log_2 ratios for each transcript varied less throughout the three biological replicas.

No enriched GO categories were found using these 218 transcripts as study count and all abundantly detected transcripts as population count. Only 12 sig. diff. and abundant transcripts coded for enzymes associated to metabolic pathways (Table VI. underlined annotations, see appendix):

- Carbohydrates: Only one transcript, up-regulated in EM, coded for an enzyme associated to carbohydrate metabolic processes.
- Pentose-phosphate cycle, glycolysis, citrate cycle, aerobic respiration: No transcripts for enzymes involved in any of these metabolic processes were found in the newly defined SuperSAGE group.
- Lipids and fatty acids: For two enzymes involved in trans,trans-farnesyl diphosphate biosynthesis, mevalonate pathway and triacylglycerol degradation, transcripts were detected as abundant and sig. diff. up-regulated in UM, while the opposite was found for transcripts of an enzyme involved in fatty acid biosynthesis and fatty acid elongation.
- Amino acids: Except for one transcript, coding for an enzyme involved in glutathion biosynthesis, all transcripts with corresponding enzymes associated with amino acid

biosynthesis-processes were up-regulated in UM. These enzymes are linked to arginine degradation, alanine biosynthesis and alanine degradation.

- **Bases:** All transcripts for enzymes involved in base synthesis detected as abundant and sig. diff. regulated had higher counts in UM.
- **Other:** For one enzyme involved in either catecholamine biosynthesis or phenylethanol biosynthesis transcripts were abundant and sig. diff. up-regulated in EM.

Uploading this refined data-set to IPA no canonical pathways were significantly enriched for sig. diff. genes, no transcription factors were detected as activated, and only three networks with more than 10 molecules were found:

1. Cell Death, Free Radical Scavenging, Lipid Metabolism.
2. Cell Cycle, Cellular Movement, Connective Tissue Development and Function.
3. Dermatological Diseases and Conditions, Immunological Disease, Post-Translational Modification.

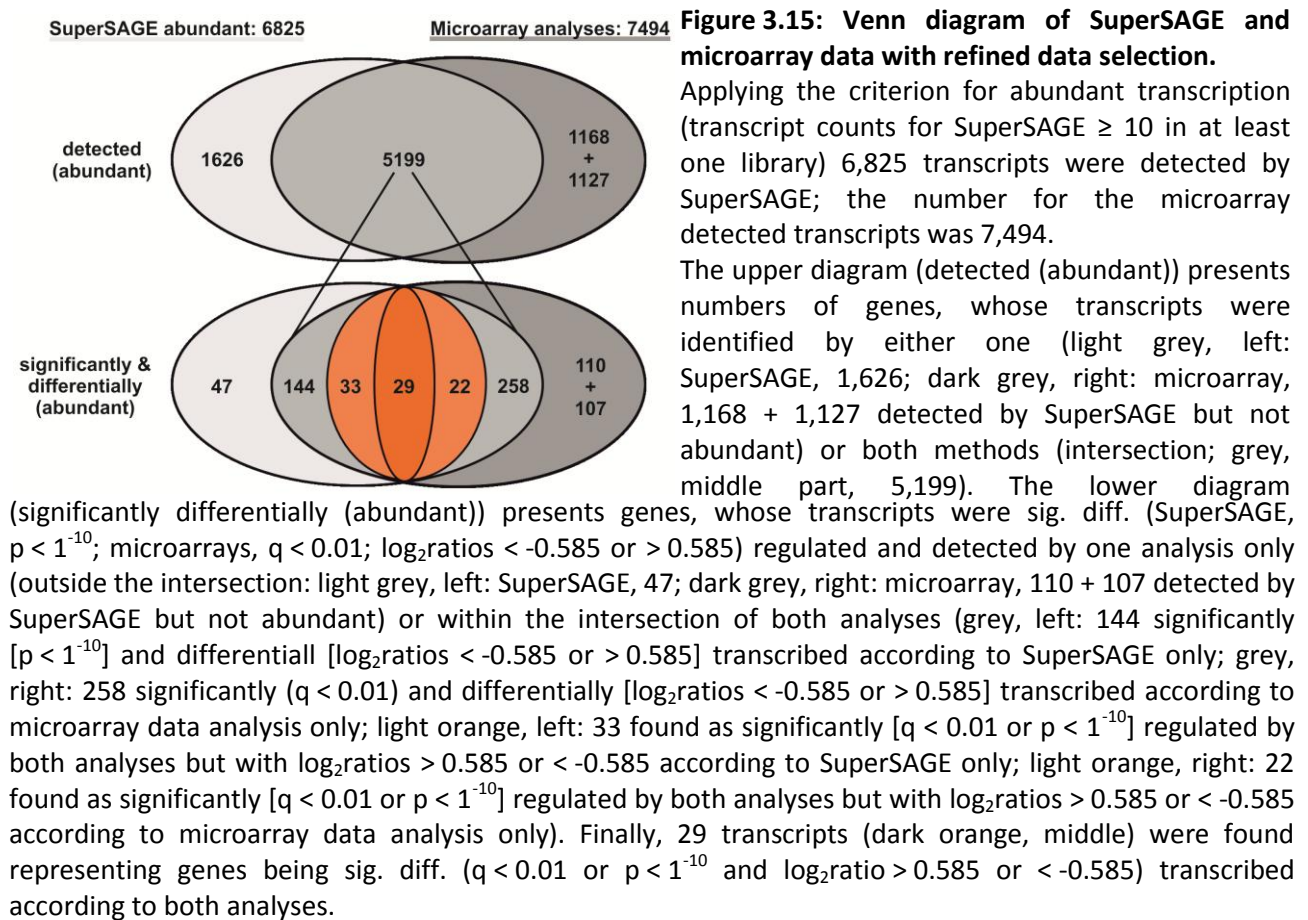
As for the refined microarray data-set the more stringently selected group of transcripts from SuperSAGE contained a lower number of significantly regulated transcripts. GO and network analyses also detected fewer enriched categories, metabolic pathways, and networks. Comparing the refined metabolic analysis of SuperSAGE and microarrays, an evidence already indicated by comparison of the less stringently selected data was confirmed: While SuperSAGE found transcripts for enzymes involved in base synthesis to be up-regulated in UM, the microarrays detected other transcripts significantly up-regulated in EM and rather linked to salvage and degradation processes of bases.

Combinatory analysis of microarray and SuperSAGE results with refined criteria

Following refinement of data analyses including only abundantly transcribed genes (abundant: transcript-counts for SuperSAGE ≥ 10 in at least one library) the overlap of microarray and SuperSAGE data was reduced to 5,199 transcripts (Figure 3.15.). Within the SuperSAGE-only group 1,626 transcripts remained, while the number of microarray-only transcripts was enhanced by 1,127. Applying the additional criterion for sig. diff. ($q < 0.01$ or $p < 1^{-10}$ and $\log_2\text{ratio} > 0.585$ or < -0.585) transcription, 47 transcripts remained in the group of SuperSAGE-only, 110 (plus 107 not abundant in SuperSAGE) in the group of microarray-only and 29 in both analyses (Figure 3.15.). These most stringently selected transcripts are represented in Table 3.4., and the hierarchical clustering is shown in figure XVIII (see appendix). Of the other genes within the intersection 144 were significant ($p < 1^{-10}$) according to SuperSAGE only and 258 were significant ($q < 0.01$) according to the microarrays only; 33 transcripts were significantly ($q < 0.01$ or $p < 1^{-10}$) regulated

3. Results

in both analyses but with an absolute value for \log_2 ratios greater than 0.585 in SuperSAGE only; and 22 were significantly ($q < 0.01$ or $p < 1^{-10}$) regulated in both analysis but with an absolute value for \log_2 ratios greater than 0.585 in the microarray only.



Submitting the 29 transcripts meeting the refined criteria for both transcriptome analyses to GO, SchistoCyc and IPA, no significantly enriched GO categories were found (using all genes detected in any analysis as population count). For only one enzyme involved in phenylethanol/catecholamine biosynthesis (DDC - Smp_135230) transcripts were found to be sig. diff. up-regulated in EM (and abundant in SuperSAGE). No canonical pathways enriched for sig. diff. genes were found, and no transcription factors were found to be activated. Only one network (> 10 molecules) was detected (Figure 3.16.): embryonic development, hair and skin development and function, organ development. It contained nine sig. diff. regulated transcripts, seven up-regulated in EM and two up-regulated in UM, including follistatin. As shown in Table 3.4. follistatin remains the outstanding signal transduction molecule. Many genes in Table 3.4., such as the the NAD dependent epimerase, sodium/dicarboxylate cotransporter, and others, seemed of minor interest with regard to the biological question, which signaling processes induce UM to become EM, able to stimulate EF. In this respect, transcripts coding for molecules involved in signal

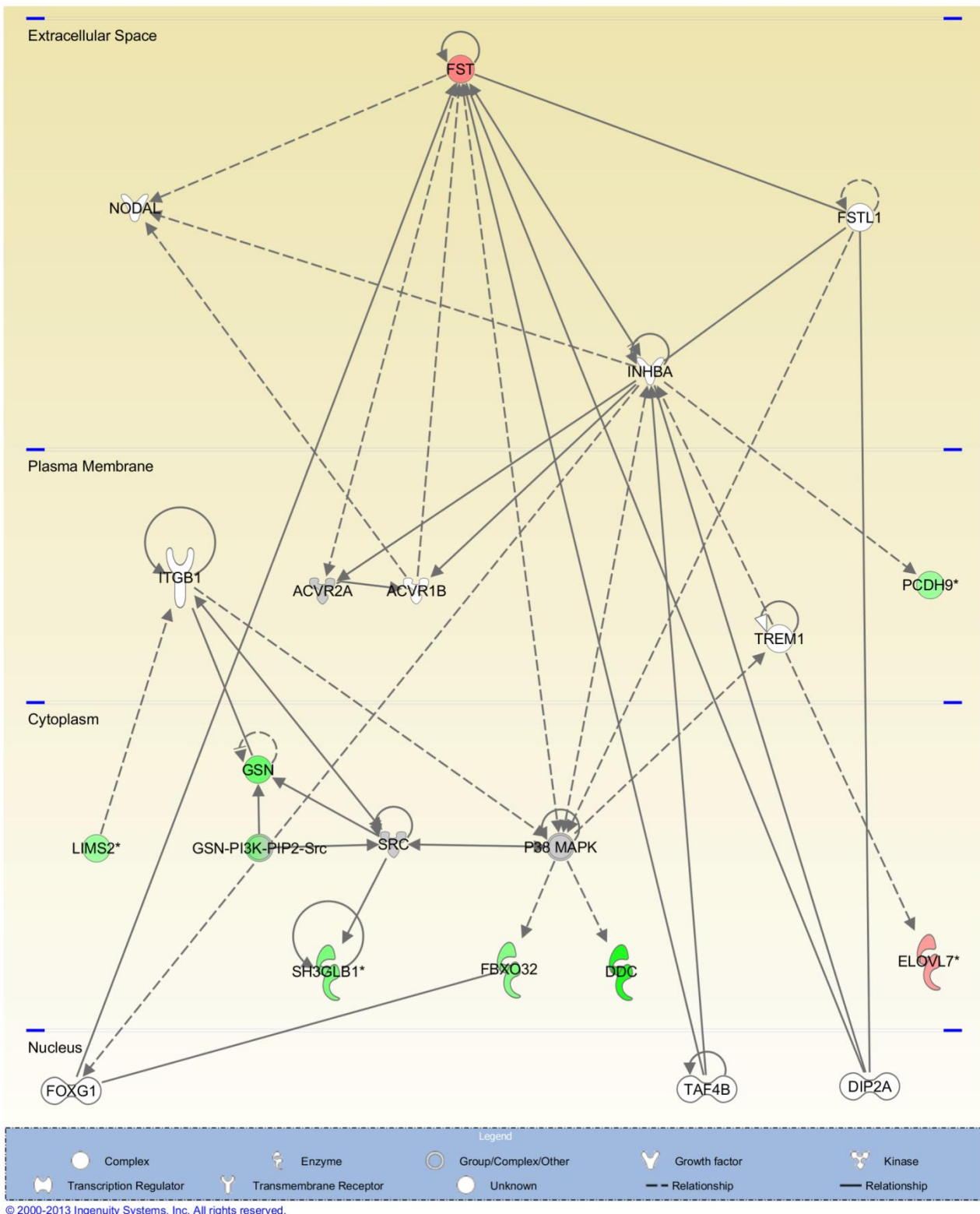


Figure 3.16: IPA-network for genes significantly differentially transcribed in SuperSAGE and microarrays. For transcripts sig. diff. regulated according to both analyses IPA created the network 'embryonic development, hair and skin development and function, organ development'. Green: up-regulated in EM; red: up-regulated in UM; grey: detected by the transcriptome analyses but not differentially regulated between EM and UM; white: located to the network by IPA but not detected by the transcriptome analyses.

3. Results

Table 3.4: Genes significantly differentially transcribed according to microarrays and SuperSAGE

NR Gene	Gene annotation Smp	array (EM/UM)	SuperSAGE (EM/UM)	SAGE- strand
Smp_135230	aromatic-L-amino-acid decarboxylase (DDC)	2.58	2.08	Exon
Smp_168940	NAD dependent epimerase/dehydratase	2.66	1.49	Exon
Smp_052230	kunitz-type protease inhibitor	1.83	1.78	Exon
Smp_008660.x	villin	0.94	1.43	Exon
Smp_163720	endophilin B1	0.83	1.40	Exon
Smp_055220.x	surface protein PspC	0.83	1.19	Exon
Smp_020540.x	<u>pinch</u>	<u>0.61</u>	<u>1.10</u>	<u>Exon</u>
Smp_040560	cancer-associated protein	0.85	1.02	Exon
Smp_073130.x	loss of heterozygosity 11 chromosomal region 2 gene a protein homolog (mast cell surface antigen 1) (masa- 1)	0.74	1.00	Exon
Smp_170080	sodium/dicarboxylate cotransporter-related	1.18	0.92	Exon
Smp_080210	lipid-binding protein	0.65	0.89	Exon
Smp_151490	nebulin	0.80	0.89	Exon
Smp_070030	snf7-related	0.71	0.79	Exon
Smp_003770	histone h1/h5	0.86	0.68	Exon
Smp_010770.x	fatty acid acyl transferase-related	-1.71	-0.89	Exon
Smp_123080	Sarcoplasmic calcium-binding protein (SCP).	-0.86	-1.00	Exon
Smp_123300	<u>follistatin</u>	<u>-2.15</u>	<u>-1.23</u>	<u>Exon</u>
Smp_036470	<u>oxalate-formate antiporter</u>	<u>-2.91</u>	<u>-1.76</u>	<u>Exon</u>
Smp_158480	<u>AMP dependent ligase</u>	<u>2.82</u>	<u>3.55</u>	<u>Intron</u>
Smp_151620	cadherin-related	0.63	1.41	Intron
Smp_135520	<u>dock</u>	<u>-1.31</u>	<u>-0.65</u>	<u>Intron</u>

Of all transcripts detected in the SuperSAGE and microarray analyses 29 met the refined criteria for abundance in SuperSAGE and sig. diff. regulation in both studies. Of these, 21 with functional annotations other than 'hypothetical protein' are presented here.

transduction seemed to be of greater interest. Though belonging in this category, dock was not chosen for further analyses, because significant regulation had been found for a putative intron-sequence. Similarly, the signaling molecule pinch was excluded from further analysis, because its regulation was contradictory in real-time PCR experiments though corresponding for microarrays and SuperSAGE. Thus follistatin remained the first choice candidate for further characterization.

3.6. First characterization studies

3.6.1 Follistatin

Follistatin was chosen for further characterization studies as it was one of the molecules showing strong and significant regulation in all analyses (see Table 3.4.). Additionally, it has a presumptive role in TGF β -pathways (Moustakas & Heldin, 2009; Massagué & Chen, 2000), which have been characterized in schistosomes as having important roles in embryonic development and gonad differentiation processes of females (Freitas *et al.*, 2007; Knobloch *et al.*, 2007; LoVerde *et al.*, 2007; reviewed in: Beall *et al.*, 2000).

Based on the gene prediction for Smp_123300 from the *S. mansoni* genome project (Berriman *et al.*, 2009), primers were designed and the full-length CDS of follistatin (SmFst) amplified. The PCR-product was cloned into the vector pDrive. Sequencing of the inserted fragment revealed minor differences to the data base prediction (as presented in SchistoDB 2.0) (Figure XIX, see appendix). Sequence parts predicted as introns were found in the sequenced stretch from the RT-PCR reaction and thus represent parts of the CDS. For more detailed classification of SmFST a SMART domain-prediction analysis of the SmFst-CDS was performed. It detected two follistatin-domains (FstD) within the sequence. FstDs are further subdivided into an EGF (epidermal growth factor) and Kazal (a protease inhibitor) –domain (Keutmann *et al.*, 2004), which, according to the SMART domain-prediction, do not follow each other directly in SmFst (amino acid positions: EGF-domains: 52-74, 312-337; Kazal-domains: 264-307, 398.434). A phylogenetic analysis placed SmFst closer to follistatin-like proteins containing only two FstDs than to Fsts containing three FstDs (Keutmann *et al.*, 2004) (Figure 3.17.).

***In situ* hybridization**

From the amplified sequence two probes were designed for *in situ* hybridization experiments with *S. mansoni* couples and UM. SmFst transcripts were detected in the testicular lobes of both EM and UM, as well as in the vitellarium and the ovary of the female (Figure 3.18). Results concerning

3. Results

the detection of sense or anti-sense transcripts varied with probe-sequence and probe batch. However, organ-specific RT-PCR reactions (Hahnel *et al.*, 2013) confirmed the presence of transcripts for SmFst within ovary and testes (Leutner *et al.*, 2013).

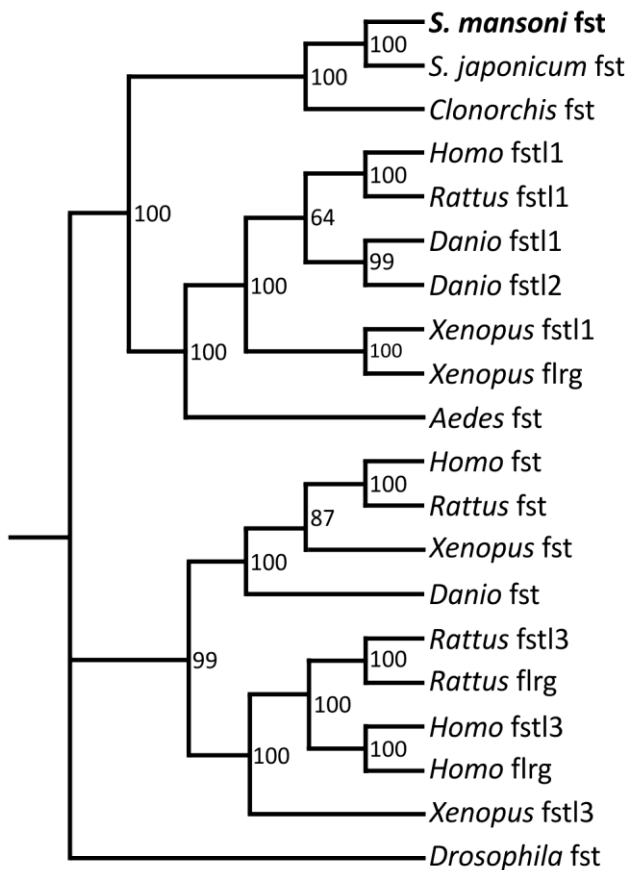


Figure 3.17: Phylogenetic analysis of SmFst in comparison to other follistatins from different organisms.

A phylogenetic analysis placed SmFst closer to 'follistatin-like proteins' than to follistatins. The following amino acid sequences were used: *Schistosoma mansoni* follistatin (KC165687); *Schistosoma japonicum* follistatin (AAW26942); *Clonorchis sinensis* follistatin (GAA49198); *Homo sapiens* follistatin-like 1 (AAH00055); *Rattus norvegicus* follistatin-like 1 (AAH87014); *Danio rerio* follistatin-like 1 (ABC48671), follistatin-like 2 (ABC48672); *Xenopus laevis* follistatin-like 1 (AAH77997), follistatin-related protein (BAB13800); *Aedes aegypti* follistatin (XP_001648919); *Homo sapiens* follistatin (AAH04107); *Rattus norvegicus* follistatin (AAB60704); *Xenopus laevis* follistatin (AAB30638); *Danio rerio* follistatin (AAI52096); *Rattus norvegicus* follistatin-like 3 (EDL89395), follistatin-related protein FLRG (BAB32664); *Homo sapiens* follistatin-like 3 (AAQ89276), follistatin-related protein FLRG (AAC64321); *Xenopus laevis* follistatin-like 3 (AAI23194); *Drosophila melanogaster* follistatin (AF454393_1).

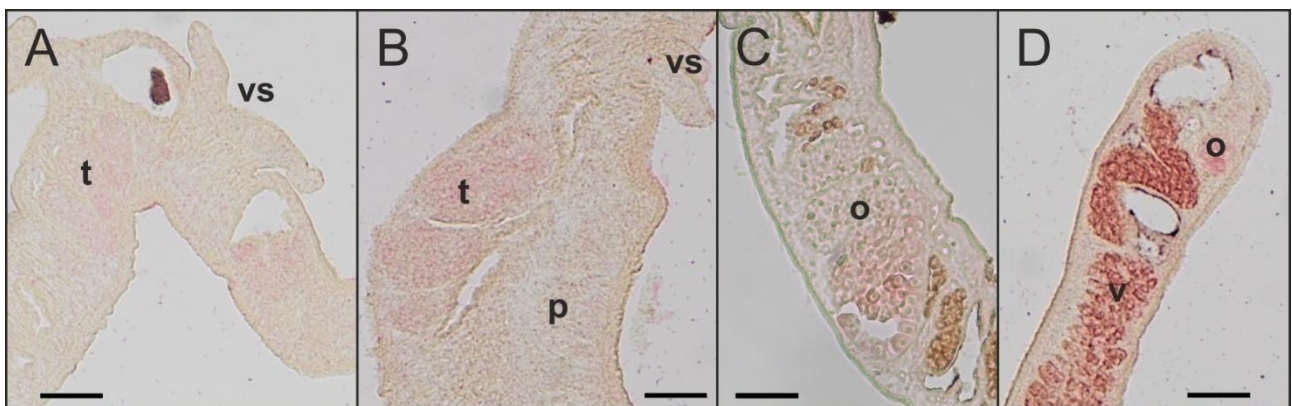


Figure 3.18: SmFst *in situ* hybridization.

Results with sense and anti-sense detecting probes (Figure XIX, see appendix) were inconsistent, but whenever signals were obtained they showed transcription of SmFst within the reproductive organs of couples and UM. A: UM, B: EM, C: EF, D: EF. o: ovary, p: parenchyma, v: vitellarium, vs: ventral sucker, t: testicular lobes. Scale bar: 50µM.

Stage-specific RT-PCR

To confirm the presence of SmFst in different life cycle stages of *S. mansoni* non-quantitative RT-PCR reactions were performed with RNAs from EM, UM, EF, UF, miracidia, and cercariae. Transcripts were detected in all tested stages except cercariae (Figure 3.19.).

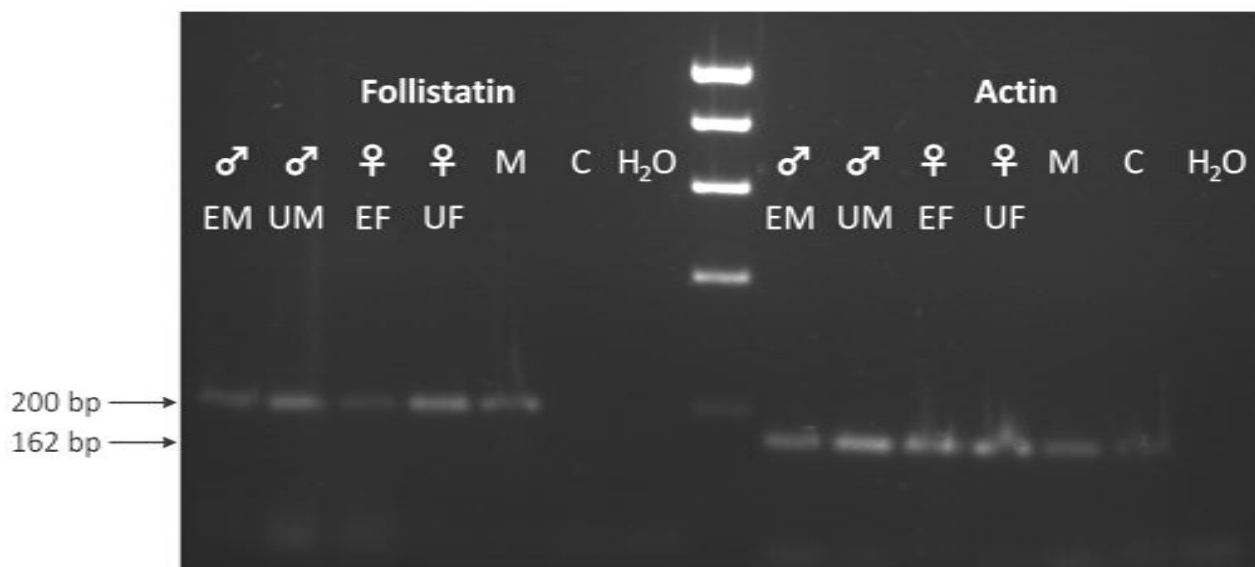


Figure 3.19: Stage-specific RT-PCR for SmFst.

A non-quantitative RT-PCR detected SmFst transcripts in different life-stage. Actin served as positive control. EM: pairing-experienced males, UM: pairing-unexperienced males, EF: pairing-experienced females, UF: pairing-unexperienced females, M: miracidia, C: cercariae, H₂O: PCR negative control, marker: Hyperladder I.

SmFst interaction studies

Previous studies demonstrated that follistatin is able to bind to activin, an agonist of the TGF β -pathway, and with less affinity to BMP (Stamler *et al.*, 2008; Lin *et al.*, 2006). In schistosomes, SmInAct, an activin/inhibin, and SmBMP were characterized (Freitas *et al.*, 2009; Freitas *et al.*, 2007). To investigate potential interactions between SmFst and SmInAct / SmBMP, Y2H analyses were performed. To this end, a full-length variant of SmFst was cloned into the Gal4-BD vector pBridge, while full-length SmInAct (Figure XX., see appendix) and four different parts of SmBMP (Figure XXI and XXII, see appendix) were cloned into the Gal4-AD vector pACT2. The SmFst-containing plasmid was transformed into yeast cells (AH109) together with either one of the other plasmids. To control successful transformation the yeast were grown on selection plates (SD-Trp/-Leu/-His). Subsequently, liquid and filter β -gal assays were performed to confirm interactions between SmFst and SmInAct / SmBMP. According to β -gal filter and liquid assays interactions between SmFst and SmInAct as well as between SmFst and SmBMP were found, while no signal was obtained for the interaction with SmBMP-C-Term and negative controls (Figure 3.20.).

3. Results

Comparison of these results indicated a stronger binding of SmFst to SmInAct. Also, the C-terminal part of SmBMP seemed to be less important for the interaction with SmFst, than the rest of the protein.

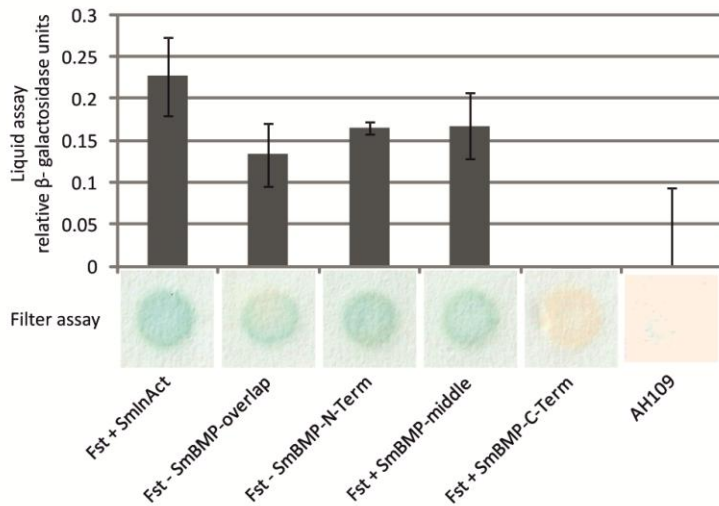


Figure 3.20: Yeast two-hybrid experiments with SmFst.

Y2H liquid and filter assays were performed with the full length sequences of SmFst and SmInAct, as well as full length SmFst and four different sequence parts of SmBMP (Figure XXII). The upper part of the figure shows the results of the β -gal liquid assay, the lower part those from a representative β -gal filter assay.

The above described experiments indicated SmFst transcription within *S. mansoni* reproductive organs of couples as well as UM. Transcription occurred in all adult *Schistosoma* life-stages and miracidia. Y2H-interaction studies provided evidence for the binding of SmFst to SmInAct and SmBMP. Thus, it seems likely that SmFst may regulate TGF β -pathways in schistosomes. To obtain further indications whether SmFst also colocalizes with SmInAct or SmBMP, *in situ* hybridization experiments for these transcripts were conducted.

3.6.2 *In situ* hybridization experiments for SmInAct and SmBMP

As potential interaction partners of SmFst, SmInAct and SmBMP were of special interest. SmInAct transcripts were detected by SuperSAGE only, although not significantly regulated between EM and UM (supplementary-file16). This was also confirmed by real-time PCR results (Figure 3.13.). SmBMP was found to be significantly and differentially down-regulated in the microarray data-set, however, this was not confirmed by SuperSAGE data (supplementary-file16) or real-time PCR (Figure 3.13.). Previous studies had localized SmInAct to the ovary and vitellarium of EF, but no information was provided on the presence of SmInAct transcripts in testicular lobes (Freitas *et al.*, 2007).

The results obtained in two replicas with a probe based on the same sequence as the one used in the previous publication (Freitas *et al.*, 2007) showed transcript detection only in the ovary of EF,

with sense and anti-sense probes. No signals were observed in the vitellarium or the testes of EM or UM (Figure 3.21.). Organ-specific RT-PCR reactions (Hahnel *et al.*, 2013) confirmed SmlnAct transcripts not only in the ovary but also in the testes (Leutner *et al.*, 2013).

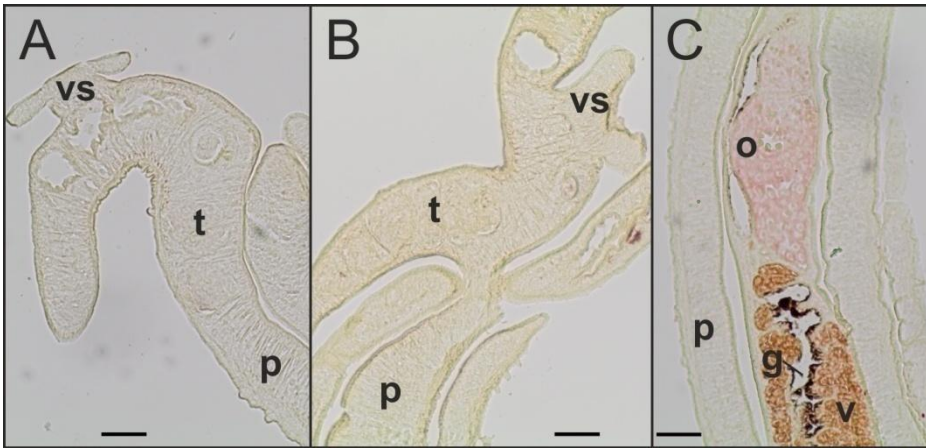


Figure 3.21: SmlnAct *in situ* hybridization.

SmlnAct-specific probes (see figure XX) detected sense and anti-sense transcripts in the ovary (o) of EF (C). No signals were obtained in the vitellarium (v) (C) or the testicular lobes (t) of UM (A) or EM (B). (Depicted results are representative for sense and anti-sense detecting probes.) g: gut, p: parenchyma, vs: ventral sucker. Scale bar: 50 μ M.

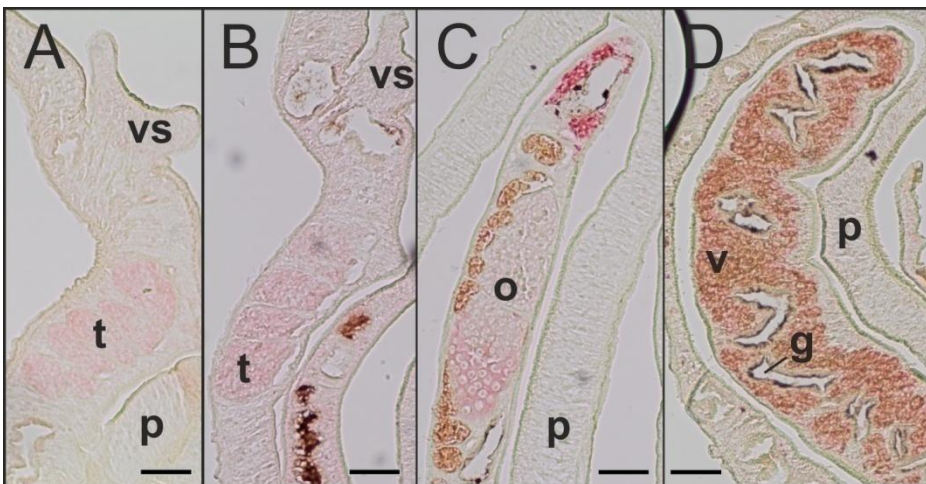


Figure 3.21: SmBMP *in situ* hybridization.

Two different probes (Figure XXI, see appendix) for SmBMP were used in *in situ* hybridization experiments, each for sense as well as anti-sense. Both probes detected transcripts in the reproductive organs of couples (B, C, D) and UM (A). The pictures are representative examples for the detection of SmBMP transcripts, independent of probes and strands. A: UM, B: EM, C: EF, D: EF. g: gut o: ovary, p: parenchyma v: vitellarium, vs: ventral sucker. t: testicular lobes. Scale bar: 50 μ M.

Two different probes were used for the localization of SmBMP (Figure XXI, see appendix). Transcripts were detected in all reproductive organs of couples as well as UM, but especially for probe 2 in the area around the ootype (Figure 3.22.). Anti-sense transcripts were detected as well as sense-transcripts, though often more weakly. Again, organ-specific RT-PCRs (Hahnel *et al.*,

3. Results

2013) detected SmBMP transcripts in the ovary and testes (Leutner *et al.*, 2013), though cDNAs had to be used undiluted to obtain a result, while a 1:20 dilution had been used in case of SmFst and SmlnAct.

The localizations of SmlnAct and SmBMP transcripts corresponded with those of SmFst. Together with the results from the Y2H-experiments evidence is provided that SmFst and SmlnAct may interact in the ovary and testes, while SmFst and SmBMP could interact in all reproductive organs.

4. Discussion

Male *S. mansoni* are essential for the unique reproduction biology of the parasite, as females will only differentiate into a sexually mature state and maintain this status if they are in a constant pairing-contact with the male (Kunz, 2001; Grevelding *et al.*, 1997a; Popiel *et al.*, 1984; Clough, 1981; Shaw, 1977; Erasmus, 1973). Research in the past has mostly focused on females (reviewed in: Beckmann *et al.*, 2010b; LoVerde *et al.*, 2009; Knobloch *et al.*, 2007; Grevelding, 2004; Kunz, 2001), while only few studies focused on males (Waisberg *et al.*, 2007; Williams *et al.*, 2007; Fitzpatrick & Hoffmann, 2006). First experiments in our group, approaching the question which processes in males are influenced by pairing, investigated the influence of pairing or TNF α on MA in males. Additionally the role of a cGMP-dependent protein kinase in *S. mansoni* was analyzed, following first evidence for its differential expression between EM and UM (Schulze, 1997). In the major analysis of the present study differences in the transcriptional activity between EM and UM were identified applying microarrays, SuperSAGE and real-time PCR. New insights into male differentiation in response to pairing were obtained including the new finding and first characterization of SmFst.

4.1. Mitotic activity in males

4.1.1. The effect of pairing on mitotic activity in males

Re-pairing experiments were performed to confirm the results of DenHollander and Erasmus (1985), who analyzed MA in virgin females paired to EM or UM. The original data indicated a faster (24 h vs. 48 h) stimulation of MA in females through pairing to EM. This result was interpreted as an indication that males are also influenced by pairing. If never paired before, they first have to reach a status of competence, which enables them to stimulate females. This interpretation was not confirmed by this study, as contradictory results were obtained for the MA in females. Also, a stimulation of MA in males following pairing, found in initial experiments performed in this thesis, could not be substantiated in subsequent experiments.

Up to date few studies have analyzed MA in adult schistosomes. Previous to the publication mentioned above, DenHollander and Erasmus reported about an analysis of MA differences between EM and UM, and EF and UF (Den Hollander & Erasmus, 1984). While differences in the MA of females were observed, none were found between EM and UM. These results were supported by more recent experiments comparing the MA of paired, separated and repaired EM and EF (Knobloch *et al.*, 2006). While MA was similar in paired and repaired females and reduced

4. Discussion

in separated females, no differences were found between the three male groups (Knobloch *et al.*, 2006). In contrast to these previous studies, which both indicated stimulation of MA in females by pairing and similar MA between different male stages (Knobloch *et al.*, 2006; Den Hollander & Erasmus, 1984), the present study detected a great variance in the MA of males and females. However, differences between paired and unpaired males or females were inconsistent and did not confirm a clear effect of pairing on MA. It is likely that this is due to methodological difficulties as indicated by inconsistencies between technical replicas. Early experiments analyzing schistosome MA applied a radioactive thymidine analogue (Den Hollander & Erasmus, 1985; Den Hollander & Erasmus, 1984), with which worms were incubated for one hour, before termination of the experiments. In contrast to this, incubation with BrdU was done throughout the whole experimental period (12 / 24 / 48 h). It can be assumed that, compared to MA-measurement over the whole pairing-period, measurement of MA for one hour at the end of a pairing-period is more accurate as it is in itself independent on the duration of the pairing-period. However, this could not be done with BrdU as an indicator of MA, because the obtained signal is much weaker than the one resulting from radioactive markers.

Two additional factors may have influenced the results, i) instead of UF (Den Hollander & Erasmus, 1985) one week-separated females were used, based on the MA data from Knobloch *et al.* (Knobloch *et al.*, 2006). However, no data exist with regard to the question if separated females and UF can be stimulated similarly well concerning their MA after culturing them for one week or more *in vitro*. ii) Aberrant from the original non-radioactive experiments (Knobloch *et al.*, 2002a), where the time for *in vitro* culture did not exceed two days, all worms used here were in culture for at least four days, females even longer as detailed above. As recently described (Galanti *et al.*, 2012), female worms are rapidly affected by culture conditions. Females shrink and have a reduced DNA content, independent of pairing. This might explain the difficulty met during this study in obtaining sufficient amounts of female DNA, which is reflected by weak DAPI-signals often detected (Figure II, Figure V). These factors, the strong influence of culture conditions and weak DAPI-signal could have caused the inconsistent results on MA in females presented here.

Even though no decline in DNA content or body size was observed in cultured males (Galanti *et al.*, 2012), other effects might play a role for the inconsistent results on MA in males. A constant DNA content does not necessarily indicate equal MA in individual worms and strong individual variances could introduce even stronger variances into group-results. While re-pairing is a clear parameter for fitness and natural behavior of a male in culture, only less clear parameters can be

defined to pick individuals from a group of unpaired males, which look very similar to the paired ones concerning vitality. Thus, the selection of control males might have had an influence on the results obtained for MA in males, even though this selection was done as standardized (and randomized) as possible.

In conclusion, it is not possible, with regard to the obtained data, to undoubtedly contradict the results of previous experiments indicating differences in the MA of females paired to EM or UM, and indifference between EM and UM (Knobloch *et al.*, 2006; Den Hollander & Erasmus, 1985; Den Hollander & Erasmus, 1984). Future repetitions of this experiment using the non-radioactive method have to be refined methodologically. Besides usage of UF, larger worm samples and media from the same batch should be used, and it might be necessary to analyze the possibility of shorter BrdU incubation periods.

4.1.2. The effect of TNF α treatment on schistosome mitotic activity

Of the host factors influencing schistosome development TNF α was reported in the past to exert a stimulatory effect on egg production (Amiri *et al.*, 1992). During preliminary studies our working group additionally detected stimulation of MA in males while researching the effect of TNF α on MA in females. This observation was further investigated in the current study.

To this end, TNF α was used in the *in vitro* culture system at concentrations of 0.2 ng/ml, 1 ng/ml, 5 ng/ml, 20 ng/ml and 50 ng/ml. While the effect on MA in females was inconsistent, MA in males was affected concentration-dependently. However, this effect also depended on the applied culture-medium. Thus lower concentrations of TNF α stimulated MA compared to higher concentrations when using M199, while the opposite was found when using Basch-medium.

Historically, TNF α was described to have an enhancing effect on granuloma formation and a concentration-dependent stimulatory effect on egg-deposition by females *in vivo* and *in vitro*, where the highest concentration of TNF α (40ng/ml) had the strongest effect (Amiri *et al.*, 1992). These findings however, were contested by other studies: for egg-production *in vitro*, the opposite results were observed (Haseeb *et al.*, 1996); *in vivo* experiments found no impact at all (Davies *et al.*, 2004); and no effect on granuloma formation (Davies *et al.*, 2004; Cheever *et al.*, 1999) was found using the same concentrations of TNF α .

Other studies on TNF α , analyzing the cytokine's influence on cell proliferation or tumor inhibition also provided contradictory results. In some experimental setups TNF α had an anti-proliferative effect, inducing tumor regression (reviewed in Baisch *et al.*, 1990), in other studies growth was

4. Discussion

stimulated (reviewed in Baisch *et al.*, 1990). As TNF α is often effective only in combination with other cytokines (reviewed in Baisch *et al.*, 1990), experiments are strongly dependent on *in vivo* or *in vitro* conditions and in the latter case also on the media applied.

Two receptors for TNF α are known and belong to different TNF α -receptor (TNFR) subfamilies, the death domain (DD)-containing receptors and the TNF α receptor associated factor (TRAF)-interacting receptors (Hehlgans & Pfeffer, 2005; Wajant *et al.*, 2003). The DD-containing receptor TNFR1 is expressed in most tissues and better characterized than the non DD-containing receptor TNFR2, which occurs more restricted in immune cells (Wajant *et al.*, 2003). Generally, TNFR1-dependent signal transduction is linked to apoptosis and cell death, while TNFR2-dependent signaling is associated with cell survival and differentiation (Locksley *et al.*, 2001). However, it has been postulated that TNFR1 is able to activate apoptotic as well as proliferative processes in parallel by simultaneous down-stream activation of caspases, and NF- κ B or c-Jun N-terminal kinase (JNK)-signaling (Bradley, 2008; Hehlgans & Pfeffer, 2005; Chen & Goeddel, 2002). TNFR2 acts through different signal transduction cascades. Through activation of the endothelial/epithelial tyrosine kinase (etk) proliferation and cell survival is influenced (Bradley, 2008). Additionally, TNFR2 may act as a modulator of TNFR1-signaling by forming heterotrimeric complexes with the other receptor (Chan, 2007) or by induction of endogenous, membrane-bound TNF α , subsequently acting on TNFR1 (Wajant *et al.*, 2003). In *Drosophila* a TNF α -homolog (Eiger) and one TNFR (Wengen) are known (Narasimamurthy *et al.*, 2009). While modulating the immune response to extracellular pathogens on the one hand, signal-transduction through a JNK-mediated pathway leads to apoptosis on the other hand (Narasimamurthy *et al.*, 2009).

One TNFR has been identified within the *S. mansoni* genome and was described in detail (Oliveira *et al.*, 2009). While phylogenetic analyses did not place SmTNFR in an ancestral position to mammalian TNFRs, neither categorizing it as type 1 nor as type 2 receptor, it was suggested to belong to the group of type 2 receptors, which lack the intracellular death domain typical for type 1 receptors (Oliveira *et al.*, 2009). Additionally, the schistosome genome encodes for more signal transduction molecules associated to TNFR2-signaling than those involved in TNFR1 signal transduction (Oliveira *et al.*, 2009). Placing SmTNFR into the group of cell survival- and differentiation-stimulating type 2 receptors supports the assumption that TNF α could stimulate egg production or even MA. However, it has also been shown, that cell death can be induced through TNFR2 (Wajant *et al.*, 2003). Also, TNFR2 has been described to induce proliferation or apoptosis in reaction to TNF α depending on the cell cycle state (Baxter *et al.*, 1999). Thus it is

unclear if SmTNFR indeed acts singularly on cell proliferation, or whether it induces multiple effects depending on the different factors influencing the signal transduction cascade.

Taken together, the results presented here, and those obtained from other studies (Oliveira *et al.*, 2009; Haseeb *et al.*, 2001), as well as the presented knowledge from mammalian TNF α signal transduction indicate the possibility that TNF α has an influence on schistosomes. This assumption is supported by a comparison of schistosome-specific experiments, revealing minor but important differences. For example, Amiri *et al.* (1992) and Cheever *et al.* (1999) used the same mice-strain and TNF α from the same source but different schistosome strains. Haseeb *et al.* (1996) used a different source of TNF α and incubated females without males, applying a different medium compared to that used by Amiri *et al.* (1992). My results were obtained using TNF α from two different companies, and differences in the effect of TNF α depending on the medium applied were observed.

In conclusion the above described observations indicate that the influence of TNF α on schistosomes is strongly dependent on the interplay with other factors of the given environment. Future studies will have to investigate the effects of TNF α under more standardized conditions. Thus the same batch of culture medium and TNF α should be used for all experiments. If a batch change in one of these parameters occurs it should be tested in the same experiments with the older components as control. With an appropriate testing-system established, RNAi experiments could be used to knock down the TNFR and subsequently investigate the effects of TNF α treatment on schistosomes lacking or containing less TNFRs.

4.2. The role of SmcGKI in schistosomes

In search for molecules relevant for processes responsible for the transformation from UM to EM and subsequent female stimulation and differentiation, PKs are of special interest. Kinases are important players in signal transduction, regulating a multitude of cellular processes (Krauss, 2008). In *S. mansoni* their importance is mainly known for different processes in the female (Long *et al.*, 2012; Wilson, 2012; Beckmann *et al.*, 2012b; Beckmann *et al.*, 2011; Dissous *et al.*, 2011; Long *et al.*, 2010; Beckmann *et al.*, 2010a; Beckmann *et al.*, 2010b; LoVerde *et al.*, 2009; Knobloch *et al.*, 2007; LoVerde *et al.*, 2007; Yan *et al.*, 2007; Knobloch *et al.*, 2002b; Kapp *et al.*, 2001) but also in spermatogenesis (Long *et al.*, 2012; Beckmann *et al.*, 2011; Dissous *et al.*, 2011; Long *et al.*, 2010; Beckmann *et al.*, 2010a; Beckmann *et al.*, 2010b; Knobloch *et al.*, 2002b; Kapp *et al.*, 2001), and larval development (Swierczewski & Davies, 2010a; Swierczewski & Davies, 2010b; Ludtmann

4. Discussion

et al., 2009; Swierczewski & Davies, 2009; Bahia *et al.*, 2006b). Furthermore, PKs are involved in neuronal and muscular activity of adults (de Saram *et al.*, 2013), and they are discussed as potential novel drug targets (Beckmann *et al.*, 2012a; Dissous & Grevelding, 2011; Andrade *et al.*, 2011; Avelar *et al.*, 2011; Dissous *et al.*, 2007; Bahia *et al.*, 2006a).

Evidence for differential transcription of a cGMP-dependent protein kinase between EM and UM was provided by results of a Diploma thesis (Schulze, 1997). The present analysis was done as a follow-up study, to i) identify the complete CDS of this cGK, ii) verify the differential transcription between EM and UM, and iii) to perform first characterization studies. Additionally, other cGK homologs were identified within the *S. mansoni* genome (Leutner *et al.*, 2011).

In mammals three cGKs are known: the two cGKI isoforms cGKI α and cGKI β and cGKII (Hofmann *et al.*, 2009). cGKs are known for their role in smooth muscle cells, platelets, neuronal tissues, spermatogenesis, sperm chemotaxis and motility (Miraglia *et al.*, 2011; Hofmann *et al.*, 2009; Teves *et al.*, 2009; Yuasa *et al.*, 2000). In *Caenorhabditis elegans* cGKs regulate body size, behavior (Raizen *et al.*, 2006; Fujiwara *et al.*, 2002) and odor perception (Lee *et al.*, 2010). A common role for cGKs across different phyla seems to be a function in locomotion (Baker & Deng, 2005; Stansberry *et al.*, 2001).

Originally, *S. mansoni* cGK transcripts were detected in RNA slot blots and northern blots using a probe based on 189 nucleotides of the C-terminal sequence. A database search with the original, partial cGK sequence (Schulze, 1997) detected a gene (Smp_123290) representing the putative full-length CDS. Following cloning, comparison of the obtained sequence and Smp_123290 revealed additional 165 nucleotides compared to the data base prediction. This may result from inaccurate sequence information for this exon or a strain difference, since a Porto Rico strain was used for the genome project, whereas a Liberian *S. mansoni* strain was used in this study.

Blast analyses of the full-length cDNA sequence and additional phylogenetic analyses were performed to classify SmcGK1. An analysis of partial sequences containing the kinase domain showed homology to mammalian cGKII, while use of full-length sequences indicated homology to invertebrate cGKs (*Drosophila*, *C. elegans*). Also the SmcGK1 sequence lacks a myristoylation motive typical for cGKIIs (Zhang & Rudnick, 2011; Vaandrager *et al.*, 1996). Thus, an intermediate position of the SmcGK1 within cGK classification was indicated. Besides SmcGK1 three more cGKs (Smp_174820, Smp_151100, Smp_080860 + Smp_078230) could be identified in *S. mansoni* combining data base and RT-PCR analyses.

Treatment of schistosome couples with 1 mM (PR)-8-pCPT-cGMPS, a cGMP analog able to block cGKI from human platelets or cGKI/cGKII from mouse (Gamm *et al.*, 1995; Butt *et al.*, 1994), resulted in reduced egg production and morphological as well as behavioral changes in the worms, depending on the worm-batch. An initial experiment revealed strong effects with regard to an oocyte congestion within the oviduct of females, disarrangement of the ovary and a disintegrated cell structure that may be a sign of apoptosis in addition to a generally reduced motility in couples (from day 3-6). However, subsequent experiments showed only a slight influence on the female phenotype after a prolonged period of time, which might be due to a new batch of inhibitor or the use of worms from a different perfusion. Different perfusional origin means worms grown from schistosomula into adults in a different hamster and thus in a different environment, depending on the host's specific blood composition. However, all three experiments performed led to a reduction in egg production. Localization studies conducted in parallel detected SmcGKI transcripts within the ovary, testes and vitellarium. These results indicated a role for SmcGKI in schistosome reproductive organs, especially the ovary. The once-only observed effect on motility also hints at a SmcGKI function during muscle activity. Transcript levels might have been too low for corresponding detection by *in situ* hybridization. In mammals cGKs are known for their participation in muscle cell signal transduction (Hofmann *et al.*, 2009; Schlossmann *et al.*, 2003). A loss in muscle activity around the female oviduct could also be the reason for the oocyte congestion. Furthermore, inhibition of normal gut peristaltic in the female, or the male movement could be responsible for the constricted oocyte transportation. The female gut peristaltic could indirectly facilitate oocyte transportation, while the male movement could have a massaging effect on the female, and thus on oocyte transportation.

Unexpectedly, *in situ* hybridization experiments repeatedly detected SmcGKI anti-sense transcripts. In recent years anti-sense RNAs have come into focus as gene regulators (Magistri *et al.*, 2012; Knowling & Morris, 2011; Su *et al.*, 2010; Werner & Sayer, 2009; Militello *et al.*, 2008). Presence of SmcGKI anti-sense RNAs in all adult schistosome life stages was confirmed by RT-PCRs. Results from RT-PCRs, however, will have to be repeated in the future and until then must be seen critically, as no "no primer controls" were included. Their necessity was pointed out by independent experiments and a following literature search, which indicated that RNA-self priming can lead to artificial results (Haddad *et al.*, 2007; Levin, 1996). Without the appropriate controls it cannot be excluded that the obtained SmcGKI anti-sense RT-PCR results might be due to such a self-priming instead of true anti-sense transcription. Still, results from *in situ* hybridization

4. Discussion

experiments and the transcriptome studies subsequently discussed, indicate the presence of SmcGKI anti-sense transcripts in EM and UM.

Opposite to the results of previous experiments (Schulze, 1997), a differential transcription of SmcGKI between EM and UM, could not be confirmed in this study. Preliminary analysis of transcriptome data comparing EM and UM indicated an up-regulation of SmcGKI in EM, while semi-quantitative RT-PCRs did not detect differences between these two male stages. The final analyses of transcriptome data obtained on EM and UM did not indicate differential transcription for SmcGKI between EM and UM (Table I.I.), whereas real-time PCR experiments showed variable results. Thus, further factors such as the final host or the *in vitro* environment before freezing the worm material for further analysis may have additionally influenced SmcGKI transcription. Of all four cGKs only Smp_151100 was differentially regulated between UM and EM (not passing the defined \log_2 ratio threshold), as found in the final transcriptome analysis (see below).

While the previously indicated evidence for differential transcription of SmcGK1 between EM and UM was not confirmed, indications for a role of this molecule in schistosome gonads, especially the ovary, and in schistosome motility exist. Future studies should include further repetitions of the inhibitor experiments to substantiate these observations. Since (PR)-8-pCPT-cGMPS is a cGMP analog which may bind to any of the *S. mansoni* cGKs, the specificity of its action has to be clarified. This may be done through germinal vesicle break down (GVBD) assays (Vicogne *et al.*, 2004; Haccard *et al.*, 1995). Constructs for the different *S. mansoni* cGKs would have to be tested for their capability to induce GVBD. Subsequently (PR)-8-pCPT-cGMPS could be used to inhibit cGK induced GVBD, thereby determining its specificity for the different *S. mansoni* cGKs. Also other cGK inhibitors could be used. Again, they would have to be tested for their specificity in schistosomes. It might also become necessary to investigate the incorporation of inhibitors into the worms. As an online search revealed, most cGK inhibitors are peptide based, and to date it has not been proven that such inhibitors can effectively enter into and affect the flukes. Verification could be done by coupling of the inhibitor to a fluorescent dye. Furthermore, functional roles and differences between the *S. mansoni* cGKs could be elucidated through knock-down studies (by RNAi) and the search for interaction partners (by Y2H). The latter would help to get deeper insights into the involved pathways.

4.3. Transcriptomic comparison between EM and UM

To identify genes differentially expressed between EM and UM two separate transcriptome analysis methods were applied. While previous studies (Waisberg *et al.*, 2007; Williams *et al.*, 2007; Fitzpatrick & Hoffmann, 2006) also used transcriptomics for the same question, these approaches covered fewer genes using one of these methods only. Furthermore, these studies referred to preliminary genome data and data from EST-projects (Verjovski-Almeida *et al.*, 2004; LoVerde *et al.*, 2004; Hu *et al.*, 2003; Verjovski-Almeida *et al.*, 2003; Merrick *et al.*, 2003; Franco *et al.*, 2000). The study presented here took advantage of combining microarray analyses, using a 44k platform (Verjovski-Almeida *et al.*, 2007), and is thus larger than those previously applied for the same question (Waisberg *et al.*, 2007; Williams *et al.*, 2007; Fitzpatrick & Hoffmann, 2006), and SuperSAGE as well as a gene annotation referring to the first version of the genome project (Berriman *et al.*, 2009).

For both transcriptome analyses three independent biological replicas of EM and UM were used. Microarray experiments were performed in technical quadruplicate (including dye swaps). Resulting data-sets were analyzed separately before they were combined and only sense-transcripts were analyzed further. To facilitate data-interpretation beyond standard statistics, different bioinformatic tools were applied. GO analyses were performed to identify enriched cellular gene categories, IPA placed detected molecules into the greater context of enriched networks, while the SchistoCyc 'omics viewer' function pointed out differences in the transcription of genes associated to metabolic processes.

It was anticipated that the combination of microarrays and SuperSAGE would ensure the detection of all present transcripts and provide independent evidence for their importance in the differentiation from UM to EM. Signaling cascades are most likely involved in such processes as is already known from female schistosomes (Beckmann *et al.*, 2012b; Beckmann *et al.*, 2010b; Knobloch *et al.*, 2007; LoVerde *et al.*, 2007). Therefore, it was expected that transcripts for signaling molecules would be regulated between EM and UM. Furthermore, the male stimulus towards the female has been proposed to be purely tactile (Armstrong, 1965) or a secreted soluble factor (Basch, 1990; Basch & Nicolas, 1989; Popiel & Basch, 1984b; Atkinson & Atkinson, 1980; Shaw *et al.*, 1977). Therefore, results of the transcriptome studies were examined for the differential regulation of surface molecules, which might indicate tactile communication between males and females; transcripts associated with the production, or coding for a secreted molecule; and transcripts related to transcription control, as they might indicate which processes are

triggered in EM. Lastly metabolism-associated transcripts were expected to be regulated between the two male stages, as previous studies had indicated such differences (Williams *et al.*, 2007; Fitzpatrick & Hoffmann, 2006).

4.3.1 Comparison of microarrays and SuperSAGE revealed methodological and statistical differences

Comparing both transcriptome analyses 6,326 gene representing transcripts were detected by both methods and additional 3,018 and 1,168 genes were exclusively detected by SuperSAGE or microarrays, respectively (Figure 3.10.). It was assumed that these differences in detection were due to a lack of according oligonucleotides on the microarray, or in case of SuperSAGE due to missing *Nla*III restriction enzyme recognition sites in the transcripts. A survey of transcripts detected by SuperSAGE only revealed that 45 % of the tested transcripts were represented by oligonucleotides on the microarray. Transcripts detected by microarray analyses only, and checked for *Nla*III restriction enzyme recognition sites showed that a minority of 7 % did not have the according sequence motive.

Further explanations for missing detection of transcripts by microarray analyses are problems during hybridization, which may have been caused by a reduced binding of specific RNAs to their respective oligonucleotides. Also, an imperfect integration of dyes during *in vitro* transcription may have occurred for specific transcripts or a partial fragmentation of RNAs previous to hybridization. In case of transcripts not found by SuperSAGE, detection problems may have been caused by incomplete restriction digestion or inaccessibility of the restriction site through RNA secondary structures; previous shearing of RNA (lack of polyA), defective PCR amplification for specific transcripts, and a reduced number of technical replicas. SuperSAGE was performed using three biological replicas, without technical replicas, while microarrays were done with four technical replicas for each biological sample. The larger amount of technical replicas enhanced chances for detection of low abundant transcripts with the microarrays compared to SuperSAGE. Additionally, the shorter tag-sequences (27 bp) created by SuperSAGE are less reliable concerning their definitive annotation than the 60mer oligonucleotides from the microarray. Thus, transcripts detected by the microarray only may be in the group of SuperSAGE tags, which remained without annotation and were therefore excluded from further analyses. Also cross-hybridizations on the microarray may be possible, though minimized through extensive bioinformatic selection of representative oligonucleotides. Cross-hybridization may lead to the false detection of a transcript

that is not present in the sample, if a different RNA hybridizes to the respective oligonucleotide. This may be a further explanation for detection of transcripts by the microarray, that are not found with SuperSAGE and contain a *Nla*III restriction site. Lastly, residual DNA contaminations not visualized with the Agilent Bioanalyzer may have led to the detection of false positives.

As expected, microarrays and SuperSAGE complemented each other, each method detecting transcripts the other did not. However, the hypotheses that additional transcripts detected by SuperSAGE or microarrays only would result from i) lacking oligonucleotide representatives on the microarray and ii) transcripts that do not contain a *Nla*III restriction enzyme recognition sites, were not affirmed. Instead, other methodological differences and technical problems were probably responsible for a lacking detection with one method. This confirmed that a combinatory approach is advantageous, altogether finding more transcripts regulated between EM and UM.

While the first statistics for SuperSAGE using EdgeR found only 53 genes significantly ($p < 0.05$) regulated, a number too small for any further bioinformatic analysis of significantly regulated genes, the second statistics applying the method of A&C (Audic & Claverie, 1997) found 815 genes significantly ($p < 10^{-10}$) regulated. A comparison of both data-sets from different SuperSAGE-statistics to the microarray data also favored the second approach. Applying the different statistics for SuperSAGE changed the number of transcripts in the overlap between microarrays and SuperSAGE from 11 to 180 (Figure 3.10.) and led to a comparable number of significantly regulated genes detected as such only by one method. Using the SuperSAGE EdgeR data-set, the combinatory data analysis of both methods would have been microarray biased (Figure 3.10.), as SAM found a great number of significantly regulated transcripts. It is possible that using a different statistical method for the microarray data or more technical replicas for the SuperSAGE would also have equilibrated the data-sets of both methods. A GO analysis of a combinatory data-set including transcripts detected by any of the two methods also indicated a microarray bias.

Detailed analysis of SuperSAGE data demonstrated the importance of the choice of a statistical test for the comparability of different data-sets. An action to avoid a bias towards one method, which may occur even with thorough choice of statistical tools, is to preferentially work with such genes that are significantly regulated in both approaches.

4.3.2 Real-time PCR experiments led to a more stringent streamlining of the data

Real-time PCR experiments were performed for a sub-set of 47 genes representing 12 technical (according to detection of the transcripts in microarray or SuperSAGE or both, with the same or different direction of regulation) and 7 functional (surface proteins, ion channels, GPCRs, signaling, transcription, metabolism, egg-shell proteins) categories. The obtained results confirmed those from the transcriptome analyses, especially in cases where microarray and SuperSAGE were already in unison. This was statistically confirmed by a Spearman's rank correlation coefficient analysis (Myers & Well, 2003) and a Wilcoxon rank sum test (Mehta & Patel, 2013; Hollander & Wolfe, 1973; Bauer, 1972). Furthermore, real-time PCR results led to two conclusions important for the further data analysis and selection of genes for further studies: i) SuperSAGE transcripts with counts below 10 for all biological samples were defined as 'low abundant'; ii) genes with a \log_2 ratio cut-off > 0.585 or < -0.585 were defined as differentially transcribed. Candidates which were significant in the statistical analyses and fulfilled these two criteria, proved most reliable during the verification process.

While an initial microarray analysis testing for significant ($q < 0.01$) regulation of transcripts between EM and UM with the program SAM detected 1,571 gene products, selection of the cut-off value (\log_2 ratio > 0.585 or < -0.585) reduced this number to 526. Accordingly, the number of enriched GO categories was reduced from 22 (of which one was enriched in EM) to 5, the number of networks detected with IPA reduced from 25 to 9, and less metabolic differences were pointed out with SchistoCyc. A similar effect was observed for SuperSAGE data. From 815 significantly ($p < 10^{-10}$) regulated genes only 253 remained after setting the cut-off. No enriched GO categories were found any longer (compared to 7 enriched in UM before), the number of IPA networks decreased from 12 to 3, and no transcription factors were found to be activated (compared to 3 before).

Also, the number of transcripts within the overlap of the two transcriptome analyses changed from 180 significantly regulated genes to 29, which were (abundant and) sig. diff. regulated between EM and UM in both microarray analysis and SuperSAGE (Figure 3.15.). Within these 29 transcripts no significantly enriched GO categories were found. IPA found only one network 'embryonic development, hair and skin development and function, organ development'. The network contained nine significantly and differentially regulated genes, seven up-regulated in EM and two up-regulated in UM.

In addition to the previously mentioned choice of statistical methods the application of a cut-off value and other selective criteria strongly influence the data analysis. It was demonstrated that the application of more stringent criteria selected as a result of real-time PCR experiments narrowed down the group of genes used for further experimental procedures.

4.3.3. Comparisons to previous studies on the differences between EM and UM support data reliability

Previous studies comparing female and male transcriptional patterns by microarray approaches (Waisberg *et al.*, 2007; Fitzpatrick & Hoffmann, 2006) or SAGE (Williams *et al.*, 2007) produced data-sets providing first evidence that pairing influences transcriptional profiling in male schistosomes. More recent studies investigated the transcriptomic patterns of specific organs (Nawaratna *et al.*, 2011) or the influence of host-sex on adult (paired) worms (Waisberg *et al.*, 2008). To support the finding that transcripts detected to be regulated between EM and UM in this study are indeed related to pairing and male competence the obtained data were compared to the above mentioned studies, as far as the data-sets were available.

To this end, 291 oligonucleotides detecting either highly transcribed genes in EM or UM or genes differentially transcribed between the two stages in the study by Fitzpatrick *et al.* (2006) were newly annotated by NCBI blastn. For 223 oligonucleotides Smp_numbers were found and matched to the data from microarray and SuperSAGE (supplementary-file17). Of the transcripts differentially regulated between male stages or strongly up-regulated in at least one male stage found in the previous study (Fitzpatrick & Hoffmann, 2006), 23 were detected as sig. diff. (and abundant in SuperSAGE) according to microarray and/or SuperSAGE, including NADH-ubiquinone oxidoreductase (Smp_038870.2), adenylate kinase 1 (Smp_061940.2), pyruvate dehydrogenase (Smp_079920), and glutathione-s-transferase omega (Smp_152710.1), which are all related to metabolic functions. Only two genes were sig. diff. regulated in both transcriptome analyses represented here: dock (Smp_135520), up-regulated in UM and the AMP-dependent ligase (Smp_158480), which was up-regulated in EM.

The comparison of the data obtained in this thesis and those previously described by Fitzpatrick *et al.* (2006) indicated a low overlap at first glance. However, experimental conditions differed with regard to hosts and the microarray-technology used. Also, another study performed in parallel to the one by Fitzpatrick and colleagues (2006) using the same host-system and microarray found no overlap between their data obtained for UM and only a very small one (4 transcripts out of 26) for

4. Discussion

EM (Waisberg *et al.*, 2007). With regard to these differences in results between studies with similar conditions it is not surprising that the performed comparison failed to detect more similarities. In contrast, the data obtained in this thesis show an even stronger correlation to those of Fitzpatrick *et al.* (2006) compared to the study performed under similar conditions (Waisberg *et al.*, 2007). Unfortunately, a comparison to the data of Waisberg and colleagues (2007) could not be performed directly as they only showed comparative diagrams for EM and UM in their publication; detailed information on specific transcripts (or oligonucleotides), significance of their regulation, or regulation-strengths were not provided.

Comparing the top 30 transcripts identified by Waisberg *et al.* (2008) to be influenced by host sex in males to the here presented data (after manual re-annotation), none were found to be sig. diff. regulated between the two tested stages (supplementary-file18). Thus, an influence of the host sex on the microarray and SuperSAGE data can be excluded.

Recently, Nawaratna *et al.* (2011) compared the transcription levels of microdissected reproductive organs from *S. mansoni* to those of whole worms. For testes they found 1,723 unique transcripts to be up-regulated (2-fold compared to whole worms). Of these 560 were not detected in the here presented analyses, however, 381 had contig annotations only, which did not allow comparison. Of the remaining 1,163 genes, 70 were sig. diff. transcribed in microarrays or SuperSAGE (supplementary-file19). With regard to the fact that the present study compared complete worms, while Nawaratna *et al.* (2011) compared testes to male hind regions, this is an astonishing large number of transcripts with a putative role for the development of UM to EM and a function in the testes. These transcripts are of future interest with regard to their specific role in testes, though at this point more than half of them are annotated as 'hypothetical' or 'expressed proteins'. Only one gene was sig. diff. regulated according to microarrays and SuperSAGE: dock (Smp_135520) was up-regulated in UM as discussed above. Two other genes with enhanced transcription in EM-testes were detected by the microarray only: the OxIT (Smp_135020), a proton pump (Ye & Maloney, 2002; Maloney *et al.*, 1994) was sig. diff. up-regulated in EM and may have a function in sperm energy budget. The putative s-adenosyl-methyltransferase mraW (Smp_053120) was sig. diff. up-regulated in UM and may have a role in methylation processes of proteins and nucleic acids, as indicated by its function in bacteria (Miller *et al.*, 2003; Carrion *et al.*, 1999).

4.3.4. EM and UM differ in metabolic processes

Comparing the results from the two separate metabolomic analyses for microarrays and SuperSAGE, transcripts representing enzymes involved in carbohydrate metabolic processes, citrate cycle, aerobic respiration, and amino acids metabolic processes were mostly down-regulated in EM compared to UM. For base metabolic processes, transcripts representing enzymes involved in synthesis were also down-regulated in EM, while transcripts for enzymes involved in degradation and salvage pathways were up-regulated in EM. This indicates differences between EM and UM for transcriptional or mitotic processes, which was previously hinted at - though inconsistently - by the re-pairing experiments performed in this thesis.

Metabolic changes between EM and UM were indicated previously by other studies researching the differences between the two male stages. One such study applying SAGE to investigate this question (Williams *et al.*, 2007) found a purin nucleoside phosphorylase (Smp_090520) to be up-regulated in EM, which was also sig. diff. up-regulated in the microarray analysis presented here. Other transcripts found to be regulated in the former study were significant in SuperSAGE, but had \log_2 ratios < 0.585 or > -0.585 : a cationic amino acid transporter (Smp_123010) (down in EM), a fatty acid binding protein (Smp_095360.x) (down in EM), and a heterogeneous nuclear ribonucleoprotein k (Smp_065580.x) (up in EM). Another study using microarrays to investigate the differences between EM and UM also found several genes coding for metabolism-associated proteins (Fitzpatrick & Hoffmann, 2006). One of them, an AMP-dependent ligase (Smp_158480) up-regulated in EM, was sig. diff. in the microarray-analysis, SuperSAGE and real-time PCR.

The regulation of s-adenosyl-methyltransferase mraW (Smp_053120) (discussed in 4.3.3) an insulinase-related gene (Smp_011100), and a 3-hydroxy-3-methylglutaryl CoA (HMG-coA)-synthase (Smp_195010), as well as ion channels like OxITs give further evidence for metabolic differences between EM and UM. Insulinases are zinc metalloproteases. Parasite metalloproteases have been linked to host invasion and anticoagulation effects (McKerrow *et al.*, 2006). Insulin receptors have been identified in *S. mansoni* and *S. japonicum* and were linked to the glucose uptake of the parasites (You *et al.*, 2010; Ahier *et al.*, 2008; Khayath *et al.*, 2007). It has been reported that EM transfer glucose to the female (Conford & Huot, 1981). The detected insulinase might have a role in the signaling process regulating glucose uptake and transfer to the female. The HMG-coA synthase is a member of the mevalonate pathway (Harris *et al.*, 2000). As schistosomes are not capable of *de novo* synthesis of sterols and fatty acids (Meyer *et al.*, 1970), the HMG-coA synthase may be involved in the transformation of host-molecules into according

4. Discussion

metabolites. Transcripts for other members of the mevalonate pathway were also sig. diff. regulated between EM and UM: hydroxymethylglutaryl-CoA synthase (Smp_195010) was up-regulated in EM according to the microarray analyses, isopentenyl-diphosphate delta isomerase (Smp_130430) was up-regulated in UM according to SuperSAGE. OxITs are known for their participation in the indirect proton pump of *Oxalobacter formigenes* (Ye & Maloney, 2002; Maloney *et al.*, 1994). Two OxITs were sig. diff. regulated in this study, one (Smp_036470) was up-regulated in UM in all transcriptome approaches and detected in male tested (Figure XXIII.), the other one (Smp_135020) was not detected by SuperSAGE and found to be up-regulated in EM-testes according to Nawaratna *et al.* (2011).

Previous to the large scale transcriptome analyses other studies already suggested that EM support females by supplementing their partner with nutrients (Silveira *et al.*, 1986; Cornford & Fitzpatrick, 1985; Haseeb *et al.*, 1985; Conford & Huot, 1981). It was described that UM have higher glycogen levels than EM, probably in preparation of pairing, while EM seem to “deplete” their storage by transferring glucose to the female (Conford & Huot, 1981). Also, females stimulate lipid accumulation and lipase activity in males (Haseeb *et al.*, 1989). Transcripts related to lipid metabolic processes were sig. diff. regulated between EM and UM including transcripts up-regulated in EM, as detailed by SchistoCyc metabolome analyses of microarray and SuperSAGE data.

GO analyses generally detected more enriched categories for transcripts up-regulated in UM. This finding is supported by a previous transcriptomic study that focused on difference between EM and UM (Fitzpatrick & Hoffmann, 2006). Thus, it seems possible that EM need a wider functional assembly of molecular processes, which includes the differential regulation of metabolic processes.

4.3.5. Signal transduction processes during UM to EM transition

Besides genes important for male metabolism those encoding for molecules involved in signal transduction were of special interest in this study. Due to the findings from a previous study in our group (Hahnel, 2010), which found GPCRs to be regulated between EM and UM, three GPCRs were tested in real-time PCR experiments. GPCRs comprise a large family of membrane receptors, which are involved in a multitude of cellular processes (Krauss, 2008). In *S. mansoni* 5 sub-families have been identified: rhodopsin-, glutamate-, adhesion-, secretin- and frizzled-receptors (Zamanian *et al.*, 2011). Transcripts for one rhodopsin-like orphan GPCR (Smp_161500) were up-regulate in EM

according to semi-quantitative PCR-analyses in our laboratory (Hahnel, 2010) and also within SuperSAGE, while it was not detected by the microarrays. Only in real-time PCR experiments sig. diff. transcription was found for this GPCR. For most other GPCRs found to be up-regulated in EM in the previous study, contradictory results were obtained by the transcriptome analyses (Table XIII.). Besides the rhodopsin-like orphan GPCR two more GPCRs were detected by SuperSAGE only. One (Smp_194740), a sex peptide receptor, was merely up-regulated in EM according to SuperSAGE and real-time PCR, the other one, a tachykinin receptor like protein / neuropeptide Y receptor like protein (Smp_170020) was sig. diff. up-regulated in UM as confirmed by real-time PCR experiments. Another neuropeptide Y prohormone (Smp_159950) was also sig. diff. up-regulated in UM according to SuperSAGE only. In *D. melanogaster* sex peptides are transmitted with the sperm and seminal fluid and alter fecundity and sexual receptivity of females through the neuronal sex peptide receptor (Gioti *et al.*, 2012; Yapici *et al.*, 2008; Kubli, 2003; Liu & Kubli, 2003). Tachykinin and neuropeptide Y are neuropeptides used throughout different phyla in different organs, and a multitude of processes including functions in the central nervous system, gut activity, feeding, and gonads (Caers *et al.*, 2012; Candenas *et al.*, 2005; Pennefather *et al.*, 2004; Gehlert, 2004; Tatemoto, 2004; Pedrazzini *et al.*, 2003; Severini *et al.*, 2002; McDonald, 1990). Up-regulation of neuropeptide Y receptors and prohormones in UM could be a preparation for pairing. With regard to the hypothesis that males have to reach a status of competence, before they are able to induce differentiation processes in the female, neuropeptide receptors could have a function in receiving the initial stimulus from the female. A neuropeptide prohormone up-regulated in UM could be a signal towards the female, in the process of establishing an initial pairing contact. Subsequent up-regulation of the sex peptide receptor in EM may be relevant for the sustenance of the male-female interaction.

In a different scenario the regulated receptors and neuropeptide Y could play a role in feeding control; then their regulation would add up to the picture of general metabolic differences between EM and UM. The latter may also be an explanation for the regulation of transcripts of the rhodopsin-like orphan GPCR (Smp_161500), which also has a reported role in feeding in nematodes and arthropods (Cardoso *et al.*, 2012). Transcripts for a previously identified *S. mansoni* neuropeptide F (NPF; Smp_088360) that was reported to be structurally similar to neuropeptide Y (Humphries *et al.*, 2004), were only detected by SuperSAGE and did not differ significantly between EM and UM.

4. Discussion

These results indicate that further research on GPCRs concerning the development from UM to EM is of interest especially with regard to the male-female interaction and therein the question whether their role in schistosomes is similar to that of e.g. the sex peptide and its receptor in *Drosophila* (Gioti *et al.*, 2012; Yapici *et al.*, 2008; Kubli, 2003; Liu & Kubli, 2003).

A further member of the GPCR family, the 7 trans-membrane receptor frizzled (Smp_155340) was sig. diff. down-regulated in EM according to the microarray analyses. One ligand of the frizzled receptors is Wnt5A (Kikuchi *et al.*, 2012; Sato *et al.*, 2010). A *S. mansoni* Wnt5A (Smp_145140) was sig. diff. up-regulated in the microarray analyses. The wnt-pathway is involved in differentiation and proliferation processes (Kikuchi *et al.*, 2012; Nishita *et al.*, 2010) and thus seemed of interest with regard to the development from UM to EM. Therefore, transcript differences between EM and UM were analyzed in real-time PCRs for frizzled, Wnt5A, glypican (Smp_105200.1), a potential up-stream regulator of wnt-pathways (Filmus *et al.*, 2008), lin-9 (Smp_133660), which was placed in the same IPA network with Wnt5A (IPA network 24 of the initial microarray analysis), and adenomatous polyposis coli protein (Smp_139190), an interaction partner of molecules within the wnt-pathway (Clevers, 2006). However, real-time PCR results rather confirmed SuperSAGE data, which did not indicate significant differences between EM and UM for transcripts of these genes. It is possible that the wnt-pathway is not of importance with respect to the differentiation from UM to EM and that the results obtained from microarray analyses indicate an influence by additional parameters independent of the pairing status, such as host-conditions.

Other signaling molecules for which sig. diff. transcription between EM and UM was indicated by all three approaches were dock (dedicator of cytokinesis) (Smp_135520, up in UM) and pinch (Smp_020540, up in EM). Both molecules are involved in cellular signaling. Pinch interacts with integrin-linked kinase and parvin to form a complex that acts down-stream of integrin receptors, regulating the actin cytoskeleton and other signaling pathways, with consequences for gene expression (Legate *et al.*, 2006). Five integrins were recently described in *S. mansoni* (Beckmann *et al.*, 2012b). *In situ* hybridization experiments for three of these integrins localized transcripts to female organs but also to the testes, and *S. mansoni* β -integrin 1 (Sm β -Int1) additionally to the parenchyma and subtegument (Beckmann *et al.*, 2012b). Though integrin action was so far linked mainly to female processes, the strong up-regulation of pinch in EM indicates further research on this gene and interaction partners of the according protein. If pinch does localize to testes like the integrins, its function in males could be associated to differentiation from immature to mature germ cells. The super-family of DOCK180 proteins also contains members participating in the

down-stream signaling of integrins (Hood & Cheresh, 2002). DOCK180 proteins are activators of the small GTPase Rac in mammalian cells, *Drosophila* and *C. elegans* and influence phagocytosis, cell motility and cytoskeletal organization during embryonic development (Miyamoto & Yamauchi, 2010; Cote & Vuori, 2002; Hood & Cheresh, 2002). A blastx analysis of Smp_135520 showed that the sequence was similar to that of DOCK7 of other organisms (identity < 50%). DOCK7 was shown to be present in neuronal cells, where it also acts through rac on e.g. regulation of the microtubule network (Yang *et al.*, 2012; Yamauchi *et al.*, 2011; Miyamoto & Yamauchi, 2010; Yamauchi *et al.*, 2008; Watabe-Uchida *et al.*, 2006). Future studies will have to detail the exact function of the *S. mansoni* dock. It's up-regulation in EM-testes (Nawaratna *et al.*, 2011) places the transcripts to the same location as integrins supporting the idea that this dock as well might have a function in sperm differentiation.

Three more genes assigned to the functional group 'signaling' were tested in real-time PCRs, but showed inconsistent results, which were insignificant for transcriptional differences between EM and UM (serin/threonin kinase PAK - Smp_17516; DdMEK1 - Smp_024290; CAMKL - Smp_094190). Also, a number of genes linked to processes in males by previous localization studies (TK3, TK4, TK5, TK6, Discs-large, SmDia; see chapter 1.4. and supplementary-file20) were not transcriptionally regulated between EM and UM, with the exception of a mucin (Hahnel *et al.* in preparation), which was sig. diff. up-regulated in EM according to SuperSAGE.

SmFst, a potential regulator of TGF β -signaling (Moustakas & Heldin, 2009; Massagué & Chen, 2000) was sig. diff. up-regulated in UM. This is a new finding since SmFst was not found to be differentially transcribed between EM and UM in previous transcriptome studies (Williams *et al.*, 2007; Fitzpatrick & Hoffmann, 2006). In case of one study (Fitzpatrick & Hoffmann, 2006) this may be due to the absence of the according oligonucleotide (the respective annotation was not found in the data-set) on the first-generation microarray used. In case of the other study (Williams *et al.*, 2007) the respective sequence was either not detected by the SAGE experiment or could not be annotated, as the genome project was incomplete. Searching for SmFst in a more recent, *S. mansoni* organ-enriched transcriptome data-set (Nawaratna *et al.*, 2011) the transcript was not found to be up-regulated in EM-testes compared to whole worms, applying a cut-off for a 2-times higher transcription, though *in situ* hybridization experiments performed in this thesis localized SmFst to the testes.

Because SmFst protruded from the analyses for its reproducibly strong regulation, other members involved in TGF β signal-transduction known in schistosomes came into focus. 'Supplementary-

4. Discussion

file17' lists TGF β -pathway linked genes identified in *S. mansoni*, as well as their regulation in microarrays and SuperSAGE. Besides SmFst and its two potential interaction partners SmlnAct and SmBMP, four other members of TGF β -pathways were tested in real-time PCR experiments: Smad4 (Smp_033950) and a predicted Smad (Smp_157540), one *S. mansoni* TGF β RI (Smp_049760) and one *S. mansoni* TGF β RII (Smp_144390). Real-time PCR confirmed the lack in transcriptional differences between EM and UM for these genes. Thus, the exceptional and consistent regulation of SmFst was additionally highlighted, which justified further functional analyses.

One molecule previously proposed to be a down-stream target of TGF β -pathways in schistosome couples is GCP (Osman *et al.*, 2006). Originally, studies with a monoclonal antibody reported GCP to be up-regulated in EM as a result of the male-female interaction (Gupta & Basch, 1987; Aronstein & Strand, 1985). Later the molecule was proposed to be essential for pairing in *S. japonicum* as indicated by siRNA studies (Cheng *et al.*, 2009). However, verifiable significant regulation of GCP between EM and UM was neither found in this thesis, nor in other comparable transcriptome studies (Williams *et al.*, 2007; Fitzpatrick & Hoffmann, 2006; Fitzpatrick *et al.*, 2005; Hoffmann *et al.*, 2002). It may be possible that this discrepancy to protein data and studies in *S. japonicum* is due to technical differences, variability among worm strains, or even post-transcriptional regulation.

The presented data confirm that signal transduction pathways are involved in the differentiation from UM to EM. A number of transcripts coding for different signaling molecules were found to be sig. diff. regulated between EM and UM. For some of these transcripts a function in neuronal signaling, the testes, or male-female interaction is indicated.

4.3.6. Involvement of the neuronal system in male differentiation

IPA analysis for genes of the intersection between microarray and SuperSAGE highlighted DCC (Smp_135230), which was further accentuated through the metabolomic data analysis, where it was associated to phenylethanol / catecholamine biosynthesis. Since DDC transforms dopa to dopamine (Holtz, 1995; Christenson *et al.*, 1972) the up-regulation of transcripts for DDC in EM indicates a role for this neurotransmitter and thus the neuronal system of schistosomes in the differentiation process from UM to EM, or even male-female interaction. Transcripts for other molecules with a known function in neuronal cells were also detected as sig. diff. regulated between EM and UM: Dock (see 4.3.5.) shows similarities to DOCK7 with a reported neuronal role (Yang *et al.*, 2012; Yamauchi *et al.*, 2011; Miyamoto & Yamauchi, 2010; Yamauchi *et al.*, 2008;

Watabe-Uchida *et al.*, 2006). A neuropeptide Y prohormone (Smp_159950) and a tachykinin receptor like protein / neuropeptide Y receptor like protein (Smp_170020) might also have a function in *S. mansoni* neuronal signaling.

The hypothesis for a role of the neuronal system in male-female interactions was previously discarded: in 1984 Popiel and Basch concluded from their experiments with transected (including decapitated) and complete worms that neuronal and especially central nervous system control was not involved in male-dependent female stimulation. However, reviewing their detailed description of results a contradictory conclusion can be drawn from their analyses. While pairing of whole UF to male segments resulted in development of the vitellarium throughout the whole female, pairing of decapitated UF to whole EM or male segments lead to scattered local development of the vitellarium. This can be interpreted as evidence for a function of the intact nervous system in the completion of female development, though, an intact nervous system seems not to be important for the initial pairing contact, since this was achieved independent of intactness or dissection of worms. However the above data justify renewed attention to neurological processes in *S. mansoni* males and couples.

4.3.7. Detection of egg-shell related transcripts indicates leaky expression in males

Surprisingly, transcripts for the egg-shell precursor protein, p14 (Smp_131110), p48, fs800-like (Smp_000270), and a not further defined “egg-shell precursor protein” (Smp_000430) were sig. diff. up-regulated in EM according to the microarray analysis. Additionally, an “egg protein CP391S” (Smp_173350.x) sig. diff. regulated was detected by SuperSAGE only. However, single \log_2 ratio values varied strongly between biological replicas in all transcriptomic methods applied. Still, the average microarray results are indirectly supported by a previous study (Nawaratna *et al.*, 2011), which provided evidence for another fs800 transcript (Smp_00280) to be up-regulated in testicular lobes of paired males. Also other supposedly female-specific transcripts were found previously in males when comparing EM and UM (Fitzpatrick & Hoffmann, 2006). Thus, it can be concluded that egg-shell precursor protein transcripts can be strongly regulated between EM and UM, depending on the worm-batch. This may be explained by a phenomenon known as leaky expression. As schistosomes have evolved from hermaphroditic organisms it is possible that genes specific for one sex might not be completely silenced in the other sex. It has been observed that males may even develop female reproductive “pseudo”organs, like vitellarium and ovary (Shaw &

Erasmus, 1982; Short, 1948; Vogel, 1947). Induction of the expression of female-specific genes and organs may also result from homosexual pairing, where one male acts as surrogate-female in the gynaecophoral canal of the other male (Ribeiro-Paes & Rodrigues, 1997; Short, 1952 in: Armstrong, 1965; Vogel, 1947). The presence of such feminized males in UM samples might be a further explanation for the variance in egg-shell-precursor protein gene transcripts between biological replicas.

4.3.8. Regulatory RNAs may be a future research focus

Microarrays as well as SuperSAGE detected transcripts complementary to the protein coding sequence. Though not further considered in the data analysis they might still be of interest in the future. Non-coding RNAs (ncRNAs) have become of great interest throughout the last decade. Originally discarded as transcriptional noise, increasing evidence was gained, especially from mammalia, that ncRNAs are important for the regulation of gene expression (reviewed in: Lee, 2012; Oliveira *et al.*, 2011; Turner & Morris, 2010). Sub-classes of ncRNAs are among others long ncRNAs, short ncRNAs, microRNAs, siRNAs, and natural anti-sense RNAs (NATs) (reviewed in: Lee, 2012; Oliveira *et al.*, 2011). NATs are regulators of gene-expression by controlling epigenetic activities, post-transcriptional gene silencing, and degradation of mRNA (reviewed in: Knowling & Morris, 2011; Werner & Sayer, 2009; Militello *et al.*, 2008). Recent publications also report the detection of anti-sense RNAs and ncRNAs (Almeida *et al.*, 2012; Oliveira *et al.*, 2011; Simoes *et al.*, 2011), as well as microRNAs (de Souza *et al.*, 2011) in *S. mansoni*. In addition, epigenetic modification by cytosine methylation, a process also regulated by long ncRNAs (reviewed in: Lee, 2012), has been shown for *S. mansoni* (Geyer *et al.*, 2011).

In this study sig. diff. regulation of anti-sense transcripts was found for 211 genes with the microarray analysis; SuperSAGE detected 261 such transcripts located in an exon-region and 107 in an intron-region. Furthermore, for two of the transcripts sig. diff. regulated according to both analyses, dock (Smp_135520) and AMP-dependent ligase (Smp_158480), SuperSAGE detected the largest tag-counts for gene loci predicted as intronic. This is of special interest in case of the dock gene locus: The intron-derived RNA could have a regulatory function in UM. Reduced transcription of this regulatory RNA upon development of UM into EM could lead to an up-regulation of dock mRNA in EM-testes as found by Nawaratna *et al.* (2011). Also, sense transcripts for the putative s-adenosyl-methyltransferase mraW (Smp_053120) was sig. diff. up-regulated in UM according to microarray and real-time PCR, and up-regulated in EM-testes (Nawaratna *et al.*, 2011). In bacteria

the function of the according protein is associated to the methylation of nucleic acids (Miller *et al.*, 2003; Carrion *et al.*, 1999). Thus, it may be possible that the s-adenosyl-methyltransferase *mraW* has a role in epigenetic processes in testes. The confirmation of these hypotheses and the unraveling of the functions of anti-sense RNAs in *S. mansoni* in general are subject of further studies.

4.3.9. Future aspects for research

Originally, it was anticipated that genes coding for proteins with an expected surface location, or with a relation to transcriptional processes would be transcriptionally regulated between EM and UM. With regard to the possibility that the male-female interaction could be based on a tactile stimulus, transcripts for surface proteins regulated between EM and UM would support this hypothesis. Target genes of the transcription factors regulated between EM and UM could provide further evidence for processes involved in the differentiation from UM to EM. However, those transcripts allocated to the functional groups “surface proteins” and “transcription”, which were tested in real-time PCR experiments showed inconsistent results that did not confirm a significance of their regulation between EM and UM. Interestingly, many of these transcripts were detected by one method only (SuperSAGE: zinc finger protein, putative – ZFP Smp_130690; RNA-binding protein musashi-related - Smp_157750; elongin - Smp_143350; MEG5 - Smp_152580; microarray: tegumental protein - Smp_169190; DNA-directed RNA polymerase III largest subunit - Smp_002890). Others had been detected by both approaches, but were found to be significantly transcribed only according to one method, and failed to produce congruent results in real-time PCRs (microarray significant: contactin - Smp_176350; tegument protein - Smp_077310; glypican - Smp_105200.1; egf-like domain protein / notch - Smp_050520; lipopolysaccharide-induced transcription factor regulating tumor necrosis factor alpha - Smp_025370; ets - Smp_126530; SuperSAGE significant: cell adhesion molecule - Smp_141410).

Therefore, the lists of transcripts sig. diff. regulated between EM and UM according to both analyses or detected by one method only were checked again for further candidates, which might be of interest for future studies. Among these are villin (Smp_008660) and nebulin (Smp_151490), actin-binding proteins (Pfuhl *et al.*, 1994; Craig & Powell, 1980) that were sig. diff. up-regulated in EM according to both analyses. Since signal-transduction in female reproductive organs was predicted among others to induce cytoskeleton reorganization (Beckmann *et al.*, 2010b) the regulation of these two transcripts could indicate similar processes in males, especially in the

4. Discussion

testes. The cadherin transcript (Smp_151620), sig. diff. up-regulated in EM in both transcriptomic approaches, codes for a protein important for cell-cell contact (Takeichi, 1991). If this cadherin is expressed on the surface of males, it could be important for tactile interaction and signal transduction from males to females. Mammalian endophilins are linked to vesicle endocytosis. An endophilin B1 (Smp_163720) was sig. diff. up-regulated in EM in both transcriptome approaches. If the male-female interaction is bidirectional as proposed (LoVerde *et al.*, 2009; LoVerde *et al.*, 2007) endocytosis might be crucial for the internalization and distribution of a signal from the female to the male. Therefore, endophilin B1 is also of interest for further characterization studies (Cheung & Ip, 2009; Schuske *et al.*, 2003). A blastx analysis of the ‘cancer-associated protein’ (Smp_040560) sig. diff. regulated according to SuperSAGE and microarrays annotated the sequence as ‘cytoplasmic tRNA 2-thiolation protein 1’. As thiolation is linked to RNA stability (Wohlgamuth-Benedum *et al.*, 2009), the function of this protein could be of regulatory nature in post-transcriptional gene regulation.

Several micro exon genes (MEGs) were sig. diff. regulated in SuperSAGE only. Since MEGs are unique to schistosomes and expressed in epithelia and gland cells (Parker-Manuel *et al.*, 2011; DeMarco *et al.*, 2010), they may have a role not only as modulators of the host response (DeMarco *et al.*, 2010) but also in male-female interaction. MEG-5 (Smp_152580) was tested in real-time PCR experiments, which did not confirm the SuperSAGE results. However, other MEGs (MEG-6 - Smp_163710; MEG-4 - Smp_085840.x; MEG-9 - Smp_125320; MEG-12 - Smp_152630) from the SuperSAGE only group were not further analyzed in this study but may be worth to be checked in future experiments.

Additional attention should be given to genes annotated as “hypothetical protein” or “expressed protein”. Since there are no obvious homologs of these genes in existing gene banks, they may represent novel, parasite-specific proteins. This is of interest in the light of the unique aspects of schistosome reproductive biology such as the still missing factors of the male that contribute to the stimulation of female maturation following pairing. Localization experiments and biochemical characterizations are needed to assign functions to these proteins.

Also the role of metabolic changes from UM to EM is worth further investigation. It has been argued, that males supply their female partners with nutrients (Silveira *et al.*, 1986; Cornford & Fitzpatrick, 1985; Haseeb *et al.*, 1985; Conford & Huot, 1981). By knocking down key molecules in metabolic processes it might be possible to identify, which of those processes or nutrients are most essential for the females.

Table 4.1. summarizes the above mentioned genes, including those from the functional group “signaling” which were proposed for future research in the previous chapters. One common aspect of dock, pinch, DDC, neuropeptide Y prohormone, and the sexpeptide and tachykinin / neuropeptide Y receptors is their potential role in neuronal processes. A most efficient way to test the impact of these genes on male development and the male-female interaction would be constant knock-out studies, hopefully available for schistosomes within the next years (Beckmann & Grevelding, 2012). Also the potential import of regulatory RNAs was pointed out.

Table 4.1: Genes of interest for further studies.

Gene	annotation
Smp_135520	dock
Smp_020540	pinch
Smp_135230	DDC
Smp_194740	sex peptide receptor
Smp_170020	tachykinin receptor like protein / neuropeptide Y receptor like protein
Smp_159950	neuropeptide Y prohormone
Smp_008660	villin
Smp_151490	nebulin
Smp_151620	cadherin
Smp_163720	endophilin B1
Smp_040560	cancer-associated protein
Smp_163710	MEG-6
Smp_085840.x	MEG-4
Smp_125320	MEG-9
Smp_152630	MEG-12

4.4. The role of SmFst in schistosomes

SmFst was identified as one of the transcripts, which were most reproducibly found to be up-regulated in UM. Because it is a potential inhibitor of the TGF β -pathway (Moustakas & Heldin, 2009; Massagué & Chen, 2000), SmFst was chosen for first characterization studies. Minor sequence differences between SmFst and the predicted follistatin gene Smp_123300 were detected, following cloning and sequencing of the CDS of *S. mansoni*. As for SmcGKI these differences may be due to either an inaccurate sequence information in the database or to differences between strains.

Further sequence and phylogenetic analyses revealed that SmFst, and also the *Clonorchis sinensis* follistatin, contain two FstDs and are thus more closely placed to follistatin-like proteins (fstl), particularly follistatin-like 1 (fstl-1). While follistatin contains three FstDs, fstl-1 contains only two such domains. Like follistatin, fstl-1 can bind activins and BMPs, when the proteins are exposed to

4. Discussion

each other (Zhou *et al.*, 2006). Fstl-1 also interacts with disco-interacting protein 2 (Dip2a) (Tanaka *et al.*, 2013; Ouchi *et al.*, 2010), a relation indicated by the IPA-network for the genes sig. diff. in both analyses. Dip2a again is an interaction partner of a putative transcription factor known from *Drosophila*, 'drosophila disconnected' (disco) (Tanaka *et al.*, 2013). A putative *S. mansoni* homolog for Dip2a (Smp_212570) exists but was not present within the microarray or SuperSAGE data-sets generated in this study. With regard to the fact that Dip2a is the putative direct binding partner of a transcription factor the confirmation of an interaction between SmFst and the *S. mansoni* Dip2a is of great interest. Further elucidation of the according down-stream signaling would provide evidence on the processes influenced by SmFst regulation. Furthermore, Fstl-1 was reported to participate in mammal neuronal processes (Li *et al.*, 2011) and tick oviposition (Zhou *et al.*, 2006). In this study SmFst transcripts were detected in miracidia and all adult schistosome stages. Y2H experiments demonstrated interactions of SmFst with SmInAct and SmBMP, agonists of the schistosome TGF β -pathway previously characterized in schistosomes (Freitas *et al.*, 2009; Freitas *et al.*, 2007). Interactions of mammalian follistatin and activin (reviewed in: Harrison *et al.*, 2005; Shi & Massague, 2003) or follistatin and bone morphogenic protein (BMP) (Beites *et al.*, 2009; Iemura *et al.*, 1998) are well known, although the follistatin binding affinity to BMP is reported to be lower (Stamler *et al.*, 2008; Lin *et al.*, 2006). SmFst interaction with both agonists was detected by filter and liquid assays, and a slight indication was found for a stronger binding of SmFst to SmInAct. Also, the C-terminal part of SmBMP seemed to be less important for the interaction with SmFst compared to the rest of the protein. This is surprising since the C-terminal part of SmBMP is most conserved in comparison to human BMPs and contains several residues essential for receptor binding (Allendorph *et al.*, 2007; Nickel *et al.*, 2001; Kirsch *et al.*, 2000), which are supposedly blocked by follistatin (Lin *et al.*, 2006; Thompson *et al.*, 2005). However, it is possible that within the quaternary structure follistatin binds to other residues primarily not of the C-terminus, but thereby prohibits the receptor binding of BMP.

In situ hybridization experiments for SmFst, SmInAct, and SmBMP showed a colocalization within the testes and ovary for all three transcripts and within the vitellarium for SmFst and SmBMP. A previous study also reported SmInAct to be transcribed within the ovary, and additionally in the vitellarium (Freitas *et al.*, 2007). Furthermore, this earlier study confirmed the here presented results of similar SmInAct transcription levels in EM and UM, However, Freitas *et al.* (2007) detected SmInAct protein only in EM but not in UM. The lack of this protein makes an interaction of SmFst and SmInAct in UM unlikely. In consequence, two possible modes of action for SmFst can

be hypothesized: (i) Assuming that SmInAct is the preferential binding partner of SmFst, as shown for other organisms (Pentek *et al.*, 2009; Stamler *et al.*, 2008; Lin *et al.*, 2006), its transcript levels detected in this study are not representative for the protein expression and the interacting molecules do not play a role in the development from UM to EM. Alternatively (ii) SmFst is translated and influences TGF β -pathways in the male through other TGF β -agonists such as SmBMP. However, contrarily to the above mentioned localization experiments, SmBMP protein was demonstrated only outside the testes (Freitas *et al.*, 2009) so far, which may be due to protein amounts beneath the detection limit.

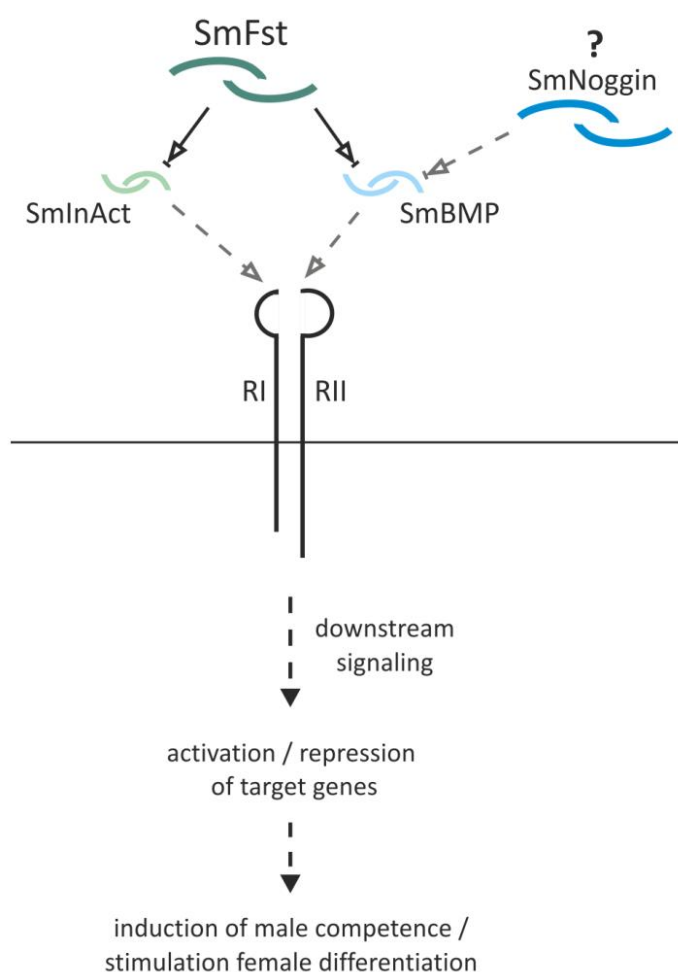


Figure 4.1: The role of SmFst in *S. mansoni*.

Interactions of SmFst with SmInAct and SmBMP were indicated by Y2H experiments. It is suggested that SmFst may bind to either of the two ligands of the TGF β R-family (RI/RII) and thus block TGF β -pathway signaling in a tissue- or stage-dependent manner.

Depending on the exact nature of the tissue or stage-specific signaling, SmFst might regulate gene expression in a way that leads to the induction of male competence and/or female differentiation.

Black continuous arrows: experimentally supported interaction. Grey dashed arrows: putative interactions.

In view of the above presented data, a tissue- and stage-dependent interplay of TGF β -family proteins in schistosomes is proposed (Figure 4.1.). It is suggested that in schistosomes different class one and class two receptors bind in various combinations. This is supported by the fact that homologs to different type one receptors can be found in the *S. mansoni* genome, but most type two receptors belong to the sub-group of activin-like receptors. Thus, the *S. mansoni* splice variant of TGF β RII (Osman *et al.* 2006) was previously described as ActRII (Forrester *et al.*, 2004), which correlates with my blast analysis. Other members of the TGF β R-family found in the *S. mansoni*

4. Discussion

genome are TGF β RI (Davies *et al.*, 1997) (Smp_049760), ActRI (Smp_093540.3), ActRI/BMPRIa (Smp_124450), ActRIIa (Smp_080120.2) and ActRIIb (Smp_144390). Different receptor-combinations would open the possibility for numerous agonist interactions governing tissue-specific activities. In this scenario SmFst, among others, may bind to SmBMP in the testes.

In this context, the role of the *S. mansoni* noggin (Smp_099440) will have to be investigated. In mammals this molecule is the natural inhibitor of BMP, binding to it more specifically than follistatin (Lin *et al.*, 2006; Massague *et al.*, 2000; Massagué, 2000). In the here presented transcriptome analyses, the schistosome noggin was not significantly regulated between EM and UM. However, to gain a detailed picture of the schistosome TGF β -pathways it is important to evaluate where and when SmBMP is bound by SmFst or noggin.

To finally pinpoint the roles of the above described molecules further, detailed studies are required. *In situ* hybridizations and Y2H experiments could provide first functional indications for the transcripts and according molecules not further investigated in this study. RNAi knock-down experiments could substantiate resulting hypotheses on the functional indication e.g. by observing the effect of RNAi-treated males on the females they are paired with. Additionally, studies at the protein level would be important, as e.g. their localization may differ from those of RNA, which would provide further and more definite indications on their functions and interplay with other members of the TGF β -family. Also, direct protein interaction assays could be performed.

With the data available at this time it can be hypothesized that SmFst has a general influence on the male as a whole organism (Figure 4.1.) and a specific one in the testes, maybe in sperm differentiation (Figure 4.2.). With regard to the fact that TGF β -pathways govern the transcription of target genes - activation as well as repression - in a tissue-dependent manner (Massagué & Gomis, 2006), it may be possible that the up-regulation of transcripts of SmFst is responsible for the arrest of UM in their pre-pairing state. Upon pairing SmFst transcription would be suppressed, and the lacking inhibition would free the pathway to activate genes related to an active condition in the testes, the male status of competence and induction of female maturation. Crosstalk with other pathways could additionally regulate these processes, as recent studies indicate (Buro *et al.*, 2013; Knobloch *et al.*, 2007). However, it is subject of future research at which point such a crosstalk occurs. While a direct interaction of two molecules from two different signaling pathways is possible, it is also possible that two pathways share a common member, or that transcription factors at the end of two different pathways target the same gene. Again, the exact nature of this cross talk could be stage- and tissue-dependent.

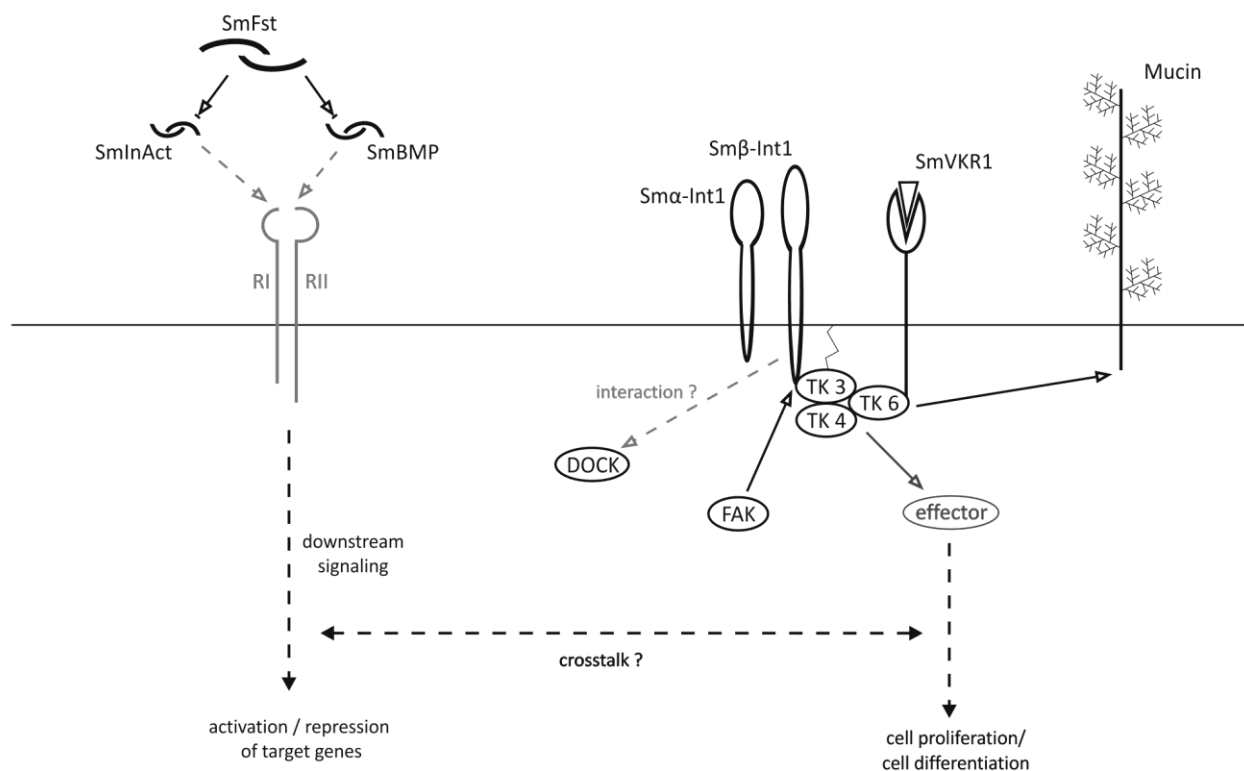


Figure 4.2: Signaling molecules in *S. mansoni* testes (modified from: Beckmann, 2008).

The here presented data could extend the model on signal transduction in the testes as proposed by Beckmann (2008). Black: molecules and interactions supported by experimental evidence. Grey: molecules and interactions proposed to be present.

4.5. Conclusion

Preliminary experiments concerning the differential transcription of SmcGKI between EM and UM, and activation of mitosis in males through pairing could not be substantiated. However, it was found that SmcGKI has an influence on schistosome muscular activity and egg production and that TNF α exerts a concentration- and medium-dependent effect on the MA of males.

The results of the two large scale transcriptome analyses showed that male gene expression on the level of transcription is influenced by pairing. The expectation that the two large scale transcriptome methods, microarray and SuperSAGE, would confirm and complement each other was met, and the influence of statistical methods pointed out. As previous studies worked with one method only, used smaller microarrays not representing the complete *S. mansoni* genome and could only refer to preliminary genome data, this work presents the most complete data-set on genes differentially transcribed between EM and UM available to date. The credibility of the data was further confirmed by real-time PCR experiments and comparison to previous analyses of male transcriptomes (Nawaratna *et al.*, 2011; Waisberg *et al.*, 2008; Williams *et al.*, 2007;

4. Discussion

Fitzpatrick & Hoffmann, 2006). First functional characterizations of SmFst, a potential TGF β -pathway inhibitor, were performed and the results encourage further research on this molecule and its interaction partners (Figure 4.1). Other candidates for future analyses were pointed out (Table 4.1), and the existing model for molecules with a function in the testes and potentially sperm differentiation could be expanded (Figure 4.2.). In contrast to previous hypothesis (Cheng *et al.*, 2009; Gupta & Basch, 1987; Aronstein & Strand, 1985) a role for GCP in male development or the male-female interaction was not indicated by my data.

The following conclusions can be drawn at this stage: (i) EM seem to lose specificity with regard to functional categories of transcripts, as was indicated by GO analyses and also found in a previous study (Fitzpatrick & Hoffmann, 2006). (ii) The development from UM to EM is a complex process, of which the male status of competence and the stimulus (or stimuli) towards the female are only two aspects. (iii) TGF β -pathways, previously described for their role in the male-female interaction and female development (LoVerde *et al.*, 2009; Knobloch *et al.*, 2007; LoVerde *et al.*, 2007), may have a central role in the differentiation of UM into EM, especially in the testes. (iv) Though sperm and seminal fluid were previously excluded as carriers of the male stimulus towards the female (Shaw *et al.*, 1977; Michaels, 1969; Armstrong, 1965), the localization of SmFst and dock in the testes and the regulation of neuropeptide Y may indicate a revision or repetition of the classical experiments leading to this exclusion. (v) The impact of neuronal processes for males and the male-female interaction has to be revised.

Summary

Schistosoma mansoni males have a key role in the unique reproduction biology of these parasitic flatworms. Without a constant pairing contact to the male the female is unable to complete or maintain its sexual maturation, which is the prerequisite for egg production. The eggs themselves are the causative agent of a disease with world-wide importance: schistosomiasis.

Little is known about the process by which males affect female development. Different types of molecules have been suggested as stimulus but none was identified so far. It was also hypothesized that males are influenced by pairing as well, obtaining a status of competence which enables them to induce female sexual maturation. Again, only scarce information is available on such processes in males. EST and genome projects for schistosomes have opened new possibilities to study these male mechanisms also on the transcriptome level. The here described study was performed to identify differences between pairing-experienced (EM) and pairing-unexperienced (UM) males.

Preliminary experiments had indicated a stimulatory effect of pairing and tumor necrosis factor α (TNF α) on the mitotic activity (MA) in males. Furthermore, evidence was provided for the differential expression of a *S. mansoni* cGMP-dependent protein kinase (SmcGK1) between EM and UM. While the effect of pairing on the MA of males was not confirmed by results obtained in this thesis, a concentration and medium-dependent stimulation of MA in males as response to TNF α was observed. SmcGK1 was not found to be differentially transcribed between EM and UM. However, localization studies detected SmcGK1 transcripts in the reproductive organs of male and female worms, and inhibitor studies indicated an influence of SmcGK1 on worm motility and egg production.

To unravel differences between EM and UM on a larger scale, the transcriptomes of these two male stages were compared combining two different methods, microarrays and SuperSAGE. As expected, both methods confirmed and complement each other. Additional confirmation of the results was obtained by real-time PCR experiments. Usage of bioinformatic tools such as gene ontology analysis, Ingenuity Pathway Analysis and schistosome-specific metabolome analysis facilitated data interpretation. Different statistical analyses were used and their influence on the data was emphasized.

Microarray analyses and SuperSAGE detected 9,344 and 7,494 sense transcripts, respectively. Merging both data-sets it was found that 6,326 transcripts were detected by both analyses, of which 29 were significantly differentially ($q < 0.01$; $p < 1^{-10}$; $\log_2\text{ratios} > 0.585$ or < -0.585)

5. Summary

transcribed between EM and UM. To date, this is the most comprehensive data-set on differential transcription in male *S. mansoni*. The data indicated differences in metabolic processes between EM and UM, confirming previous hypotheses. Beyond that evidence was obtained for the contribution of neuronal signaling, anti-sense regulation and schistosome-specific protein coding genes, in the male-female interaction. Genes protruding from the analyses were among others, a dopa-decarboxylase, the signaling molecules dock and pinch, and the TGF β -pathway inhibitor follistatin (SmFst). First characterization studies provided evidence for SmFst transcription in the reproductive organs of EM, UM and females. Furthermore, the interaction of SmFst with an inhibin/activin-like protein (SmInAct) and a bone morphogenic protein (SmBMP) of *S. mansoni* was shown by yeast-two-hybrid experiments. Localization studies demonstrated that all three transcripts localize in the testes of EM and UM. These findings indicate a yet unknown function of the TGF β -pathway in male schistosomes and a possible influence of pairing on the male gonad.

Zusammenfassung

Schistosoma mansoni Männchen haben eine Schlüsselrolle in der einzigartigen Reproduktionsbiologie dieser parasitären Plattwürmer. Ohne einen konstanten Paarungskontakt mit dem Männchen kann das Weibchen seine geschlechtliche Reife weder erlangen noch erhalten. Diese ist jedoch die Grundlage für die Produktion der Eier, welche die Auslöser der weltweit bedeutenden Krankheit Schistosomiasis sind.

Über die Prozesse, durch die Männchen auf die Entwicklung der Weibchen wirken, ist wenig bekannt. Verschiedene Arten von Molekülen wurden als Stimulanzen vorgeschlagen, doch wurde bisher keines verifiziert. Weiterhin gibt es die Hypothese, dass auch Männchen durch die Paarung beeinflusst werden, wobei sie einen Kompetenz-Status erreichen, der es ihnen ermöglicht, die Reifung des Weibchens zu stimulieren. Auch hierfür gibt es derzeit nur wenige Daten. Die EST- und Genomprojekte für Schistosomen haben neue Möglichkeiten eröffnet, die Prozesse in Männchen auch durch Transkriptomanalysen zu untersuchen. Die hier beschriebene Studie wurde durchgeführt, um Unterschiede zwischen paarungserfahrenen (EM) und paarungsunerfahrenen (UM) Männchen aufzudecken.

Vorhergehende Experimente hatten angedeutet, dass sowohl die Paarung als auch TNF α einen Einfluss auf die mitotische Aktivität (MA) in Männchen hatten. Weiterhin gab es Hinweise darauf, dass eine *S. mansoni* cGMP-abhängige Protein-Kinase (SmcGK1) differentiell zwischen EM und UM transkribiert wurde. Während ein Einfluss der Paarung auf die MA in Männchen in der

vorliegenden Studie nicht bestätigt werden konnte, wurde ein Konzentrations- und Medium-abhängiger Effekt von TNF α auf die MA von Männchen gefunden. Differentielle Transkription von SmcGK1 zwischen EM und UM wurde nicht nachgewiesen. Allerdings zeigten Lokalisationsstudien, dass SmcGK1-Transkripte in den Reproduktionsorganen weiblicher und männlicher *S. mansoni* vorliegen. Weiterhin gaben Inhibitorstudien Hinweise darauf, dass SmcGK1 einen Einfluss auf die Beweglichkeit und die Eiproduktion der Würmer hat.

Um Unterschiede zwischen EM und UM in größerem Maß aufzudecken, wurden zwei unterschiedliche Methoden zur Transkriptomanalyse, Microarrays und SuperSAGE, kombiniert. Wie erwartet bestätigten und ergänzten sich beide Methoden gegenseitig. Zusätzliche Bestätigung der erhaltenen Ergebnisse wurde durch ‚real-time‘ PCR-Experimente erzielt. Die Verwendung bioinformatischer Programme wie ‚gene ontology‘, Ingenuity Pathway Analysis‘, sowie einer *S. mansoni*-spezifische Metablomanalyse vereinfachte zusätzlich die Dateninterpretation. Unterschiedliche statistische Verfahren wurden angewendet und ihr Einfluss auf die Daten hervorgehoben.

Mittels Microarray-Analysen und SuperSAGE wurden insgesamt je 9,344 und 7,394 sense-Transkripte detektiert. Der Vergleich beider Datensätze ergab, dass 6,326 Transkripte mit beiden Methoden nachgewiesen wurden, wobei 29 dieser Gene signifikant und differenziell ($q < 0.01$; $p < 1^{-10}$; $\log_2\text{ratios} > 0.585$ oder < -0.585) zwischen EM und UM transkribiert waren. Zu diesem Zeitpunkt ist dies der umfassendste Datensatz bezüglich differentieller Transkription in *S. mansoni* Männchen. Die Daten beinhalteten Hinweise auf Unterschiede zwischen EM und UM in metabolischen Prozessen, ein Befund, der frühere Studien bestätigt. Zusätzlich wurden Hinweise auf die Beteiligung neuronale Signaltransduktion, anti-sense Regulation und Schistosomen-spezifischer, Protein-kodierender Gene gefunden, die an der Männchen-Weibchen-Interaktion beteiligt sein könnten. Verschiedene Gene wurden durch die Datenanalyse hervorgehoben, darunter sind eine Dopa-Decarboxylase, die Signalmoleküle Dock und Pinch und der TGF β -Signalweg-Inhibitor Follistatin (SmFst). Anhand erster Charakterisierungsstudien wurden Transkripte für SmFst in den Reproduktionsorganen von EM, UM und Weibchen gefunden. Weiterhin konnte die Interaktion von SmFst mit einem Inhibin/Activin-ähnlichen Protein (SmInAct), sowie einem ‚bone morphogenic protein‘ (SmBMP) aus *S. mansoni* mittels ‚yeast-two-hybrid‘-Analysen nachgewiesen werden. Transkripte aller drei Gene wurden in den Testes von EM und UM lokalisiert. Diese Ergebnisse legen eine bisher unbekannt Funktion des TGF β -Signalweges

5. Summary

in Schistosomenmännchen nahe, sowie eine mögliche Beeinflussung der männlichen Gonaden durch die Paarung.

6. References

- Abràmoff, M. D.; Magalhaes, P. J.; Ram, S. J. (2004)** Umage Processing with ImageJ. *Biophotonics International* **11**:36-42.
- Adams, S. P. (2013)** Data analysis and reporting. Pp. 39-62 in Real-time PCR, M. T. Dorak, ed. *Taylor & Francis group*, Abingdon.
- Ahier, A.; Khayath, N.; Vicogne, J.; Dissous, C. (2008)** Insulin receptors and glucose uptake in the human parasite *Schistosoma mansoni*. *Parasite* **15**:573-579.
- Allendorph, G. P.; Isaacs, M. J.; Kawakami, Y.; Izpisua Belmonte, J. C.; Choe, S. (2007)** BMP-3 and BMP-6 structures illuminate the nature of binding specificity with receptors. *Biochemistry* **46**:12238-12247.
- Almeida, G. T.; Amaral, M. S.; Beckedorff, F. C. F.; Kitajima, J. P.; DeMarco, R.; Verjovski-Almeida, S. (2012)** Exploring the *Schistosoma mansoni* adult male transcriptome using RNA-seq. *Exp. Parasitol.* **132**:22-31.
- Amiri, P.; Locksley, R. M.; Parslow, T. G.; Sadick, M.; Rector, E.; Ritter, D.; McKerrow, J. H. (1992)** Tumour necrosis factor alpha restores granulomas and induces parasite egg-laying in schistosome-infected SCID mice. *Nature* **356**:604-607.
- Andrade, L. F.; Nahum, L. A.; Avelar, L. G.; Silva, L. L.; Zerlotini, A.; Ruiz, J. C.; Oliveira, G. (2011)** Eukaryotic protein kinases (ePKs) of the helminth parasite *Schistosoma mansoni*. *BMC. Genomics* **12**:215.
- Armstrong, J. C. (1965)** Mating behavior and development of schistosomes in the mouse. *J. Parasitol.* **51**:605-616.
- Aronstein, W. S. and Strand, M. (1985)** A glycoprotein antigen of *Schistosoma mansoni* expressed on the gynecophoral canal of mature male worms. *Am. J. Trop. Med. Hyg.* **34**:508-512.
- Ashton, P. D.; Harrop, R.; Shah, B.; Wilson, R. A. (2001)** The schistosome egg: development and secretion. *Parasitology* **122**:329-338.
- Atkinson, K. H. and Atkinson, B. G. (1980)** Biochemical basis for the continuous copulation of female *Schistosoma mansoni*. *Nature* **283**:478-479.
- Audic, S. and Claverie, J. M. (1997)** The significance of digital gene expression profiles. *Genome Res.* **7**:986-995.
- Avelar, L. G.; Nahum, L. A.; Andrade, L. F.; Oliveira, G. (2011)** Functional Diversity of the *Schistosoma mansoni* Tyrosine Kinases. *J. Signal. Transduct.* **2011**:603290.
- Bahia, D.; Andrade, L. F.; Ludolf, F.; Mortara, R. A.; Oliveira, G. (2006a)** Protein tyrosine kinases in *Schistosoma mansoni*. *Mem Inst Oswaldo Cruz* **101**:137-143.
- Bahia, D.; Avelar, L.; Mortara, R. A.; Khayath, N.; Yan, Y.; Noel, C.; Capron, M.; Dissous, C.; Pierce, R. J.; Oliveira, G. (2006b)** SmPKC1, a new protein kinase C identified in the platyhelminth parasite *Schistosoma mansoni*. *Biochem. Biophys. Res. Commun.* **345**:1138-1148.
- Baisch, H.; Otto, U.; Kloppel, G. (1990)** Antiproliferative and cytotoxic effects of single and combined treatment with tumor necrosis factor alpha and/or alpha interferon on a human renal cell carcinoma xenotransplanted into nu/nu mice: cell kinetic studies. *Cancer Res.* **50**:6389-6395.

6. References

- Baker, D. A. and Deng, W. (2005)** Cyclic GMP-dependent protein kinases in protozoa. *Front Biosci.* **10**:1229-1238.
- Basch, P. F. and Basch, N. (1984)** Intergeneric reproductive stimulation and parthenogenesis in *Schistosoma mansoni*. *Parasitology* **89** (Pt 2):369-376.
- Basch, P. F. (1986)** Immunocytochemical localization of ecdysteroids in the life history stages of *Schistosoma mansoni*. *Comp Biochem. Physiol A Comp Physiol* **83**:199-202.
- Basch, P. F. and Nicolas, C. (1989)** *Schistosoma mansoni*: pairing of male worms with artificial surrogate females. *Exp. Parasitol.* **68**:202-207.
- Basch, P. F. (1990)** Why do schistosomes have separate sexes? *Parasitol. Today* **6**:160-163.
- Bauer, D. F. (1972)** Constructing confidence sets using rank statistics. *Journal of the American Statistical Association* **67**:687-690.
- Baxter, G. T.; Kuo, R. C.; Jupp, O. J.; Vandenabeele, P.; MacEwan, D. J. (1999)** Tumor necrosis factor-alpha mediates both apoptotic cell death and cell proliferation in a human hematopoietic cell line dependent on mitotic activity and receptor subtype expression. *J. Biol. Chem.* **274**:9539-9547.
- Beall, M. J.; McGonigle, S.; Pearce, E. J. (2000)** Functional conservation of *Schistosoma mansoni* Smads in TGF-beta signaling. *Mol. Biochem. Parasitol.* **111**:131-142.
- Beall, M. J. and Pearce, E. J. (2001)** Human transforming growth factor-beta activates a receptor serine/threonine kinase from the intravascular parasite *Schistosoma mansoni*. *J. Biol. Chem.* **276**:31613-31619.
- Beckmann, S. (2008)** *Schistosoma mansoni*: Tyrosinkinase-Signalwege in den Reproduktionsorganen und Aktin-Promotoranalysen im Transgemodell. *Justus-Liebig Universität Gießen*.
- Beckmann, S. and Grevelding, C. G. (2010)** Imatinib has a fatal impact on morphology, pairing stability and survival of adult *Schistosoma mansoni* in vitro. *Int. J. Parasitol.* **40**:521-526.
- Beckmann, S.; Buro, C.; Dissous, C.; Hirzmann, J.; Grevelding, C. G. (2010a)** The Syk kinase SmTK4 of *Schistosoma mansoni* is involved in the regulation of spermatogenesis and oogenesis. *PLoS. Pathog.* **6**:e1000769.
- Beckmann, S.; Quack, T.; Burmeister, C.; Buro, C.; Long, T.; Dissous, C.; Grevelding, C. G. (2010b)** *Schistosoma mansoni*: signal transduction processes during the development of the reproductive organs. *Parasitology* **137**:497-520.
- Beckmann, S.; Hahnel, S.; Cailliau, K.; Vanderstraete, M.; Browaeys, E.; Dissous, C.; Grevelding, C. G. (2011)** Characterization of the Src/Abl hybrid kinase SmTK6 of *Schistosoma mansoni*. *J. Biol. Chem.* **286**:42325-42336.
- Beckmann, S. and Grevelding, C. G. (2012)** Paving the way for transgenic schistosomes. *Parasitology* **139**:651-668.
- Beckmann, S.; Leutner, S.; Gougnard, N.; Dissous, C.; Grevelding, C. G. (2012a)** Protein kinases as potential targets for novel anti-schistosomal strategies. *Curr. Pharm. Des* **18**:3579-3594.

- Beckmann, S.; Quack, T.; Dissous, C.; Cailliau, K.; Lang, G.; Grevelding, C. G. (2012b) Discovery of platyhelminth-specific alpha/beta-integrin families and evidence for their role in reproduction in *Schistosoma mansoni*. *PLoS. One.* **7**:e52519.
- Beites, C. L.; Hollenbeck, P. L.; Kim, J.; Lovell-Badge, R.; Lander, A. D.; Calof, A. L. (2009) Follistatin modulates a BMP autoregulatory loop to control the size and patterning of sensory domains in the developing tongue. *Development* **136**:2187-2197.
- Berriman, M.; Haas, B. J.; LoVerde, P. T.; Wilson, R. A.; Dillon, G. P.; Cerqueira, G. C.; Mashiyama, S. T.; Al-Lazikani, B.; Andrade, L. F.; Ashton, P. D.; Aslett, M. A.; Bartholomeu, D. C.; Blandin, G.; Caffrey, C. R.; Coghlan, A.; Coulson, R.; Day, T. A.; Delcher, A.; DeMarco, R.; Djikeng, A.; Eyre, T.; Gamble, J. A.; Ghedin, E.; Gu, Y.; Hertz-Fowler, C.; Hirai, H.; Hirai, Y.; Houston, R.; Ivens, A.; Johnston, D. A.; Lacerda, D.; Macedo, C. D.; McVeigh, P.; Ning, Z.; Oliveira, G.; Overington, J. P.; Parkhill, J.; Pertea, M.; Pierce, R. J.; Protasio, A. V.; Quail, M. A.; Rajandream, M. A.; Rogers, J.; Sajid, M.; Salzberg, S. L.; Stanke, M.; Tivey, A. R.; White, O.; Williams, D. L.; Wortman, J.; Wu, W.; Zamanian, M.; Zerlotini, A.; Fraser-Liggett, C. M.; Barrell, B. G.; El-Sayed, N. M. (2009) The genome of the blood fluke *Schistosoma mansoni*. *Nature* **460**:352-358.
- Bertin, B.; Oger, F.; Cornette, J.; Caby, S.; Noel, C.; Capron, M.; Fantappie, M. R.; Rumjanek, F. D.; Pierce, R. J. (2006) *Schistosoma mansoni* CBP/p300 has a conserved domain structure and interacts functionally with the nuclear receptor SmFtz-F1. *Mol. Biochem. Parasitol.* **146**:180-191.
- Bradley, J. R. (2008) TNF-mediated inflammatory disease. *J. Pathol.* **214**:149-160.
- Buro, C.; Beckmann, S.; Quack, T.; Grevelding, C. G. (2010) Photometric quantification of the β -galactosidase activity for the analysis of the relative interaction strength between signal transduction proteins from *Schistosoma mansoni*. *Eppendorf Application Note* **221**:1-6.
- Buro, C.; Oliveira, K. C.; Beckmann, S.; Leutner, S.; Lu, Z.; Dissous, C.; Cailliau, K.; Verjovski-Almeida, S.; Grevelding, C. G. (2013) Transcriptome analyses of inhibitor-treated schistosome females provide evidence for cooperating Src-kinase and TGF β receptor pathways controlling mitosis and eggshell formation. *PLoS. Pathog.* **9**:e1003448.
- Butt, E.; Eigenthaler, M.; Genieser, H. G. (1994) (Rp)-8-pCPT-cGMPS, a novel cGMP-dependent protein kinase inhibitor. *Eur. J. Pharmacol.* **269**:265-268.
- Caers, J.; Verlinden, H.; Zels, S.; Vandersmissen, H. P.; Vuerinckx, K.; Schoofs, L. (2012) More than two decades of research on insect neuropeptide GPCRs: an overview. *Front Endocrinol. (Lausanne)* **3**:151.
- Candenas, L.; Lecci, A.; Pinto, F. M.; Patak, E.; Maggi, C. A.; Pennefather, J. N. (2005) Tachykinins and tachykinin receptors: effects in the genitourinary tract. *Life Sci.* **76**:835-862.
- Cardoso, J. C.; Felix, R. C.; Fonseca, V. G.; Power, D. M. (2012) Feeding and the rhodopsin family g-protein coupled receptors in nematodes and arthropods. *Front Endocrinol. (Lausanne)* **3**:157.
- Carlo, J. M.; Osman, A.; Niles, E. G.; Wu, W.; Fantappie, M. R.; Oliveira, F. M.; LoVerde, P. T. (2007) Identification and characterization of an R-Smad ortholog (SmSmad1B) from *Schistosoma mansoni*. *FEBS J.* **274**:4075-4093.
- Carrion, M.; Gomez, M. J.; Merchante-Schubert, R.; Dongarra, S.; Ayala, J. A. (1999) mraW, an essential gene at the dcw cluster of *Escherichia coli* codes for a cytoplasmic protein with methyltransferase activity. *Biochimie* **81**:879-888.

6. References

- Causton, H. C.; Quackenbush, J.; Brazma, A. (2003)** Microarray gene expression data analysis - a beginner's guide. *Oxford: Blackwell Publishing*.
- Chan, F. K. (2007)** Three is better than one: pre-ligand receptor assembly in the regulation of TNF receptor signaling. *Cytokine* **37**:101-107.
- Cheever, A. W.; Poindexter, R. W.; Wynn, T. A. (1999)** Egg laying is delayed but worm fecundity is normal in SCID mice infected with *Schistosoma japonicum* and *S. mansoni* with or without recombinant tumor necrosis factor alpha treatment. *Infect. Immun.* **67**:2201-2208.
- Chen, G. and Goeddel, D. V. (2002)** TNF-R1 signaling: a beautiful pathway. *Science* **296**:1634-1635.
- Cheng, G.; Fu, Z.; Lin, J.; Shi, Y.; Zhou, Y.; Jin, Y.; Cai, Y. (2009)** *In vitro* and *in vivo* evaluation of small interference RNA-mediated gynaecophoral canal protein silencing in *Schistosoma japonicum*. *J. Gene Med.* **11**:412-421.
- Cheung, Z. H. and Ip, N. Y. (2009)** Endophilin B1: Guarding the gate to destruction. *Commun. Integr. Biol.* **2**:130-132.
- Chien, C. T.; Bartel, P. L.; Sternglanz, R.; Fields, S. (1991)** The two-hybrid system: a method to identify and clone genes for proteins that interact with a protein of interest. *Proc. Natl. Acad. Sci. U. S. A* **88**:9578-9582.
- Chitsulo, L.; Loverde, P.; Engels, D. (2004)** Schistosomiasis. *Nat. Rev. Microbiol.* **2**:12-13.
- Christenson, J. G.; Dairman, W.; Udenfriend, S. (1972)** On the Identity of DOPA Decarboxylase and 5-Hydroxytryptophan Decarboxylase. *Proc. Nat. Acad. Sci. U. S. A* **69**:343-347.
- Cioli, D. and Pica-Mattocchia, L. (2003)** Praziquantel. *Parasitol Res.* **90**:S3-S9.
- Clevers, H. (2006)** Wnt/beta-catenin signaling in development and disease. *Cell* **127**:469-480.
- Clough, E. R. (1981)** Morphology and reproductive organs and oogenesis in bisexual and unisexual transplants of mature *Schistosoma mansoni* females. *J. Parasitol.* **67**:535-539.
- Conford, E. M. and Huot, M. E. (1981)** Glucose transfer from male to female schistosomes. *Science* **213**:1269-1271.
- Cornford, E. M. and Fitzpatrick, A. M. (1985)** The mechanism and rate of glucose transfer from male to female schistosomes. *Mol. Biochem. Parasitol.* **17**:131-141.
- Cote, J. F. and Vuori, K. (2002)** Identification of an evolutionarily conserved superfamily of DOCK180-related proteins with guanine nucleotide exchange activity. *J. Cell Sci.* **115**:4901-4913.
- Craig, S. W. and Powell, L. D. (1980)** Regulation of actin polymerization by villin, a 95,000 dalton cytoskeletal component of intestinal brush borders. *Cell* **22**:739-746.
- Davies, S. J.; Shoemaker, C. B.; Pearce, E. J. (1998)** A divergent member of the transforming growth factor beta receptor family from *Schistosoma mansoni* is expressed on the parasite surface membrane. *J. Biol. Chem.* **273**:11234-11240.
- Davies, S. J.; Grogan, J. L.; Blank, R. B.; Lim, K. C.; Locksley, R. M.; McKerrow, J. H. (2001)** Modulation of blood fluke development in the liver by hepatic CD4+ lymphocytes. *Science* **294**:1358-1361.

- Davies, S. J.; Lim, K. C.; Blank, R. B.; Kim, J. H.; Lucas, K. D.; Hernandez, D. C.; Sedgwick, J. D.; McKerrow, J. H. (2004) Involvement of TNF in limiting liver pathology and promoting parasite survival during schistosome infection. *Int. J. Parasitol.* **34**:27-36.
- DeBont, J. and Vercruyse, J. (1998) Schistosomiasis in cattle. *Adv. Parasitol.* **41**:285-364.
- De Marco, R.; Mathieson, W.; Manuel, S. J.; Dillon, G. P.; Curwen, R. S.; Ashton, P. D.; Ivens, A. C.; Berriman, M.; Verjovski-Almeida, S.; Wilson, R. A. (2010) Protein variation in blood-dwelling schistosome worms generated by differential splicing of micro-exon gene transcripts. *Genome Res.* **20**:1112-1121.
- De Moraes, J.; Almeida, A. A.; Brito, M. R.; Marques, T. H.; Lima, T. C.; Sousa, D. P.; Nakano, E.; Mendonca, R. Z.; Freitas, R. M. (2013) Anthelmintic activity of the natural compound (+)-limonene epoxide against *Schistosoma mansoni*. *Planta Med.* **79**:253-258.
- De Mendonca, R. L.; Bouton, D.; Bertin, B.; Escriva, H.; Noel, C.; Vanacker, J. M.; Cornette, J.; Laudet, V.; Pierce, R. J. (2002) A functionally conserved member of the FTZ-F1 nuclear receptor family from *Schistosoma mansoni*. *Eur. J. Biochem.* **269**:5700-5711.
- De Moraes Maciel, R.; de Silva Dutra, D. L.; Rumjanek, F. D.; Juliano, L.; Juliano, M. A.; Fantappi , M. R. (2004) *Schistosoma mansoni* histone acetyltransferase GCN5: linking histone acetylation to gene activation. *Mol. Biochem. Parasitol* **133**:131-135.
- De Saram, P. S.; Ressurreicao, M.; Davies, A. J.; Rollinson, D.; Emery, A. M.; Walker, A. J. (2013) Functional mapping of protein kinase A reveals its importance in adult *Schistosoma mansoni* motor activity. *PLoS. Negl. Trop. Dis.* **7**:e1988.
- De Souza, G. M.; Muniyappa, M. K.; Carvalho, S. G.; Guerra-Sa, R.; Spillane, C. (2011) Genome-wide identification of novel microRNAs and their target genes in the human parasite *Schistosoma mansoni*. *Genomics* **98**:96-111.
- Den Hollander, J. E. and Erasmus, D. A. (1984) *Schistosoma mansoni*: DNA synthesis in males and females from mixed and single-sex infections. *Parasitology* **88 (Pt 3)**:463-476.
- Den Hollander, J. E. and Erasmus, D. A. (1985) *Schistosoma mansoni*: male stimulation and DNA synthesis by the female. *Parasitology* **91 (Pt 3)**:449-457.
- Dettman, C. D.; Higgins-Opitz, S. B.; Saikoolal, A. (1989) Enhanced efficacy of the paddling method for schistosome infection of rodents by a four-step pre-soaking procedure. *Parasitol. Res.* **76**:183-184.
- Dissous, C.; Ahier, A.; Khayath, N. (2007) Protein tyrosine kinases as new potential targets against human schistosomiasis. *Bioessays* **29**:1281-1288.
- Dissous, C. and Greveling, C. G. (2011) Piggy-backing the concept of cancer drugs for schistosomiasis treatment: a tangible perspective? *Trends Parasitol.* **27**:59-66.
- Dissous, C.; Greveling, C. G.; Long, T. (2011) *Schistosoma mansoni* Polo-like kinases and their function in control of mitosis and parasite reproduction. *An. Acad. Bras. Cienc.* **83**:627-635.
- Doenhoff, M.; Musallam, R.; Bain, J.; McGregor, A. (1978) Studies on the host-parasite relationship in *Schistosoma mansoni*-infected mice: the immunological dependence of parasite egg excretion. *Immunology* **35**:771-778.

6. References

- Doenhoff, M. J.; Hagan, P.; Cioli, D.; Southgate, V.; Pica-Mattoccia, L.; Botros, S.; Coles, G.; Tchuem Tchuente, L. A.; Mbaye, A.; Engels, D. (2009) Praziquantel: its use in control of schistosomiasis in sub-Saharan Africa and current research needs. *Parasitology* **136**:1825-1835.
- Dönges, J. (1988) *Parasitologie*. Thieme Verlag, Stuttgart.
- Duvall, R. H. and DeWitt, W. B. (1967) An improved perfusion technique for recovering adult schistosomes from laboratory animals. *Am. J. Trop. Med. Hyg.* **16**:483-486.
- Erasmus, D. A. (1973) A comparative study of the reproductive system of mature, immature and "unisexual" female *Schistosoma mansoni*. *Parasitology* **67**:165-183.
- Filmus, J.; Capurro, M.; Rast, J. (2008) Glypicans. *Genome Biol.* *Epub 2008 May 22.*
- Fitzpatrick, J. M.; Johansen, M. V.; Johnston, D. A.; Dunne, D. W.; Hoffmann, K. F. (2004) Gender-associated gene expression in two related strains of *Schistosoma japonicum*. *Mol. Biochem. Parasitol.* **136**:191-209.
- Fitzpatrick, J. M.; Johnston, D. A.; Williams, G. W.; Williams, D. J.; Freeman, T. C.; Dunne, D. W.; Hoffmann, K. F. (2005) An oligonucleotide microarray for transcriptome analysis of *Schistosoma mansoni* and its application/use to investigate gender-associated gene expression. *Mol. Biochem. Parasitol.* **141**:1-13.
- Fitzpatrick, J. M. and Hoffmann, K. F. (2006) Dioecious *Schistosoma mansoni* express divergent gene repertoires regulated by pairing. *Int. J. Parasitol.* **36**:1081-1089.
- Fitzpatrick, J. M.; Peak, E.; Perally, S.; Chalmers, I. W.; Barrett, J.; Yoshino, T. P.; Ivens, A. C.; Hoffmann, K. F. (2009) Anti-schistosomal intervention targets identified by lifecycle transcriptomic analyses. *PLoS. Negl. Trop. Dis.* **3**:e543.
- Forrester, S. G.; Warfel, P. W.; Pearce, E. J. (2004) Tegumental expression of a novel type II receptor serine/threonine kinase (SmRK2) in *Schistosoma mansoni*. *Mol. Biochem. Parasitol.* **136**:149-156.
- Franco, G. R.; Valadao, A. F.; Azevedo, V.; Rabelo, E. M. (2000) The *Schistosoma* gene discovery program: state of the art. *Int. J. Parasitol.* **30**:453-463.
- Freebern, W. J.; Niles, E. G.; LoVerde, P. T. (1999a) RXR-2, a member of the retinoid x receptor family in *Schistosoma mansoni*. *Gene* **233**:33-38.
- Freebern, W. J.; Osman, A.; Niles, E. G.; Christen, L.; LoVerde, P. T. (1999b) Identification of a cDNA encoding a retinoid X receptor homologue from *Schistosoma mansoni*. Evidence for a role in female-specific gene expression. *J. Biol. Chem.* **274**:4577-4585.
- Freitas, T. C.; Jung, E.; Pearce, E. J. (2007) TGF-beta signaling controls embryo development in the parasitic flatworm *Schistosoma mansoni*. *PLoS. Pathog.* **3**:e52.
- Freitas, T. C.; Jung, E.; Pearce, E. J. (2009) A bone morphogenetic protein homologue in the parasitic flatworm, *Schistosoma mansoni*. *Int. J. Parasitol.* **39**:281-287.
- Fujiwara, M.; Sengupta, P.; McIntire, S. L. (2002) Regulation of body size and behavioral state of *C. elegans* by sensory perception and the EGL-4 cGMP-dependent protein kinase. *Neuron* **36**:1091-1102.
- Galanti, S. E.; Huang, S. C.; Pearce, E. J. (2012) Cell death and reproductive regression in female *Schistosoma mansoni*. *PLoS. Negl. Trop. Dis.* **6**:e1509.

- Gamm, D. M.; Francis, S. H.; Angelotti, T. P.; Corbin, J. D.; Uhler, M. D. (1995)** The type II isoform of cGMP-dependent protein kinase is dimeric and possesses regulatory and catalytic properties distinct from the type I isoforms. *J. Biol. Chem.* **270**:27380-27388.
- Gehlert, D. R. (2004)** Introduction to the reviews on neuropeptide Y. *Neuropeptides* **38**:135-140.
- Geyer, K. K.; Rodriguez Lopez, C. M.; Chalmers, I. W.; Munshi, S. E.; Truscott, M.; Heald, J.; Wilkinson, M. J.; Hoffmann, K. F. (2011)** Cytosine methylation regulates oviposition in the pathogenic blood fluke *Schistosoma mansoni*. *Nat. Commun.* **2**:424.
- Gioti, A.; Wigby, S.; Wertheim, B.; Schuster, E.; Martinez, P.; Pennington, C. J.; Partridge, L.; Chapman, T. (2012)** Sex peptide of *Drosophila melanogaster* males is a global regulator of reproductive processes in females. *Proc. Biol. Sci.* **279**:4423-4432.
- Gobert, G. N.; Moertel, L.; Brindley, P. J.; McManus, D. P. (2009a)** Developmental gene expression profiles of the human pathogen *Schistosoma japonicum*. *BMC. Genomics* **10**:128.
- Gobert, G. N.; McManus, D. P.; Nawaratna, S.; Moertel, L.; Mulvenna, J.; Jones, M. K. (2009b)** Tissue specific profiling of females of *Schistosoma japonicum* by integrated laser microdissection microscopy and microarray analysis. *PLoS. Negl. Trop. Dis.* **3**:e469.
- Gouignard, N.; Vanderstraete, M.; Cailliau, K.; Lescuyer, A.; Browaeys, E.; Dissous, C. (2012)** *Schistosoma mansoni*: Structural and biochemical characterization of two distinct Venus Kinase Receptors. *Exp. Parasitol.* **132**:32-39.
- Greenberg, R. M. and . (2005)** Are Ca²⁺ channels targets of praziquantel action? *Int. J. Parasitol.* **35**:1-9.
- Grevelding, C. G. (1995)** The female-specific W1 sequence of the Puerto Rican strain of *Schistosoma mansoni* occurs in both genders of a Liberian strain. *Mol. Biochem. Parasitol.* **71**:269-272.
- Grevelding, C. G.; Sommer, G.; Kunz, W. (1997a)** Female-specific gene expression in *Schistosoma mansoni* is regulated by pairing. *Parasitology* **115 (Pt 6)**:635-640.
- Grevelding, C. G.; Kampkotter, A.; Kunz, W. (1997b)** *Schistosoma mansoni*: sexing cercariae by PCR without DNA extraction. *Exp. Parasitol.* **85**:99-100.
- Grevelding, C. G. (2004)** *Schistosoma*. *Curr. Biol.* **14**:R545.
- Gupta, B. C. and Basch, P. F. (1987)** Evidence for transfer of a glycoprotein from male to female *Schistosoma mansoni* during pairing. *J. Parasitol.* **73**:674-675.
- Haccard, O.; Lewellyn, A.; Hartley, R. S.; Erikson, E.; Maller, J. L. (1995)** Induction of *Xenopus* oocyte meiotic maturation by MAP kinase. *Dev. Biol.* **168**:677-682.
- Haddad, F.; Qin, A. X.; Giger, J. M.; Guo, H.; Baldwin, K. M. (2007)** Potential pitfalls in the accuracy of analysis of natural sense-antisense RNA pairs by reverse transcription-PCR. *BMC. Biotechnol.* **7**:21.
- Hahnel, S. (2010)** Identifizierung, Klonierung und erste Untersuchungen von Transmembranrezeptoren aus *Schistosoma mansoni*. *Justus-Liebig-Universität Gießen*.
- Hahnel, S.; Lu, Z.; Wilson, R.A.; Grevelding, C.G.; Quack, T. (2013)** Whole-organ isolation approach as a basis for tissue-specific analyses in *Schistosoma mansoni*. *PLoS Negl Trop Dis.* **7**:e2336.
- Hanahan, D. (1983)** Studies on transformation of *Escherichia coli* with plasmids. Pp. 557-580

6. References

- Harris, I. R.; Hoppner, H.; Siefken, W.; Farrell, A. M.; Wittern, K. P. (2000) Regulation of HMG-CoA synthase and HMG-CoA reductase by insulin and epidermal growth factor in HaCaT keratinocytes. *J. Invest Dermatol.* **114**:83-87.
- Harrison, C. A.; Gray, P. C.; Vale, W. W.; Robertson, D. M. (2005) Antagonists of activin signaling: mechanisms and potential biological applications. *Trends Endocrinol. Metab* **16**:73-78.
- Haseeb, M. A.; Eveland, L. K.; Fried, B. (1985) The uptake, localization and transfer of [4-¹⁴C]cholesterol in *Schistosoma mansoni* males and females maintained *in vitro*. *Comp Biochem. Physiol A Comp Physiol* **82**:421-423.
- Haseeb, M. A.; Fried, B.; Eveland, L. K. (1989) *Schistosoma mansoni*: female-dependent lipid secretion in males and corresponding changes in lipase activity. *Int. J. Parasitol.* **19**:705-709.
- Haseeb, M. A.; Solomon, W. B.; Palma, J. F. (1996) *Schistosoma mansoni*: effect of recombinant tumor necrosis factor alpha on fecundity and [¹⁴C]-tyrosine uptake in females maintained *in vitro*. *Comp Biochem. Physiol C. Pharmacol. Toxicol. Endocrinol.* **115**:265-269.
- Haseeb, M. A.; Shirazian, D. J.; Preis, J. (2001) Elevated serum levels of TNF-alpha, sTNF-RI and sTNF-RII in murine schistosomiasis correlate with schistosome oviposition and circumoval granuloma formation. *Cytokine* **15**:266-269.
- Hehlgans, T. and Pfeffer, K. (2005) The intriguing biology of the tumour necrosis factor/tumour necrosis factor receptor superfamily: players, rules and the games. *Immunology* **115**:1-20.
- Hertz-Fowler, C.; Peacock, C. S.; Wood, V.; Aslett, M.; Kerhornou, A.; Mooney, P.; Tivey, A.; Berriman, M.; Hall, N.; Rutherford, K.; Parkhill, J.; Ivens, A. C.; Rajandream, M. A.; Barrell, B. (2004) GeneDB: a resource for prokaryotic and eukaryotic organisms. *Nucleic Acids Res.* **32**:D339-D343.
- Hoffmann, K. F.; Johnston, D. A.; Dunne, D. W. (2002) Identification of *Schistosoma mansoni* gender-associated gene transcripts by cDNA microarray profiling. *Genome Biol.* **3**:RESEARCH0041.
- Hofmann, F.; Bernhard, D.; Lukowski, R.; Weinmeister, P. (2009) cGMP Regulated Protein Kinases (cGK). Pp. 137-162 in Handbook of Experimental Pharmacology, Schmidt *et al.*, ed. *Springer-Verlag*, Berlin Heidelberg.
- Hollander, M. and Wolfe, D. A. (1973) Nonparametric statistical inference. *New York: John Wiley Sons.*
- Holtz, P. (1995) Role of L-Dopa decarboxylase in the biosynthesis of catecholamines in nervous tissue and the adrenal medulla. *Pharmacol. Rev.* **11**:317-329.
- Hood, J. D. and Cheresch, D. A. (2002) Role of integrins in cell invasion and migration. *Nat. Rev. Cancer* **2**:91-100.
- Hu, W.; Yan, Q.; Shen, D. K.; Liu, F.; Zhu, Z. D.; Song, H. D.; Xu, X. R.; Wang, Z. J.; Rong, Y. P.; Zeng, L. C.; Wu, J.; Zhang, X.; Wang, J. J.; Xu, X. N.; Wang, S. Y.; Fu, G.; Zhang, X. L.; Wang, Z. Q.; Brindley, P. J.; McManus, D. P.; Xue, C. L.; Feng, Z.; Chen, Z.; Han, Z. G. (2003) Evolutionary and biomedical implications of a *Schistosoma japonicum* complementary DNA resource. *Nat. Genet.* **35**:139-147.
- Humphries, J. E.; Kimber, M. J.; Barton, Y. W.; Hsu, W.; Marks, N. J.; Greer, B.; Harriott, P.; Maule, A. G.; Day, T. A. (2004) Structure and bioactivity of neuropeptide F from the human parasites *Schistosoma mansoni* and *Schistosoma japonicum*. *J. Biol. Chem.* **279**:39880-39885.

- Iemura, S.; Yamamoto, T. S.; Takagi, C.; Uchiyama, H.; Natsume, T.; Shimasaki, S.; Sugino, H.; Ueno, N. (1998) Direct binding of follistatin to a complex of bone-morphogenetic protein and its receptor inhibits ventral and epidermal cell fates in early *Xenopus* embryo. *Proc. Natl. Acad. Sci. U. S. A* **95**:9337-9342.
- Kapp, K.; Schussler, P.; Kunz, W.; Grevelding, C. G. (2001) Identification, isolation and characterization of a Fyn-like tyrosine kinase from *Schistosoma mansoni*. *Parasitology* **122**:317-327.
- Kaushal, D. and Naeve, C. W. (2004) Analyzing and visualizing expression data with Sportfire. *Current Protocols in Bioinformatics*.
- Keutmann, H. T.; Schneyer, A. L.; Sidis, Y. (2004) The role of follistatin domains in follistatin biological action. *Mol. Endocrinol.* **18**:228-240.
- Khayath, N.; Vicogne, J.; Ahier, A.; BenYounes, A.; Konrad, C.; Trolet, J.; Viscogliosi, E.; Brehm, K.; Dissous, C. (2007) Diversification of the insulin receptor family in the helminth parasite *Schistosoma mansoni*. *FEBS J.*:659-676.
- Kikuchi, A.; Yamamoto, H.; Sato, A.; Matsumoto, S. (2012) Wnt5a: its signalling, functions and implication in diseases. *Acta Physiol* **204**:17-33.
- King, D. H. (2010) Parasites and poverty: the case of schistosomiasis. *Acta Trop* **13**:95-104.
- Kirsch, T.; Nickel, J.; Sebald, W. (2000) BMP-2 antagonists emerge from alterations in the low-affinity binding epitope for receptor BMPR-II. *EMBO J.* **19**:3314-3324.
- Knobloch, J.; Kunz, W.; Grevelding, C. G. (2002a) Quantification of DNA synthesis in multicellular organisms by a combined DAPI and BrdU technique. *Dev. Growth Differ.* **44**:559-563.
- Knobloch, J.; Winnen, R.; Quack, M.; Kunz, W.; Grevelding, C. G. (2002b) A novel Syk-family tyrosine kinase from *Schistosoma mansoni* which is preferentially transcribed in reproductive organs. *Gene* **294**:87-97.
- Knobloch, J.; Rossi, A.; Osman, A.; LoVerde, P. T.; Klinkert, M. Q.; Grevelding, C. G. (2004) Cytological and biochemical evidence for a gonad-preferential interplay of SmFKBP12 and SmTbetaR-I in *Schistosoma mansoni*. *Mol. Biochem. Parasitol.* **138**:227-236.
- Knobloch, J.; Kunz, W.; Grevelding, C. G. (2006) Herbimycin A suppresses mitotic activity and egg production of female *Schistosoma mansoni*. *Int. J. Parasitol.* **36**:1261-1272.
- Knobloch, J.; Beckmann, S.; Burmeister, C.; Quack, T.; Grevelding, C. G. (2007) Tyrosine kinase and cooperative TGFbeta signaling in the reproductive organs of *Schistosoma mansoni*. *Exp. Parasitol.* **117**:318-336.
- Knowling, S. and Morris, K. V. (2011) Non-coding RNA and antisense RNA. Nature's trash or treasure? *Biochimie* **93**:1922-1927.
- Köster, B.; Dargatz, H.; Schröder, J.; Hirzmann, J.; Haarmann, C.; Symmons, P.; Kunz, W. (1988) Identification and localisation of the products of a putative eggshell precursor gene in the vitellarium of *Schistosoma mansoni*. *Mol Biochem Parasitol.* **31**:183-98.
- Krauss, G. (2008) Biochemistry of Signal Transduction and Regulation. WILEY-VCH Verlag GmbH & Co. KGaA, Weinheim.

6. References

- Kristiansen, K. (2004)** Molecular mechanisms of ligand binding, signaling, and regulation within the superfamily of G-protein-coupled receptors: molecular modeling and mutagenesis approaches to receptor structure and function. *Pharmacol. Ther.* **103**:21-80.
- Kubli, E. (2003)** Sex-peptides: seminal peptides of the *Drosophila* male. *Cell Mol. Life Sci.* **60**:1689-1704.
- Kunz, W. (2001)** Schistosome male-female interaction: induction of germ-cell differentiation. *Trends Parasitol.* **17**:227-231.
- Lamb, E. W.; Walls, C. D.; Pesce, J. T.; Riner, D. K.; Maynard, S. K.; Crow, E. T.; Wynn, T. A.; Schaefer, B. C.; Davies, S. J. (2010)** Blood fluke exploitation of non-cognate CD4+ T cell help to facilitate parasite development. *PLoS. Pathog.* **6**:e1000892.
- Larkin, M. A.; Blackshields, G.; Brown, N. P.; Chenna, R.; McGettigan, P. A.; McWilliam, H.; Valentin, F.; Wallace, I. M.; Wilm, A.; Lopez, R.; Thompson, J. D.; Gibson, T. J.; Higgins, D. G. (2007)** Clustal W and Clustal X version 2.0. *Bioinformatics* **23**:2947-2948.
- Lee, J. I.; O'Halloran, D. M.; Eastham-Anderson, J.; Juang, B. T.; Kaye, J. A.; Scott, H. O.; Lesch, B.; Goga, A.; L'Etoile, N. D. (2010)** Nuclear entry of a cGMP-dependent kinase converts transient into long-lasting olfactory adaptation. *Proc. Natl. Acad. Sci. U. S. A* **107**:6016-6021.
- Lee, J. T. (2012)** Epigenetic regulation by long noncoding RNAs. *Science* **338**:1435-1439.
- Legate, K. R.; Montanez, E.; Kudlacek, O.; Fassler, R. (2006)** ILK, PINCH and parvin: the tIPP of integrin signalling. *Nat. Rev. Mol. Cell Biol.* **7**:20-31.
- Letunic, I.; Doerks, T.; Bork, P. (2012)** SMART 7: recent updates to the protein domain annotation resource. *Nucleic Acids Res.* **40**:D302-D305.
- Leutner, S.; Beckmann, S.; Grevelding, C. G. (2011)** Characterization of the cGMP-dependent protein kinase SmcGK1 of *Schistosoma mansoni*. *An. Acad. Bras. Cienc.* **83**:637-648.
- Leutner, S.; Oliveira, K.C.; Rotter, B.; Beckmann, S.; Buro, C.; Hahnel, S.; Kitajima, J.P.; Verjovski-Almeida, S.; Winter, P.; Grevelding, CG. (2013)** Combinatory microarray and SuperSAGE analyses identify pairing-dependently transcribed genes in *Schistosoma mansoni* males, including follistatin. *Plos NTD.* (accepted October 2013)
- Levin, H. L. (1996)** An unusual mechanism of self-primed reverse transcription requires the RNase H domain of reverse transcriptase to cleave an RNA duplex. *Mol. Cell Biol.* **16**:5645-5654.
- Li, K. C.; Zhang, F. X.; Li, C. L.; Wang, F.; Yu, M. Y.; Zhong, Y. Q.; Zhang, K. H.; Lu, Y. J.; Wang, Q.; Ma, X. L.; Yao, J. R.; Wang, J. Y.; Lin, L. B.; Han, M.; Zhang, Y. Q.; Kuner, R.; Xiao, H. S.; Bao, L.; Gao, X.; Zhang, X. (2011)** Follistatin-like 1 suppresses sensory afferent transmission by activating Na⁺,K⁺-ATPase. *Neuron* **69**:974-987.
- Lin, S. J.; Lerch, T. F.; Cook, R. W.; Jardetzky, T. S.; Woodruff, T. K. (2006)** The structural basis of TGF-beta, bone morphogenetic protein, and activin ligand binding. *Reproduction.* **132**:179-190.
- Liu, H. and Kubli, E. (2003)** Sex-peptide is the molecular basis of the sperm effect in *Drosophila melanogaster*. *Proc. Natl. Acad. Sci. U. S. A* **100**:9929-9933.
- Locksley, R. M.; Killeen, N.; Lenardo, M. J. (2001)** The TNF and TNF receptor superfamilies: integrating mammalian biology. *Cell* **104**:487-501.

- Lodish, H.; Berk, A.; Zipursky, S. L.; Matsudaira, P.; Baltimore, D.; Darnell, J. E.; Lange, C.; Mahke, K.; Trager, L. (2001) Molekulare Zellbiologie. *Spektrum Akademischer Verlag*.
- Loker, E. S. and Brant, S. V. (2006) Diversification, dioecy and dimorphism in schistosomes. *Trends Parasitol.* **22**:521-528.
- Long, T.; Cailliau, K.; Beckmann, S.; Browaeys, E.; Trolet, J.; Greveling, C. G.; Dissous, C. (2010) *Schistosoma mansoni* Polo-like kinase 1: A mitotic kinase with key functions in parasite reproduction. *Int. J. Parasitol.* **40**:1075-1086.
- Long, T.; Vanderstraete, M.; Cailliau, K.; Morel, M.; Lescuyer, A.; Gouignard, N.; Greveling, C. G.; Browaeys, E.; Dissous, C. (2012) SmSak, the second Polo-like kinase of the helminth parasite *Schistosoma mansoni*: conserved and unexpected roles in meiosis. *PLoS. One.* **7**:e40045.
- Lorsuwannarat, N.; Saowakon, N.; Ramasoota, P.; Wanichanon, C.; Sobhon, P. (2013) The anthelmintic effect of plumbagin on *Schistosoma mansoni*. *Exp. Parasitol.* **133**:18-27.
- LoVerde, P. T.; Hirai, H.; Merrick, J. M.; Lee, N. H.; El-Sayed, N. (2004) *Schistosoma mansoni* genome project: an update. *Parasitol. Int.* **53**:183-192.
- LoVerde, P. T.; Osman, A.; Hinck, A. (2007) *Schistosoma mansoni*: TGF-beta signaling pathways. *Exp. Parasitol.* **117**:304-317.
- LoVerde, P. T.; Andrade, L. F.; Oliveira, G. (2009) Signal transduction regulates schistosome reproductive biology. *Curr. Opin. Microbiol.* **12**:422-428.
- Ludtmann, M. H.; Rollinson, D.; Emery, A. M.; Walker, A. J. (2009) Protein kinase C signalling during miracidium to mother sporocyst development in the helminth parasite, *Schistosoma mansoni*. *Int. J. Parasitol.* **39**:1223-1233.
- Machado-Silva, J. R.; Lanfredi, R. M.; Gomes, D. C. (1997) Morphological study of adult male worms of *Schistosoma mansoni* Sambon, 1907 by scanning electron microscopy. *Mem Inst Oswaldo Cruz* **92**:647-653.
- Magistri, M.; Faghihi, M. A.; St, L. G., III; Wahlestedt, C. (2012) Regulation of chromatin structure by long noncoding RNAs: focus on natural antisense transcripts. *Trends Genet.* **28**:389-396.
- Malagon, D.; Gray, D.; Botterill, B.; Lovas, E.; Duke, M.; Gray, C.; Kopp, S. R.; Knott, L. M.; McManus, D. P.; Daly, N. L.; Mulvenna, J.; Craik, D. J.; Jones, M. K. (2013) Anthelmintic activity of the cyclotides (kalata B1 and B2) against schistosome parasites. *Biopolymers*.
- Maloney, P. C.; Yan, R. T.; Abe, K. (1994) Bacterial anion exchange: reductionist and integrative approaches to membrane biology. *J. Exp. Biol.* **196**:471-482.
- Massague, J. (2000) How cells read TGF-beta signals. *Nat. Rev. Mol. Cell Biol.* **1**:169-178.
- Massague, J. and Wotton, D. (2000) Transcriptional control by the TGF-beta/Smad signaling system. *EMBO J.* **19**:1745-1754.
- Massague, J. and Chen, Y. G. (2000) Controlling TGF-beta signaling. *Genes Dev.* **14**:627-644.
- Massague, J.; Blain, S. W.; Lo, R. S. (2000) TGFbeta signaling in growth control, cancer, and heritable disorders. *Cell* **103**:295-309.
- Massague, J. and Gomis, R. R. (2006) The logic of TGFβ signaling. *FEBS Lett.* **580**:2811-2820.

6. References

- Matsumura, H.; Reich, S.; Ito, A.; Saitoh, H.; Kamoun, S.; Winter, P.; Kahl, G.; Reuter, M.; Kruger, D. H.; Terauchi, R. (2003)** Gene expression analysis of plant host-pathogen interactions by SuperSAGE. *Proc. Natl. Acad. Sci. U. S. A* **100**:15718-15723.
- Matsumura, H.; Yoshida, K.; Luo, S.; Kimura, E.; Fujibe, T.; Albertyn, Z.; Barrero, R. A.; Kruger, D. H.; Kahl, G.; Schroth, G. P.; Terauchi, R. (2010)** High-throughput SuperSAGE for digital gene expression analysis of multiple samples using next generation sequencing. *PLoS. One.* **5**:e12010.
- McDonald, J. K. (1990)** Role of neuropeptide Y in reproductive function. *Ann. N. Y. Acad. Sci.* **611**:258-272.
- McKerrow, J. H.; Caffrey, C.; Kelly, B.; Loke, P.; Sajid, M. (2006)** Proteases in Parasitic Diseases. *Annu. Rev. Pathol. Mech. Dis.*:497-536.
- Mehlhorn, H. and Piekarski, G. (2002)** Grundriß der Parasitenkunde - Parasiten des Menschen und der Nutztiere. *Spektrum Akademischer Verlag*, Heidelberg.
- Mehta, C. R. and Patel, N. R. (2013)** StatXact-5 for Windows. *Cytel Software Cooperation*, Cambridge, USA.
- Melman, S. D.; Steinauer, M. L.; Cunningham, C.; Kubatko, L. S.; Mwangi, I. N.; Wynn, N. B.; Mutuku, M. W.; Karanja, D. M.; Colley, D. G.; Black, C. L.; Secor, W. E.; Mkoji, G. M.; Loker, E. S. (2009)** Reduced susceptibility to praziquantel among naturally occurring Kenyan isolates of *Schistosoma mansoni*. *PLoS Negl. Trop Dis.* **3**:e504.
- Merrick, J. M.; Osman, A.; Tsai, J.; Quackenbush, J.; LoVerde, P. T.; Lee, N. H. (2003)** The *Schistosoma mansoni* gene index: gene discovery and biology by reconstruction and analysis of expressed gene sequences. *J. Parasitol.* **89**:261-269.
- Meyer, F.; Meyer, H.; Bueding, E. (1970)** Lipid metabolism in the parasitic and free-living flatworms, *Schistosoma mansoni* and *Dugesia dorotocephala*. *Biochim. Biophys. Acta* **210**:257-266.
- Michaels, R. M. (1969)** Mating of *Schistosoma mansoni* in vitro. *Exp. Parasitol.* **25**:58-71.
- Militello, K. T.; Refour, P.; Comeaux, C. A.; Duraisingh, M. T. (2008)** Antisense RNA and RNAi in protozoan parasites: Working hard or hardly working. *Mol. Biochem. Parasitol.*:117-126.
- Miller, D. J.; Ouellette, N.; Evdokimova, E.; Savchenko, A.; Edwards, A.; Anderson, W. F. (2003)** Crystal complexes of a predicted S-adenosylmethionine-dependent methyltransferase reveal a typical AdoMet binding domain and a substrate recognition domain. *Protein Science* **12**:1432-1442.
- Miller, J. H. (1972)** Experiments in molecular genetics. *Cold Spring Harbor Laboratory*, Cold Spring Harbor.
- Miller, J. H. (1992)** A short course in bacterial genetics. *Cold Spring Harbor Laboratory Press*, Plainview.
- Miraglia, E.; De, A. F.; Gazzano, E.; Hassanpour, H.; Bertagna, A.; Aldieri, E.; Revelli, A.; Ghigo, D. (2011)** Nitric oxide stimulates human sperm motility via activation of the cyclic GMP/protein kinase G signaling pathway. *Reproduction.* **141**:47-54.
- Miyamoto, Y. and Yamauchi, J. (2010)** Cellular signaling of Dock family proteins in neural function. *Cell Signal.* **22**:175-182.
- Moertel, L.; McManus, D. P.; Piva, T. J.; Young, L.; McInnes, R. L.; Gobert, G. N. (2006)** Oligonucleotide microarray analysis of strain- and gender-associated gene expression in the human blood fluke, *Schistosoma japonicum*. *Mol. Cell Probes* **20**:280-289.

- Molina, C.; Rotter, B.; Horres, R.; Udupa, S. M.; Besser, B.; Bellarmino, L.; Baum, M.; Matsumura, H.; Terauchi, R.; Kahl, G.; Winter, P. (2008) SuperSAGE: the drought stress-responsive transcriptome of chickpea roots. *BMC. Genomics* 9:553.
- Moore, D. V. and Sandground, J. H. (1956) The relative egg producing capacity of *Schistosoma mansoni* and *Schistosoma japonicum*. *Am J Trop Med Hyg.* 5:831-40.
- Moore, D. V.; Yolles, T. K.; Meleney, H. E. (1954) The relationship of male worms to the sexual development of female *Schistosoma mansoni*. *J. Parasitol.*:166-185.
- Morais, E. R.; Oliveira, K. C.; Magalhaes, L. G.; Moreira, E. B.; Verjovski-Almeida, S.; Rodrigues, V. (2013) Effects of curcumin on the parasite *Schistosoma mansoni*: a transcriptomic approach. *Mol. Biochem. Parasitol* 187:91-97.
- Moustakas, A. and Heldin, C. H. (2009) The regulation of TGFbeta signal transduction. *Development* 136:3699-3714.
- Mühlhardt, C. (2000) Der Experimentator - Molekularbiologie. *Spektrum Akademischer Verlag Heidelberg.*
- Mullis, K.; Faloona, F.; Scharf, S.; Saiki, R.; Horn, G.; Erlich, H. (1986) Specific enzymatic amplification of DNA *in vitro*: the polymerase chain reaction. *Cold Spring Harb. Symp. Quant. Biol.* 51 Pt 1:263-273.
- Myers, J. L. and Well, A. D. (2003) Research Design and Statistical Analysis. *Lawrence Erlbaum Associates.*
- Narasimamurthy, R.; Geuking, P.; Ingold, K.; Willen, L.; Schneider, P.; Basler, K. (2009) Structure-function analysis of Eiger, the *Drosophila* TNF homolog. *Cell Res.* 19:392-394.
- Nawaratna, S. S.; McManus, D. P.; Moertel, L.; Gobert, G. N.; Jones, M. K. (2011) Gene Atlasing of digestive and reproductive tissues in *Schistosoma mansoni*. *PLoS. Negl. Trop. Dis.* 5:e1043.
- Neto, E. D.; Harrop, R.; Correa-Oliveira, R.; Wilson, R. A.; Pena, S. D. J.; Simpson, A. J. G. (1997) Minilibraries constructed from cDNA generated by arbitrarily primed RT-PCR: an alternative to normalized libraries for the generation of ESTs from nanogram quantities of mRNA. *Gene* 186:135-142.
- Neves, R. H.; de Lamare Biolchini, C.; Machado-Silva, J. R.; Carvalho, J. J.; Branguiho, T. B.; Lenzi, H. L.; Hulstijn, M.; Gomes, D. C. (2005) A new description of the reproductive system of *Schistosoma mansoni* (Trematoda: *Schistosomatidae*) analyzed by confocal laser scanning microscopy. *Parasitol Res.* 95:43-49.
- New England Biolabs. (2008) NEB 10-beta Competent *E. coli* (High Efficiency)-Manual. www.neb.com
- Nickel, J.; Dreyer, M. K.; Kirsch, T.; Sebald, W. (2001) The crystal structure of the BMP-2:BMPr-IA complex and the generation of BMP-2 antagonists. *J. Bone Joint Surg. Am.* 83-A Suppl 1:S7-14.
- Nirde, P.; Torpier, G.; De Reggi, M. L.; Capron, A. (1983) Ecdysone and 20 hydroxyecdysone: new hormones for the human parasite *Schistosoma mansoni*. *FEBS Lett.* 151:223-227.
- Nirde, P.; De Reggi, M. L.; Tsoupras, G.; Torpier, G.; Fressancourt, P.; Capron, A. (1984) Excretion of ecdysteroids by schistosomes as a marker of parasite infection. *FEBS Lett.* 168:235-240.
- Nishita, M.; Enomoto, M.; Yamagata, K.; Minami, Y. (2010) Cell/tissue-tropic functions of Wnt5a signaling in normal and cancer cells. *Trends Cell Biol.* 20:346-354.
- Oliveira, G. (2007) The *Schistosoma mansoni* transcriptome: an update. *Exp. Parasitol* 117:229-235.

6. References

- Oliveira, K. C.; Carvalho, M. L.; Venancio, T. M.; Miyasato, P. A.; Kawano, T.; DeMarco, R.; Verjovski-Almeida, S. (2009) Identification of the *Schistosoma mansoni* TNF-alpha receptor gene and the effect of human TNF-alpha on the parasite gene expression profile. *PLoS. Negl. Trop. Dis.* **3**:e556.
- Oliveira, K. C.; Carvalho, M. L.; Maracaja-Coutinho, V.; Kitajima, J. P.; Verjovski-Almeida, S. (2011) Non-coding RNAs in schistosomes: an unexplored world. *An. Acad. Bras. Cienc.* **83**:673-694.
- Osman, A.; Niles, E. G.; LoVerde, P. T. (2001) Identification and characterization of a Smad2 homologue from *Schistosoma mansoni*, a transforming growth factor-beta signal transducer. *J. Biol. Chem.* **276**:10072-10082.
- Osman, A.; Niles, E. G.; LoVerde, P. T. (2004) Expression of functional *Schistosoma mansoni* Smad4: role in Erk-mediated transforming growth factor beta (TGF-beta) down-regulation. *J. Biol. Chem.* **279**:6474-6486.
- Osman, A.; Niles, E. G.; Verjovski-Almeida, S.; LoVerde, P. T. (2006) *Schistosoma mansoni* TGF-beta receptor II: role in host ligand-induced regulation of a schistosome target gene. *PLoS. Pathog.* **2**:e54.
- Ouchi, N.; Asaumi, Y.; Ohashi, K.; Higuchi, A.; Sono-Romanelli, S.; Oshima, Y.; Walsh, K. (2010) DIP2A functions as a FSTL1 receptor. *J. Biol. Chem.* **285**:7127-7134.
- Parker-Manuel, S. J.; Ivens, A. C.; Dillon, G. P.; Wilson, R. A. (2011) Gene expression patterns in larval *Schistosoma mansoni* associated with infection of the mammalian host. *PLoS. Negl. Trop. Dis.* **5**:e1274.
- Pedrazzini, T.; Pralong, F.; Grouzmann, E. (2003) Neuropeptide Y: the universal soldier. *Cell Mol. Life Sci.* **60**:350-377.
- Pennefather, J. N.; Lecci, A.; Candenas, M. L.; Patak, E.; Pinto, F. M.; Maggi, C. A. (2004) Tachykinins and tachykinin receptors: a growing family. *Life Sci.* **74**:1445-1463.
- Pentek, J.; Parker, L.; Wu, A.; Arora, K. (2009) Follistatin preferentially antagonizes activin rather than BMP signaling in *Drosophila*. *Genesis.* **47**:261-273.
- Pfaffl, M. W. (2004) Real-time RT-PCR: Neue Ansätze zur exakten mRNA Quantifizierung. *Biospektrum*:92-95.
- Pfuhl, M.; Winder, S. J.; Pastore, A. (1994) Nebulin, a helical actin binding protein. *EMBO J.* **13**:1782-1789.
- Pica-Mattoccia, L.; Carlini, D.; Guidi, A.; Climica, V.; Vigorosi, F.; Cioli, D. (2006) The schistosome enzyme that activates osamniquin has the characteristics of a sulfotransferase. *Mem Inst Oswaldo Cruz* **101**:307-312.
- Popiel, I. and Basch, P. F. (1984a) Reproductive development of female *Schistosoma mansoni* (Digenea: Schistosomatidae) following bisexual pairing of worms and worm segments. *J. Exp. Zool.* **232**:141-150.
- Popiel, I. and Basch, P. F. (1984b) Putative polypeptide transfer from male to female *Schistosoma mansoni*. *Mol. Biochem. Parasitol.* **11**:179-188.
- Popiel, I.; Cioli, D.; Erasmus, D. A. (1984) The morphology and reproductive status of female *Schistosoma mansoni* following separation from male worms. *Int. J. Parasitol.* **14**:183-190.
- Popiel, I. (1986) The reproductive biology of schistosomes. *Parasitol. Today* **2**:10-15.
- Popiel, I. and Basch, P. F. (1986) *Schistosoma mansoni*: cholesterol uptake by paired and unpaired worms. *Exp. Parasitol.* **61**:343-347.

- Protasio, A. V.; Tsai, I. J.; Babbage, A.; Nichol, S.; Hunt, M.; Aslett, M. A.; De, S. N.; Velarde, G. S.; Anderson, T. J.; Clark, R. C.; Davidson, C.; Dillon, G. P.; Holroyd, N. E.; LoVerde, P. T.; Lloyd, C.; McQuillan, J.; Oliveira, G.; Otto, T. D.; Parker-Manuel, S. J.; Quail, M. A.; Wilson, R. A.; Zerlotini, A.; Dunne, D. W.; Berriman, M. (2012) A systematically improved high quality genome and transcriptome of the human blood fluke *Schistosoma mansoni*. *PLoS. Negl. Trop. Dis.* **6**:e1455.
- Quack, T.; Beckmann, S.; Greveling, C. G. (2006) Schistosomiasis and the molecular biology of the male-female interaction of *S. mansoni*. *Berl Munch. Tierarztl. Wochenschr.* **119**:365-372.
- Quack, T.; Knobloch, J.; Beckmann, S.; Vicogne, J.; Dissous, C.; Greveling, C. G. (2009) The formin-homology protein SmDia interacts with the Src kinase SmTK and the GTPase SmRho1 in the gonads of *Schistosoma mansoni*. *PLoS. One.* **4**:e6998.
- R Development Core Team. (2013) R: A language and environment for statistical computing. *R Foundation for Statistical Computing*, Vienna, Austria.
- Raizen, D. M.; Cullison, K. M.; Pack, A. I.; Sundaram, M. V. (2006) A novel gain-of-function mutant of the cyclic GMP-dependent protein kinase egl-4 affects multiple physiological processes in *Caenorhabditis elegans*. *Genetics* **173**:177-187.
- Ramachandran, H.; Skelly, P. J.; Shoemaker, C. B. (1996) The *Schistosoma mansoni* epidermal growth factor receptor homologue, SER, has tyrosine kinase activity and is localized in adult muscle. *Mol. Biochem. Parasitol.* **83**:1-10.
- Rasband, W. S. (2012) ImageJ In. *U.S.National Institutes of Health*, Bethesda, Maryland, USA.
- Ribeiro-Paes, J. T. and Rodrigues, V. (1997) Sex determination and female reproductive development in the genus *Schistosoma*: a review. *Rev. Inst. MEd. Trop. Sao Paulo* **39**:337-344.
- Robinson, M. D.; McCarthy, D. J.; Smyth, D. J. (2010) edgeR: a Bioconductor package for differential expression analysis of digital gene expression data. *Bioinformatics* **26**:139-140.
- Robinson, P. N.; Wollstein, A.; Bohme, U.; Beattie, B. (2004) Ontologizing gene-expression microarray data: characterizing clusters with Gene Ontology. *Bioinformatics.* **20**:979-981.
- Ross, A. G.; McManus, D. P.; Farrar, J.; Hunstman, R. J.; Gray, D. J.; Li, Y. S. (2012) Neuroschistosomiasis. *J. Neurol.* **259**:22-32.
- Ruppel, A. and Cioli, D. (1977) A comparative analysis of various developmental stages of *Schistosoma mansoni* with respect to their protein composition. *Parasitology* **75**:339-343.
- Salzet, M.; Capron, A.; Stefano, G. B. (2000) Molecular crosstalk in host-parasite relationships: schistosome- and leech-host interactions. *Parasitol Today.* **16**:536-40.
- Sambrook, J.; Fritsch, E. F.; Maniatis, T. (1989) Molecular Cloning, A Laboratory Manual. **2nd edn** Cold Spring Harbor Laboratory Press, NY
- Sanger, F.; Nicklen, S.; Coulson, A. R. (1977) DNA sequencing with chain-terminating inhibitors. *Proc. Natl. Acad. Sci. U. S. A* **74**:5463-5467.
- Sato, A.; Yamamoto, H.; Sakane, H.; Koyama, H.; Kikuchi, A. (2010) Wnt5a regulates distinct signalling pathways by binding to Frizzled2. *The EMBO Journal* **29**:41-54.

6. References

- Schallig, H. D. F. H.; Young, N. J.; Magee, R. M.; de Jong-Brink, M.; Rees, H. H. (1991) Identification of free and conjugated ecdysteroids in cercariae of the schistosome *Trichobilharzia ocellata*. *Mol. Biochem. Parasitol.* **49**:169-176.
- Schistosoma japonicum Genome Sequencing and Functional Analysis Consortium; Zhou, H.; Zheng, H.; Chen, Y.; Zhang, L.; Wang, K.; Guo, J.; Huang, Z.; Zhang, B.; Huang, W.; Jin, K.; Dou, T.; Hasegawa, M.; Wang, L.; Zhang, Y.; Zhou, J.; Tao, L.; Cao, Z.; Li, Y.; Vinar, T.; Brejova, B.; Brown, D.; Li, M.; Miller, D. J.; Blair, D.; Zhong, Y.; Chen, Z.; Liu, F.; Hu, W.; Wang, Z. Q.; Zhang, Q. H.; Song, H. D.; Chen, S.; Xu, X.; Xu, B.; Ju, C.; Huang, Y.; Brindley, P. J.; McManus, D. P.; Feng, Z.; Han, Z. G.; Lu, G.; Ren, S.; Wang, Y.; Gu, W.; Kang, H.; Chen, J.; Chen, X.; Chen, S.; Wang, L.; Yan, J.; Wang, B.; Lv, X.; Jin, L.; Wang, B.; Pu, S.; Zhang, X.; Zhang, W. H. Q.; Zhu, G.; Wang, J.; Yu, J.; Wang, J.; Yang, H.; Ning, Z.; Beriman, M.; Wei, C. L.; Ruan, Y.; Zhao, G.; Wang, S.; Liu, F.; Zhou, Y.; Wang, Z. Q.; Lu, G.; Zheng, H.; Brindley, P. J.; McManus, D. P.; Blair, D.; Zhang, Q. H.; Zhong, Y.; Wang, S.; Han, Z. G.; Chen, Z.; Wang, S.; Han, Z. G.; Chen, Z. (2009) The *Schistosoma japonicum* genome reveals features of host-parasite interplay. *Nature* **460**:345-351.
- Schlossmann, J.; Feil, R.; Hofmann, F. (2003) Signaling through NO and cGMP-dependent protein kinases. *Ann. Med.* **35**:21-27.
- Schneider, C. A.; Rasband, W. S.; Eliceiri, K. W. (2012) NIH Image to ImageJ: 25 years of image analysis. *Nature Methods*:671.
- Schramm, G.; Haas, H.; (2010) Th2 immune response against *Schistosoma mansoni* infection. *Microbes Infect.* **12**:881-8.
- Schultz, J.; Milpetz, F.; Bork, P.; Ponting, C. P. (1998) SMART, a simple modular architecture research tool: identification of signaling domains. *Proc. Natl. Acad. Sci. U. S. A* **95**:5857-5864.
- Schulze, K. M. M. (1997) Untersuchungen zur differentiellen Genexpression bei *Schistosoma mansoni*. *Heinrich-Heine-Universität Düsseldorf*.
- Schuske, K. R.; Richmond, J. E.; Matthies, D. S.; Davis, W. S.; Runz, S.; Rube, D. A.; van der Bliek, A. M.; Jorgensen, E. M. (2003) Endophilin is required for synaptic vesicle endocytosis by localizing synaptojanin. *Neuron* **40**:749-762.
- Severinghaus, A. E. (1928) Sex studies on *Schistosoma japonicum*. *Quarterly Journal of Microscopical Science* s2-71:653-702.
- Severini, C.; Improta, G.; Falconieri-Erspamer, G.; Salvadori, S.; Erspamer, V. (2002) The tachykinin peptide family. *Pharmacol. Rev.* **54**:285-322.
- Shaw, J. R. (1977) *Schistosoma mansoni*: pairing *in vitro* and development of females from single sex infections. *Exp. Parasitol.* **41**:54-65.
- Shaw, J. R.; Marshall, I.; Erasmus, D. A. (1977) *Schistosoma mansoni*: *in vitro* stimulation of vitelline cell development by extracts of male worms. *Exp. Parasitol.* **42**:14-20.
- Shaw, M. K. and Erasmus, D. A. (1982) *Schistosoma mansoni*: the presence and ultrastructure of vitelline cells in adult males. *J. Helminthol.* **56**:51-53.
- Shi, Y. and Massague, J. (2003) Mechanisms of TGF-beta signaling from cell membrane to the nucleus. *Cell* **113**:685-700.

- Shoemaker, C. B.; Ramachandran, H.; Landa, A.; dos Reis, M. G.; Stein, L. D. (1992)** Alternative splicing of the *Schistosoma mansoni* gene encoding a homologue of epidermal growth factor receptor. *Mol. Biochem. Parasitol.* **53**:17-32.
- Short, R. B. (1948)** Hermaphrodites in a Puerto Rican strain of *Schistosoma mansoni*. *J. Parasitol.* **34**:240-242.
- Silveira, A. M.; Friche, A. A.; Rumjanek, F. D. (1986)** Transfer of [¹⁴C] cholesterol and its metabolites between adult male and female worms of *Schistosoma mansoni*. *Comp Biochem. Physiol B* **85**:851-857.
- Simoës, M. C.; Lee, J.; Djikeng, A.; Cerqueira, G. C.; Zerlotini, A.; da Silva-Pereira, R. A.; Dalby, A. R.; Loverde, P.; El-Sayed, N. M.; Oliveira, G. (2011)** Identification of *Schistosoma mansoni* microRNAs. *BMC Genomics* **12**:47.
- Smithers, S. R. and Terry, R. J. (1965)** The infection of laboratory hosts with cercariae of *Schistosoma mansoni* and the recovery of the adult worms. *Parasitology* **55**:695-700.
- Stamler, R.; Keutmann, H. T.; Sidis, Y.; Kattamuri, C.; Schneyer, A.; Thompson, T. B. (2008)** The structure of FSTL3.activin A complex. Differential binding of N-terminal domains influences follistatin-type antagonist specificity. *J. Biol. Chem.* **283**:32831-32838.
- Stansberry, J.; Baude, E. J.; Taylor, M. K.; Chen, P. J.; Jin, S. W.; Ellis, R. E.; Uhler, M. D. (2001)** A cGMP-dependent protein kinase is implicated in wild-type motility in *C. elegans*. *J. Neurochem.* **76**:1177-1187.
- Su, W. Y.; Xiong, H.; Fang, J. Y. (2010)** Natural antisense transcripts regulate gene expression in an epigenetic manner. *Biochem. Biophys. Res. Commun.* **396**:177-181.
- Swierczewski, B. E. and Davies, S. J. (2009)** A schistosome cAMP-dependent protein kinase catalytic subunit is essential for parasite viability. *PLoS. Negl. Trop. Dis.* **3**:e505.
- Swierczewski, B. E. and Davies, S. J. (2010a)** Conservation of protein kinase a catalytic subunit sequences in the schistosome pathogens of humans. *Exp. Parasitol.* **125**:156-160.
- Swierczewski, B. E. and Davies, S. J. (2010b)** Developmental regulation of protein kinase A expression and activity in *Schistosoma mansoni*. *Int. J. Parasitol.* **40**:929-935.
- Takeichi, M. (1991)** Cadherin cell adhesion receptors as a morphogenetic regulator. *Science* **251**:1451-1455.
- Tanaka, M.; Murakami, K.; Ozaki, S.; Imura, Y.; Tong, X. P.; Watanabe, T.; Sawaki, T.; Kawanami, T.; Kawabata, D.; Fujii, T.; Usui, T.; Masaki, Y.; Fukushima, T.; Jin, Z. X.; Umehara, H.; Mimori, T. (2013)** DIP2 disco-interacting protein 2 homolog A (*Drosophila*) is a candidate receptor for follistatin-related protein/follistatin-like 1--analysis of their binding with TGF-beta superfamily proteins. *FEBS J.* **277**:4278-4289.
- Tatemoto, K. (2004)** Neuropeptide Y and Related Peptides. <http://www.springer.com>.
- Teves, M. E.; Guidobaldi, H. A.; Unates, D. R.; Sanchez, R.; Miska, W.; Publicover, S. J.; Morales Garcia, A. A.; Giojalas, L. C. (2009)** Molecular mechanism for human sperm chemotaxis mediated by progesterone. *PLoS. One.* **4**:e8211.
- Thomas, S. and Bonchev, D. (2010)** A survey of current software for network analysis in molecular biology. *Hum. Genomics* **4**:353-360.

6. References

- Thompson, T. B.; Lerch, T. F.; Cook, R. W.; Woodruff, T. K.; Jardetzky, T. S. (2005)** The structure of the follistatin:activin complex reveals antagonism of both type I and type II receptor binding. *Dev. Cell* **9**:535-543.
- Torpier, G.; Hirn, M.; Nirde, P.; De, R. M.; Capron, A. (1982)** Detection of ecdysteroids in the human trematode, *Schistosoma mansoni*. *Parasitology* **84**:123-130.
- Turner, A. M. and Morris, K. V. (2010)** Controlling transcription with noncoding RNAs in mammalian cells. *Biotechniques* **48**:ix-xvi.
- Tusher, V. G.; Tibshirani, R.; Chu, G. (2001)** Significance analysis of microarrays applied to the ionizing radiation response. *Proc. Natl. Acad. Sci. U. S. A* **98**:5116-5121.
- Vaandrager, A. B.; Ehlert, E. M.; Jarchau, T.; Lohmann, S. M.; de Jonge, H. R. (1996)** N-terminal myristoylation is required for membrane localization of cGMP-dependent protein kinase type II. *J. Biol. Chem.* **271**:7025-7029.
- Velculescu, V. E.; Zhang, L.; Vogelstein, B.; Kinzler, K.W. (1995)** Serial analysis of gene expression. *Science*. **270**:484-487.
- Verjovski-Almeida, S.; DeMarco, R.; Martins, E. A.; Guimaraes, P. E.; Ojopi, E. P.; Paquola, A. C.; Piazza, J. P.; Nishiyama, M. Y., Jr.; Kitajima, J. P.; Adamson, R. E.; Ashton, P. D.; Bonaldo, M. F.; Coulson, P. S.; Dillon, G. P.; Farias, L. P.; Gregorio, S. P.; Ho, P. L.; Leite, R. A.; Malaquias, L. C.; Marques, R. C.; Miyasato, P. A.; Nascimento, A. L.; Ohlweiler, F. P.; Reis, E. M.; Ribeiro, M. A.; Sa, R. G.; Stukart, G. C.; Soares, M. B.; Gargioni, C.; Kawano, T.; Rodrigues, V.; Madeira, A. M.; Wilson, R. A.; Menck, C. F.; Setubal, J. C.; Leite, L. C.; Dias-Neto, E. (2003)** Transcriptome analysis of the acoelomate human parasite *Schistosoma mansoni*. *Nat. Genet.* **35**:148-157.
- Verjovski-Almeida, S.; Leite, L. C.; Dias-Neto, E.; Menck, C. F.; Wilson, R. A. (2004)** Schistosome transcriptome: insights and perspectives for functional genomics. *Trends Parasitol.* **20**:304-308.
- Verjovski-Almeida, S.; Venancio, T. M.; Oliveira, K. C.; Almeida, G. T.; DeMarco, R. (2007)** Use of a 44k oligoarray to explore the transcriptome of *Schistosoma mansoni* adult worms. *Exp. Parasitol.* **117**:236-245.
- Vicogne, J.; Pin, J. P.; Lardans, V.; Capron, M.; Noel, C.; Dissous, C. (2003)** An unusual receptor tyrosine kinase of *Schistosoma mansoni* contains a Venus Flytrap module. *Mol. Biochem. Parasitol.* **126**:51-62.
- Vicogne, J.; Cailliau, K.; Tulasne, D.; Browaey, E.; Yan, Y. T.; Fafeur, V.; Vilain, J. P.; Legrand, D.; Trolet, J.; Dissous, C. (2004)** Conservation of epidermal growth factor receptor function in the human parasitic helminth *Schistosoma mansoni*. *J. Biol. Chem.* **279**:37407-37414.
- Vogel, H. (1947)** Hermaphrodites of *Schistosoma mansoni*. *Ann. Trop. Med. Parasitol.* **41**:266-277.
- Wahab, M. F.; Warren, K. S.; Levy, R. P. (1971)** Function of the thyroid and the host-parasite relation in murine schistosomiasis mansoni. *J. Infect. Dis.* **124**:161-171.
- Waisberg, M.; Lobo, F. P.; Cerqueira, G. C.; Passos, L. K.; Carvalho, O. S.; Franco, G. R.; El-Sayed, N. M. (2007)** Microarray analysis of gene expression induced by sexual contact in *Schistosoma mansoni*. *BMC Genomics* **8**:181.
- Waisberg, M.; Lobo, F. P.; Cerqueira, G. C.; Passos, L. K.; Carvalho, O. S.; El-Sayed, N. M.; Franco, G. R. (2008)** *Schistosoma mansoni*: Microarray analysis of gene expression induced by host sex. *Exp. Parasitol.* **120**:357-363.

- Wajant, H.; Pfizenmaier, K.; Scheurich, P. (2003)** Tumor necrosis factor signaling. *Cell Death. Differ.* **10**:45-65.
- Watabe-Uchida, M.; John, K. A.; Janas, J. A.; Newey, S. E.; Van, A. L. (2006)** The Rac activator DOCK7 regulates neuronal polarity through local phosphorylation of stathmin/Op18. *Neuron* **51**:727-739.
- Werner, A. and Sayer, J. A. (2009)** Naturally occurring antisense RNA: function and mechanisms of action. *Curr. Opin. Nephrol. Hypertens.* **18**:343-349.
- White, T. J.; Arnheim, N.; Erlich, H. A. (1989)** The polymerase chain reaction. *Trends Genet.* **5**:185-189.
- Williams, D. L.; Sayed, A. A.; Bernier, J.; Birkeland, S. R.; Cipriano, M. J.; Papa, A. R.; McArthur, A. G.; Taft, A.; Vermeire, J. J.; Yoshino, T. P. (2007)** Profiling *Schistosoma mansoni* development using serial analysis of gene expression (SAGE). *Exp. Parasitol.* **117**:246-258.
- Wilson, R. A. (2012)** The cell biology of schistosomes: a window on the evolution of the early metazoa. *Protoplasma* **249**:503-518.
- Wohlgamuth-Benedum, J. M.; Rubio, M. A.; Paris, Z.; Long, S.; Poliak, P.; Lukes, J.; Alfonzo, J. D. (2009)** Thiolation controls cytoplasmic tRNA stability and acts as a negative determinant for tRNA editing in mitochondria. *J. Biol. Chem.* **284**:23947-23953.
- Wolowczuk, I.; Roye, O.; Nutten, S.; Delacre, M.; Trottein, F.; Auriault, C. (1999)** Role of interleukin-7 in the relation between *Schistosoma mansoni* and its definitive vertebrate host. *Microbes. Infect.* **1**:545-551.
- Yamauchi, J.; Miyamoto, Y.; Chan, J. R.; Tanoue, A. (2008)** ErbB2 directly activates the exchange factor Dock7 to promote Schwann cell migration. *J. Cell Biol.* **181**:351-365.
- Yamauchi, J.; Miyamoto, Y.; Hamasaki, H.; Sanbe, A.; Kusakawa, S.; Nakamura, A.; Tsumura, H.; Maeda, M.; Nemoto, N.; Kawahara, K.; Torii, T.; Tanoue, A. (2011)** The atypical Guanine-nucleotide exchange factor, dock7, negatively regulates schwann cell differentiation and myelination. *J. Neurosci.* **31**:12579-12592.
- Yan, Y.; Tulasne, D.; Browaeys, E.; Cailliau, K.; Khayath, N.; Pierce, R. J.; Trolet, J.; Fafeur, V.; Ben, Y. A.; Dissous, C. (2007)** Molecular cloning and characterisation of SmSLK, a novel Ste20-like kinase in *Schistosoma mansoni*. *Int. J. Parasitol.* **37**:1539-1550.
- Yang, Y. T.; Wang, C. L.; Van, A. L. (2012)** DOCK7 interacts with TACC3 to regulate interkinetic nuclear migration and cortical neurogenesis. *Nat. Neurosci.* **15**:1201-1210.
- Yapici, N.; Kim, Y. J.; Ribeiro, C.; Dickson, B. J. (2008)** A receptor that mediates the post-mating switch in *Drosophila* reproductive behaviour. *Nature* **451**:33-37.
- Ye, L. and Maloney, P. C. (2002)** Structure/function relationships in OxIT, the oxalate/formate antiporter of *Oxalobacter formigenes*: assignment of transmembrane helix 2 to the translocation pathway. *J. Biol. Chem.* **277**:20372-20378.
- Yeast Protocols Handbook. (2001)** Clontech Laboratories, Inc.
- You, H.; Zhang, W.; Jones, M. K.; Gobert, G. N.; Mulvenna, J.; Rees, G.; Spanevello, M.; Blair, D.; Duke, M.; Brehm, K.; McManus, D. P. (2010)** Cloning and characterisation of *Schistosoma japonicum* insulin receptors. *PLoS. One.* **5**:e9868.

6. References

- You, H.; McManus, D. P.; Hu, W.; Smout, M. J.; Brindley, P. J.; Gobert, G. N. (2013)** Transcriptional responses of *in vivo* praziquantel exposure in schistosomes identifies a functional role for calcium signalling pathway member CamKII. *PLoS Pathog.* **9**:e1003254.
- Young, N. D.; Jex, A. R.; Li, B.; Liu, S.; Yang, L.; Xiong, Z.; Li, Y.; Cantacessi, C.; Hall, R. S.; Xu, X.; Chen, F.; Wu, X.; Zerlotini, A.; Oliveira, G.; Hofmann, A.; Zhang, G.; Fang, X.; Kang, Y.; Campbell, B. E.; Loukas, A.; Ranganathan, S.; Rollinson, D.; Rinaldi, G.; Brindley, P. J.; Yang, H.; Wang, J.; Wang, J.; Gasser, R. B. (2012)** Whole-genome sequence of *Schistosoma haematobium*. *Nat. Genet.* **44**:221-225.
- Yuasa, K.; Omori, K.; Yanaka, N. (2000)** Binding and phosphorylation of a novel male germ cell-specific cGMP-dependent protein kinase-anchoring protein by cGMP-dependent protein kinase I alpha. *J. Biol. Chem.* **275**:4897-4905.
- Zamanian, M.; Kimber, M. J.; McVeigh, P.; Carlson, S. A.; Maule, A. G.; Day, T. A. (2011)** The repertoire of G protein-coupled receptors in the human parasite *Schistosoma mansoni* and the model organism *Schmidtea mediterranea*. *BMC. Genomics* **12**:596.
- Zerlotini, A.; Heiges, M.; Wang, H.; Moraes, R. L.; Dornitini, A. J.; Ruiz, J. C.; Kissinger, J. C.; Oliveira, G. (2009)** SchistoDB: a *Schistosoma mansoni* genome resource. *Nucleic Acids Res.* **37**:D579-D582.
- Zhang, Y. W. and Rudnick, G. (2011)** Myristoylation of cGMP-dependent protein kinase dictates isoform specificity for serotonin transporter regulation. *J. Biol. Chem.* **286**:2461-2468.
- Zhou, J.; Liao, M.; Hatta, T.; Tanaka, M.; Xuan, X.; Fujisaki, K. (2006)** Identification of a follistatin-related protein from the tick *Haemaphysalis longicornis* and its effect on tick oviposition. *Gene* **372**:191-198.

Abbreviations

A&C	Audic and Claverie
AD	activation domain
AMP	adenosine monophosphate dependent
ADE	adenin
BD	DNA binding domain
BMP	bone morphogenic protein
bp	base pairs
BrdU	Bromo-deoxy-Uridine
β-gal	β-galactosidase
CaMKII	calcium/calmodulin dependent kinase II
CDS	coding sequence
CEBPA	CCAAT/enhancer binding protein (C/EBP), alpha
cGMP	cyclic guanosine monophosphate
cGK	cGMP-dependent protein kinase
CLSM	confocal laser scanning microscopy
CREB	cAMP response element-binding protein
ct	cycle
DAPI	4',6-Diamidin-2-phenylindol
DD	death domain
DDC	dopadecarboxylase
DEPC	diethylpyrocarbonate
Dip2a	disco-interacting protein 2
DLG	discs-large homolog
DMSO	dimethyl sulfoxide
DNA	deoxyribonucleic acid
dNTPs	deoxyribonucleotide triphosphates
EDTA	ethylene diamine tetra acetic acid
e.g.	for example
EGF	epidermal growth factor
EF	pairing-experienced females
EM	pairing-experienced males
ESRRA	estrogen-related receptor alpha
etk	endothelial/epithelial tyrosine kinase

Abbreviations & Units

ets	E26 transform-ation-specific (transcription factor)
FAK	focal adhesion kinase
fstl	follistatin-like
FstD	follistatin domain
GCN	'general control non-repressed'
GCP	gynaecophoral canal protein
GDF	growth and differentiation factor
GO	gene ontology
GOI	gene of interest
GPCRs	G protein-coupled receptors
GTP	Guanosine-5'-triphosphat
GVBD	germinal vesicle break down
HATs	histone acetyltransferases
HIS	histidin
HMG-coA	3-hydroxy-3-methylglutaryl CoA
IPA	Ingenuity Pathway Analysis
IPTG	isopropyl- β -D-thiogalactopyranosid
JNK	c-Jun N-terminal kinase
kb	kilo bases
LacZ	β -gal encoding gene
lin-9	abnormal cell LINEage
MA	mitotic activity
MAPK	mitogen-activate protein kinase
MEG	micro exon gene
MM	master mix
MOPS	3-(N-morpholino) propanesulfonic acid
NATs	natural anti-sense RNAs
ncRNAs	non-coding RNAs
NF- κ B	nuclear factor 'kappa-light-chain-enhancer' of activated B-cells
nt	nucleotides
ONPG	o-Nitrophenyl- β -D-galactopyranosid
OxIT	oxalate-formate antiporter
PCR	polymerase chain reaction
PBS	phosphate buffered saline

PDI	protein disulfide isomerase
p.i.	post infection
PK	protein kinase
PKA	cyclic-AMP protein kinase
PKC	protein kinase C
PLK	polo-like kinase
PPARGC1A	peroxisome proliferator-activator receptor gamma, coactivator 1 alpha
PZQ	praziquantel
RNA	ribonucleic acid
RNAi	RNA interference
RT	reverse transcription
RTC	room temperature (in °C)
SAGE	serial analysis of gene expression
SAM	significance analysis for microarray
SDS	sodium dodecyl sulfate
sig. diff.	significantly differentially
Sm β -Int	<i>Schistosoma mansoni</i> β integrin
SmBMP	<i>Schistosoma mansoni</i> BMP
SmCBP	<i>Schistosoma mansoni</i> CREB-binding protein
SmcGK	<i>Schistosoma mansoni</i> cGK
SmFTZ	<i>S. mansoni</i> fushi tarazu factor
SmGCN5	<i>Schistosoma mansoni</i> 'general control nonrepressed'
SmInAct	<i>Schistosoma mansoni</i> ihibin/activin
SmPLK	<i>Schistosoma mansoni</i> polo like kinase
SmRKI	<i>Schistosoma mansoni</i> receptor kinase I
SmRTK1	<i>Schistosoma mansoni</i> receptor tyrosine kinase 1
SmTGF β	<i>Schistosoma mansoni</i> transforming growth factor β
SmTGF β RI	<i>Schistosoma mansoni</i> transforming growth factor β receptor I
SmTGF β RII	<i>Schistosoma mansoni</i> transforming growth factor β receptor II
SmTNFR	<i>Schistosoma mansoni</i> tumor necrosis factor α receptor
SSC	saline-sodium citrate
SuperSAGE	advancement of SAGE
TGF β	transforming growth factor β
TGF β R	transforming growth factor receptor

Abbreviations & Units

TNF α	tumor necrosis factor α
TNFR	tumor necrosis factor α receptor
TK	tyrosine kinase
TRAF	TNF α receptor-associated factor
SmSLK	<i>Schistosoma mansoni</i> Ste20-like kinase
SmTK3	<i>Schistosoma mansoni</i> tyrosine kinase 3 (Src kinase)
SmTK4	<i>Schistosoma mansoni</i> tyrosine kinase 4 (Syk kinase)
SmTK5	<i>Schistosoma mansoni</i> tyrosine kinase 5 (Fyn-like kinase)
SmTK6	<i>Schistosoma mansoni</i> tyrosine kinase 6 (Src/Abl hybrid kinase)
UF	pairing-unexperienced females
UM	pairing-unexperienced males
UTP	uracil triphosphate
VKR	venus kinase receptor
Wnt5a	wingless-related MMTV integration site
X-Gal	5-Brom-4-Chlor-3-indoyl- β -D-galactosid
Y2H	yeast two-hybrid

Units

°C	degree in Celsius
d	days
g	gram
h	hours
k	kilo
kb	kilo bases
kDa	kilo dalton
l	liter
M	Molar
min	minutes
mg	milli gram
ml	milli liter
mM	milli Molar
μg	micro gram
μl	micro liter
ng	nano gram
nm	nano meter
OD	optical density
rpm	rotations per minute
s	seconds
(v/v)	volume per volume
vol	volume
μg	micro gram
μl	micro liter
μmol	micro mol
μM	micro Molar

Figures

Figure 1.1.	<i>S. mansoni</i> life cycle _____	2
Figure 2.1.	Transcript blot setup _____	48
Figure 2.2.	Flowchart of microarray and SuperSAGE experimental procedures and analyses _	53
Figure 2.3.	Flowchart of the SuperSAGE experimental procedure _____	56
Figure 3.1.	Amplification products from RT-PCR reactions for different <i>Schistosoma</i> cGKs ____	64
Figure 3.2.	Effects of the treatment of <i>S. mansoni</i> couples with a cGK inhibitor _____	65
Figure 3.3.	<i>In situ</i> hybridization with SmcGKI-specific anti-sense probes _____	66
Figure 3.4.	Strand-specific RT-PCRs for SmcGKI _____	66
Figure 3.5.	Real-time PCR for SmcGK1 _____	67
Figure 3.6.	Hierarchical clustering of transcripts significant after SAM _____	70
Figure 3.7.	Gene Ontology - enriched categories for transcripts significantly regulated between EM and UM according to the microarray-analysis _____	72
Figure 3.8.	Hierarchical clustering of transcripts significantly regulated in SuperSAGE data according the statistics of Audic and Claverie _____	76
Figure 3.9.	Gene Ontology - enriched categories for transcripts significantly regulated between EM and UM according to SuperSAGE _____	77
Figure 3.10.	Venn diagram of SuperSAGE and microarray data _____	80
Figure 3.11.	Hierarchical clustering of transcripts significantly regulated in SuperSAGE and/or microarray analyses _____	80
Figure 3.12.	Gene Ontology - enriched categories for transcripts significantly regulated between EM and UM in both analyses _____	86
Figure 3.13.	Results of real-time PCR –verification experiments for microarray and SuperSAGE data _____	92
Figure 3.14.	GO for transcripts significantly and differentially regulated according to the microarray analyses _____	97
Figure 3.15.	Venn diagram of SuperSAGE and microarray data with refined data selection ____	100
Figure 3.16.	IPA-network for genes significantly differentially transcribed in SuperSAGE and microarray _____	101
Figure 3.17.	Phylogenetic analysis of SmFst in comparison to other follistatins from different organisms _____	104
Figure 3.18.	SmFst <i>in situ</i> hybridization _____	104
Figure 3.19.	Stage-specific RT-PCR for SmFst _____	105
Figure 3.20.	Yeast two-hybrid experiments with SmFst _____	106
Figure 3.21.	SmInAct <i>in situ</i> hybridization _____	107
Figure 3.21.	SmBMP <i>in situ</i> hybridization _____	107
Figure 4.1.	The role of SmFst in <i>S. mansoni</i> _____	135
		169

Figure 4.2.	Signaling molecules in <i>S. mansoni</i> testes _____	137
Figure I.	Male dependent mitotic activity in females _____	I
Figure II.	Mitotic activity in females as a result of re-pairing with EM or UM; initial experiments _____	I
Figure III.	Pairing-dependent mitotic activity in males; initial experiments _____	II
Figure IV.	Pairing-dependent mitotic activity in males, technical replica of initial experiments _____	II
Figure V.	Mitotic activity in females as a result of re-pairing with EM or UM _____	III
Figure VI.	Pairing-dependent male mitotic activity _____	IV
Figure VII.	Mitotic activity of male worms treated with TNF α _____	V
Figure VIII.	Mitotic activity of female worms treated with TNF α _____	V
Figure IX.	Sequence alignment of SmcGK1 and its SchistoDB (2.0) prediction Smp_123290 ____	VI
Figure X.	Phylogenetic analyses of SmcGK1 in comparison to other cGKs from different organisms _____	VII
Figure XI.	Initial semi-quantitative RT-PCR results for SmcGK1 transcription in EM and UM ____	VII
Figure XII.	Results from additional cGK inhibitor treatments _____	VIII
Figure XIII.	hierarchical clustering of SuperSAGE EdgeR significantly regulated genes _____	XII
Figure XIV.	Gene Ontology - enriched categories for genes significantly regulated between EM and UM according to SuperSAGE, microarray or both analyses _____	XV
Figure XV.	Hierarchical clustering of 180 significant in both analyses _____	XVIII
Figure XVI.	Hierarchical clustering of microarray transcripts significantly and differentially regulated _____	XX
Figure XVII.	Hierarchical clustering of SuperSAGE detected transcripts abundantly significantly differentially regulated _____	XXV
Figure XVIII.	Hierarchical clustering of the SuperSAGE microarray overlap after refined analysis _____	XXVI
Figure XIX.	SmFst CDS _____	XXVI
Figure XX.	SmInAct CDS _____	XXVI
Figure XXI.	SmBMP CDS _____	XXVII
Figure XXII.	Schematic representation of SmBMP Y2H-constructs _____	XXVII
Figure XXIII.	Oxalate-formate antiporter <i>in situ</i> hybridization _____	XXVIII

Tables

Table 3.1.	Selection of transcripts detected by SuperSAGE only _____	83
Table 3.2.	Selection of transcripts detected only by microarray-experiments _____	85
Table 3.3.	Genes selected for real-time PCR verification _____	90
Table 3.4.	Genes significantly differentially transcribed according to microarray and SuperSAGE _____	102
Table 4.1.	Genes of interest for further studies _____	133
Table I.I.	Regulation of <i>Schistosoma</i> cGKs in according to microarray and SuperSAGE transcriptome analyses _____	VIII
Table II.	GO – microarray _____	IX
Table III.	SchistosCyc – microarray _____	X
Table IV.	SuperSAGE EdgeR significantly regulated genes _____	XII
Table V.	GO - SuperSAGE A&C _____	XIII
Table VI.	SchistosCyc - SuperSAGE A&C _____	XIV
Table VII.	180 genes significantly transcribed according to both analyses _____	XVI
Table VIII.	GO - 180 significant in both analyses _____	XVIII
Table IX.	SchistoCyc - 180 significant in both analyses _____	XIX
Table X.	Real-time PCR MasterMix tests _____	XIX
Table XI.	Genes significantly and differentially regulated in the microarray analyses _____	XX
Table XII.	GO for genes significantly and differentially regulated in the microarray analyses _____	XXV
Table XIII.	Comparison to previous results on the regulation of GPCRs between EM and UM _____	XXVII

Supplementary files

For readers of the online publication:

Supplementary files can be accessed on the CDs within the copies of this thesis available at the library of the Justus-Liebig-University Gießen.

Supplementary-file1: Microarray intensities.

Text-file containing information on average intensities of all oligonucleotides for each microarray experiment and dye, as extracted from the Agilent software. (The file was needed in this form for calculation of supplementary-file2 with “R”.)

Supplementary-file2: Microarray log₂ratios.

Text-file containing log₂ratios for each oligonucleotide in each microarray experiment, calculated from supplementary-file1, with the software “R”, using EM-values as controls ($\log_2 \frac{\text{intensity} - UM}{\text{intensity} - EM}$)

Supplementary-file3: Microarray detection.

Text-file containing information on signal detection (0 = no detection; 1 = detection) for each oligonucleotide for each microarray experiment and dye, as extracted from the Agilent software. (The file was needed in this form for combination with supplementary-file1 and -2, and subsequent data-filtering.)

Supplementary-file4: Microarray – general information.

The table presents general information on the microarray used, including annotations, and is an exact copy from the original file publicized (Oliveira *et al.*, 2011).

Supplementary-file5: Microarray results.

The file presents the data for the microarray experiments including information on the oligonucleotide, significance, log₂ratios, annotations and applicability in further analysis procedures, such as GO and IPA.

Supplementary-file6: Effects of cGK1-inhibitor treatment.

A cGK1-inhibitor affected motility of schistosomes. The file provides video-information on controls and treated forms after two and four days (Leutner *et al.*, 2011).

Supplementary-file7: SuperSAGE data with EdgeR statistics.

The file presents the data for the SuperSAGE experiments, after application of EdgeR statistics. (Information on the different sheets is given in the sheet “description”)

Supplementary-file8: SuperSAGE data with A&C statistics.

The file presents the data for the SuperSAGE experiments after application of A&C statistics. (Information on the different sheets is given in the sheet “description”)

Supplementary-file9: SuperSAGE IPA transcription factors.

The table lists transcription factors regulated according to IPA, as indicated through transcripts regulated in SuperSAGE. Three transcription factors predicted to be activated are highlighted in bold letters and detailed further in subsequent sheets of the file.

Supplementary-file10: Microarray & SuperSAGE intersection (EdgeR).

Transcripts detected by microarrays and SuperSAGE. Information on log₂ratios, significances, and gene annotations is given. The table only shows SuperSage data for EdgeR statistical analysis.

Supplementary-file11: Microarray & SuperSAGE intersection (A&C).

Transcripts detected by microarray and SuperSAGE. Information on log₂ratios, significances, and gene annotations is given. The file only shows SuperSAGE data for A&C statistical analysis. (Information on the different sheets is given in the sheet “description”)

Supplementary-file12: Transcripts detected only by SuperSAGE.

The file gives information on the transcripts detected by SuperSAGE alone and not by the microarrays. (Information on the different sheets is given in the sheet “description”)

Supplementary-file13: Transcripts detected only by microarrays.

The file gives information on the transcripts detected by the microarrays alone and not by SuperSAGE. (Information on the different sheets is given in the sheet “description”)

Supplementary-file14: BeestKeeper reference gene analysis

A number of potential reference genes was tested for EM and UM and evaluated with the Excel-implementation BestKeeper (Pfaffl, 2004). The table presents the results.

Supplementary-file15: Genes tested in real-time PCR.

The file provides information on genes tested in real-time PCR experiments.

Supplementary-file16: TGFβ-pathway associated transcripts.

The file lists genes associated with the TGFβ-pathway and their regulation and significance in microarray and SuperSAGE data.

Supplementary-file17: Comparison to Fitzpatrick et al. (2006).

The file contains two tables. The first presents data from Fitzpatrick *et al.* (2006) and compares them to data obtained by microarray or SuperSAGE (described here with the term male data) The second table shows these data for a selection of transcripts significantly regulated between EM and UM.

Supplementary-file18: Comparison to Waisberg et al. (2008).

The file contains two tables. The first represents table 2 from Waisberg *et al.* (2008) supplemented with Smp_numbers detected by blasting the sequences of given accession numbers at Schisto DB 2.0. The second table shows the comparison to data obtained by microarray and SuperSAGE (described here with the term male data), with significances and log₂ratios.

Supplementary-file19: Comparison to Nawaratna et al. (2011)

The table gives transcripts significantly up-regulated in testes compared to whole worms as detected in the study of Nawaratna *et al.* (2011), and the according information on differences in transcription detection between EM and UM according to SuperSAGE or microarray analysis (described here with the term male data). A second sheet provides this data for a selection of transcripts significantly regulated between EM and UM.

Supplementary-file20: Signaling associated transcripts.

The file lists genes associated to signaling, which were previously localized in testes (see chapter 1.4.). Their regulation and significance in microarray and SuperSAGE data is given.

Publications and scholarships

Scientific publications

S. Leutner, K.C. Oliveira, B. Rotter, S. Beckmann, C. Buro, S. Hahnel, JP. Kitajima, S. Verjovski-Almeida, P. Winter, CG. Grevelding. Combinatory microarray and SuperSAGE analyses identify pairing-dependently transcribed genes in *Schistosoma mansoni* males, including follistatin. Plos NTD. (accepted October 2013)

C. Buro, K.C. Oliveira, S. Beckmann, S. Leutner, Z. Lu, C. Dissous, K. Cailliau, S. Verjovski-Almeida, C.G. Grevelding. Transcriptome analyses of inhibitor-treated schistosome females provide evidence for cooperating Src-kinase and TGF β receptor pathways controlling mitosis and eggshell formation. PLoS Pathog. (2013) 9:e1003448

S. Leutner, S. Beckmann, C.G. Grevelding. Characterization of the cGMP-dependent protein kinase SmcGK1 of *Schistosoma mansoni*. (2011) Anais da Academia Brasileira de Ciências 83(2). 1-12

S. Beckmann, S. Leutner, N. Gouignard, C. Dissous, C.G. Grevelding. (2012) Protein Kinases as Potential Targets for Novel Anti-Schistosomal Strategies. Curr Pharm Des.;18(24).3579-94. Review.

Conference contributions

Talks

S. Leutner, T. Quack, C.G.Grevelding. Expression of a cGMP-dependent protein kinase in *Schistosoma mansoni*. DGP 3rd Short Course for Young Parasitologists, 01 - 04.03.2008.

S. Leutner, K.C. Oliveira, S. Verjovski-Almeida, C.G. Grevelding. Microarray analyses of pairing-dependent, differential transcription in *Schistosoma mansoni* males. 2nd GGL Conference on Life Sciences, 30.09 - 01.10.2009.

S. Leutner, K.C. Oliveira, S. Verjovski-Almeida, B. Rotter, P. Winter, C.G. Grevelding. Microarray analyses and Super-SAGE of *Schistosoma mansoni* male transcriptomes. 1st Workshop of the „Forum Bioinformatik“, 11.-12.02.2010.

S. Leutner, K.C. Oliveira, S. Verjovski-Almeida, B. Rotter, P. Winter, C.G. Grevelding. Combining microarray-analysis and Super-SAGE to detect pairing-dependent transcription in *Schistosoma mansoni* males. 24. Jahrestagung der Deutschen Gesellschaft für Parasitologie, 16. - 20.03.2010.

S. Leutner, K.C. Oliveira, S. Verjovski-Almeida, B. Rotter, P. Winter, C.G. Grevelding. Analyses of *Schistosoma mansoni* male transcriptomes. Semiar. Current topics in infection biology SS2010, 07.05.2010.

Posters

S. Leutner, T. Quack, C.G. Grevelding. Expression of a cGMP-dependent protein kinase in *Schistosoma mansoni*. 23. Jahrestagung der Deutschen Gesellschaft für Parasitologie, 05. - 07.03.2008.

S. Leutner, T. Quack, C.G. Grevelding. Analysis of mitotic activity in paired *Schistosoma mansoni* males and characterization of a cGMP-dependent protein kinase". 1st GGL Conference on Life Sciences, 30.09 - 01.10.2008.

S. Leutner, K.C. Oliveira, S. Verjovski-Almeida, B. Rotter, P. Winter, C.G. Grevelding. A combined study applying microarray and Super-SAGE detects pairing-dependent transcription in *Schistosoma mansoni* males. Molecular and Cellular Biology of Helminths VI, 05.-10.09.2010.

S. Hahnel, T. Quack, S. Leutner, C. Buro, C. G. Grevelding. In silico identification and further investigation of G protein-coupled receptors from adult *Schistosoma mansoni*. BSP (British Society for Parasitology) Spring meeting 2011, 12.-14.04.2011.

K. C. Oliveira, M. L. P. Carvalho, S. Leutner, S. Beckmann, C. Buro, E. Szyleyco, C. G. Grevelding, J. McKerrow, S. Verjovski-Almeida. Molecular characterization of TNF-alpha Receptor and TNF Receptor Associated Factors in *Schistosoma mansoni*. ASTMH (The American Society of Tropical Medicine and hygiene) 60th Annual Meeting, 4.-8.12.2011.

Scholarships

Traveling scholarship of the Boehringer Ingelheim Fonds.

Associate of the post-graduate program „Molekulare Veterinärmedizin“ with a grant for laboratory material and traveling expenses.

Support through the ‘Studienstiftung des deutschen Volkes‘ with a personal scholarship.

Participant in the ‘Gießener Graduiertenzentrum für Lebenswissenschaften‘ (GGL).

Grant of the GlaxoSmithKline Stiftung for the participation in the conference „Molecular and Cellular Biology of Helminths VI“.

Acknowledgements

To Prof. Albrecht Bindereif I am very grateful for accepting this thesis, and his monitoring of its progress.

I thank my supervisor Prof. Christoph Grevelding for the possibility to work on this project, with deep appreciation for his endurance during our discussions, lots of advice on English grammar, and his belief in my work.

This thesis would not have been possible without the help of my collaboration partners. To Sergio Verjovsky-Almeida and particularly Katia Oliveira I would like to express my gratitude for introducing me to the methodology of microarrays as well as their advice and our discussions. I also thank Björn Rotter and Peter Winter for performing the SuperSAGE experiments and Joao Kitajima for his grand help in annotating the microarray and SuperSAGE data.

Dr. Gerrit Eichner I thank for many inspiring conversations on statistics and his lectures on statistics with R.

I especially thank Christine Henrich – the world-best technical assistant - for her relentless work on diverse PCR reactions and her help with other experiments.

Christina Scheld, Brigitte Hoffmann and Bianca Kulik I thank for their persistent work on sustaining the schistosome life cycle, which provided me with the worm samples needed for this dissertation.

I wish to express my deepest thanks to my colleagues Dr. Christin Buro, Steffen Hahnel, Gabriele Lang, Dr. Svenja Beckmann, and Dr. Thomas Quack for their constructive advice, experimental help, encouragement and kind words in scientific as well as personal crisis. I especially thank Dr. Svenja Beckmann for her help with yeast experiments, and Gabriele Lang for her technical assistance in *in situ* hybridizations.

To my friends I am intensely grateful for their support and strength throughout the last years. Especially Dr. Denis Wolf, Martin Leustik Ph.D., Dr. Christiane Riedel, and Dr. Claudia Schulz have been a great source of comfort and advice.

Thanks again to all of you mentioned above, who participated in proof reading the manuscript of this thesis!

Finally I would like to express my gratitude to my parents who gave me the possibility to study biology. I am particularly thankful to my father for giving me the initial opportunity to perform my thesis as well as for his support and belief in me.

Appendix

I. Mitotic activity in male worms

Subsequently presented figures supplement data described in chapter 3.1. 'Analyses on mitotic activity in male worms'.

I.I. Pairing experiments

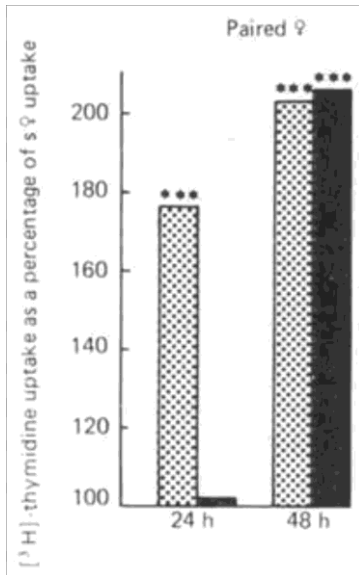


Figure I: Male dependent mitotic activity in females.

Results from DenHollander and Erasmus (1985), showed mitotic activity in females to depend on pairing to either EM or UM: Females from unisexual infections were paired to UM or EM for 24 or 48 hours. Subsequently couples were incubated for one hour in medium containing [³H-methyl]thymidine. The thymidine uptake was measured as indicator for mitotic activity. Dotted bars: females paired to EM; black bars: females paired to UM.

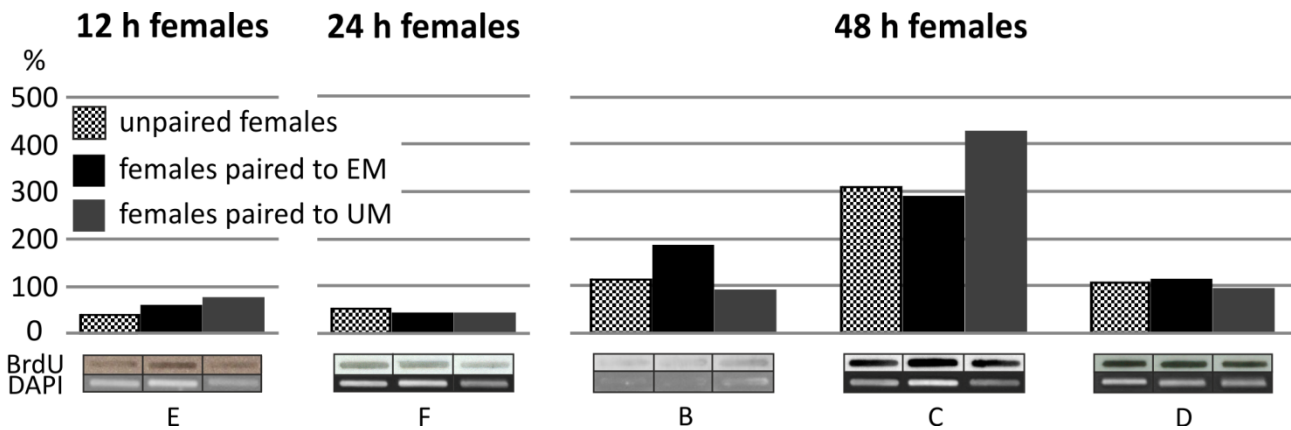


Figure II: Mitotic activity in females as a result of re-pairing with EM or UM; initial experiments.

First experiments analyzing the mitotic activity in un-paired females and females re-paired with either EM or UM were inhomogeneous and thus did not confirm the results of DenHollander and Erasmus (1985), shown in Figure I. Mitotic activity is given in percent of positive control. Below each bar for mitotic activity the according BrdU and DAPI-signals used for the respective calculation are given. B-F represent different experimental series, during which separated females, which were kept in culture for at least one week, were re-paired with EM or UM and incubated in the presence of 1 mM BrdU for 12 h or 24 h or 48 h.

Appendix

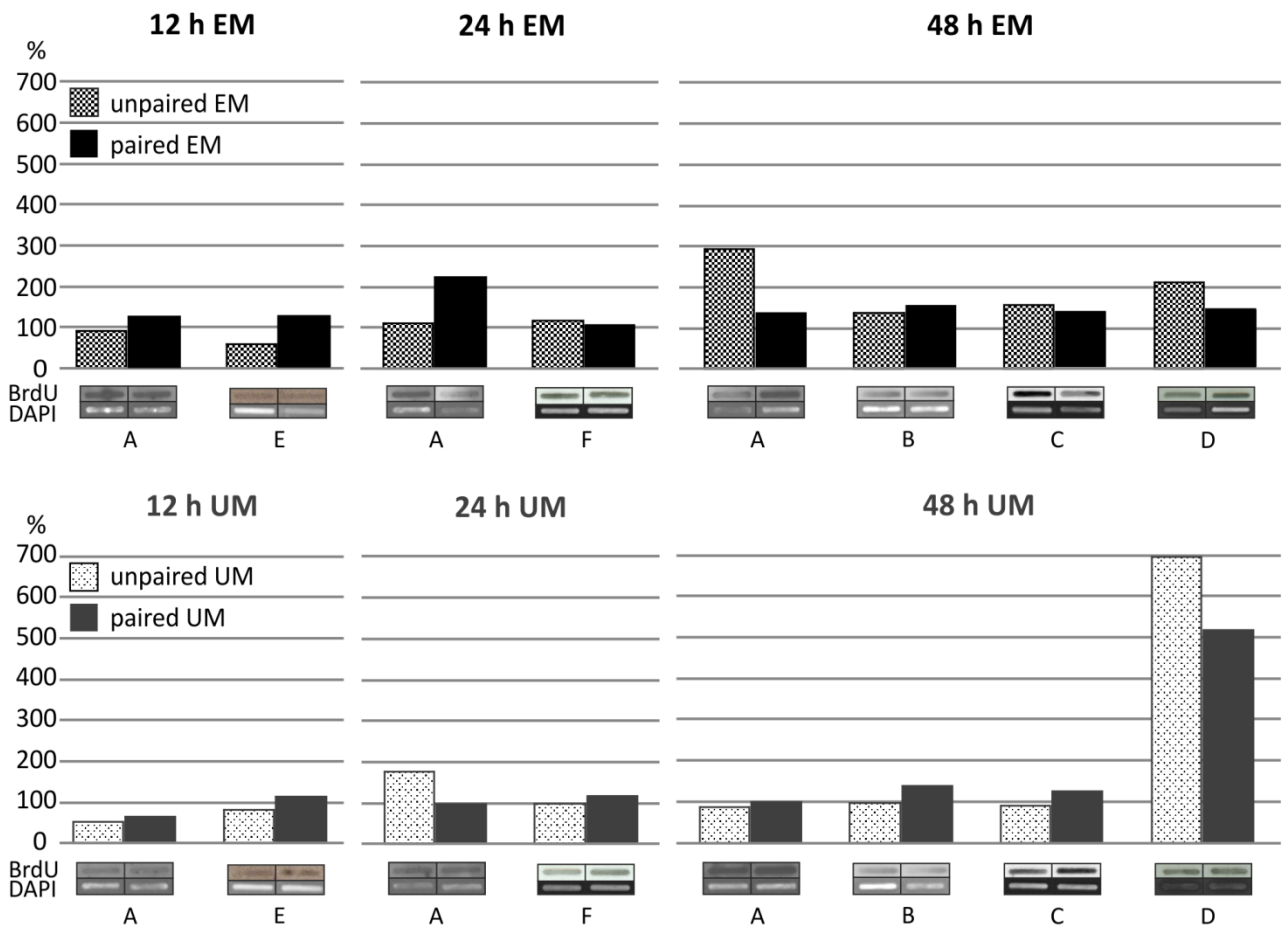


Figure III: Pairing-dependent mitotic activity in males; initial experiments.

First experiments analyzing mitotic activity in EM or UM as a result of pairing indicated enhanced mitotic activity in paired males in several experimental setups and especially for previously pairing-unexperienced males. Mitotic activity is given as percent of positive control. Below each bar for mitotic activity the according BrDU and DAPI-signals used for the respective calculation are given. A-F represent different experimental series, during which males were paired to females (separated and kept un-paired for one week) and incubated in the presence of 1 mM BrDU for 12 h , 24 h or 48 h .

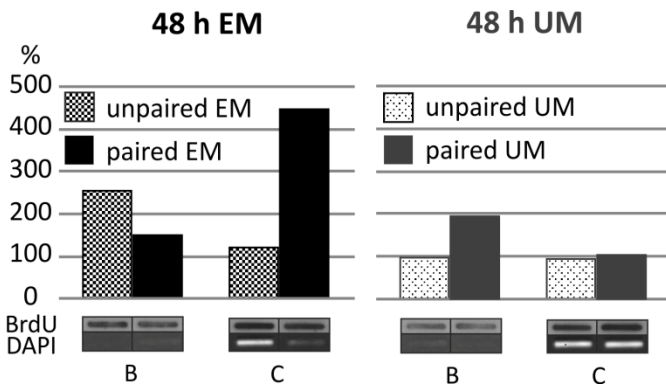


Figure IV: Pairing-dependent mitotic activity in males, technical replica of initial experiments.

For two of the experiments from Figure III (B and C) enough DNA was extracted from males, to allow a repetition of the mitotic activity estimation (given in percent of positive control). Especially for EM strong technical variation can be observed, when comparing this result to figure Figure III.

Below each bar for mitotic activity the according BrDU and DAPI-signals used for the respective calculation are given.

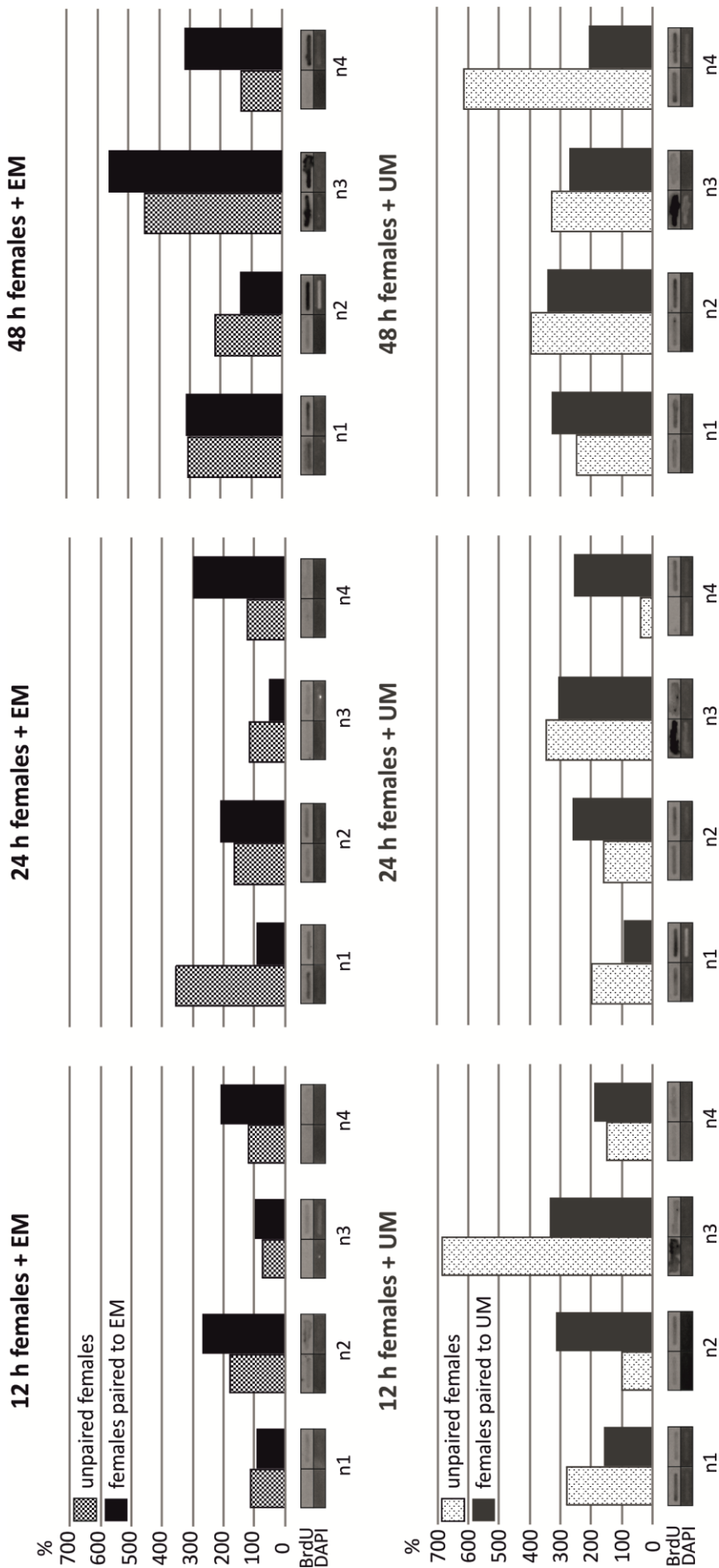


Figure V: Mitotic activity in females as a result of re-pairing with EM or UM.

A collection of four independent experiments (n1-n4, experimental setup as in Figure II did not confirm the results of DenHollander and Erasmus (1985) (Figure I), due to strong variations of paired female mitotic activity in comparison to respective controls within each pairing-time. Mitotic activity is given in percent of positive control. Below each bar the according BrdU and DAPI-signals used for calculation of mitotic activity are given.



Figure VI: Pairing-dependent male mitotic activity.

Four independent experiments (n1-n4, experimental setup as described in Figure III.), giving results for all tested time frames, could not confirm the indication that pairing leads to enhanced mitotic activity in males; results are strongly variable. Mitotic activity is given in percent of positive control. Below each bar the according BrdU and DAPI-signals used for calculation of mitotic activity are given.

I.II. TNF α treatment

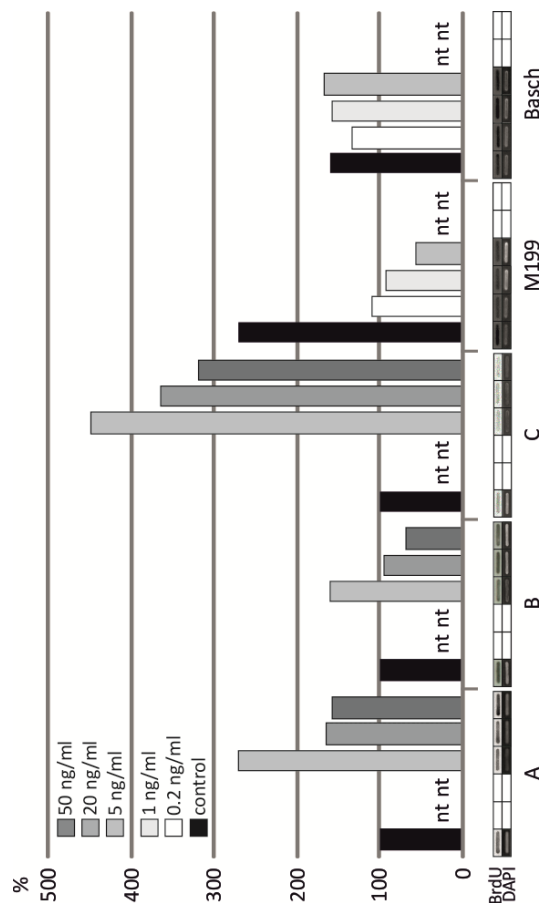


Figure VII: Mitotic activity of male worms treated with TNF α .

To analyze the effect of TNF α on mitotic activity, couples were treated for three days with different concentrations. Of the cytokine All experiments indicated a dose-dependent effect of TNF α on male mitotic activity. However, strength and direction of this effect varied widely. While the early experiments A-C (done with M199 only), showed a stimulatory effect for two out of three experiments (always at a concentration of 5 ng/ml), the later experiments with M199 or Basch medium, where the influence of the respective culture medium was tested in addition to further concentrations of TNF α , showed a reduction of mitotic activity. Depending on the medium, higher concentrations (M199) or lower concentration (Basch) led to a stronger reduction of mitotic activity. Mitotic activity is given in percent of control. BrdU and DAPI-signals for each sample are shown below the bars.

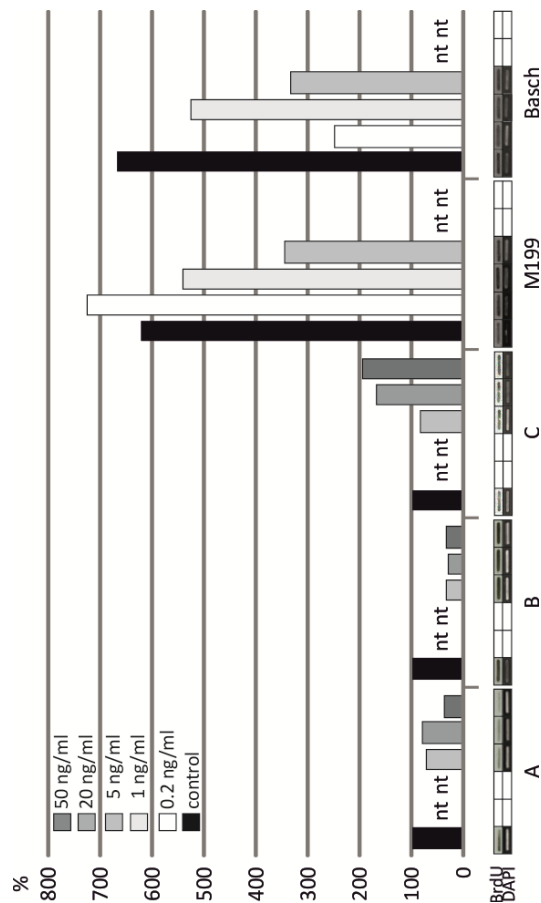


Figure VIII: Mitotic activity of female worms treated with TNF α .

Couples were treated for three days with different concentrations of TNF α to analyze its effect on mitotic activity. Results for females were not homogenous and indicated strong biological variance as well as an equally strong influence of the medium components. A-C; early experiments done with M199 only. M199, Basch: experiments, where the influence of the respective culture medium was tested in addition to further concentrations of TNF α . Mitotic activity is given in percent of control (A-C) or in percent of positive control (M199, Basch). BrdU and DAPI-signals for each sample are shown below the bars.

II. The cGMP-dependent protein kinase SmcGKI

Subsequent presented figures and tables supplement data described in chapter 3.2. ‘The cGMP-dependent protein kinase SmcGKI may have a function in schistosome gonads’.

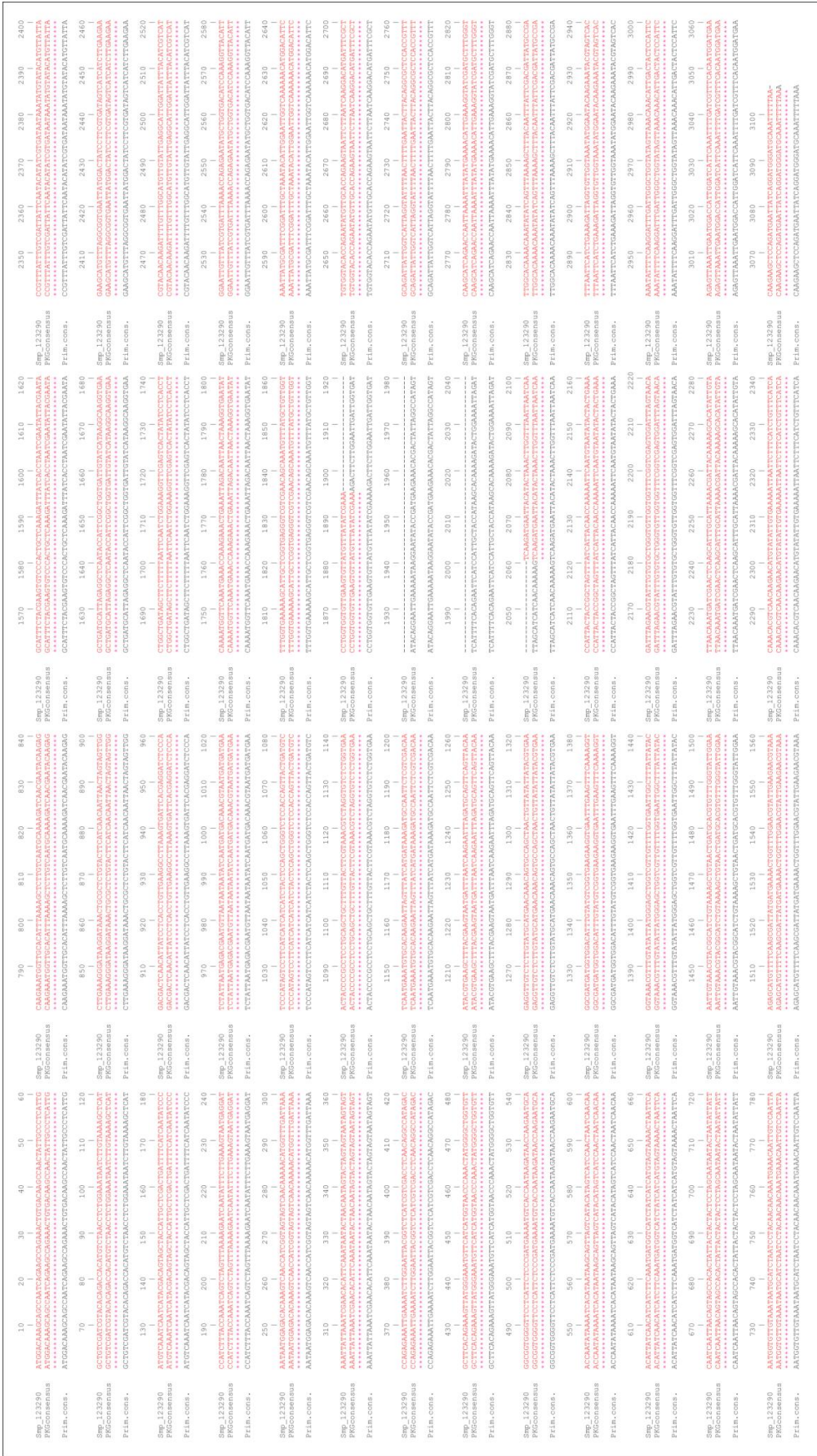


Figure IX: Sequence alignment of SmcGKI and its Schistodb (2.0) prediction Smp_123290. Sequences are identical apart from an insertion of 165 nucleotides at position 1896-2060.

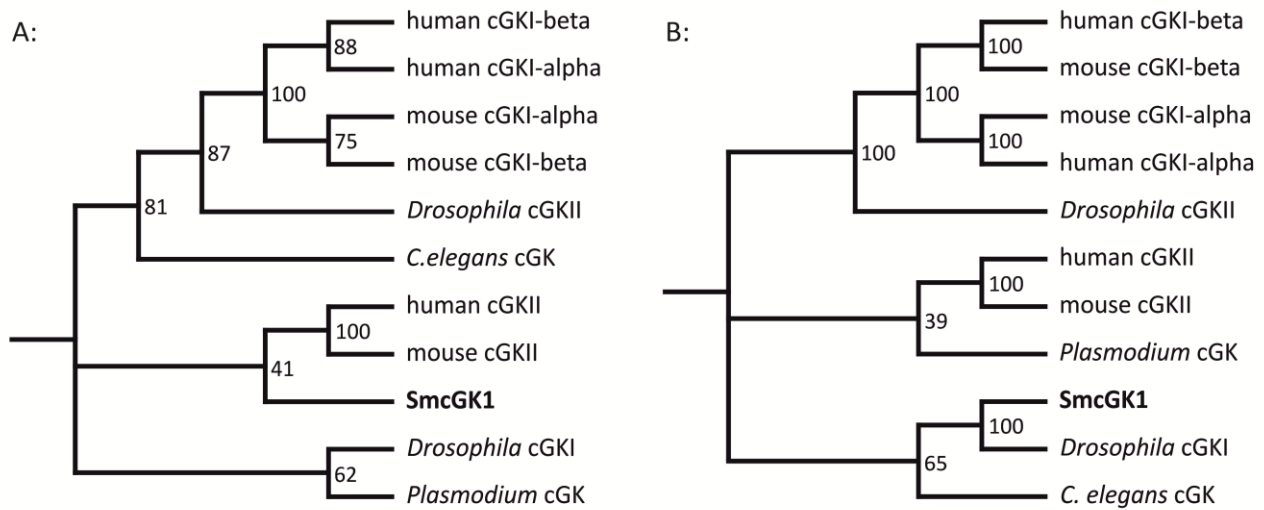


Figure X: Phylogenetic analyses of SmcGK1 in comparison to other cGKs from different organisms.

A: A phylogenetic analysis of partial sequences representing the kinase domains, places SmcGK1 closer to mammal cGKII, as found with a full-length amino acids blastx search at NCBI (Leutner *et al.* 2011). **B:** A phylogenetic analysis with full-length amino acid sequences places SmcGK1 closer to the cGKs of other invertebrates. The following amino acid sequences were used for phylogenetic analyses, besides SmcGK1 (FR749994): human cGKI-beta (CAA68810.1), human cGKI-alpha (BAA08297.1), human cGKII (EAX05867), *Drosophila* cGKII (NP_477487.1), *Drosophila* cGKI (AAB03405.1), *Plasmodium falciparum* cGK (AAN36959.1), *Caenorhabditis elegans* (NP_500141.1).

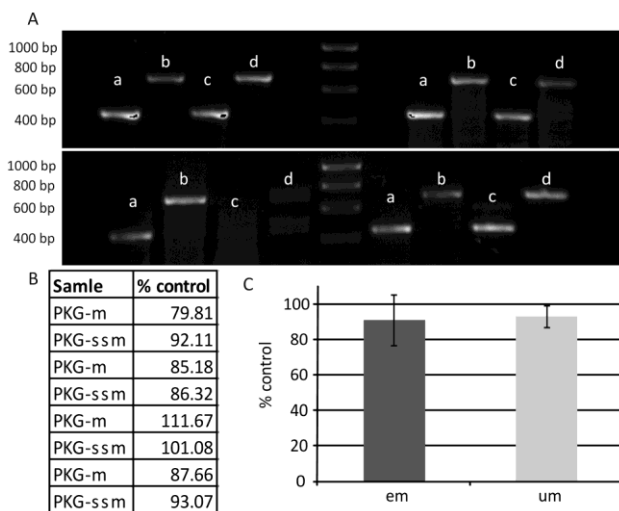


Figure XI: Initial semi-quantitative RT-PCR results for SmcGK1 transcription in EM and UM.

The figure demonstrates results from semi-quantitative RT-PCRs comparing SmcGK1 transcription in EM and UM with PDI as reference. **A:** Pictures from agarose gels show results from four biological replicas of the experiment. Samples were loaded in the order a: EM-cGK, b: EM-PDI, c: UM-cGK, d: UM-PDI (marker: Hyperaldder 1). **B:** Results from densitometric analyses are given. **C:** average values from B are depicted graphically: No difference could be detected in the transcription level of SmcGK1 between EM and UM.

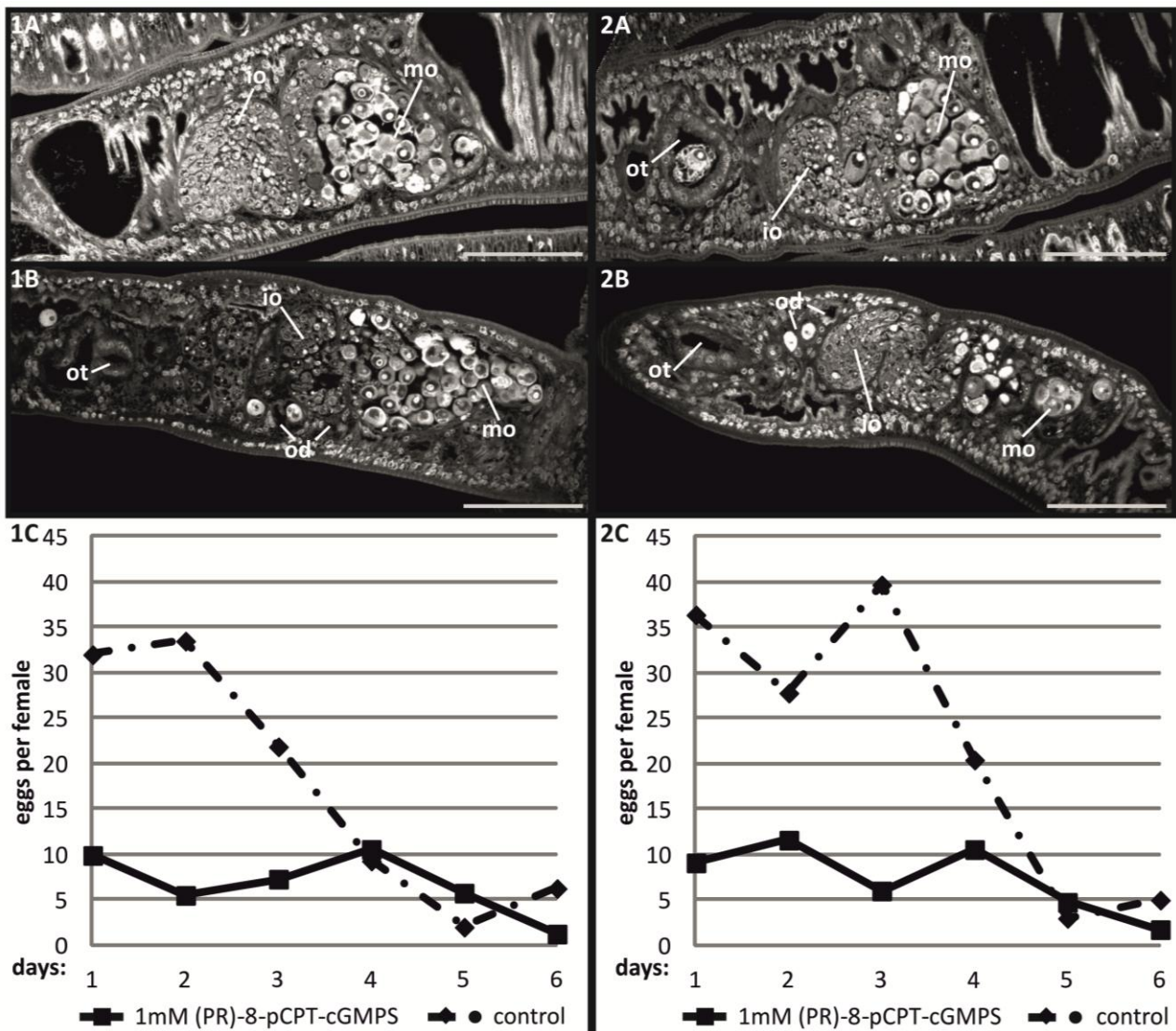


Figure XII: Results from additional cGK inhibitor treatments.

The figure shows results from two more experiments testing the effect of cGK inhibition on Schistosomes. In these experiments a slight increase of oocytes in the oviduct was found only after 6 d of treatment, while a previous experiment showed a stronger effect after 2 d. Inhibition of eggproduction was similar in all experiments. 1A, 2A: respective control females after 6 d in culture. 1B, 2B: females after 6 d treatment with (PR)-8-pCPT-cGMPS. 1C, 2C: effect on egg production resulting from inhibitor treatment. (scale bar: 75 μ m; io: immature oocytes; mo: mature oocytes; od: oviduct; ot: ootype).

Table I.I: Regulation of *Schistosoma* cGKs according to microarray and SuperSAGE transcriptome analyses.

cGK	PCR-amplification	Microarray			SuperSAGE		
		q-value	average-log ₂ (EM/UM)	as-detection	p-value	average-log ₂ (EM/UM)	as-detection
Smp_078230	yes	31.395	0.061	no	0.069	1.479	yes
Smp_080860	yes	9.612	0.133	no	0.003	0.766	yes
Smp_123290	yes	5.884	0.151	yes	0.009	0.073	yes
Smp_151100	yes	0.735	-0.336	yes	0.006	0.882	yes
Smp_168670	no	2.454	-0.290	no	0.003	-0.416	yes
Smp_174820	(yes)	41.433	0.013	no	0.457	-0.007	no

The table gives results from microarray and SuperSAGE (final analyses) for the various *Schistosoma* cGKs. Fat print: SmcGK1, analyzed in this thesis; red: significant in statistical analysis; yellow log₂ratio > 0.585 or < -0.585.

III. Transcriptome analyses

Subsequently presented figures and tables supplement data described in chapter 3.3. 'Transcriptome analyses comparing EM and UM'.

III.I. Microarray

Table II: GO - microarray.

Ontology	GO term description	Go term	Counts	p.adjusted
EM				
membrane	Double layer of lipid molecules that encloses all cells, and, in eukaryotes, many organelles; may be a single or double lipid bilayer; also includes associated proteins.	GO:0016020	170/1786	3.51E-02
UM				
generation of precursor metabolites and energy	The chemical reactions and pathways resulting in the formation of precursor metabolites, substances from which energy is derived, and any process involved in the liberation of energy from these substances.	GO:0006091	38/89	7.99E-11
mitochondrion	A semiautonomous, self replicating organelle that occurs in varying numbers, shapes, and sizes in the cytoplasm of virtually all eukaryotic cells. It is notably the site of tissue respiration.	GO:0005739	71/223	5.44E-09
oxidoreductase activity	Catalysis of an oxidation-reduction (redox) reaction, a reversible chemical reaction in which the oxidation state of an atom or atoms within a molecule is altered. One substrate acts as a hydrogen or electron donor and becomes oxidized, while the other acts as hydrogen or electron acceptor and becomes reduced.	GO:0016491	63/199	1.81E-07
cytoplasm	All of the contents of a cell excluding the plasma membrane and nucleus, but including other subcellular structures.	GO:0005737	368/2599	7.73E-05
envelope	A multilayered structure surrounding all or part of a cell; encompasses one or more lipid bilayers, and may include a cell wall layer; also includes the space between layers.	GO:0031975	45/170	1.85E-04
catalytic activity	Catalysis of a biochemical reaction at physiological temperatures. In biologically catalyzed reactions, the reactants are known as substrates, and the catalysts are naturally occurring macromolecular substances known as enzymes. Enzymes possess specific binding sites for substrates, and are usually composed wholly or largely of protein, but RNA that has catalytic activity (ribozyme) is often also regarded as enzymatic.	GO:0003824	348/2309	1.85E-04
carbohydrate metabolic process	The chemical reactions and pathways involving carbohydrates, any of a group of organic compounds based of the general formula $C_x(H_2O)_y$. Includes the formation of carbohydrate derivatives by the addition of a carbohydrate residue to another molecule.	GO:0005975	41/170	1.86E-04
electron carrier activity	Any molecular entity that serves as an electron acceptor and electron donor in an electron transport system.	GO:0009055	22/57	3.32E-04
cellular nitrogen compound biosynthetic process	The chemical reactions and pathways resulting in the formation of organic and inorganic nitrogenous compounds.	GO:0044271	29/135	1.09E-03
cofactor binding	Interacting selectively and non-covalently with a cofactor, a substance that is required for the activity of an enzyme or other protein. Cofactors may be inorganic, such as the metal atoms zinc, iron, and copper in certain forms, or organic, in which case they are referred to as coenzymes. Cofactors may either be bound tightly to active sites or bind loosely with the substrate.	GO:0048037	29/100	2.45E-03
cell surface receptor linked signaling pathway	Any series of molecular signals initiated by the binding of an extracellular ligand to a receptor on the surface of the target cell.	GO:0007166	26/108	3.01E-03
amine metabolic process	The chemical reactions and pathways involving any organic compound that is weakly basic in character and contains an amino or a substituted amino group, as carried out by individual cells. Amines are called primary, secondary, or tertiary according to whether one, two, or three carbon atoms are attached to the nitrogen atom.	GO:0009308	27/121	1.01E-02
extracellular region	The space external to the outermost structure of a cell. For cells without external protective or external encapsulating structures this refers to space outside of the plasma membrane. This term covers the host cell environment outside an intracellular parasite.	GO:0005576	40/176	1.96E-02
carboxylic acid binding	Interacting selectively and non-covalently with a carboxylic acid, any organic acid containing one or more carboxyl (COOH) groups or anions (COO ⁻).	GO:0031406	9/19	2.84E-02
small molecule metabolic process	The chemical reactions and pathways involving small molecules, any monomeric molecule of small relative molecular mass.	GO:0044281	129/767	2.89E-02
oxidation reduction	The process of removal or addition of one or more electrons with or without the concomitant removal or addition of a proton or protons.	GO:0055114	13/36	2.89E-02

Appendix

cofactor metabolic process	The chemical reactions and pathways involving a cofactor, a substance that is required for the activity of an enzyme or other protein. Cofactors may be inorganic, such as the metal atoms zinc, iron, and copper in certain forms, or organic, in which case they are referred to as coenzymes. Cofactors may either be bound tightly to active sites or bind loosely with the substrate.	GO:0051186	21/82	2.89E-02
biological adhesion	The attachment of a cell or organism to a substrate or other organism.	GO:0022610	28/111	3.04E-02
alcohol metabolic process	The chemical reactions and pathways involving alcohols, any of a class of compounds containing one or more hydroxyl groups attached to a saturated carbon atom.	GO:0006066	33/116	3.04E-02
ion transport	The directed movement of charged atoms or small charged molecules into, out of or within a cell, or between cells by means of some agent such as a transporter or pore.	GO:0006811	47/238	3.38E-02
ion binding	Interacting selectively and non-covalently with ions, charged atoms or groups of atoms.	GO:0043167	197/1255	4.53E-02

Enriched GO categories detected, when analyzing transcripts significantly regulated between EM and UM in the microarray experiments.

Table III: SchistosCyc - microarray.

	Pathway	Enzymes	Gene
carbohydrates	glycogen biosynthesis II (from UDP-D-Glucose)	glycogen synthase, putative	Smp_018260
		udp-glucose-1-phosphate uridylyltransferase 2 (udp-glucose pyrophosphorylase 2), putative	Smp_133600
	UDP-galactose biosynthesis (salvage pathway from galactose using UDP-glucose)	udp-glucose 4-epimerase, putative	Smp_070780
		udp-glucose-1-phosphate uridylyltransferase 2 (udp-glucose pyrophosphorylase 2), putative	Smp_133600
	galactose degradation II	galactokinase, putative	Smp_078400
		udp-glucose 4-epimerase, putative	Smp_070780
		udp-glucose-1-phosphate uridylyltransferase 2 (udp-glucose pyrophosphorylase 2), putative	Smp_133600
	UDP-N-acetyl-D-galactosamine biosynthesis I	galactokinase, putative	Smp_078400
		udp-glucose-1-phosphate uridylyltransferase 2 (udp-glucose pyrophosphorylase 2), putative	Smp_133600
	GDP-mannose biosynthesis I	glucose-6-phosphate isomerase, putative	Smp_022400
GDP-L-fucose biosynthesis I	GDP-mannose 4,6-dehydratase	Smp_153490	
	NAD dependent epimerase/dehydratase, putative	Smp_104720	
GDP- α -D-perosamine biosynthesis	GDP-mannose 4,6-dehydratase	Smp_153490	
	glycolysis	glucose-6-phosphate isomerase, putative	Smp_022400
		6-phosphofructokinase	Smp_043670
		fructose 1,6-bisphosphate aldolase, putative	Smp_042160
		phosphoglycerate kinase	Smp_187370
		pyruvate kinase, putative	Smp_156360
citrate cycle	TCA cycle variation III (eukaryotic)	succinyl-CoA synthetase-related	Smp_052060
		isocitrate dehydrogenase [NAD] subunit gamma, mitochondrial, putative	Smp_056200
		aconitase, mitochondrial, putative	Smp_063090
aerobic respiration	aerobic respiration -- electron donor II	NADH-ubiquinone oxidoreductase subunit B17.2, putative	Smp_082940
		NADH-ubiquinone oxidoreductase 1, chain, putative	Smp_042590.x
		NADH-ubiquinone oxidoreductase, putative	Smp_038870.x
		cytochrome C oxidase, subunit II, putative	Smp_095540
	aerobic respiration -- electron donors reaction list	cytochrome C oxidase subunit IV, putative	Smp_128610
		glycerol-3-phosphate dehydrogenase, putative	Smp_168310.x
		glycerol-3-phosphate dehydrogenase, putative	Smp_169570
		NADH-ubiquinone oxidoreductase subunit B17.2, putative	Smp_082940
lipids and fatty acids	mevalonate pathway	NADH-ubiquinone oxidoreductase 1, chain, putative	Smp_042590.x
		NADH-ubiquinone oxidoreductase, putative	Smp_038870.x
	fatty acid β -oxidation I	glycerol-3-phosphate dehydrogenase, putative	Smp_030500.x
		hydroxymethylglutaryl-CoA synthase, putative	Smp_195010
	phospholipid biosynthesis II	farnesyl pyrophosphate synthase	Smp_070710
		long-chain-fatty-acid CoA ligase, putative	Smp_165850
phosphatidylinositol synthase, putative		Smp_132640	
		ethanolaminephosphotransferase, putative	Smp_084320
		ethanolaminephosphotransferase, putative	Smp_071020
		1-acylglycerol-3-phosphate acyltransferase, putative	Smp_028490

	CDP-diacylglycerol biosynthesis	glycerol-3-phosphate dehydrogenase, putative	Smp_030500.x
		1-acylglycerol-3-phosphate acyltransferase, putative	Smp_028490
	triacylglycerol biosynthesis	diacylglycerol o-acyltransferase, putative	Smp_158520
		1-acylglycerol-3-phosphate acyltransferase, putative	Smp_028490
	glycerol degradation	glycerol-3-phosphate dehydrogenase, putative	Smp_030500.x
		glycerol kinase, putative	Smp_141770
glycerol-3-phosphate dehydrogenase, putative		Smp_169570	
glycerol-3-phosphate dehydrogenase, putative		Smp_168310	
amino acids	alanine degradation II (to D-lactate)	alanine aminotransferase, putative	Smp_130540
		alanine aminotransferase, putative	Smp_007760
	alanine biosynthesis II	alanine aminotransferase, putative	Smp_130540
		alanine aminotransferase, putative	Smp_007760
	glycine degradation	glycine amidinotransferase, mitochondrial precursor, putative	Smp_144220
	arginine degradation VI / proline biosynthesis III	pyrroline-5-carboxylate reductase	Smp_049390
	aspartate biosynthesis / asparagin biosynthesis III / glutamate degradation II	asparagine synthetase, putative	Smp_133540
glutamate / glutamine biosynthesis I	glutamate synthase, putative	Smp_128380	
pyridoxal 5'-phosphate salvage pathway	pyridoxine kinase	Smp_164250	
bases	degradation of purine ribonucleosides	purine nucleoside phosphorylase, putative	Smp_090520
	salvage pathways of guanine, xanthine, and their nucleosides	purine nucleoside phosphorylase, putative	Smp_090520
	salvage pathways of pyrimidine ribonucleotides	uridine phosphorylase, putative	Smp_082430
		uridine phosphorylase, putative	Smp_082420
	salvage pathways of adenine, hypoxanthine, and their nucleosides	Adenine phosphoribosyltransferase, putative	Smp_054410
		purine nucleoside phosphorylase, putative	Smp_090520
	de novo biosynthesis of uridine-5'-monophosphate	orotidine 5'-phosphate decarboxylase / orotate phosphoribosyltransferase	Smp_050540
de novo biosynthesis of pyrimidine deoxyribonucleotides	ribonucleoside-diphosphate reductase, alpha subunit, putative	Smp_009030	
formyltetrahydrofolate biosynthesis	folylpolyglutamate synthase	Smp_162030	
other	sulfide oxidation I (sulfide-quinone reductase)	sulfide quinone reductase, putative	Smp_062070.x
	betaxanthin biosynthesis (via dopaxanthin)	tyrosinase 2 precursor, putative	Smp_013540
	betacyanin biosynthesis (via dopamine)	tyrosinase 2 precursor, putative	Smp_013540
	phenylethanol biosynthesis	aromatic amino acid decarboxylase, putative	Smp_135230
	catecholamine biosynthesis	Tyrosine 3-monooxygenase (Tyrosine 3-hydroxylase) (TH), putative	Smp_007690
		aromatic amino acid decarboxylase, putative	Smp_135230
	colanic acid building blocks biosynthesis	udp-glucose 4-epimerase, putative	Smp_070780
		udp-glucose-1-phosphate uridylyltransferase 2 (udp-glucose pyrophosphorylase 2), putative	Smp_133600
		NAD dependent epimerase/dehydratase, putative	Smp_104720
		galactokinase, putative	Smp_078400
	heme biosynthesis	uroporphyrinogen decarboxylase	Smp_143740
	glutathione biosynthesis	gamma-glutamylcysteine synthetase, putative	Smp_025030
	geranyldiphosphat biosynthesis	farnesyl pyrophosphate synthase	Smp_070710
geranylgeranyldiphosphate biosynthesis II (plastidic)	farnesyl pyrophosphate synthase	Smp_070710	
	geranylgeranyl pyrophosphate synthase, putative	Smp_134230	

The table present results from metabolic analysis with the online tool SchistoCyc (Zerlotini *et al.*, 2009), for genes significantly regulated between EM and UM in the microarray analysis. green: genes up-regulated in EM; red: genes up-regulated in UM; underlined: genes significantly regulated between the two stages with more than 1.5 times higher transcription in either stage compare to the other.

III.II. SuperSAGE

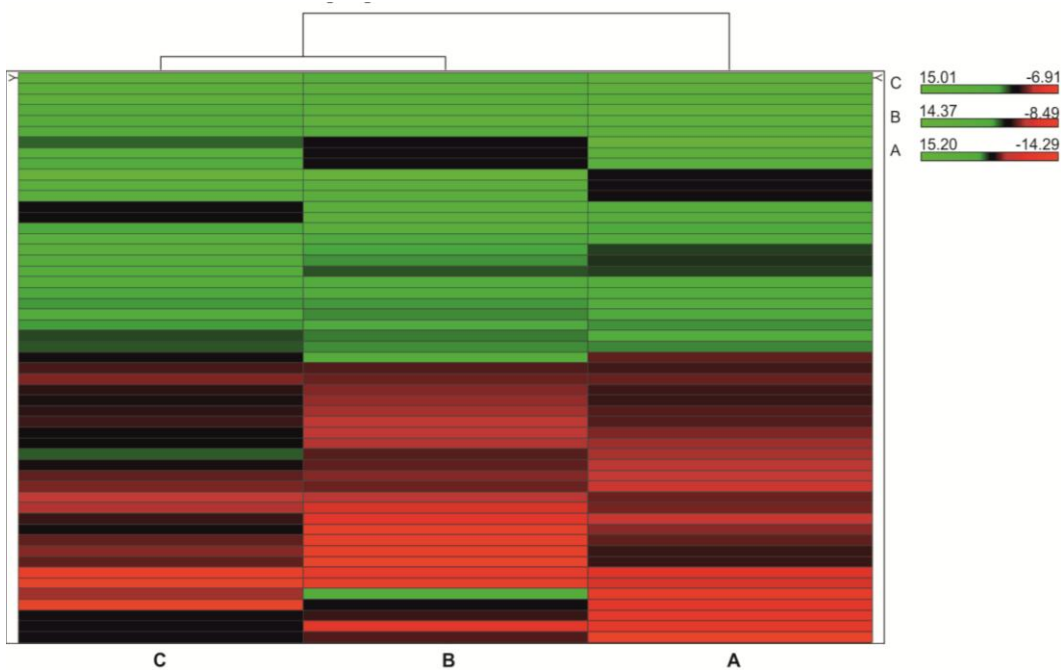


Figure XIII: hierarchical clustering of SuperSAGE EdgeR significantly regulated genes.

EdgeR statistical analysis of the SuperSAGE data detected only 53 transcripts to be significantly regulated between EM and UM. Green: transcripts up-regulated in EM. Red: transcripts up-regulated in UM.

Table IV: SuperSAGE EdgeR significantly regulated genes.

h.c.	NR-codes	Source	Gene annotation Smp	Average log ₂ ratio (EM/UM)	p#adjustBH
1	Smp_093720	Exon	hypothetical protein	9.571	4.960E-23
2	Smp_179420	Exon	hypothetical protein	8.334	6.650E-07
3	Smp_024390.x	Intron	microsomal signal peptidase 25 kD subunit	7.950	9.650E-06
4	Smp_141410	Exon	cell adhesion molecule	9.040	2.130E-26
5	Smp_130690	Exon	zinc finger protein	8.542	6.310E-14
6	Smp_165980	Exon	rna polymerase III (DNA directed), 39kD subunit- related	6.179	2.720E-08
7	JAP09507.C	Exon	dynein, axonemal, heavy chain 10 [Homo sapiens]	5.568	6.752E-03
8	gi 60692940	Exon	-	5.096	2.747E-03
9	Smp_010620.x	Intron	hypothetical protein	3.554	3.643E-02
10	JAP03296.C	Exon	-	9.794	8.470E-46
11	Smp_136240.x	Intron	vesicle-associated membrane protein (vamp)	5.271	8.844E-04
12	Smp_145980.x	Intron	sodium/dicarboxylate symporter-related	4.800	3.643E-02
13	Smp_011100	Exon	M16 family peptidase	4.303	3.643E-02
14	Smp_191570	Exon	-	4.153	4.603E-02
15	Smp_016490.x	Intron	hypothetical protein	3.943	4.641E-02
16	Smp_180750	Exon	hypothetical protein	4.566	7.853E-03
17	Smp_157750	Exon	rna-binding protein musashi-related	3.313	2.818E-04
18	Smp_158480	Intron	AMP dependent ligase	2.430	2.436E-03
19	Smp_135230	Exon	aromatic-L-amino-acid decarboxylase	2.081	3.590E-05
20	Smp_169450	Intron	DNA replication licensing factor MCM8	3.832	9.930E-12
21	Smp_103420	Intron	hypothetical protein	3.076	3.753E-02
22	Smp_173350.x	Exon	egg protein CP391S-like	2.704	2.770E-05
23	Smp_176400	Exon	hypothetical protein	2.764	2.652E-04
24	Smp_122830	Intron	hypothetical protein	2.416	3.254E-02

25	Smp_087810	Intron	GTP binding protein	2.042	4.980E-03
26	Smp_179530	Exon	hypothetical protein	1.824	2.995E-02
27	Smp_172960	Exon	kunitz-type protease inhibitor	1.138	5.094E-03
28	Smp_123300	Exon	folistatin	-1.226	4.526E-02
29	C800058.1	Exon	kinesin heavy chain	-1.823	1.773E-02
30	Smp_142800	Exon	hypothetical protein	-1.354	3.765E-02
31	Smp_134550	Exon	hypothetical protein	-1.356	1.309E-02
32	Smp_162520	Intron	cadherin-related	-1.628	2.083E-02
33	Smp_159950	Exon	neuropeptide Y precursor	-1.801	4.980E-03
34	Smp_036470	Exon	oxalate:formate antiporter	-1.764	8.801E-04
35	Smp_157910.x	Intron	hypothetical protein	-1.891	2.238E-03
36	C813377.1	Exon	-	-0.892	1.773E-02
37	Smp_180620	Intron	hypothetical protein	-1.728	2.330E-02
38	Smp_104760	Intron	hypothetical protein	-2.308	2.397E-02
39	Smp_166510	Intron	hypothetical protein	-2.671	1.749E-02
40	Smp_128470	Intron	hypothetical protein	-2.548	1.577E-02
41	Smp_141480	Exon	hypothetical protein	-3.040	2.440E-11
42	Smp_140600	Intron	Jagged	-3.341	4.980E-03
43	Smp_154900	Exon	rhoGAP protein	-3.381	1.068E-02
44	Smp_168800.x	Intron	family C12 unassigned peptidase (C12 family)	-3.497	4.641E-02
45	Smp_095410.x	Exon	Magnesium-dependent phosphatase 1 (EC 3.1.3.-)	-3.605	1.711E-02
46	Smp_025160.x	Intron	acyl-protein thioesterase 1,2 (lysophospholipase I,II)	-3.692	1.749E-02
47	Smp_169990.x	Intron	golgi reassembly stacking protein 2 (grasp2)	-6.517	3.643E-02
48	Smp_120960.x	Intron	ribonuclease pH related	-6.574	1.749E-02
49	Smp_128290	Exon	hypothetical protein	-2.969	4.050E-03
50	Smp_098780	Exon	forkhead protein/ forkhead protein domain	-4.850	1.749E-02
51	Smp_180400	Intron	serine/threonine kinase	-3.359	4.980E-03
52	Smp_045860.x	Intron	histidine acid phosphatase	-4.655	2.747E-03
53	JAP10881.C	Exon	muclipin 2 [Homo sapiens]	-5.210	2.112E-03

The table shows details for the 53 transcripts detected as significantly regulated between EM and UM according to SuperSAGE EdgeR statistics. h.c.: hierarchical clustering.

Table V: GO - SuperSAGE A&C.

Ontology	GO term description	Go term	Counts	p.adjusted
generation of precursor metabolites and energy	The chemical reactions and pathways resulting in the formation of precursor metabolites, substances from which energy is derived, and any process involved in the liberation of energy from these substances.	GO:0006091	20/95	2,43E-06
envelope	A multilayered structure surrounding all or part of a cell; encompasses one or more lipid bilayers, and may include a cell wall layer; also includes the space between layers.	GO:0031975	27/180	2,48E-05
mitochondrion	A semiautonomous, self replicating organelle that occurs in varying numbers, shapes, and sizes in the cytoplasm of virtually all eukaryotic cells. It is notably the site of tissue respiration.	GO:0005739	34/232	2,48E-05
hydrogen transport	The directed movement of hydrogen (H ₂ or H ⁺), into, out of or within a cell, or between cells by means of some agent such as a transporter or pore.	GO:0006818	14/80	1,67E-02
respiratory chain	The protein complexes that form the electron transport system (the respiratory chain), associated with a cell membrane, usually the plasma membrane (in prokaryotes) or the inner mitochondrial membrane (on eukaryotes). The respiratory chain complexes transfer electrons from an electron donor to an electron acceptor and are associated with a proton pump to create a transmembrane electrochemical gradient.	GO:0070469	8/28	1,67E-02
proton-transporting two-sector ATPase complex	A large protein complex that catalyzes the synthesis or hydrolysis of ATP by a rotational mechanism, coupled to the transport of protons across a membrane. The complex comprises a membrane sector (F ₀ , V ₀ , or A ₀) that carries out proton transport and a cytoplasmic compartment sector	GO:0016469	7/20	2,38E-02

Appendix

	(F1, V1, or A1) that catalyzes ATP synthesis or hydrolysis. Two major types have been characterized: V-type ATPases couple ATP hydrolysis to the transport of protons across a concentration gradient, whereas F-type ATPases, also known as ATP synthases, normally run in the reverse direction to utilize energy from a proton concentration or electrochemical gradient to synthesize ATP. A third type, A-type ATPases have been found in archaea, and are closely related to eukaryotic V-type ATPases but are reversible.			
oxidoreductase activity	Catalysis of an oxidation-reduction (redox) reaction, a reversible chemical reaction in which the oxidation state of an atom or atoms within a molecule is altered. One substrate acts as a hydrogen or electron donor and becomes oxidized, while the other acts as hydrogen or electron acceptor and becomes reduced.	GO:0016491	21/211	3,45E-02

Enriched GO categories detected, when analyzing transcripts significantly regulated between EM and UM in the SuperSAGE A&C experiments. All presented categories are significantly enriched for transcripts up-regulated in UM, for transcripts up-regulated in EM no significantly enriched categories were found.

Table VI: SchistosCyc - SuperSAGE A&C.

	Pathway	Enzymes	Gene
carbohydrates	GDP-mannose biosynthesis I	glucose-6-phosphate isomerase, putative	Smp_022400
	D-mannose degradation	hexokinase From Schistosoma Mansoni Complexed With Glucose, putative	Smp_043030
pentose phosphate pathwa		6-phosphogluconolactonase	Smp_081460.x
glycolysis		glucose-6-phosphate isomerase, putative	Smp_022400
		6-phosphofructokinase	Smp_043670
		fructose 1,6-bisphosphate aldolase, putative	Smp_042160
		pyruvate kinase, putative	Smp_065610
		phosphoglycerate mutase	Smp_096760
		triosephosphate isomerase, putative	Smp_003990
citrate cycle	TCA cycle variation III (eukaryotic)	aconitase, mitochondrial	Smp_063090
aerobic respiration	aerobic respiration - electron donor II	L-lactate dehydrogenase, putative	Smp_038950
		cytochrome C oxidase, subunit II	Smp_095540
		-	Smp_181810
	electron donors	NADH-ubiquinone oxidoreductase 1, chain, putative	Smp_042590.x
		glycerol-3-phosphate dehydrogenase, putative	Smp_030500
		NADH-ubiquinone oxidoreductase 1, chain, putative	Smp_042590.x
lipids and fatty acids	trans,trans-farnesyl diphosphate biosynthesis	lipase containing protein, putative	Smp_128680
	CDP-diacylglycerol biosynthesis	glycerol-3-phosphate dehydrogenase, putative	Smp_030500.x
	mevalonate pathway /trans,trans-farnesyl diphosphate biosynthesis	isopentenyl-diphosphate delta isomerase, putative	Smp_130430
	triacylglycerol degradation	acetyl-CoA C-acyltransferase, putative	Smp_129330
		lipase containing protein, putative	Smp_128680
	glycerol degradation	hormone-sensitive lipase, putative	Smp_000130.x
		glycerol-3-phosphate dehydrogenase, putative	Smp_030500.x
	fatty acid biosynthesis - initial steps I	glycerol-3-phosphate dehydrogenase, putative	Smp_121990.x
	fatty acid elongation -- saturated	3-oxoacyl-[acyl-carrier-protein] synthase, putative	Smp_009150.x
fatty acid β -oxidation I	3-oxoacyl-[acyl-carrier-protein] synthase, putative	Smp_009150.x	
amino acids	arginine degradation I (arginase pathway)	acetyl-CoA C-acyltransferase	Smp_129330
	arginine degradation VI (arginase 2 pathway)	aldehyde dehydrogenase, putative	Smp_050390
	alanine biosynthesis II	arginase, putative	Smp_059980
		alanine aminotransferase, putative	Smp_130540
	alanine degradation II (to D-lactate)	alanine aminotransferase, putative	Smp_007760
		alanine aminotransferase, putative	Smp_130540
	thioredoxin biosynthesis	alanine aminotransferase, putative	Smp_007760
	glutathione biosynthesis	thioredoxin glutathione reductase	Smp_048430
S-adenosyl-L-methionine cycle	glutamate cysteine ligase, putative	Smp_013860	
bases	de novo biosynthesis of pyrimidine deoxyribonucleotides	adenosylhomocysteinase, putative	Smp_096020.x
		nucleoside diphosphate kinase, putative	Smp_168270
		nucleoside diphosphate kinase, putative	Smp_092750
	pyrimidine ribonucleotides interconversion	putative Thymidylate Kinase	Smp_032810
		nucleoside diphosphate kinase, putative	Smp_168270
	salvage pathways of pyrimidine ribonucleotides	nucleoside diphosphate kinase, putative	Smp_092750
		nucleoside diphosphate kinase, putative	Smp_168270
		nucleoside diphosphate kinase, putative	Smp_092750

	formyltetrahydrofolate biosynthesis	folylpolyglutamate synthase	Smp_162030
other	catecholamine biosynthesis	<u>aromatic amino acid decarboxylase, putative</u>	Smp_135230
	phenylethanol biosynthesis	<u>aromatic amino acid decarboxylase, putative</u>	Smp_135230

The table presents results from metabolic analysis with the online tool SchistoCyc, for genes significantly regulated between EM and UM in the SuperSAGE A&C. green: genes up-regulated in EM; red: genes up-regulated in UM; underlined: genes significantly regulated between the two stages with more than 1.5 times higher transcript detection in either stage compare to the other.

III.III. Comparison of microarray and SuperSAGE data

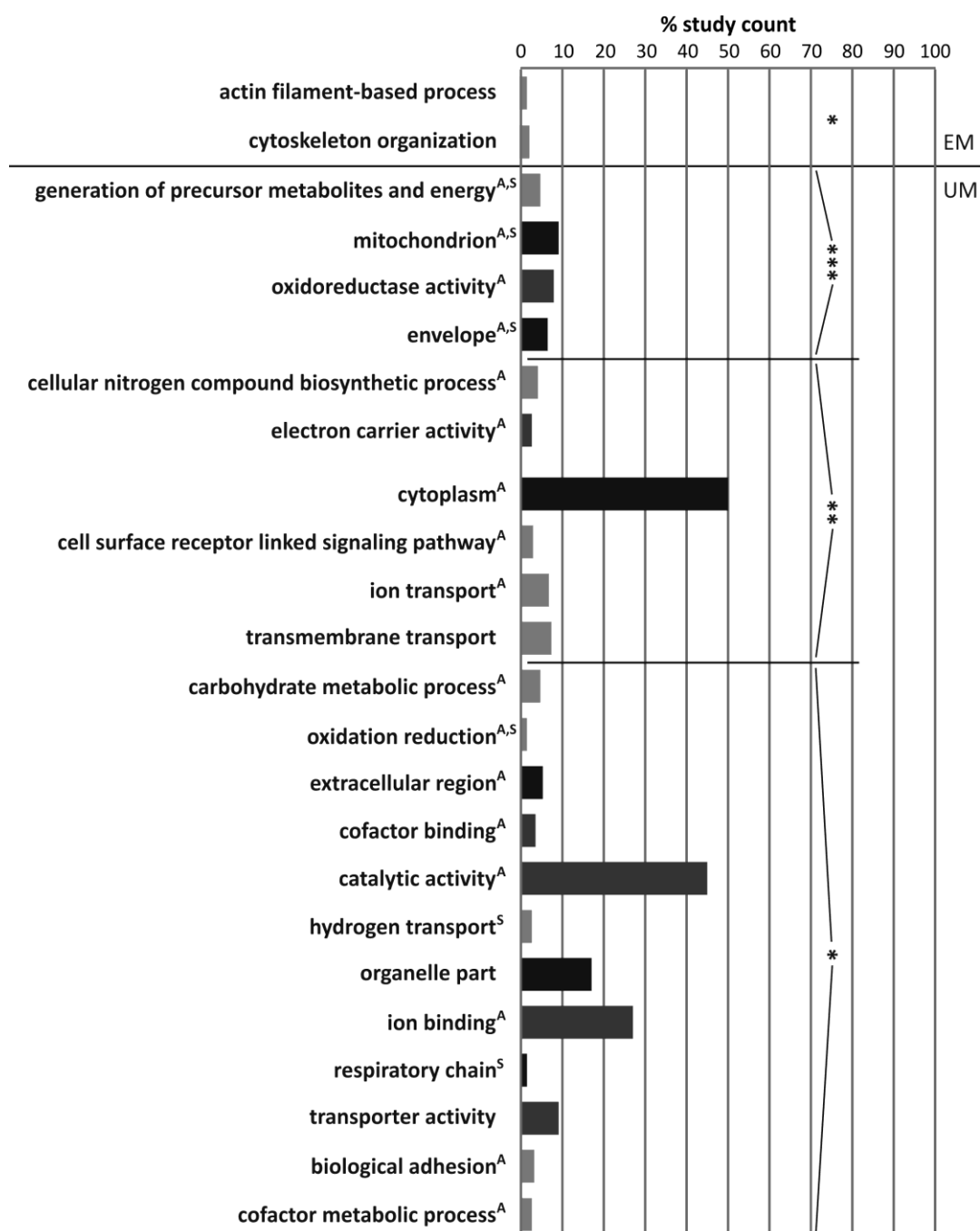


Figure XIV: Gene Ontology - enriched categories for genes significantly regulated between EM and UM according to SuperSAGE, microarray or both analyses:

GO analysis was performed for genes significantly regulated according to microarray experiments and/or SuperSAGE. Two categories were significantly enriched for genes with higher transcript detection in EM, while 21 were significantly enriched for genes with a higher transcript detection in UM. Light grey: biological process; grey: molecular function; black: cellular component; p-values for the GO-analysis: *p < 0.05; **p < 0.005; ***p < 0.0001; A: category also detected as enriched in microarray analysis; S: category also detected as enriched in SuperSAGE analysis.

Appendix

Table VII: 180 genes significantly transcribed according to both analyses.

NR Gene	Gene annotation Smp	log2(EM/UM) microarray	log2(EM/UM) SuperSAGE
Smp_135230	aromatic-L-amino-acid decarboxylase	2.58	2.08
Smp_168940	NAD dependent epimerase/dehydratase, putative	2.66	1.49
Smp_052230	kunitz-type protease inhibitor, putative	1.83	1.78
Smp_008660.x	villin, putative	0.94	1.43
Smp_163720	endophilin B1, putative	0.83	1.40
Smp_055220.x	surface protein PspC , putative	0.83	1.19
Smp_000430.x	eggshell protein, chorion, putative	2.29	0.56
Smp_020540.x	pinch, putative	0.61	1.10
Smp_040560	cancer-associatedprotein protein, putative	0.85	1.02
Smp_073130.x	loss of heterozygosity 11 chromosomal region 2 gene a protein homolog (mast cell surface antigen 1) (masa- 1), putative	0.74	1.00
Smp_170080	sodium/dicarboxylate cotransporter-related	1.18	0.92
Smp_080210	lipid-binding protein, putative	0.65	0.89
Smp_151490	nebulin, putative	0.80	0.89
Smp_070030	snf7-related	0.71	0.79
Smp_003770	histone h1/h5, putative	0.86	0.68
Smp_031300	universal stress protein, putative	0.77	0.54
Smp_174510	dynein light chain, putative	1.23	0.40
Smp_059480	Peroxiredoxin, Prx1	0.64	0.41
Smp_062420.x	heat shock protein 70 (hsp70)-interacting protein, putative	0.69	0.40
Smp_019310	cytoplasmic dynein light chain, putative	0.69	0.27
Smp_000130.x	hormone-sensitive lipase (S09 family)	0.74	0.38
Smp_047370	malate dehydrogenase, putative	-0.64	-0.16
Smp_083720	mitochondrial phosphate carrier protein, putative	-0.63	-0.18
gi 256073395	expressed protein	-1.07	-0.17
Smp_161680	phosphorylase B kinase beta, kpbp, putative	-0.77	-0.21
Smp_007760	alanine aminotransferase, putative	-0.71	-0.27
Smp_194770	ATP:guanidino kinase (Smc74), putative	-0.87	-0.41
Smp_034550	alpha-actinin, putative	-1.13	-0.43
Smp_095540	cytochrome-c oxidase	-1.10	-0.47
Smp_003440	SPFH domain / Band 7 family protein, putative	-1.40	-0.55
Smp_010770.x	fatty acid acyl transferase-related	-1.71	-0.89
Smp_123080	Sarcoplasmic calcium-binding protein (SCP). , putative	-0.86	-1.00
gi 76153071	conserved hypothetical protein	-1.45	-1.40
Smp_123300	follistatin, putative	-2.15	-1.23
Smp_036470	oxalate:formate antiporter, putative	-2.91	-1.76
Smp_154040	sugar nucleotide epimerase related	-0.91	-2.88
Smp_041350	bruno-like rna binding protein	-0.78	-2.88
Smp_131050	camp-dependent protein kinase type II regulatory subunit, putative	-0.67	-2.88
Smp_158480	AMP dependent ligase, putative	2.82	3.55
Smp_151620	cadherin-related	0.63	1.41
Smp_135520	dock, putative	-1.31	0.16
Smp_126640	neurotracting/lsamp/neurotrimin/obcam related cell adhesion molecule	-0.70	0.03
Smp_123350	G-protein coupled receptor fragment, putative	-1.07	-0.28
Smp_167630	solute carrier family, putative	-0.86	-0.14
Smp_144130	lachesin	-0.81	0.97
Smp_194460	dihydroliipoamide acetyltransferase component of pyruvate dehydrogenase, putative	-0.60	-0.26
Smp_034500	dual specificity protein phosphatase, putative	0.35	0.69
Smp_169010	adenylate cyclase, putative	0.54	0.99
Smp_005160	muscleblind-like protein	0.40	0.80
Smp_008900	eukaryotic translation initiation factor 4 gamma, putative	0.34	0.84
Smp_153870	protein kinase	0.41	0.76
Smp_057650	protein kiaa0174, putative	0.35	0.82
Smp_073680.x	TATA-box binding protein, putative	0.35	0.71
Smp_059690.x	kappa B-ras, putative	0.46	0.59
Smp_072190	Sm29, putative	0.49	0.61
Smp_103470.x	mago nashi protein homolog	0.24	0.69
Smp_171850	yippee protein, putative	0.34	0.61
Smp_060480	copine, putative	-0.45	-2.88

gi 76161853	diras family, GTP-binding ras- like	-0.49	-4.32
Smp_168220	protein regulator of cytokinesis 1 prc1, putative	-0.33	-4.85
Smp_130980	cyclin k, putative	-0.25	-3.55
Smp_005290	cytochrome C1, putative	-0.36	-0.09
Smp_130540	alanine aminotransferase, putative	-0.49	-0.12
gi 256089072	tripartite motif protein trim9, putative	-0.44	-2.88
Smp_073790	gaba(A) receptor-associated protein, putative	0.33	0.53
Smp_137920	chloride intracellular channel, putative	0.52	0.58
Smp_050110	gamma-secretase subunit aph-1, putative	0.36	0.54
Smp_140510	transmembrane protein 56 , putative	0.32	0.47
Smp_125640	Syntaxin-12, putative	0.34	0.47
Smp_154200	CD63 antigen, putative	0.49	0.46
gi 256087236	rabb and C, putative	0.44	0.49
Smp_195190	13 kDa tegumental antigen Sm13	0.37	0.43
Smp_150500	recs1 protein (responsive to centrifugal force and shear stressprotein 1 protein), putative	0.39	0.46
Smp_124050.x	venom allergen-like (VAL) 6 protein	0.39	0.49
Smp_013300.x	yip1-related	0.32	0.48
Smp_097020.x	fbxl20, putative	0.52	0.42
Smp_154960.x	cop-coated vesicle membrane protein P24 (emp24/gp25l family), putative	0.32	0.42
Smp_042090.x	60S ribosomal protein L10a, putative	0.29	0.41
Smp_006390	cystatin B, putative	0.43	0.35
Smp_030300.x	endoplasmin, putative	-0.54	0.00
Smp_044010.x	tropomyosin, putative	-0.56	-0.07
Smp_034420.x	cystatin, putative	-0.30	-0.11
Smp_022400	glucose-6-phosphate isomerase, putative	-0.44	-0.18
Smp_037910	succinate dehydrogenase, putative	-0.35	-0.13
Smp_079220	ADP,ATP carrier protein, putative	-0.53	-0.18
Smp_106080.x	NADH-ubiquinone oxidoreductase 39 kD subunit, putative	-0.26	-0.13
Smp_042160.x	fructose 1,6-bisphosphate aldolase, putative	-0.31	-0.24
Smp_068170.x	pyruvate dehydrogenase, putative	-0.39	-0.13
Smp_079450	subfamily M16B non-peptidase homologue (M16 family)	-0.52	-0.17
Smp_043670.x	6-phosphofructokinase	-0.41	-0.22
Smp_013410.x	28S ribosomal protein S11, putative	-0.33	-0.20
Smp_106130.x	heat shock protein 70 (hsp70), putative	-0.40	-0.21
Smp_055210	Microsomal GST-3	-0.33	-0.24
Smp_154530	mitochondrial ATP synthase B chain, putative	-0.27	-0.21
Smp_077090	nitrogen fixation protein nifu, putative	-0.36	-0.23
Smp_063090	aconitate hydratase	-0.38	-0.31
Smp_163570	ryanodine receptor related	-0.51	-0.37
Smp_038100	ATP synthase beta subunit, putative	-0.58	-0.29
Smp_134440.x	malic enzyme, putative	-0.38	-0.31
Smp_030500.x	glycerol-3-phosphate dehydrogenase, putative	-0.21	-0.30
Smp_162030	folypolyglutamate synthase	-0.31	-0.46
Smp_008360	adenosine kinase, putative	-0.56	-0.54
Smp_165980	rna polymerase III (DNA directed), 39kD subunit- related	-0.22	6.18
Smp_160410.x	Transmembrane protein 106C (Endoplasmic reticulum membrane protein overexpressed in cancer), putative	-0.48	0.60
Smp_049550	heat shock protein 70 (hsp70), putative	-0.83	0.49
Smp_067900	cdc37-related	-0.34	0.56
Smp_105410	glucose transport protein, putative	-0.52	0.35
Smp_141290.x	innexin, putative	-0.47	0.44
Smp_049600.x	DNAj (hsp40) homolog, subfamily C, member, putative	-0.27	0.46
Smp_152710.x	glutathione-s-transferase omega, putative	-0.59	0.45
Smp_156770	major tegumental antigen SM15, putative	-0.48	0.40
Smp_018250.x	troponin I, putative	-0.45	0.22
Smp_085540.x	myosin heavy chain, putative	-0.50	0.06
Smp_030730	tubulin beta chain, putative	-0.30	0.10
Smp_079270	crp-related	-0.29	0.01
Smp_038560.x	Prothymosin alpha-B, putative	0.28	-0.08
Smp_148530	heat shock protein hsp16, putative	0.54	-0.12
Smp_006320.x	gap associated protein - related	0.57	-0.12

Appendix

Smp_127650	secretory carrier membrane protein, putative	0.24	-0.18
Smp_130100	saposin containing protein	0.49	-0.24
Smp_045860.x	histidine acid phosphatase, putative	0.46	2.71
Smp_008620	RHBDF1 protein (S54 family)	0.74	0.70
Smp_039650	Crumbs complex protein	0.38	0.09

Of the 180 genes significantly regulated according to both transcriptome analyses 123, with a functional annotation other than 'hypothetical protein', are represented.

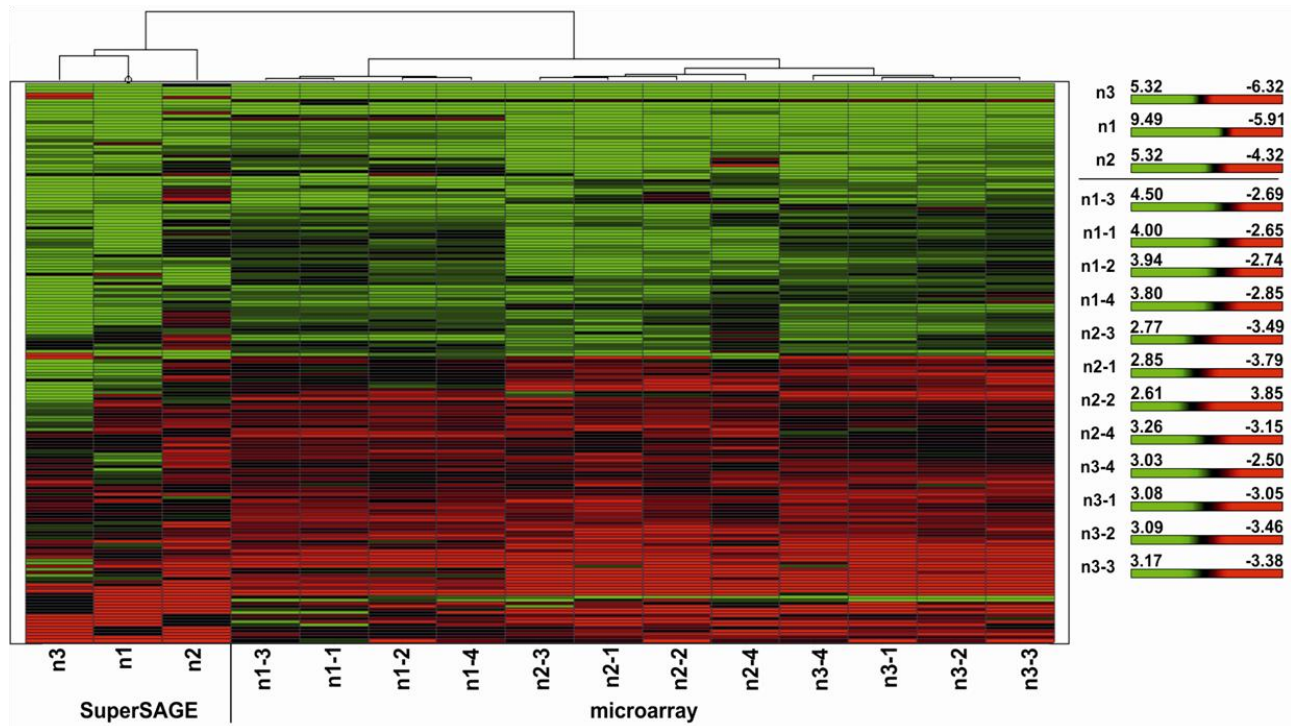


Figure XV: Hierarchical clustering of 180 significant in both analyses.

Hierarchical clustering of the 180 transcripts significantly regulated in both analyses shows, strong differences in regulation between the two methodological approaches for individual transcripts, similar to the hierarchical clustering performed for significantly regulated transcripts from either one or both analyses (Fig. 3.11.).

Table VIII: GO - 180 significant in both analyses.

Ontology	GO term description	Go term	Counts	p.adjusted
generation of precursor metabolites and energy	The chemical reactions and pathways resulting in the formation of precursor metabolites, substances from which energy is derived, and any process involved in the liberation of energy from these substances.	GO:0006091	10/93	2,30E-05
mitochondrion	A semiautonomous, self replicating organelle that occurs in varying numbers, shapes, and sizes in the cytoplasm of virtually all eukaryotic cells. It is notably the site of tissue respiration.	GO:0005739	17/231	3,27E-04
envelope	A multilayered structure surrounding all or part of a cell; encompasses one or more lipid bilayers, and may include a cell wall layer; also includes the space between layers.	GO:0031975	11/179	1,16E-03
cellular alkene metabolic process	The chemical reactions and pathways involving an alkene, any cyclic branched or unbranched hydrocarbon having one carbon-carbon double bond and the general formula C _n H _{2n} , as carried out by individual cells.	GO:0043449	3/7	5,42E-03
cytoplasmic part	Any constituent part of the cytoplasm, all of the contents of a cell excluding the plasma membrane and nucleus, but including other subcellular structures.	GO:0044444	25/1032	5,42E-03
hydrogen transport	The directed movement of hydrogen (H ₂ or H ⁺), into, out of or within a cell, or between cells by means of some agent such as a transporter or pore.	GO:0006818	6/79	2,49E-02
phosphotransferase activity, nitrogenous group as acceptor	Catalysis of the transfer of a phosphorus-containing group from one compound (donor) to a nitrogenous group (acceptor).	GO:0016775	2/3	2,49E-02

Enriched GO categories detected, when analyzing the 180 transcripts significantly regulated between EM and UM according to both transcriptome analyses. No significantly enriched categories were found for transcripts up-regulated in EM. All categories presented here were significantly enriched for transcripts up-regulated in UM.

Table IX: SchistoCyc - 180 significant in both analyses.

	Pathway	Enzymes	Genes
carbohydrates	GDP-mannose biosynthesis I	<u>glucose-6-phosphate isomerase, putative</u>	Smp_022400
aerobic respiration	aerobic respiration -- electron donor II	<u>cytochrome C oxidase, subunit II, putative</u>	Smp_095540
glycolysis		<u>glucose-6-phosphate isomerase, putative</u>	Smp_022400
		<u>6-phosphofructokinase</u>	Smp_043670
		<u>fructose 1,6-bisphosphate aldolase, putative</u>	Smp_042160
citrate cycle	TCA cycle variation III (eukaryotic)	<u>aconitase, mitochondrial</u>	Smp_063090
aerobic respiration	aerobic respiration - electron donor II	<u>cytochrome C oxidase, subunit II</u>	Smp_095540
	aerobic respiration -- electron donors reaction list	<u>glycerol-3-phosphate dehydrogenase, putative</u>	Smp_030500
lipids and fatty acids	CDP-diacylglycerol biosynthesis	<u>glycerol-3-phosphate dehydrogenase, putative</u>	Smp_030500.x
	CDP-diacylglycerol biosynthesis	<u>glycerol-3-phosphate dehydrogenase, putative</u>	Smp_030500.x
amino acids	alanine biosynthesis II	<u>alanine aminotransferase, putative</u>	Smp_130540
	alanine degradation II (to D-lactate)	<u>alanine aminotransferase, putative</u>	Smp_007760
bases	formyltetrahydrofolate biosynthesis	<u>folypolyglutamate synthase</u>	Smp_162030
other	catecholamine biosynthesis	<u>aromatic amino acid decarboxylase, putative</u>	Smp_135230
	phenylethanol biosynthesis	<u>aromatic amino acid decarboxylase, putative</u>	Smp_135230

The table present results from metabolic analysis with the online tool SchistoCyc, for the 180 genes significantly regulated between EM and UM in both analyses, microarray and SuperSAGE. green: genes up-regulated in EM; red: genes up-regulated in UM; underlined: genes significantly regulated between the two stages with more than 1.5 times higher transcription in either stage compared to the other.

IV. Real-time PCR

There here presented table summarizes the different master mixes tested during real-time PCR.

Table X: Real-time PCR MasterMix tests.

company	Kit	dye	dimer	product	E	Primer tested
SolisBiodyne	Hot FIREPol EvaGreen qPCR Mix Plus (noROX)	eva green	yes	concentration dependency	1.36	sigmaL20
			yes	concentration dependency	0.96	AcetT
Qiagen	Rotor-Gene SYBR Green PCR Kit	sybr green	no	good	0.82	sigmaL20
			no	ok	0.82	AcetT
Applied	Power SYBR® Green PCR Master Mix	sybr green	no	good	0.83	sigmaL20
Biorad	iQ SYBRGreen Supermix	sybr green	slightly	ok	0.85	sigmaL20
Eurogenetec	MESA FAST qPCR MasterMix Plus for SYBR Assay No ROX	sybr green	yes	ok	1.33	sigmaL20
NEB	DyNAmo HS SYBR Green qPCR Kit	sybr green	no	ok	0.57	sigmaL20
Invitrogen	EXPRESS SYBR FreenER qPCR Supermix	sybr green	no	weak	0.93	sigmaL20
Invitrogen	Platinum SYBR Green qPCR SuperMix-UDG	sybr green	no	weak	1.33	sigmaL20
Bioline	SensiMix SYBR No-ROX Kit	sybr green	no	good	0.56	sigmaL20
Fermentas	Maxima SYBR Green qPCR Master Mix	sybr green	no	weak	0.72	sigmaL20
molegene	5xHOT MOLPol EvaGreen qPCR Mix Plus (no Rox)	eva green	yes	ok	1.22	sigmaL20
thermo scientific	thermo scientific Absolute qPCR SYBR Green Mix	sybr green	no	very weak	1.5	sigmaL20
peqlab	KAPA SYBR FAST QPCR MasterMix Universal	sybr green	yes	good	0.95	AcetT
	diatheva	sybr green	slightly	strong	0.92	sigmaL20
Clontech	TAKARA SYBR PremixExTaqII (Perfect real time) sample	sybr green	no	stark	0.91	sigmaL20
Sprime	REalMasterMix SYBR ROX	sybr green	yes	good	0.78	sigmaL20
VWR	Quanta	sybr green	no	ok	0.86	sigmaL20

First results from real-timer PCR MasterMix tests, influencing later (after refined testing) choice of Quanta MM as standard reagent.

V. Data-analyses with refined criteria

Subsequently presented figures supplement data described in chapter 3.5. 'Data-analyses with refined criteria drastically reduced the number of interesting genes'.

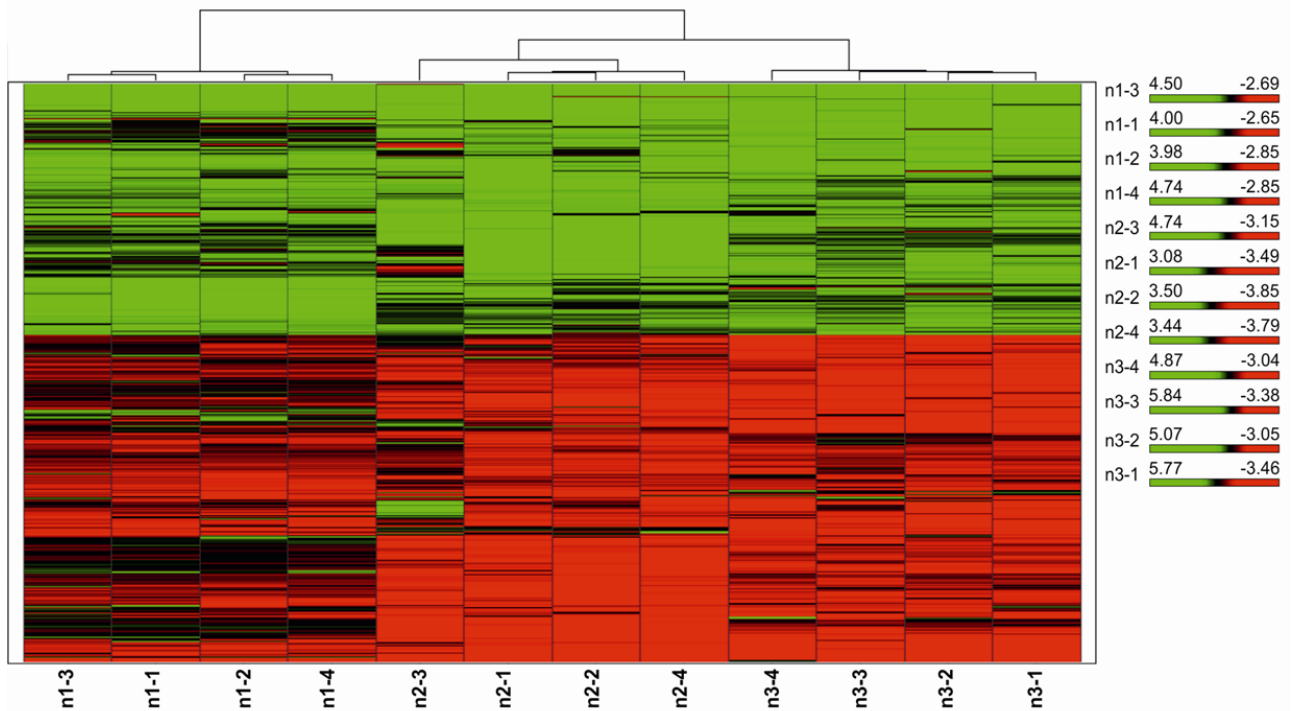


Figure XVI: Hierarchical clustering of microarray transcripts significantly and differentially regulated.

Refined analysis of microarray data, according to the criteria defined in 3.4.2 lead to a more equal distribution between EM and UM up-regulated transcripts: 229 up in EM, 297 up in UM.

Table XI: Genes significantly and differentially regulated in the microarray analyses.

NR Gene	Gene annotation Smp	average ratio (EM/UM)	q-value (%)
Smp_123300	follistatin	-2.15	0.00
Smp_136050	leucine-rich repeat-containing protein	-2.31	0.00
Smp_166960	Ubiquitin-protein ligase BRE1	-1.69	0.00
Smp_036470	oxalate:formate antiporter	-2.91	0.00
Smp_194770	ATP:guanidino kinase (Smc74)	-0.87	0.00
Smp_034550	alpha-actinin	-1.13	0.00
Smp_144220	glycine amidinotransferase	-0.75	0.00
Smp_161680	phosphorylase B kinase beta, kpbp	-0.77	0.00
Smp_146840	netrin	-1.33	0.00
Smp_038440	heart-specific myosin light chain phosphatase small subunit	-0.77	0.00
Smp_088950	hypoxia upregulated 1 (hyou1)-related	-0.95	0.00
Smp_135530	leishmanolysin-2 (M08 family)	-0.92	0.00
Smp_015670	paraxis	-1.06	0.00
Smp_123080	Sarcoplasmic calcium-binding protein (SCP).	-0.86	0.00
Smp_003440	SPFH domain / Band 7 family protein	-1.40	0.00
Smp_098710	quiescin q6-related sulfhydryl oxidase	-0.60	0.00
Smp_056200	Isocitrate dehydrogenase [NAD] subunit gamma, mitochondrial	-0.64	0.00
Smp_136710.x	calcium-transporting atpase sarcoplasmic/endoplasmic reticulum type (calcium pump)	-0.99	0.00
Smp_176930	cationic amino acid transporter	-0.75	0.00
Smp_049550	heat shock protein 70 (hsp70)	-0.83	0.00
Smp_018260	glycogen synthase	-0.73	0.00
Smp_047370	malate dehydrogenase	-0.64	0.00
Smp_019630	aminoacylase (M20 family)	-0.69	0.00
Smp_153700	protein phosphatase 1 binding protein	-0.91	0.00
Smp_134800	tyrosine kinase	-1.50	0.00
Smp_145210	cadherin	-0.91	0.00

Smp_062980	tetraspanin	-0.73	0.00
Smp_037900	family S12 unassigned peptidase (S12 family)	-0.65	0.00
Smp_095630	CD9-like protein Sm-TSP-1	-0.71	0.00
Smp_156540	wnt related	-1.04	0.00
Smp_010770.x	fatty acid acyl transferase-related	-1.71	0.00
Smp_154730	rna-binding protein musashi-related	-1.08	0.00
Smp_010820	peptidyl-glycine alpha-amidating monooxygenase	-0.94	0.00
Smp_124540	serine-rich repeat protein	-1.20	0.00
Smp_010930	heat shock protein 70 (hsp70)-interacting protein	-0.81	0.00
Smp_126350	glutamate receptor, NMDA	-0.73	0.00
Smp_083220	protocadherin alpha	-1.35	0.00
Smp_083720	mitochondrial phosphate carrier protein	-0.63	0.00
Smp_173340	transcription factor	-1.04	0.00
Smp_096480	Cys-loop ligand gated ion channel subunit	-0.97	0.00
Smp_079920	pyruvate dehydrogenase	-0.75	0.00
Smp_038870.x	NADH-ubiquinone oxidoreductase	-0.88	0.00
Smp_161480	eukaryotic translation initiation factor 3 subunit (eif-3)	-0.68	0.00
Smp_121780	serine/threonine kinase	-0.64	0.00
Smp_062070.x	sulfide quinone reductase	-0.84	0.00
Smp_135520	dock	-1.31	0.00
Smp_180240	f-spondin	-0.71	0.00
Smp_172510.x	DNAj-related	-0.68	0.00
Smp_145140	wnt-5	-0.75	0.00
Smp_194460	dihydropolipoamide acetyltransferase component of pyruvate dehydrogenase	-0.60	0.00
Smp_050520	notch	-0.79	0.00
Smp_135140	high voltage-activated calcium channel beta subunit 1	-0.62	0.00
Smp_151960	rho gtpase activating protein	-1.16	0.00
Smp_133600	utp-glucose-1-phosphate uridylyltransferase 2 (udp- glucose pyrophosphorylase 2)	-0.65	0.00
Smp_176540	cadherin	-0.77	0.00
Smp_176470	cadherin	-1.40	0.00
Smp_013440	solute carrier protein	-0.84	0.00
Smp_148790	laminin beta chain-related	-0.81	0.00
Smp_057530	subfamily S9B unassigned peptidase (S09 family)	-0.74	0.00
Smp_126640	neurotracting/lsamp/neurotrimin/obcam related cell adhesion molecule	-0.70	0.00
Smp_079960	tubulin beta chain	-0.59	0.00
Smp_196150	Selenoprotein O-like	-0.63	0.00
Smp_142190	carboxypeptidase N (M14 family)	-0.76	0.00
Smp_083450	DNAj homolog subfamily C member	-0.62	0.00
Smp_157070	cysteine-rich with egf-like domains protein	-0.69	0.00
Smp_056620	DNA helicase recq1	-0.90	0.00
Smp_131050	camp-dependent protein kinase type II regulatory subunit	-0.67	0.00
Smp_044060	camp-specific cyclic nucleotide phosphodiesterase	-0.90	0.00
Smp_144450	apobec-1 complementation factor-related	-0.60	0.00
Smp_141980	camp-specific 3,5-cyclic phosphodiesterase	-1.07	0.00
Smp_145970	recombining binding protein suppressor of hairless	-0.99	0.00
Smp_007550	leukotriene A4 hydrolase (M01 family)	-1.18	0.00
Smp_073560.x	G beta-like protein gbl	-0.91	0.00
Smp_152710.x	glutathione-s-transferase omega	-0.59	0.00
Smp_154680	glycosyltransferase 14 family member	-1.27	0.00
Smp_195010	HMG-CoA synthase	-0.64	0.00
Smp_168730	carbonic anhydrase	-0.74	0.00
Smp_075690	translation elongation factor G	-0.62	0.00
Smp_163230	propionyl-CoA carboxylase beta chain, mitochondrial precursor	-0.81	0.00
Smp_041350	bruno-like rna binding protein	-0.78	0.00
Smp_139840	kunitz-type protease inhibitor	-0.75	0.00
Smp_142630	taln 2	-0.71	0.00
Smp_070630	uncoordinated protein 112 (mitogen inducible mig- 2 protein like)	-0.75	0.00
Smp_180810	kunitz-type protease inhibitor	-0.66	0.00
Smp_007760	alanine aminotransferase	-0.71	0.00
Smp_132700	nephrin	-0.63	0.00
Smp_053120	S-adenosyl-methyltransferase mraW	-0.69	0.00

Appendix

Smp_194050	Clumping factor A precursor (Fibrinogen-binding protein A) (Fibrinogen receptor A)	-0.75	0.00
Smp_126530	ets	-0.88	0.00
Smp_139980	ataxin 2-binding protein (hexaribonucleotide binding protein 1)	-0.60	0.06
Smp_165820	dynein heavy chain	-1.62	0.06
Smp_123350	G-protein coupled receptor fragment	-1.07	0.06
Smp_070780	UDP-glucose 4-epimerase	-0.60	0.06
Smp_155970	twik family of potassium channels-related	-0.63	0.06
Smp_022740	tumor necrosis factor induced protein	-0.99	0.06
Smp_136330	lip-related protein (liprin) alpha	-0.69	0.06
Smp_061940.x	adenylate kinase 1	-0.60	0.06
Smp_155340	frizzled	-1.02	0.06
Smp_159190	thiamin pyrophosphokinase-related	-0.60	0.06
Smp_010660	60S ribosomal protein L6	-0.59	0.06
Smp_095540	cytochrome-c oxidase	-1.10	0.06
Smp_063070.x	rabb and C	-0.61	0.06
Smp_124910	stoned-related	-0.70	0.06
Smp_134250	heparan sulfate n-deacetylase/n- sulfotransferase	-0.59	0.06
Smp_157100	sphingoid long chain base kinase	-1.11	0.06
Smp_167630	solute carrier family	-0.86	0.06
Smp_167660	protein phosphatase 1 binding protein	-0.93	0.06
Smp_147450	serine/threonine kinase	-0.69	0.06
Smp_039300	trim56 protein	-0.67	0.06
Smp_154040	sugar nucleotide epimerase related	-0.91	0.10
Smp_123650	peroxidasin	-0.59	0.10
Smp_121190	voltage-gated potassium channel	-0.63	0.10
Smp_161900	innexin	-0.79	0.10
Smp_158510	diacylglycerol O-acyltransferase 1	-1.05	0.10
Smp_132740	fatty acid desaturase	-0.71	0.10
Smp_084270	rhodopsin-like orphan GPCR	-0.75	0.10
Smp_143420	actin bundling/missing in metastasis-related	-0.83	0.18
Smp_194720	family S33 non-peptidase homologue (S33 family)	-0.59	0.18
Smp_096520	sialin (solute carrier family 17 member 5) (sodium/sialic acid cotransporter) (ast) (membrane glycoprotein hp59)	-0.70	0.18
Smp_059170.x	troponin I	-0.63	0.18
Smp_175760	endosomal trafficking protein	-0.74	0.18
Smp_127160	cytochrome b5	-0.67	0.18
Smp_176770	dock-9	-0.78	0.18
Smp_126050	cadherin	-0.81	0.23
Smp_024290	MAP kinase kinase protein DdMEK1	-0.70	0.23
Smp_157550	partition defective complex protein	-0.65	0.23
Smp_046640	twik family of potassium channels-related	-0.74	0.23
Smp_131580	lysosomal alpha-mannosidase (mannosidase alpha class 2b member 1)	-0.82	0.30
Smp_173180.x	developmentally regulated GTP-binding protein 1 (drg 1)	-0.74	0.30
Smp_144130	lachesin	-0.81	0.41
Smp_006760	fasting-inducible integral membrane protein tm6p1-related	-0.60	0.41
Smp_016600	solute carrier family 1 (glial high affinity glutamate transporter	-0.62	0.41
Smp_129120	shoc2	-0.75	0.41
Smp_137410	calpain C (C02 family)	-0.66	0.41
Smp_172750	cation transporting ATPase	-0.67	0.41
Smp_169940	kelch-like protein	-0.61	0.41
Smp_147390	glutamate receptor, NMDA	-0.80	0.41
Smp_158400	receptor protein tyrosine phosphatase r (pcptp1)	-0.65	0.55
Smp_121920	vesicular amine transporter	-0.72	0.55
Smp_148200	Junctophilin	-0.86	0.55
Smp_151220	beta-1,3-n-acetylglucosaminyltransferase,putati ve	-0.73	0.55
Smp_196090	TGF-beta receptor	-0.62	0.55
Smp_168940	NAD dependent epimerase/dehydratase	2.66	0.00
Smp_095980	superoxide dismutase precursor (EC 1.15.1.1)	2.35	0.00
Smp_158480	AMP dependent ligase	2.82	0.00
Smp_000430.x	eggshell protein, chorion	2.29	0.00
Smp_013540	tyrosinase precursor	1.77	0.00

Smp_170080	sodium/dicarboxylate cotransporter-related	1.18	0.00
Smp_082430	uridine phosphorylase	2.33	0.00
Smp_077920	Trematode Eggshell Synthesis domain containing protein	2.29	0.00
Smp_082420	uridine phosphorylase	1.09	0.00
Smp_000280	similar to female-specific protein 800 (fs800)	2.02	0.00
Smp_135020	oxalate:formate antiporter	1.18	0.00
Smp_000420	Pro-His-rich protein	1.98	0.00
Smp_055220.x	surface protein PspC	0.83	0.00
Smp_151490	nebulin	0.80	0.00
Smp_176350	contactin	0.69	0.00
Smp_135230	aromatic-L-amino-acid decarboxylase	2.58	0.00
Smp_174510	dynein light chain	1.23	0.00
Smp_090520	purine nucleoside phosphorylase	1.11	0.00
Smp_133770	glutamine synthetase bacteria	1.94	0.00
Smp_138570	spore germination protein	1.98	0.00
Smp_075850	rrm-containing protein seb-4	0.67	0.00
Smp_025370	lipopolysaccharide-induced transcription factor regulating tumor necrosis factor alpha	0.62	0.00
Smp_008620	RHBDF1 protein (S54 family)	0.74	0.00
Smp_003770	histone h1/h5	0.86	0.00
Smp_052230	kunitz-type protease inhibitor	1.83	0.00
Smp_157080	ceramide glucosyltransferase	0.81	0.00
Smp_020550	low-density lipoprotein receptor (ldl)	1.42	0.00
Smp_170340	Collagen alpha-1(V) chain precursor	1.45	0.00
Smp_051400	cytoplasmic dynein light chain	1.21	0.00
Smp_070030	snf7-related	0.71	0.00
Smp_138740	Alpha-(1,6)-fucosyltransferase (EC 2.4.1.68) (Glycoprotein 6-alpha-L-fucosyltransferase) (GDP-fucose--glycoprotein fucosyltransferase) (GDP-L-Fuc:N-acetyl-beta-D-glucosaminide alpha1,6-fucosyltransferase) (alpha1-6FucT) (Fucosyltransferase 8)	0.84	0.00
Smp_005710.x	egg protein CP391S	1.32	0.00
Smp_028990.x	protein phosphatase-1	0.75	0.00
Smp_163720	endophilin B1	0.83	0.00
Smp_051410	septate junction protein	0.73	0.00
Smp_169190	tegumental protein	1.80	0.00
Smp_031300	universal stress protein	0.77	0.00
Smp_164730	growth hormone secretagogue receptor	0.68	0.00
Smp_139190	adenomatous polyposis coli protein	1.16	0.00
Smp_044870	zinc finger protein	0.92	0.00
Smp_008640	gelsolin	0.76	0.00
Smp_087940.x	gaba(A) receptor-associated protein	0.63	0.00
Smp_140420	5'-3' exoribonuclease	0.86	0.00
Smp_060190.x	ctg4a-related	1.07	0.00
Smp_162190	crp-related	0.81	0.00
Smp_094190	serine/threonine kinase	0.80	0.00
Smp_141450	subfamily S1A unassigned peptidase (S01 family)	1.20	0.00
Smp_151620	cadherin-related	0.63	0.00
Smp_138750	Alpha-(1,6)-fucosyltransferase (EC 2.4.1.68) (Glycoprotein 6-alpha-L-fucosyltransferase) (GDP-fucose--glycoprotein fucosyltransferase) (GDP-L-Fuc:N-acetyl-beta-D-glucosaminide alpha1,6-fucosyltransferase) (alpha1-6FucT) (Fucosyltransferase 8)	0.75	0.00
Smp_009070	zinc finger protein	0.65	0.00
Smp_054300	alpha(1,3)fucosyltransferase	0.80	0.00
Smp_131190	diacylglycerol kinase, zeta, iota	0.69	0.00
Smp_195070	conserved Schistosoma protein, unknown function	0.87	0.00
Smp_129920	sodium-dependent neurotransmitter transporter	0.87	0.00
Smp_020540.x	pinch	0.61	0.00
Smp_194960	similar to tetraspanin TE736	1.06	0.00
Smp_059480	Peroxiredoxin, Prx1	0.64	0.00
Smp_062420.x	heat shock protein 70 (hsp70)-interacting protein	0.69	0.00
Smp_000130.x	hormone-sensitive lipase (S09 family)	0.74	0.00
Smp_163790	nuclear hormone receptor	1.03	0.00
Smp_033000	calcium-binding protein	1.28	0.00
Smp_140270	carbonyl reductase	0.59	0.00
Smp_125650	inositol polyphosphate multikinase	0.75	0.00

Appendix

Smp_082360	protein tyrosine kinase	1.02	0.00
Smp_094500	choline dehydrogenase	1.03	0.00
Smp_015020	sodium potassium transporting ATPase alpha subunit	0.78	0.00
Smp_144440	replication A protein	0.81	0.00
Smp_125890	DNA photolyase	0.69	0.00
Smp_009390.x	prefoldin subunit	0.59	0.08
Smp_132260	serine/threonine kinase	0.99	0.08
Smp_000270	Trematode Eggshell Synthesis domain containing protein	1.14	0.08
Smp_127960	tubulin-specific chaperone E	0.59	0.08
Smp_194610	serine/threonine kinase	0.60	0.08
Smp_125660	heterogeneous nuclear ribonucleoprotein-related	0.67	0.08
Smp_008660.x	villin	0.94	0.08
Smp_161430	monocarboxylate transporter	0.90	0.08
Smp_080210	lipid-binding protein	0.65	0.08
Smp_004680	interferon-related developmental regulator- related	0.68	0.08
Smp_172890	protein tyrosine phosphatase	0.69	0.10
Smp_174110	protein phosphatase 1 regulatory inhibitor subunit 16a	0.60	0.10
Smp_147140	transient receptor potential cation channel	0.77	0.10
Smp_019310	cytoplasmic dynein light chain	0.69	0.10
Smp_155560	serpin	0.65	0.10
Smp_173240	cement precursor protein 3B variant 3	0.85	0.10
Smp_028490	1-acyl-sn-glycerol-3-phosphate acyltransferase epsilon, fragment	0.60	0.18
Smp_160890	STARP antigen	0.61	0.18
Smp_167010	talin	0.77	0.18
Smp_073130.x	loss of heterozygosity 11 chromosomal region 2 gene a protein homolog (mast cell surface antigen 1) (masa- 1)	0.74	0.18
Smp_133660	lin-9	1.07	0.18
Smp_174880	FOG precursor	0.94	0.18
Smp_154400	tomosyn	0.71	0.23
Smp_081140	dbl related	0.79	0.23
Smp_072620	Dynein light chain 1, cytoplasmic	0.86	0.23
Smp_041770	serine/threonine kinase	0.65	0.23
Smp_040560	cancer-associated protein protein	0.85	0.30
Smp_105910	CREB-binding protein 1 (SmCBP1)	0.79	0.41
Smp_007670	ank repeat-containing	0.61	0.41
Smp_169610	zinc finger protein	0.68	0.41
Smp_074470	30S ribosomal protein S12 family member	0.59	0.41
Smp_032950	Calmodulin (CaM)	0.59	0.55
Smp_165850	long-chain-fatty-acid--CoA ligase	0.63	0.55
Smp_148120	ctd sr related rna binding protein	0.89	0.55
Smp_077310	tegumental protein	0.61	0.55
Smp_028550	DEAD/DEAH box helicase, fragment	0.78	0.73
Smp_168130	phosphatase and actin regulator	0.59	0.73

Genes significantly and differentially regulated between EM and UM according to the microarray analysis (with refined criteria from 3.4.2). Give are those 247 of 256 transcripts with functional annotations other than hypothetical protein.

Table XII: GO for genes significantly and differentially regulated in the microarray analyses.

Ontology	GO term description	Go term	Counts	p.adjusted
membrane	Double layer of lipid molecules that encloses all cells, and, in eukaryotes, many organelles; may be a single or double lipid bilayer; also includes associated proteins.	GO:0016020	99/2025	2,37E-04
biological adhesion	The attachment of a cell or organism to a substrate or other organism.	GO:0022610	17/144	1,76E-03
extracellular region	The space external to the outermost structure of a cell. For cells without external protective or external encapsulating structures this refers to space outside of the plasma membrane. This term covers the host cell environment outside an intracellular parasite.	GO:0005576	19/205	1,73E-02
generation of precursor metabolites and energy	The chemical reactions and pathways resulting in the formation of precursor metabolites, substances from which energy is derived, and any process involved in the liberation of energy from these substances.	GO:0006091	10/95	1,73E-02
carbohydrate metabolic process	The chemical reactions and pathways involving carbohydrates, any of a group of organic compounds based of the general formula $C_x(H_2O)_y$. Includes the formation of carbohydrate derivatives by the addition of a carbohydrate residue to another molecule.	GO:0005975	13/189	4,47E-02

Enriched GO categories detected, when analyzing the transcripts significantly and differentially (according to criteria in 3.4.2) regulated between EM and UM according to both transcriptome analyses. For transcripts up-regulated in EM no significantly enriched categories were found. All categories presented here were significantly enriched for transcripts up-regulated in UM.

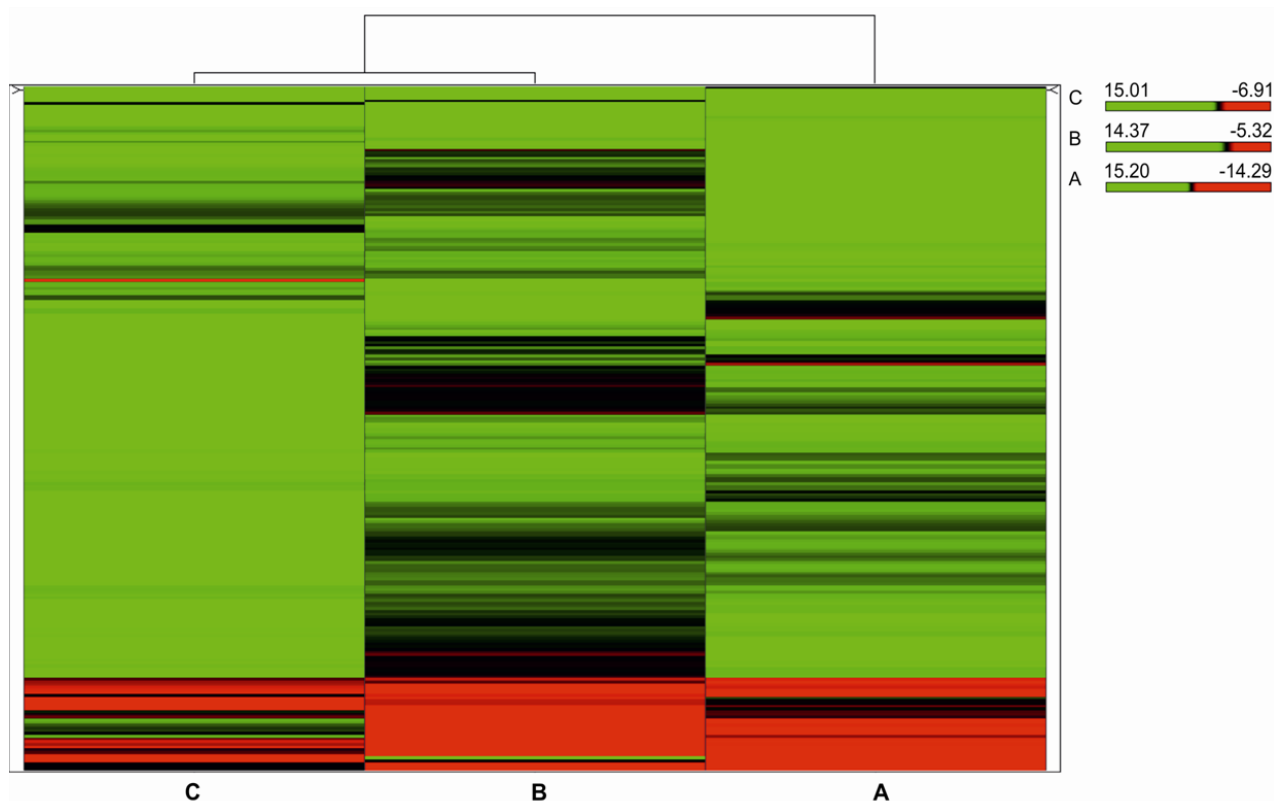


Figure XVII: Hierarchical clustering of SuperSAGE detected transcripts abundantly significantly differentially regulated.

Refined criteria, to select only those transcripts detected by SuperSAGE with a normalized count of at least 10 in at least one biological replica of either EM or UM, and of these only those significantly regulated between the two male stages with an absolute \log_2 ratio greater than 0.585, detected 253 transcripts. Of these 218 were up-regulated in EM (green) and 35 in UM (red). Within this refined data-set \log_2 ratios for each transcript are more homogenous throughout the three biological replicas.

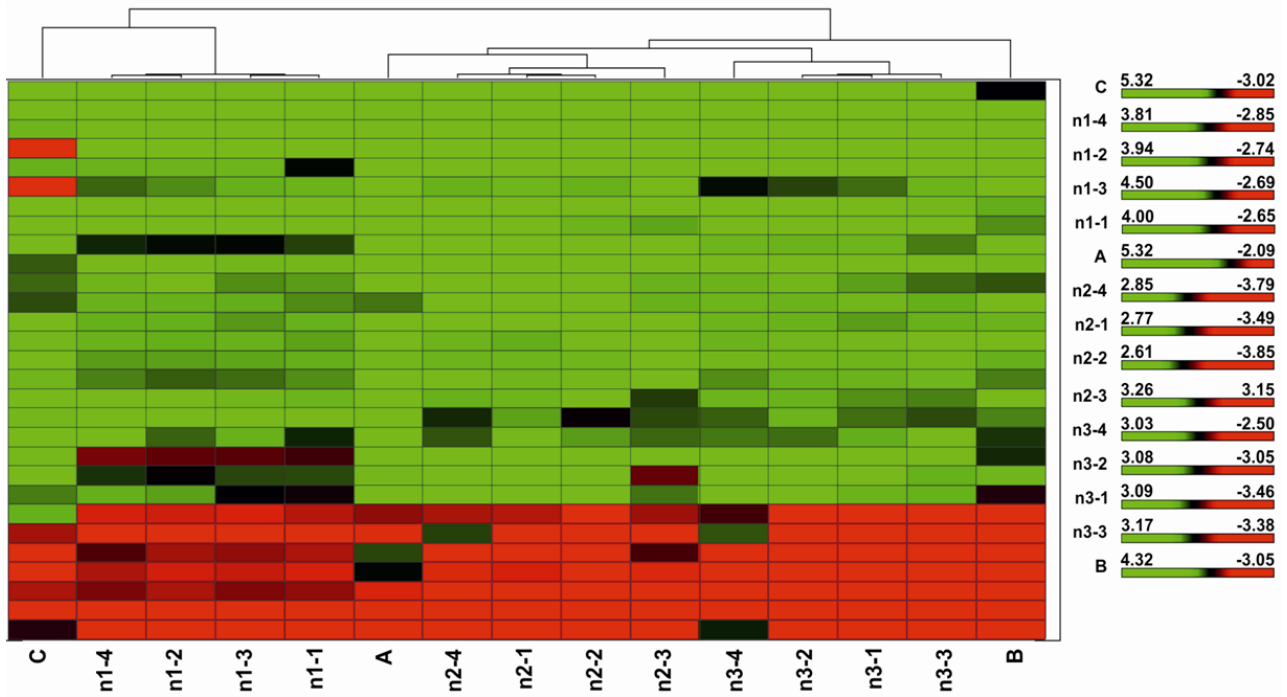


Figure XVIII: Hierarchical clustering of the SuperSAGE microarray overlap after refined analysis. Refined criteria (3.4.2) lead to a reduced list of genes abundantly significantly and differentially regulated between EM and UM according to both transcriptome analyses. The hierarchical clustering shows that most transcripts in this group (22) are up-regulated in EM (green) and only 7 are up-regulated in UM (red). Biological replicas cluster independent of experimental origin.

VI. First characterization studies

Subsequently presented figures supplement data described in chapter 3.6. 'First characterization studies'.

```

ATGGAAGAGAGTATATCACAATTAGAATGTTGTAACGTTGGATTCTATTTAAATCGTCAAATAACTCAACAAGAATATTTAACTGATCATTAT
TATTTGAATCTGGTACACCAAATTTGTTCAAGCATGTAATGAAGAATTACCTTCAACATGTAAGGATATGTATGTCCTGAAGGACATTATTGTCG
TATGATTAATAATGAACCAAAATGCAAAATGTCGCTTCAATGTAATACAGCAGATTATTTAACTGGTCCATTATGTACAATAATTTAAGACGATTT
CATAATCAATGCCATTTAAAACAAGCTCGTTGTAATCACCAAAAGAAAGTCTTGAAGTAATACCATGTCAGATGAAGGTTTACGATGTTGAGATT
TAAGTATATTATCTGAAAAAATTTAAATCTTAATTCCTATTTAAAACATTATATGCTGAATATGAAGAAAAGAAAGGTTACCTTCATACCATC
ATCATCATCCTTGCCTTCATCAACTTCAACAACAAATCGTCACTATCATCAACAGATAATCAAGAGTATACCACAATGAAGATGATAATGTCATC
ATTTGAATCGTAGAACATCAACAGATCTCAAAACATATATTGATAAAATGAATGATGAATCCATTTTCGATGAGAAGTCACCTTATCTAATGATG
AATTATCTAAAGAATTAATATGTAATGCTAATGAATATTGTTTATTACGACAATTTGATGGAGTCCATCATGTGAATATGGAAATGAACAATCATG
GCAAAACATTAATAATTTGTCAGAGTCTACATTTAATGAACCAATATGTAGTACAGATAATCAACATTTTATAATAGTTGTGATCTTAAATTAAC
GGATAAAAAATCAATTAGAAGTAAGAATTCATATAAAGGTGAATGTCGAAGCAAGGTAACCTGCTCTGATATTCAATGTCCAAGACCTGATATGA
GATGTAGTCCACATCATTTAACTGGTCAACCAATTTGTATGGATTGTGCTAAATTACCATTAGATTGTAATGCATCATTTAGAAATGGACAAGAAAC
ACTAACTTCATCAACATCTTCATCATCATCATCATCATCATCATCATCATCATCATCATCATCATCATCATCATCATCATCATCATCATCATCATCAT
TGGAAAACACCAGTTCAAACATATGGTTGGCCAGTTGTTTGTGGATCAAATGGGAAAACCTTATCGTAATACATGTTTTCTCATGTTGTTAACTGTT
TAAGTGATAAATTTGTCGGATTGAAAAACCAGAATTTGTAGTGAACACTATTCATCAAACATGATGATTGGAGAAGACATTTGGAAAAATATTC
AAATTTATTCTAA
    
```

Figure XIX: SmFst CDS. The sequence of *Schistosoma mansoni* follistatin (SmFst) comprises of 1,371 nt. In comparison to the CDS predicted in the *S. mansoni* genome project SchistoDB 2.0 (Smp_123300) two sequence stretches predicted as introns were found to be part of the CDS (fat print). Underlined: *in situ* hybridization probes, grey: predicted exon-exon borders.

```

ATGAATAGAATGTTTAAATTAATAAAACCAGAAATCGATAAAACTATCTTACCTGAAAAATTTTAAACATCTATGGTAACATTTAATATAACAATCGTATGA
TTAATTGGTTAAATATAATAGAAATAATCAACCATATAAACCATTACATGTTATATAATGATAATATGTAATAATTGTGATCATGAACAACAAAATATTAT
GATCCAAAAAGGTTGTTATGGAAATTAATATCGTCCAGCTTTAAAAAGACAGAGGCGATCATTAACTAAAGGAGATGAGACAATATACAATGATGTCGTTT
TAATGGACACCATTAAGTTGTTGACACAAGCATTATCTGTTAAATTTTCTGATATTGGTTGGGATAACTGGATTATACACCCGAAAAGTTTGAACCGAATTAT
TGTCGAGGATCCTGTAAGTACATCAACAAAAAGTTTACACTATGATGTTATGGATTTATTATTACGTAATAAATTTATCACAATTTGGTAATGTTCAACGTGAT
GAAGTACAATCTGTTGTCATCCAACCAATTAAGTATGCTGTTTATATTGATTCAAATCGTGAATTACAAATGCATACTTTACATAAATTAATGTTTT
AGGATGTGCTGTAGTTAA
    
```

Figure XX: SmlnAct CDS. The amplified sequence for SmlnAct confirmed the CDS prediction from SchistoDB 2.0 (Smp_063190) which contains 162 more bp at the 5'-end than the published sequence (DQ863513, Freitas *et al.*, 2007) (fat print). Underlined: *in situ* hybridization probe, grey: predicted exon-exon borders.

Appendix

Besides transcripts associated with TGF β -signalling, further *in situ* hybridizations were performed to localize an oxalate-formate antiporter, which was strongly up-regulated (significantly and differentially) in UM according to all transcriptome approaches. A first experiment detected sense-transcripts for this molecules in all reproductive organs of EM, UM, and EF:

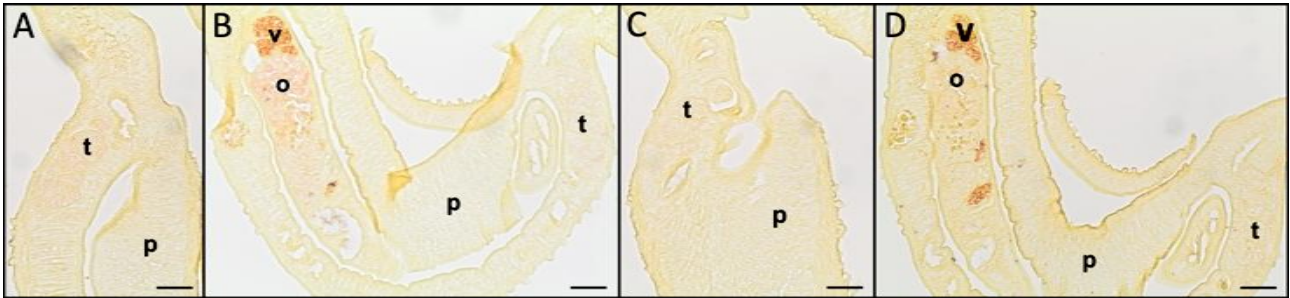


Figure XXIII: Oxalate-formate antiporter *in situ* hybridization.

Anti-sense detecting probes for the oxalate-formate antiporter (Smp_036470) detected sense-transcripts (A,B) in the testicular lobes (t) of UM (A) and EM (B), and in the ovary (o) of females (B). The respective sense control reactions (C, D) did not result in a color signal. Scale bar: 50 μ M.